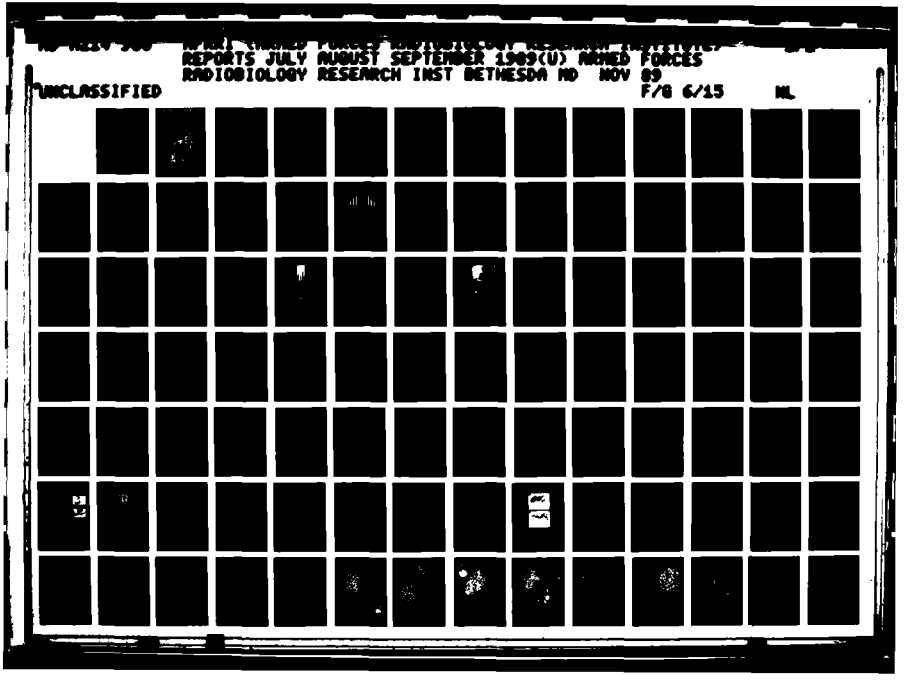
REPORTS JULY AUGUST SEPTEMBER 1989(U) ARMED FORCES
RADIOBIOLOGY RESEARCH INST BETHESDA MD NOV 89
UNCLASSIFIED
F/G 6/15
NL

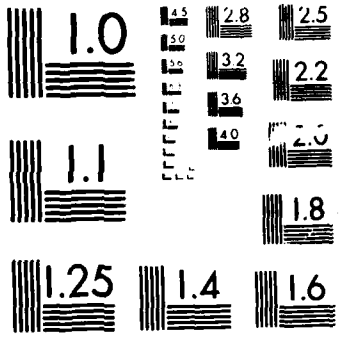
1.0
1.1
1.25
1.4
1.6
1.8
2.0
2.2
2.5
2.8
3.2
3.6
4.0
4.5
5.0

AFRRI··REPORTS

(2)

AD-A214 960

DTIC FILE COPY

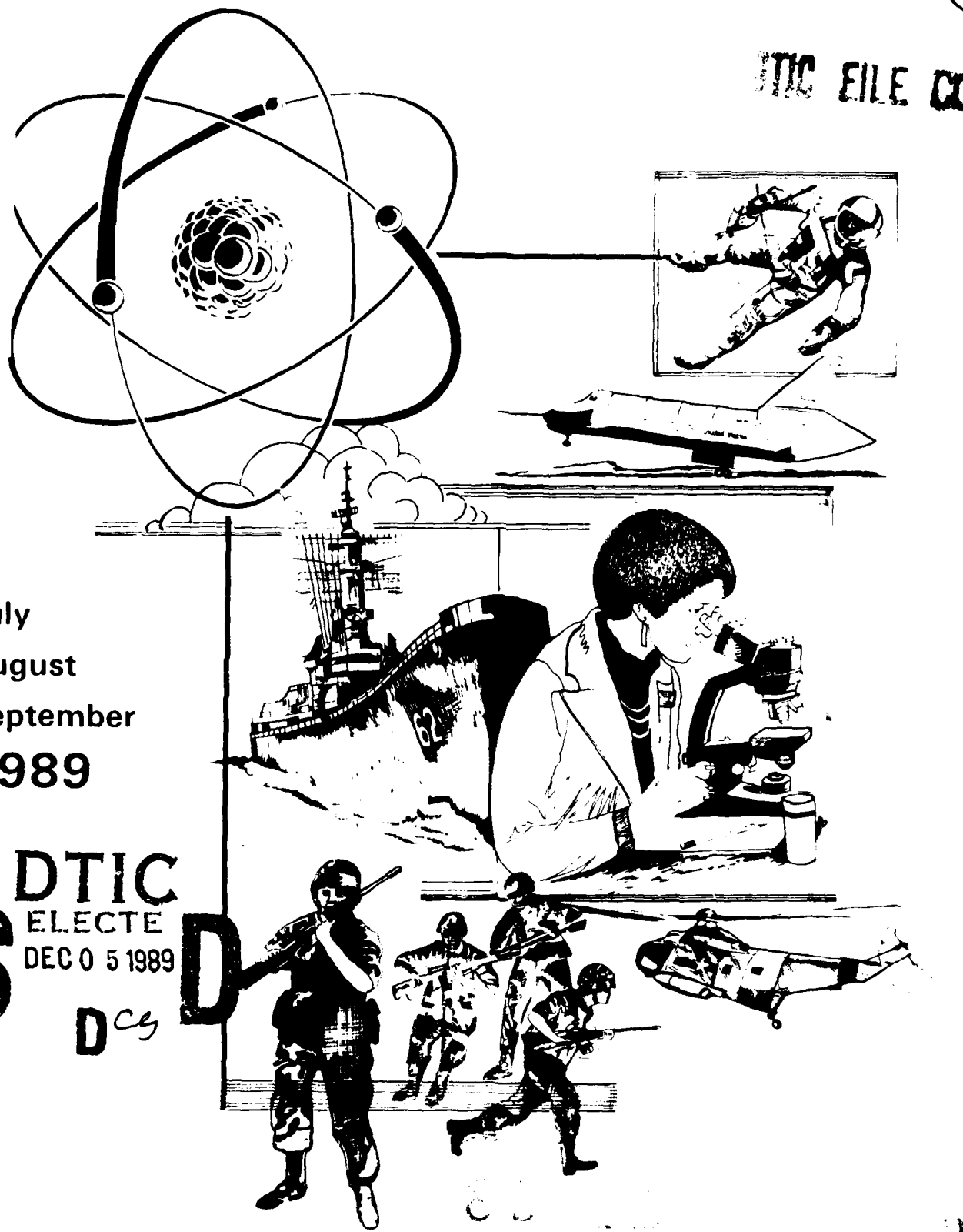

July
August
September
1989

DTIC
ELECTE
DEC 0 5 1989
S D
D Cg

Defense Nuclear Agency
Armed Forces Radiobiology Research Institute
Bethesda, Maryland 20814-5145

Approved for public release, distribution unlimited

UNCLASSIFIED
SECURITY CLASSIFICATION OF THIS PAGE

REPORT DOCUMENTATION PAGE

1a REPORT SECURITY CLASSIFICATION UNCLASSIFIED	1b RESTRICTIVE MARKINGS
2a SECURITY CLASSIFICATION AUTHORITY	3 DISTRIBUTION / AVAILABILITY OF REPORT Approved for public release; distribution unlimited.
2b DECLASSIFICATION / DOWNGRADING SCHEDULE	
4 PERFORMING ORGANIZATION REPORT NUMBER(S) SR89-26 - SR89-39, TR89-1	5 MONITORING ORGANIZATION REPORT NUMBER(S)
6a NAME OF PERFORMING ORGANIZATION Armed Forces Radiobiology Research Institute 6b OFFICE SYMBOL (If applicable) AFRRI	7a NAME OF MONITORING ORGANIZATION
6c ADDRESS (City, State, and ZIP Code) Defense Nuclear Agency Bethesda, Maryland 20814-5145	7b ADDRESS (City, State, and ZIP Code)
8a NAME OF FUNDING / SPONSORING ORGANIZATION Defense Nuclear Agency 8b OFFICE SYMBOL (If applicable) DNA	9 PROCUREMENT INSTRUMENT IDENTIFICATION NUMBER
8c ADDRESS (City, State, and ZIP Code) Washington, DC 20305	10 SOURCE OF FUNDING NUMBERS PROGRAM ELEMENT NO: NWED QAXM PROJECT NO: TASK NO: WORK UNIT ACCESSION NO:
11 TITLE (Include Security Classification) AFRRI Reports, Jul-Sep 1989	
12 PERSONAL AUTHOR(S)	
13a TYPE OF REPORT Reprints/Technical 13b TIME COVERED FROM _____ TO _____ 14 DATE OF REPORT (Year, Month, Day) 1989 November 15 PAGE COUNT	
16 SUPPLEMENTARY NOTATION	

17 COSATI CODES			18 SUBJECT TERMS (Continue on reverse if necessary and identify by block number)
FIELD	GROUP	SUB-GROUP	

19 ABSTRACT (Continue on reverse if necessary and identify by block number)

This volume contains AFRRI Scientific Reports SR89-26 through SR89-39 and Technical Report TR89-1 for Jul-Sep 1989.

20 DISTRIBUTION / AVAILABILITY OF ABSTRACT ☐ UNCLASSIFIED/UNLIMITED ☒ SAME AS RPT. ☐ DTIC USERS	21 ABSTRACT SECURITY CLASSIFICATION UNCLASSIFIED
22a NAME OF RESPONSIBLE INDIVIDUAL Gloria Ruggiero	22b TELEPHONE (Include Area Code) (301) 295-2017 22c OFFICE SYMBOL ISDP

DD FORM 1473, 84 MAR — 83 APR edition may be used until exhausted. All other editions are obsolete.

SECURITY CLASSIFICATION OF THIS PAGE

UNCLASSIFIED

CONTENTS

Scientific Reports

SR89-26: Allalunis-Turner, M. J., Walden, T. L., Jr., and Sawich, C. Induction of marrow hypoxia by radioprotective agents.

SR89-27: Blakely, E., Chang, P., Lommel, L., Bjornstad, K., Dixon, M., Tobias, C., Kumar, K., and Blakely, W. F. Cell-cycle radiation response: Role of intracellular factors.

SR89-28: Burghardt, W. F., Jr., and Hunt, W. A. Characteristics of radiation-induced performance changes in bar-press avoidance with and without a preshock warning cue.

SR89-29: Carcillo, J. A., Litten, R. Z., and Roth, B. L. Norepinephrine-induced phosphorylation of a 25 kd phosphoprotein in rat aorta is altered in intraperitoneal sepsis.

SR89-30: Fuciarelli, A. F., Wegher, B. J., Gajewski, E., Dizdaroglu, M., and Blakely, W. F. Quantitative measurement of radiation-induced base products in DNA using gas chromatography-mass spectrometry.

SR89-31: Gruber, D. F., and Farese, A. M. Tropism of canine neutrophils to xanthine oxidase.

SR89-32: Maier, D. M., and Landauer, M. R. Effects of acute sublethal gamma radiation exposure on aggressive behavior in male mice: A dose-response study.

SR89-33: Mickley, G. A., Ferguson, J. L., Mulvihill, M. A., and Nemeth, T. J. Progressive behavioral changes during the maturation of rats with early radiation-induced hypoplasia of fascia dentata granule cells.

SR89-34: Nold, J. B., Weichbrod, R. H., and Alderks, C. E. Stomach nodules in pigeons.

SR89-35: Rabin, B. M., Hunt, W. A., and Joseph, J. A. An assessment of the behavioral toxicity of high-energy iron particles compared to other qualities of radiation.

SR89-36: Raff, R. F., Severns, E., Storb, R., Martin, P., Graham, T., Sandmaier, B., Schuening, F., Sale, G., and Appelbaum, F. R. L-leucyl-L-leucine methyl ester treatment of canine marrow and peripheral blood cells.

SR89-37: Schmauder-Chock, E. A., and Chock, S. P. Localization of cyclo-oxygenase and prostaglandin E_2 in the secretory granule of the mast cell.

SR89-38: Schwartz, G. N. Radioprotection of mice with interleukin-1: Relationship to the number of spleen colony-forming units.

SR89-39: Vigneulle, R. M., Vriesendorp, H. M., Taylor, P., Burns, W., and Pelkey, T. Survival after total-body irradiation. I. Effects of partial small bowel shielding.

Technical Reports

AFRRI TR89-1: Mohaupt, T. H., Zeman, G. H., Blakely, W. F., and Elkind, M. M. Laboratory x-ray irradiator for cellular radiobiology research studies: Dosimetry report.

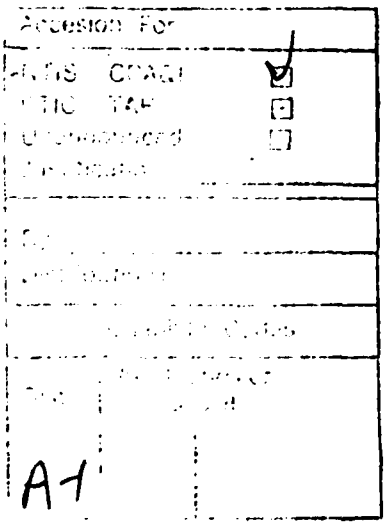

ARMED FORCES RADIOBIOLOGY
RESEARCH INSTITUTE
SCIENTIFIC REPORT
SR89-26

RADIATION RESEARCH 118, 581–586 (1989)

SHORT COMMUNICATION

Induction of Marrow Hypoxia by Radioprotective Agents

M. JOAN ALLALUNIS-TURNER,*† THOMAS L. WALDEN, JR.,‡
AND CHERYL SAWICH*

*Cross Cancer Institute and †University of Alberta, Edmonton, Alberta, Canada T6G 1Z2
‡Radiation Biochemistry Department, Armed Forces Radiobiology
Research Institute, Bethesda, Maryland 20814-5145

ALLALUNIS-TURNER, M. J., WALDEN, T. L., JR., AND SAWICH, C. Induction of Marrow Hypoxia by Radioprotective Agents. *Radiat. Res.* **118**, 581–586 (1989).

The ability of thiol and non-thiol radioprotectors to induce hypoxia was determined using the binding of [^{3}H]misonidazole by bone marrow cells as a measure of hypoxia. When administered at maximally radioprotective doses, four drugs (WR-2721, cysteamine, 5-hydroxytryptamine, and 16,16-dimethyl prostaglandin E_2) significantly increased the amount of [^{3}H]misonidazole bound by marrow cells, while no significant increase in binding was observed with three other agents (endotoxin, AET, superoxide dimutase). Doses of WR-2721 previously shown to provide suboptimal radioprotection did not significantly increase ^{3}H-misonidazole binding. These results suggest that the physiological effects of some radioprotectors, that is, their ability to induce marrow hypoxia, may contribute to their efficacy *in vivo*. © 1989 Academic Press, Inc.

INTRODUCTION

Many compounds which possess sulfhydryl groups have been shown to protect bone marrow from radiation injury. The most effective thiol radioprotective agent is ethiofos [*S*-2-(3-aminopropylamino)ethylphosphorothioic acid or WR-2721] (*1*). Several mechanisms of action have been postulated. These include hydrogen atom donation, OH radical scavenging, formation of mixed disulfides, metal chelation, and the production of hypoxia (*2*). Actual radioprotection may occur through a combination of these mechanisms. Studies using model biomolecule systems show that sulfhydryls do interact with radiation-induced free radicals, but direct evaluation in animal models has been more difficult to achieve because of the short half-life of various radical species. Nonetheless, it is believed that chemical mechanisms play a major role in the radioprotective effects of these drugs in *in vivo* systems.

The possibility that the production of tissue hypoxia by radioprotectors contributed to the protective effects observed with these drugs has also been considered. Some radioprotectors produce profound physiological changes including hypertension, apnea, brachycardia, and altered blood flow (*3*). Many of these altered physiologies can be induced by WR-2721 (*4*) and also by 16,16-dimethyl prostaglandin E_2 ($DiPGE_2$) (*5, 6*). The biological responses to these radioprotectors may have an impact on marrow oxygenation. WR-2721 has been postulated to reduce the peripheral

0033-7587/89 $3.00
Copyright © 1989 by Academic Press, Inc.
All rights of reproduction in any form reserved.

oxygen tension (*4*). Tissue hypoxia may also explain the protection observed with certain non-thiol compounds, including 5-hydroxytryptamine (5-HT).

Direct evaluation of the role of marrow hypoxia in the radioprotection of the hematopoietic system has been hampered by the lack of a suitable method for quantifying tissue hypoxia *in vivo*. With current microelectrode technology, the pO_2 cannot be accurately determined in the marrow of small rodents. Attempts to correlate hypoxia with other physiological parameters such as blood flow or production of lactic acid are complicated since they may be influenced by changes unrelated to hypoxia. To overcome these problems and directly evaluate the role of marrow hypoxia in radioprotection we have used the sensitizer–adduct technique to assess the extent of marrow hypoxia following treatment with radioprotective agents. This system is based on the metabolic reduction and subsequent binding of misonidazole to tissues as a function of the tissue oxygen concentration (*7, 8*). Misonidazole (Miso) is preferentially bound by hypoxic tissue. Using Miso binding as a measure of tissue oxygenation, we have demonstrated that treatment with WR-2721, $DiPGE_2$, cysteamine (Cys), or 5-HT induces significant hypoxia in mouse bone marrow.

MATERIALS AND METHODS

Mice. Six- to twelve-week-old BALB/c female mice obtained from Jackson Laboratories (Bar Harbor, ME) were used in these experiments. Mice were housed in a Canadian Council on Animal Care accredited facility on a 12-h light/dark cycle. Mice were provided with a standard rodent pellet diet and with acidified water *ad libitum*.

[^{3}H]Misonidazole. ^{3}H-labeled misonidazole ([^{3}H]Miso) (sp act 356.7 μCi/mg) was prepared by Dr. James Raleigh as described (*9*). Animals received a single intraperitoneal (ip) injection of [^{3}H]Miso in a 0.5 ml volume of phosphate-buffered saline (PBS) according to the schedule detailed below. The dose of [^{3}H]Miso was calculated to achieve a peak plasma concentration of approximately 100 μM.

Drugs and treatment schedule. 16,16-Dimethyl prostaglandin E_2 was obtained in the free oil form as the generous gift of Dr. Douglas Morton (Upjohn Co., Kalamazoo, MI). Stock solutions were prepared by dissolution in ethanol to a concentration of 10 mg/ml and diluted to the indicated concentration in PBS prior to administration as a single subcutaneous injection into the nape of the neck in a 0.1 ml volume. WR-2721 was obtained from the Cancer Treatment Division of the National Cancer Institute. All other drugs were purchased from Sigma Chemical Co. (St. Louis, MO) and were prepared in PBS immediately prior to use. Superoxide dimutase (SOD) was administered intravenously, while the remaining drugs were given as a single ip injection in a volume of 0.01 ml/g body wt. Mice were treated first with radioprotectors. Miso was injected at various intervals thereafter corresponding to the expected time of maximum radioprotective effect. Specifically, [^{3}H]Miso was administered 5 min after 5-HT (300 mg/kg); 10 min after $DiPGE_2$ (40 μg/mouse) or Cys (100 mg/kg); 15 min after 2-(2-aminoethyl)-2-thiopseudorea dihydrobromide (AET) (300 mg/kg); 30 min after WR-2721 (200–400 mg/kg); 60 min after SOD (200 mg/kg); and 24 h after endotoxin (LPS) (50 μg/mouse). In each experiment, control animals received 0.01 ml/g of PBS (ip) followed by [^{3}H]Miso at intervals equivalent to those used for the radioprotectors.

Bone marrow assay. Sixty minutes after [^{3}H]Miso, animals (three to five per group) were killed by cervical dislocation and the femurs were removed. Marrow cells were isolated by flushing femurs of individual animals with ice-cold complete medium (MEM Spinner with 5% fetal calf serum). Known numbers of cells were placed in duplicate tubes and washed four times with complete medium to remove any unbound [^{3}H]Miso. Following the last wash, the acid-soluble and acid-precipitable cellular fractions were isolated according to techniques previously described (*10*), and the total amount of [^{3}H]Miso bound to these fractions was determined by liquid scintillation counting. The results calculated for individual animals were expressed as pmol [^{3}H]Miso bound per 10^6 cells. Each drug was evaluated on two or three separate occasions. A Student's *t* test was used to determine significant differences between control and experimental groups.

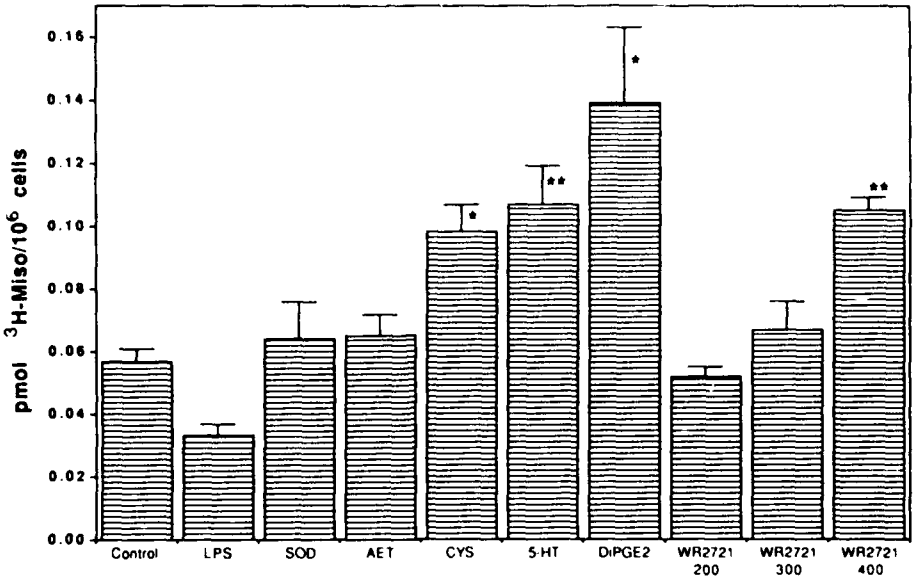

FIG. 1. Effect of *in vivo* treatment with various radioprotective agents on [^{3}H]Miso binding by bone marrow cells. Drug treatments and sample preparation are detailed under Materials and Methods. The doses of WR-2721 are provided as milligrams per kilogram body weight. Standard error bars are provided. (*) $P < 0.01$ or (**) $P < 0.001$.

RESULTS

Seven chemicals with known radioprotective properties were screened for their effects on [^{3}H]Miso binding to normal bone marrow cells *in vivo*. Cys, DiPGE$_2$, 5-HT, and WR-2721 treatment resulted in significantly increased binding to the acid-insoluble, macromolecular fraction (Fig. 1). No significant increase in marrow binding was observed following treatment with LPS, SOD, or AET.

In these studies, the dose and exposure time of each radioprotector duplicated that previously reported to produce maximum radioprotective effects (*6, 11–16*). We also determined the dose dependency of the degree of marrow hypoxia produced by increasing concentrations of WR-2721 by administering graded doses of WR-2721 (200–400 mg/kg) 30 min prior to [^{3}H]Miso. The results in Fig. 1 indicate that as the dose of WR-2721 was increased, the amount of [^{3}H]Miso bound to the marrow also increased. The response was statistically significant only at the optimal radioprotective dose of 400 mg WR-2721/kg of body weight.

DISCUSSION

The oxygen dependence of the metabolic reduction and covalent binding of misonidazole has been well described (*7, 8*). Because the K_m for the oxygen inhibition of the binding is similar to the K_m of the oxygen effect on radiosensitivity (*8*), misonidazole binding can be used as a reliable marker of radiobiological hypoxia. In this study, the binding of Miso to the macromolecular fraction of bone marrow cells was used

to indirectly assess the extent of hypoxia produced by treatment with radioprotective agents. Previous studies showed that increased binding of Miso occurs to both the small molecular weight species found in the acid-soluble fractions and to macromolecules such as DNA which are associated with the acid-precipitable fraction (*10*). The ratio of bound products between the acid-soluble and -precipitable fractions is dependent upon cell line and handling procedures, but the binding kinetics is similar for both fractions (*10, 17*). In this study, only the binding to the macromolecular fraction was considered to avoid possible problems in interpretation arising from an increased concentration of small molecular weight thiol species to which [^{3}H]Miso is capable of binding, although this would not be a problem for non-thiol containing compounds such as 5-HT or $DiPGE_2$.

Four of seven agents tested (WR-2721, $DiPGE_2$, Cys, 5-HT) produced significant increases in [^{3}H]Miso binding, suggesting that the marrow of animals treated with these drugs would be less oxygenated at times associated with peak radioprotective effects. In support of this hypothesis is evidence that various physiological and chemical properties of these drugs are such that they may contribute to the production of relative marrow hypoxia. For example, the largest uptake of [^{3}H]Miso occurred in bone marrow cells from animals receiving $DiPGE_2$. This concentration of $DiPGE_2$ produces a 16% increase in hematocrit (6) and a 30% reduction in breathing rate (*18*) 15 min after administration. A dose-dependent reduction in peripheral blood flow with blood pooling in the spleen also has been noted for WR-2721 (*4*). Similarly, the hypotensive and vasoactive effects of 5-HT (*15*) and Cys (*19*) have been described. Changes in blood flow distribution and respiration rate might reasonably be expected to have indirect effects on the oxygen supply of the marrow. In addition, a chemical reduction in the amount of oxygen available to the marrow may directly contribute to hypoxia. WR-1065, the dephosphorylated product of WR-2721, consumes oxygen in an *in vitro* system (*20*). Our preliminary results measuring the oxygen consumption of marrow cells treated *in vivo* with WR-2721 suggest that increased oxygen consumption also occurs in the host animal. Other thiol containing compounds such as Cys have been shown to undergo autooxygenation *in vitro* (*21*); however, their ability to produce the same effects *in vivo* have yet to be evaluated. These physiological/chemical drug effects coupled with the known dependence of Miso binding on oxygen concentration are consistent with the hypothesis that the observed increase in [^{3}H]-Miso binding was a consequence of a shift of marrow oxygen tension to lower values. A counterargument to this proposal is the possibility that these drugs affect the *in vivo* reduction of Miso which is independent of any changes in marrow pO_2. However, this latter possibility is unlikely because (1) the addition of exogeneous thiols has been shown to decrease, not increase, the binding of misonidazole to cellular macromolecules (*7*), and (2) even if these drugs were to increase the metabolism of Miso (through the stimulation of nitroreductase enzymes, for example), the resultant reactive species would be oxidized back to the parent compound under conditions of normal marrow pO_2.

In the case of WR-2721, the increase in marrow binding was found to be dose dependent, with only the optimally protective dose (400 mg/kg) producing significantly increased binding. However, other studies have demonstrated that smaller doses of WR-2721 (75–300 mg/kg) afford some marrow protection (*22*). This suggests

that several mechanisms contribute to the radioprotective effects of WR-2721, and that at low drug doses, chemical rather than physiological mechanisms predominate. Similarly, the failure of AET or SOD to alter [^{3}H]Miso binding suggests that any physiological changes produced by these drugs were insufficient to render the marrow relatively hypoxic and that chemical and/or alternative physiological changes must be postulated to account for their radioprotective properties. In the case of LPS, less [^{3}H]Miso binding was observed in drug-treated animals than in controls. The reason for this has yet to be determined. However, the possibility that LPS treatment altered the pharmacokinetics of Miso or resulted in increased oxygen delivery to the marrow should be considered.

Several investigators have drawn attention to the fact that protection with WR-2721 appears to be most effective for cells or tissues that are at intermediate oxygen tensions (*23, 24*). In such cases, it has been postulated that small reductions in oxygen tension are sufficient to render the tissues hypoxic. Previous studies by Meyn and Jenkins (*25*) which measured the induction of DNA strand breaks *in vivo* and *in vitro* have suggested that marrow resides at relatively low oxygen tensions *in vivo*. In such a case, small shifts in the availability of oxygen to critical hematopoietic targets may exert protective effects. Confirmation of the hypothesis that small changes in physiological oxygen concentrations produce radiobiological hypoxia awaits techniques for accurately measuring the *in vivo* pO_2 of cell populations.

ACKNOWLEDGMENTS

Supported by awards from the National Cancer Institute of Canada, the Alberta Cancer Board, and the Armed Forces Radiobiology Research Institute, Defense Nuclear Agency, work unit 00152. The views presented in this paper are those of the authors. No endorsement by the Defense Nuclear Agency has been given or should be inferred. The authors thank Drs. J. D. Chapman, A. J. Franko, and J. A. Raleigh for helpful discussions.

RECEIVED: October 11, 1988; ACCEPTED: February 6, 1989

REFERENCES

1. J. M. YUHAS, J. M. SPELLMAN and F. CULO, The role of WR-2721 in radiotherapy and/or chemotherapy. *Cancer Clin. Trials* **3**, 211–216 (1980).
2. K. D. HELD, G. D. BREN, and D. C. MELDER, Interactions of radioprotectors and oxygen in cultured mammalian cells. *Radiat. Res.* **108**, 296–306 (1986).
3. V. DISTEFANO, D. E. LEARY, and K. D. LITTLE, The pharmacological effects of some cogeners of 2-amino-ethylisothiuronium bromide (AET). *J. Pharmacol. Exp. Ther.* **126**, 304–311 (1959).
4. J. H. YUHAS, J. O. PROCTOR, and L. H. SMITH, Some pharmacologic effects of WR-2721: Their role in toxicity and radioprotection. *Radiat. Res.* **54**, 223–233 (1973).
5. W. R. HANSON, Radiation protection of murine intestine by WR-2721, 16,16-dimethyl prostaglandin E_2, and the combination of both agents. *Radiat. Res.* **111**, 361–373 (1987).
6. T. L. WALDEN, JR., M. PATCHEN, and S. L. SNYDER, 16,16-Dimethyl prostaglandin E_2 increases survival in mice following irradiation. *Radiat. Res.* **109**, 440–448 (1987).
7. J. D. CHAPMAN, K. BAER, and J. LEE, Characteristics of the metabolism-induced binding of misonidazole to hypoxic mammalian cells. *Cancer Res.* **43**, 1523–1528 (1983).
8. A. J. FRANKO, C. J. KOCH, B. M. GARRECHT, J. SHARPLIN, and D. HUGHES, Oxygen dependence of binding of misonidazole to rodent and human tumors in vitro. *Cancer Res.* **47**, 5367–5376 (1987).
9. J. L. BORN and B. R. SMITH, The synthesis of tritium-labelled misonidazole. *J. Labelled Compds. Radiopharm.* **20**, 429–432 (1983).

10. C. J. KOCH, C. C. STOBBE, and K. A. BAER, Metabolism induced binding of ^{14}C-misonidazole to hypoxic cells: Kinetic dependence on oxygen concentration and misonidazole concentration. *Int. J. Radiat. Oncol. Biol. Phys.* **10,** 1327–1331 (1984).

11. A. PETKAU, Radiation protection by superoxide dismutase. *Photochem. Photobiol.* **28,** 765–774 (1978).

12. B. L. SZTANYIK and V. VARTERESZ, Radioprotective effect of a mixture of AET and 5-methyoxytryptamine in X-irradiated mice. In *Radiation Protection and Sensitization* (H. L. Moroson and M. Quintilani, Eds.), pp. 363–367. Taylor & Francis, London, 1970.

13. J. R. MAISIN, G. MATTELIN, and M. LAMBIET-COLLIER, Reduction of short- and long-term radiation effects by mixtures of chemical protectors. In *Radiation Protection and Sensitization* (H. L. Moroson and M. Quintilani, Eds.), pp. 355–361. Taylor & Francis, London, 1970.

14. E. J. AINSWORTH and R. M. LARSEN, Colon-forming units and survival of irradiated mice treated with AET or endotoxin. *Radiat. Res.* **40,** 149–176 (1969).

15. C. VAN DER MEER and D. W. VAN BEKKUM, A study on the mechanism of radiation protection by 5-hydroxytryptamine and tryptamine. *Int. J. Radiat. Biol.* **4,** 105–110 (1961).

16. J. DENEKAMP, A. ROJAS, and F. A. STEWART, Is radiation protection by WR-2721 restricted to normal tissues? In *Radioprotectors and Anticarcinogens* (O. F. Nygaard and M. G. Simic, Eds.), pp. 665–679. Academic Press, New York, 1983.

17. G. G. MILLER, J. NGAN-LEE, and J. D. CHAPMAN, Intracellular localization of radioactively labelled misonidazole in EMT-6 tumor cells in vitro. *Int. J. Radiat. Oncol. Biol. Phys.* **8,** 741–744, (1982).

18. T. L. WALDEN, JR., and M. J. ALLALUNIS-TURNER, Radioprotection by 16,16-dimethyl prostaglandin E_2: Is hypoxia a contributing factor? *Proc. Am. Assoc. Cancer Res.* **29,** 515 (1988). [Abstract]

19. J. MISUSTOVA, B. HOSEK, and J. KAUTSKA, Characterization of the protective effect of radioprotective substances by means of long-term changes in oxygen consumption. *Strahlentherapie* **156,** 790–794 (1980).

20. J. W. PURDIE, E. R. INHABEN, H. SCHNEIDER, and J. L. LABELLE, Interaction of cultured mammalian cells with WR-2721 and its thiol WR-1065: Implication for mechanisms of radio-protection. *Int. J. Radiat. Biol* **43,** 417–527 (1983).

21. J. E. BIAGLOW, R. W. ISSELS, L. E. GERWECK, M. E. VARNES, B. JACOBSON, J. B. MITCHELL, and A. RUSSO, Factors influencing the oxidation of cysteamine and other thiols: Implications for hyperthermic sensitization and radiation protection. *Radiat. Res.* **100,** 298–312 (1984).

22. D. E. DAVIDSON, M. M. GRENAN, and T. R. SWEENEY, Biological characteristics of some improved radioprotectors. In *Radiation Sensitizers, Their Use in the Clinical Management of Cancer* (L. W. Brady, Ed.), pp. 309–320. Masson, New York, 1980.

23. J. DENEKAMP, B. D. MITCHELL, A. ROJAS, and F. A. STEWART, Thiol radioprotection in vivo: The critical role of tissue oxygen concentration. *Br. J. Radiol* **54,** 1112–1114 (1981).

24. R. E. DURAND, Radioprotection by WR-2721 in vitro at low oxygen tensions: Implications for its mechanism of action. *Br. J. Cancer* **47,** 387–392 (1983).

25. R. E. MEYN and W. T. JENKINS, Variation in normal and tumor sensitivity mice to ionizing radiation-induced DNA strand breaks in vivo. *Cancer Res.* **43,** 5668–5673 (1983).

Adv. Space Res. Vol. 9, No. 10, pp. (10)177 (10)186, 1989
Printed in Great Britain. All rights reserved

0273-1177/89 $0.00 + .50
Copyright © 1989 COSPAR

ARMED FORCES RADIOBIOLOGY RESEARCH INSTITUTE
SCIENTIFIC REPORT
SR89-27

CELL-CYCLE RADIATION RESPONSE: ROLE OF INTRACELLULAR FACTORS

E. Blakely,* P. Chang,* L. Lommel,* K. Bjornstad,* M. Dixon,* C. Tobias,* K. Kumar** and W. F. Blakely**

**Cell and Molecular Biology Division, Lawrence Berkeley Laboratory, Berkeley, CA 94720, U.S.A.*
***Radiation Biochemistry Department, Armed Forces Radiobiology Research Institute, Bethesda, MD 20814-5145, U.S.A.*

ABSTRACT

We have been studying variations of radiosensitivity and endogenous cellular factors during the course of progression through the human and hamster cell cycle. After exposure to low-LET radiations, the most radiosensitive cell stages are mitosis and the G_1/S interface. The increased activity of a specific antioxidant enzyme such as superoxide dismutase in G_1-phase, and the variations of endogenous thiols during cell division are thought to be intracellular factors of importance to the radiation survival response. These factors may contribute to modifying the age-dependent yield of lesions or more likely, to the efficiency of the repair processes. These molecular factors have been implicated in our cellular measurements of the larger values for the radiobiological oxygen effect late in the cycle compared to earlier cell ages. Low-LET radiation also delays progression through S phase which may allow more time for repair and hence contribute to radioresistance in late-S-phase. The cytoplasmic and intranuclear milieu of the cell appears to have less significant effects on lesions produced by high-LET radiation compared to those made by low-LET radiation. High-LET radiation fails to slow progression through S phase, and there is much less repair of lesions evident at all cell ages; however, high-LET particles cause a more profound block in G_2 phase than that observed after low-LET radiation. Hazards posed by the interaction of damage from sequential doses of radiations of different qualities have been evaluated and are shown to lead to a cell-cycle-dependent enhancement of radiobiological effects. A summary comparison of various cell-cycle-dependent endpoints measured with low- or high-LET radiations is given and includes a discussion of the possible additional effects introduced by microgravity.

INTRODUCTION

The quantitative understanding of long-term effects of the components of space radiation on carcinogenesis and nervous system functions depends on the nature of the molecular injury produced by particles of various atomic numbers and energies. Of particular interest is the functional dependence of individual lesions, their repair and misrepair, and the time-dependent interactions that can occur at low dose rates.

Many types of cancer cells have chromosomal defects, frequently including band deletions or reciprocal translocations /1/. Correlations have been made between what are termed "inherited fragile sites" and the chromosomal break points involved in the structural rearrangements associated with some neoplasms /2,3/. It has been suggested that certain genes of differentiated cells require submicroscopic rearrangements for normal functional activity, and these changes could provide a mechanism whereby unique chromosome sites become inherently susceptible to further rearrangements caused by various chemical or physical agents in specific cell types /4/. Thus, both inherited genetic susceptibility as well as normal programmed genetic functions occurring during cell division could contribute to the vulnerability of cellular targets to damage from ionizing radiations.

Of serious concern in the space environment are particle radiations that are capable of causing an assortment of types and degrees of chromosomal damage depending on particle charge and energy, and the cellular targets at risk. Lesions produced by particles from protons to uranium can result in minor to severe chromosomal aberrations /5,6/. There is a high probability that, especially where low doses are concerned, the chances are increased for cellular survival, and therefore there is a greater likelihood for expression of transformation events.

Specific intracellular factors, including for example antioxidant enzymes like superoxide dismutase (SOD) and catalase (CAT), are known to inhibit carcinogenic transformation by X-rays and certain chemotherapeutic drugs like bleomycin, and are also known to reduce the promotional action of 12-O-tetradecanoylphorbol 13-acetate (TPA) in vitro /7/. This suggests that oncogenic action can be mediated in part by free radicals and that antioxidants can inhibit oncogenesis and late events in the progression of cell transformation associated with promotion. Additional evidence indicating these factors may contribute to variations

in cell competence to transformation is that the cell content of SOD and CAT is reported to vary from one cell type to another /8/.

We have been studying human and other mammalian cells in culture that are synchronized with respect to their stage in the cell cycle. Our goal is to investigate when cells are most sensitive to modifications that can influence radiation survival and can also ultimately lead to mutation or transformation. We have used split-dose techniques to elucidate the significance of the cell cycle to the enhancement of particle effects. In order to understand the mechanisms underlying these effects we have begun characterizing intracellular factors that are thought to play a role in detoxifying radical-induced damage. We report here a study demonstrating cell-stage dependent enhancement of the lethal effects of split-doses of charged particle beams of low- and high-linear energy transfer (LET). We include cell age-dependent measurements of SOD enzyme activity and a speculative discussion of the relevance of this antioxidant and other intracellular factors to the ultimate effects of ionizing radiations.

METHODOLOGY

Human T-1 cell fibroblasts cultured in vitro were used in these experiments. The cell line was originally established by Van Der Veen et al. /9/ and was kindly provided to us by G.W. Barendsen of the TNO Radiobiology Laboratories, Rijswijk, The Netherlands. The cells were maintained in minimum essential medium (MEM) with Earle's salts supplemented with 12.8% fetal bovine serum and were grown at 37°C in a humidified atmosphere of 5% CO_2 and 95% air. The concentration of glutamine (0.25 g/liter) was doubled for experimental cultures which were not replenished with fresh media during incubation to measure survival. Routine screening for mycoplasma has indicated that the cultures are free of contamination.

Experiments were completed with exponentially growing cell populations, as well as those synchronized by mitotic selection. The techniques used to obtain large numbers of highly synchronized cells in various phases of the cell division cycle have been described in detail elsewhere /10/. The cell cycle time is approximately 20 hrs. In each experiment the quality of the synchrony was evaluated by cell volume distributions, and cell progression was monitored by autoradiographic analysis of cells pulse-labeled for 20 mins with [^{3}H]dThd at various times after mitotic selection. Representative autoradiography data from a typical experiment are given in Figure 1. Cell populations at two ages post-mitotic-selection were irradiated for survival studies: mid G_1-phase (3 hours) and late-S phase (14 hours).

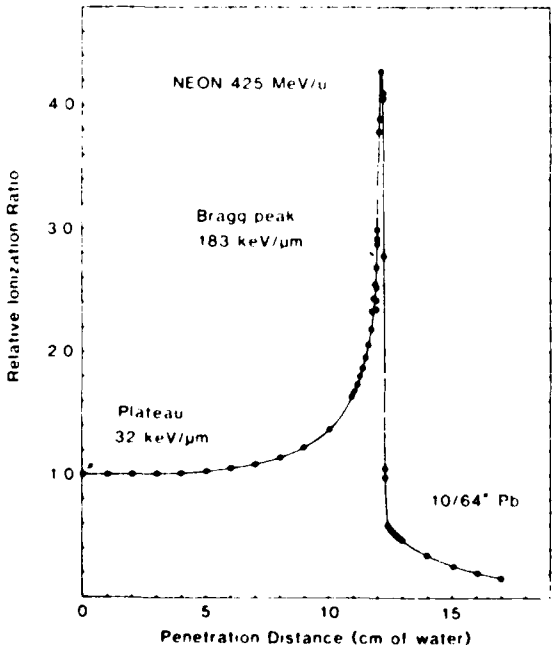

Fig. 1. Representative autoradiography data from unirradiated human T 1 cell populations pulse-labeled for 20 minutes with tritiated thymidine at various times after synchronization. Data are from one of the experiments reported here, and the ages and incorporation levels of the synchronized populations studied are indicated.

The level of activity of the antioxidant enzyme superoxide dismutase (SOD) was measured in unirradiated populations of synchronized cells. Mitotically-selected cells were plated into 75 cm² tissue culture flasks and were either processed immediately or were allowed to progress at 37°C to appropriate ages throughout the cell cycle. SOD activity levels are therefore reported for populations synchronized at three cell ages post mitotic selection: M phase (0 hours), G_1 phase (4 hours) or mid S phase (12 hours). At the appropriate time the attached cells were trypsinized and washed twice in a phosphate buffered saline (PBS) solution containing EDTA but free of calcium and magnesium. Aliquots were counted with a Coulter Counter to determine the cell concentration. The remaining cells were transferred to 1.5 ml plastic vials and rapidly frozen to -50°C. Cell protein was extracted by the addition of digitonin (2.5 mg/ml) immediately after a rapid thawing of each sample. Aliquots of the supernatants of the digitonin-treated samples were used for protein and enzyme assays.

Total superoxide dismutase (SOD) activity, including Cu/Zn SOD and Mn SOD, was determined according to the method of McCord and Fridovich /11/. Total cellular protein was determined by the Coomassie brilliant blue dye binding method /12/ using standard protein reagents from BioRad. The mean of the ratio of enzyme activity (U/mg total protein) and protein concentration (mg/10^6

cells) from three separate measurements of both enzyme activity and protein concentration are reported in each of two experiments. The standard error of this ratio reflects the variance associated with both enzyme activity and protein concentration (mg/10^6) measurements as described by Cleland /13/.

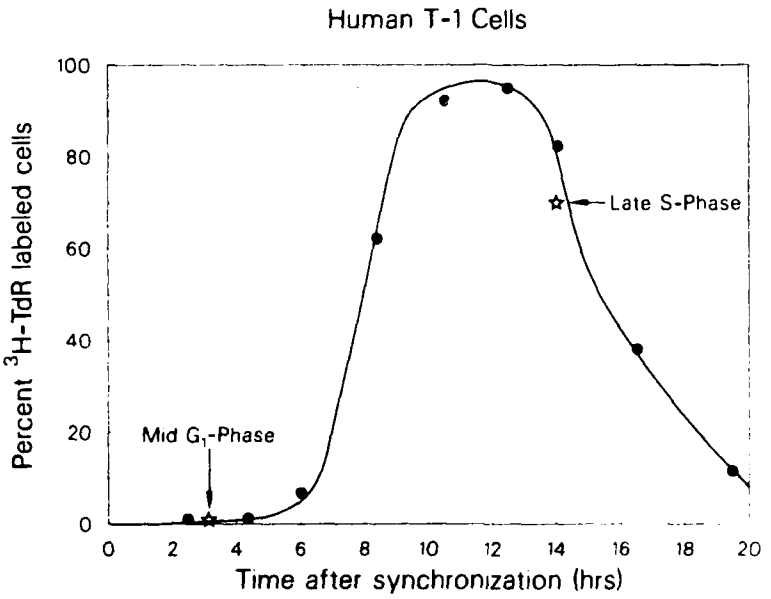

Fig. 2. Bragg ionization curve of Neon 425 MeV/u ion beam. Cellular monolayers were placed at the depths indicated in the entrance plateau and in the Bragg peak

For radiation exposures, cells were distributed into tissue culture flasks and allowed to attach as a monolayer. The cells were irradiated through the wall of the flask. Heavy-ion exposures were made at the Bevalac facility. Parallel-plate ionization chambers were used for dose measurements. Dose calibrations were made with ionization chambers. Neon ion beams of 425 MeV/u initial energy were used for these experiments. A typical Bragg ionization curve is given in Figure 2. Exposures were made in the plateau (dose-average LET = 32 keV/μm) and in the Bragg peak (dose-average LET = 183 keV/μm) of the beam. The physical properties of the particle beams including the calculated LET distributions of the primary particles and the fragments have been described elsewhere /14,15/. In the case of experiments with synchronized cells, at the appropriate culture age, flasks were removed from the 37°C incubator, were cooled down to 4°C to prevent the cells from further progression, and were transported to the Bevalac facility for irradiation. Unirradiated control cultures were handled in a similar fashion. In some experiments the cells received split doses of the plateau ions (low LET), or split doses of the Bragg peak ions (high LET), or split doses of high-LET followed by low-LET radiations. Split-repair-times varied from one hour to 24 hours. Control samples were unirradiated, or received only the first dose fraction, or received both dose fractions in an immediate sequence.

When irradiations were completed, the samples were returned to 37°C and assayed for colony-forming ability by standard techniques. Cells were trypsinized, resuspended, counted, plated into MEM, and incubated at 37°C in a 95% air and 5% CO_2 incubator for 10 to 12 days. Colony-forming ability was scored by staining and fixing the cultures with 1% methylene blue in 30% ethyl alcohol. Clones containing at least 50 cells were scored as survivors. Colony counts on four or more 25-cm² tissue culture flasks were averaged for each data point. Eight or more flasks were used for control and high dose samples. Survival curves were obtained from computer-fits of the data to the linear quadratic model of cell inactivation using programs developed by N.W. Albright /16/.

RESULTS

Split-Dose Effects of Low- or High-LET Particles on Survival

Dose-response curves for exponentially growing human T-1 cell populations irradiated with single- or split-doses of either plateau or Bragg peak ions from a neon beam with an initial energy of 425 MeV/u are presented in Figure 3. The fractionation interval was 24 hours. The data indicate that there is split-dose recovery of the damage from the low LET particles, but no recovery is observed after irradiation with ions of the Bragg peak. The kinetics of split-dose recovery were studied at shorter time intervals. Figure 4 is a compilation of data from two replicate experiments to investigate split-dose effects of 425 MeV/u neon plateau or Bragg peak ions where the time between the two doses was one to twenty-four hours. The data show dose-dependent recovery in the plateau, but no recovery in the Bragg peak.

The split-dose effects of low- and high-LET neon beams on synchronized cell populations are presented in Figure 5. Populations of cells in mid G_1 phase or late S phase at the time of the first dose were studied. In agreement with the asynchronous experiments, the data show split-dose recovery of damage from plateau ions and a lack of recovery from Bragg peak ions.

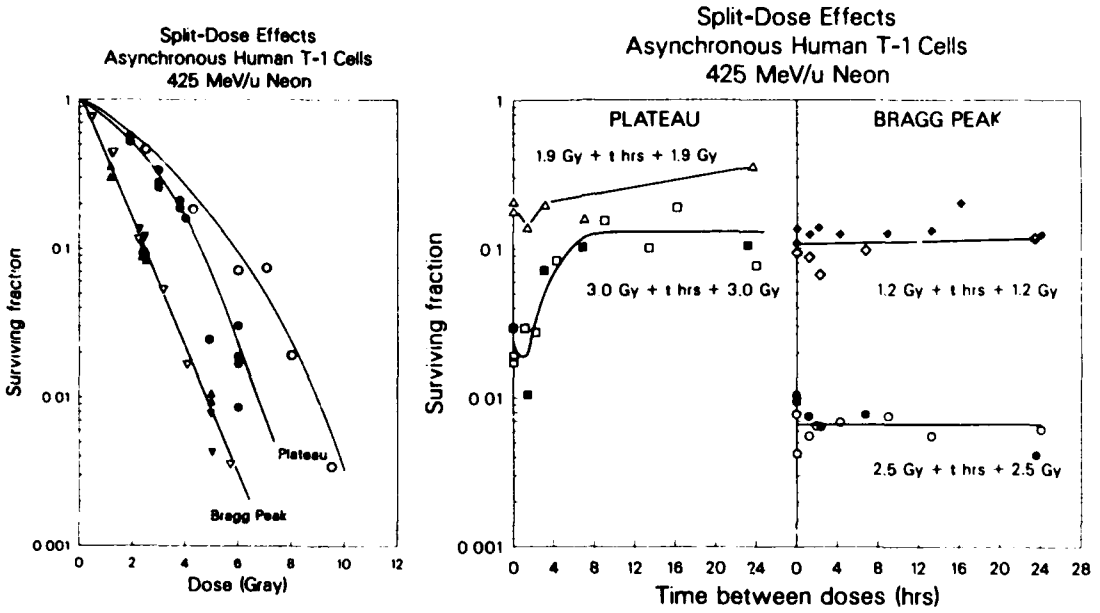

Fig. 3. Dose-response curves for asynchronous cell populations irradiated with single doses (solid symbols) or split doses (open symbols) or either plateau (circles) or Bragg peak (triangles) ions. Different symbols represent different experiments. The fractionation interval was 24 hrs.

Fig. 4. Kinetics of split-dose recovery of asynchronous human T1 cells irradiated with 425 MeV/u plateau or Bragg peak ions. Experiments were repeated twice. The data show dose-dependent recovery in the plateau, but no recovery in the Bragg peak.

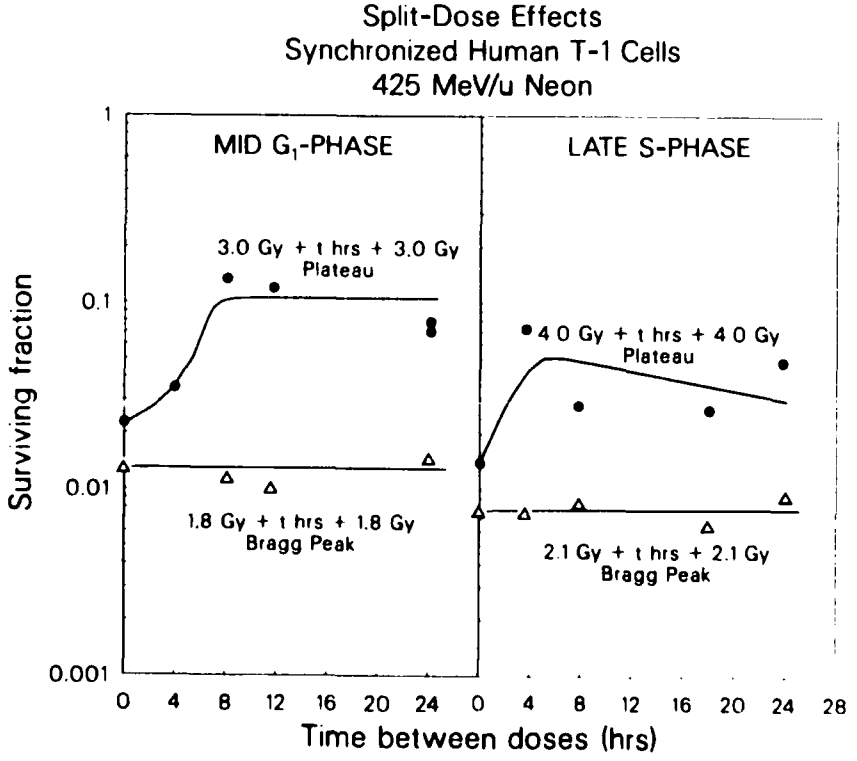

Fig. 5. Effects of 425 MeV/u Neon plateau (●) or Bragg peak (Δ) ions on synchronized cell populations in mid G_1-phase or late-S-phase at the time of the first dose.

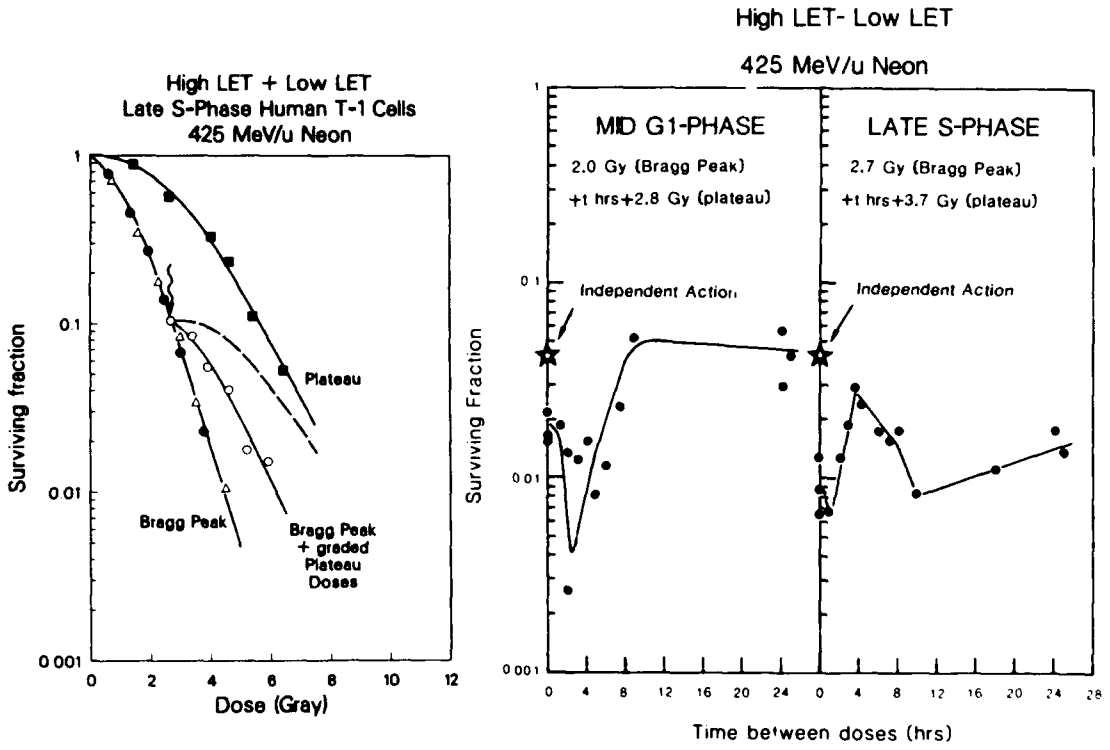

Fig. 6. Dose-response curves for late-S-phase cells cooled to ice temperatures and irradiated with single doses of plateau ions alone (■), or single doses of Bragg peak ions alone (●). Some cells were also irradiated with Bragg peak ions at room temperature (Δ). Also shown are the survival data for cooled cells irradiated sequentially with 2.7 Gy Bragg peak ions followed within 2 minutes by graded doses of plateau ions (o). Survival expected from the independent action of the two radiations (---).

Fig. 7. Survival data measured with populations of cells synchronized either in mid G_1-phase or late S-phase at the time of a first dose of Bragg peak ions followed at various times by a dose of plateau ions. The stars represent the survival level expected from the independent action of each radiation.

Enhancement of Cell Killing from Sequential Doses of High- and Low-LET Radiation

Dose-response curves for late-S phase cells irradiated with plateau neon ions alone, or with Bragg peak ions alone are shown in Figure 6. The cells were cooled to ice temperature just before irradiation to inhibit cell progression. Repair processes may have also been inhibited. The survival data from cultures irradiated in the Bragg peak at room temperature also are shown however and are not different from identical cultures irradiated at the reduced temperature. The survival curves show clearly that the late-S-phase cells are resistant to radiation damage from low LET neon ion beams in the plateau of the Bragg curve, and more sensitive to doses in the Bragg peak. Included in this study are survival data for cells precooled on ice and irradiated sequentially with 2.7 Gy Bragg peak ions followed within two minutes by graded doses of plateau ions. The survival of this cell population was much less than that expected from the independent action of the two radiations (shown as a dashed line on Figure 6).

To explore further the age-dependence of the enhanced lethal effects from sequential doses of high-LET and low-LET ion beams, survival data were obtained from populations of cells synchronized either in mid G_1-phase or late-S-phase at the time of a first dose of Bragg peak ions, followed at various times by a dose of plateau ions (Figure 7). Comparisons of the measured survival with the survival expected from the independent action of each radiation were made. The data show that G_1-phase cells are more sensitive than expected and become even more radiosensitive with a 2-hr interval between the two doses as the cells move to the G_1/S border. The cells then show increasing radioresistance that levels off with an 8-hr fractionation interval at a survival fraction that is equivalent to what would be expected initially from the independent action of the two radiations. The late-S-phase cells are also much more sensitive than expected with the combined radiation treatment, but become more resistant with split-times up to 4 hrs and then more radiosensitive when the cells divide and enter G_1-phase. The cell progression was confirmed with results obtained using flow cytometry methodology (data not shown).

Cell-Age-Dependent SOD Activity

In three replicate experiments, exponentially growing human T-1 cells were found to have a total (Cu-Zn- and Mn-containing) SOD enzyme activity level of 21.3 + 1.9 U/mg total protein (mean ± std. error). Biochemical results from experiments with synchronized cell populations show a high quality of synchrony with a 50% reduction in cellular protein from 0.24 mg/10^6 in M-phase to 0.12 mg/10^6 in G_1-phase (mean of two experiments - see Figure 8, left panel). The specific activity of SOD however exhibited an opposite trend from the protein content data with a significant peak of 30 U/mg total protein in G_1 phase compared to 17 U/mg total protein in mitosis. Intermediate levels of protein content and SOD activity were measured for S-phase cells. The observation of a peak of SOD activity in G_1-phase has also been found in synchronized Chinese hamster cells /17/.

DISCUSSION

Particle Split-Dose Effects

The synergistic effects of low- and high-LET radiations have been reported in sequential /18-24/, as well as simultaneous /25,26/ exposures of exponentially growing asynchronous mammalian cells to radiations of different qualities (e.g., low- and high-LET). The cell killing effects due to damage interaction after sequential irradiations with a high-LET particle beam and X-rays have also recently been reported to vary throughout the Chinese hamster cell cycle /27/. The greatest effect was observed in late-S-phase which was most resistant to either of the radiations. In this paper we report that human T-1 cells show a dose-dependent recovery from split doses of plateau 425 MeV/u neon ions (32 keV/μm). Most of the recovery is completed within 6-8 hours. In contrast, no recovery is measured in split-dose experiments with Bragg peak neon ions (183 keV/μm) even after a 24 hr fractionation time. Secondly, split-dose experiments with synchronized cell populations indicate cell-cycle dependent differences in recovery kinetics from plateau neon-ion damage, while both mid G_1- and late S-phase cells show no recovery from Bragg peak damage. Finally, we show that sequential doses of Bragg peak ions followed immediately by doses of plateau neon ions are more effective than expected from the independent action of the two radiations. This effect is dependent on the age of the cell at the time of the high-LET radiation exposure, and also on the fractionation interval before the exposure to the low-LET radiation.

Our data clearly show that there are differences in the effects of split-doses of low- and high-LET radiations and, also, that split-dose effects are processed differently by cells in G_1- and in S-phase. Under certain conditions enhancing effects occur between low- and high-LET radiation dose components. The simplest explanation for the data in Figures 4 and 5 is that single high-LET particle tracks produced by ions in the Bragg peak are by themselves sufficient to kill cells. This may be because each of these tracks is capable of producing several DNA lesions in close proximity along the track, which then may interact resulting in enhanced misrepair /28/. The lethal effects of high-LET radiation, hence, become somewhat independent of the temporal sequence of its administration. Low-LET neon ions produce more diffuse lesions. Lesions produced by the first dose are more likely to be repaired, or otherwise modified, before more lesions are produced by the second dose.

Data such as are shown in Figures 6 and 7, indicate that high-LET tracks made by particles in the neon Bragg peak produce sublethal lesions in cell nuclei. These lesions can then interact with a subsequent low-LET dose. Why there is a time-dependent structure of the effects shown in Figure 7, and why these effects are different in G_1- and in S-phase is not completely understood at present. One possibility is that the high concentration of cellular factors including SOD activity in G_1-phase reduces, via a decrease in oxygen radicals, the concentration of DNA lesions produced by low-LET radiations. In contrast, as shown in Figure 8, the activity of SOD is reduced in late-S-phase, and therefore, the enhancing effects of low- and high-LET radiations can be greater. Another possibility is that the first high-LET dose may perturb the cellular radioprotective factors in the period following the exposure to the neon peak. Further work is needed to explain the molecular mechanisms underlying these effects and to investigate additional cell-cycle dependent modifications of these effects with time between the two radiation doses.

Radiation Age Response: Intracellular Factors

It has been known since the early 1960s that there are variations in the radiosensitivity of cultured mammalian cells at different phases of the division cycle /29-32/. In the late 1960s and early 1970s high-LET radiations, including fast neutrons, alpha particles, pions and heavy-ion particle beams, were found to diminish the amplitude of the variation between the most sensitive and the most resistant phases (see /33/ for review). Rodent cell lines with a short G_1 phase (about 2 h) were primarily used in these studies which indicated that the reduced age response was still qualitatively similar to that of low-LET radiations in that cells at (or near) mitosis and at the G_1-S phase interface are more radiosensitive than late-S phase cells.

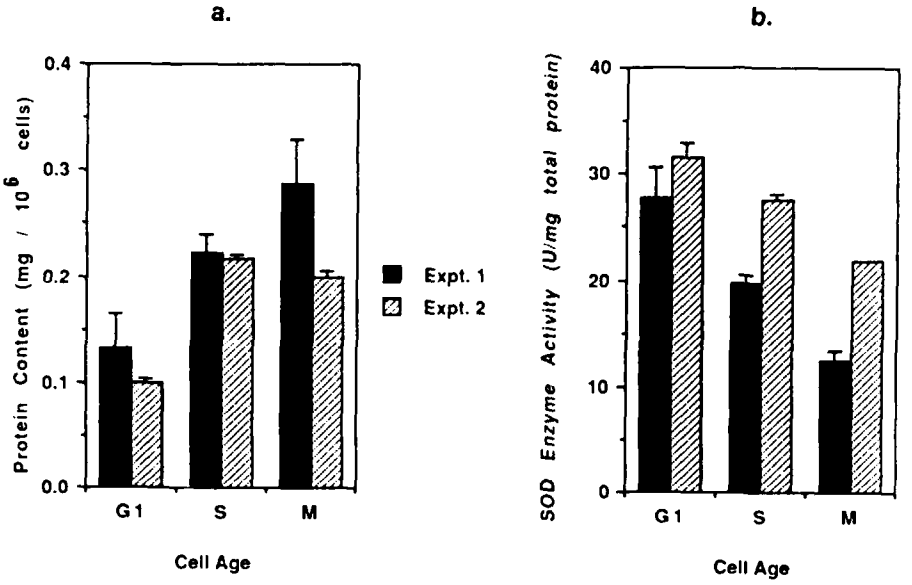

Fig. 8. Human T-1 cell-cycle stage dependence of total cell protein content in mg per 10^6 cells (left panel) and total SOD enzyme activity per mg of total protein (right panel). The data are from two separate experiments. Error estimates represent in each case the standard error of the mean of three replicate samples.

In human cells which have generally a much longer G_1-phase, two peaks of radioresistance to low LET radiation are usually seen, one in G_1- and one in S-phase /34/. Recent work has indicated that high-LET radiations eliminate the X-ray-resistant peak of survival at early G_1-phase in synchronized human cells, but not the resistant peak at late-S-phase, thus suggesting a differential age dependence of *radiolesions and/or* repair effects depending on radiation quality /35-37/.

Early attempts to correlate a single molecular factor or activity like DNA synthesis as an explanation for the age dependence of radiosensitivity through the cell cycle proved to be inadequate since it failed to explain radioresistance in G_1-phase. Based on measurements of sulfhydryl variation that indicate non protein sulfhydryls are greatest in G_1-phase, whereas glutathione levels are greatest in S-phase /38,39/, Sinclair proposed a factor "Q" that may be some small fraction of the intracellular pool which varied as a function of cell cycle position to control cell survival /40/. We have recently demonstrated that cell age-dependent fluctuations in glutathione (GSH) and glutathione disulfide in human T-1 cells are correlated with changes in X-ray oxygen enhancement ratio (OER) for cell survival /41/, however, this effect may be a consequence of fluctuations in GSH and/or other cellular factors resulting in differences in the initial damage and/or the cells' ability to repair these lesions.

DNA damage, measured as DNA strand breaks, has been shown to be readily modified by GSH concentrations at oxygen levels typically found in tissues /42/. The types and yield of radiation-induced base damage are clearly dependent on the oxygen concentration as demonstrated from model system studies using nucleic acids /43/. DNA conformation also can influence the yield and type of base lesions formed from OH radical attack on DNA /44/. In cellular studies, Dewey et al. /45/ examined changes in radiosensitivity and dispersion of chromatin during the cell cycle of synchronous Chinese hamster cells. They found that the decrease in X-ray radiosensitivity as cells moved from mitosis to S-phase correlates well with the dispersion of chromatin that occurs during these parts of the cell cycle. They hypothesized that based on DNA fiber dimensions and how tightly they are packed, the probability for lesion interactions between lesions could explain the similarity of sublethal and potentially lethal lesion repair kinetics. They could not account for the increase in radiosensitivity at the G_1/S interface. With regard to high LET lesions it is likely that the increasing dispersion of chromatin /45,46/ and/or its association with membranes /47/ through the G_1-phase nucleus as the cell ages could result in changes in the volume or distribution of critical targets irradiated with particle beams compared to X-rays /10/ and thereby explain LET-differences in relative radiosensitivity

If we return to the concept of the age dependency of the cell's ability to repair lesions, the cellular levels of GSH may contribute to the maintenance of the cellular redox capacity, a prerequisite for normal metabolism to occur. Further studies on the importance of redox state in radiosensitization, however, are needed. The isolation of radiation repair deficient mammalian mutant cell lines, notably a Chinese hamster cell line that is extremely sensitive to killing by gamma-irradiation in the G_1 and early S phases of the cell cycle, but which has normal resistance in late S phase /48/, has significantly enhanced our under

standing. The mutant is able to repair single-strand DNA breaks (ssb), but is deficient in the repair of double-strand DNA breaks (dsb) produced by γ-irradiation during the sensitive G_1- and early S-phase. In the resistant late-S period, repair is nearly the same for both the mutant and parent cell types. This correlation between γ-ray sensitivity and repair, strongly suggested that an inability to repair double-strand DNA breaks in G_1-phase is the basis for the hypersensitivity of the mutant to the lethal effects of γ-rays during this phase of the cell cycle. These researchers have stated that their work also implies that in normal cells there are at least two pathways for the repair of double-strand breaks, one of which functions primarily in late-S phase, and the other, either throughout the cell cycle or only in the G_1- and early-S phases. Radiosensitive mutant Chinese hamster ovary cell lines isolated by Jeggo and Kemp /49/ have also recently been shown to have a defect in double strand-break rejoining /50/. Additional work involving genomic DNA transfection experiments have shown that after gene uptake, revertant cells are able to survive γ-irradiation as well as the wild type CHO line, and in one of the cells studied, normal dsb repair and the normal reversible nature of the G_2-block in division was restored /51/.

Delays in cell division from exposure to low-LET ionizing radiations are known to prolong the duration of S phase and cause a G_2-phase delay. A pronounced increase in the effectiveness of high-LET radiations in delaying cells in G_2-phase has been reported /52/. In space under the combined stresses of exposure to transit vibration and acceleration and radiations of different LET, alterations in cell progression could be further altered by microgravity. It has been reported that at high g, cells divide faster at the expense of reduced motility, since energy consumption remains the same, while in microgravity, lymphocytes show a dramatic reduction in proliferation rate, reduced glucose consumption, but a strong increase of interferon secretion /53/. WI-38 embryonic lung cells which do not undergo differentiation steps grow and move normally at zero gravity, but they also consume less glucose /54/. This has led to the conclusion that cells are sensitive to gravity, especially those which are differentiating.

Alterations caused by weightlessness on the effect of radiation have for the most part been in the form of an enhancement of the radiation effect /55/. This is especially noted in the direct genetic studies in which there is enhancement in a large number of cases involving chromosome breakage and rejoining /56-58/. Developmental anomalies are also enhanced by weightlessness, related very likely to genetic alterations /59-61/, as perhaps is also the significant loss of xanthine dehydrogenase activity in Drosophila larvae /62/.

New satellite bioexperiments to be discussed at this meeting will likely contribute to our basic understanding of the molecular mechanisms operating under weightless conditions that are responsible for altering chromosome damage from radiation. Further experimentation is needed to systematically evaluate the consequences of the combined stresses of weightlessness and the damage interaction of radiations of different quality on various phases of the cell division cycle. We have reported preliminary measurements of cell age-dependent activity of SOD enzyme that indicate a peak level in G_1-phase prior to DNA synthesis. Gamma-radiation induction of SOD enzyme activity has been reported /63,64/ as well as the radioresistance of Drosophila larvae with a highly active SOD allele /65/. It may be important to explore radiation-induced alterations in SOD enzyme activity as a part of the modification of radiation response, especially under the stresses of the space environment.

ACKNOWLEDGEMENTS

We appreciated helpful discussions with Dr. Tracy C.H. Yang during the preparation of this Manuscript. The assistance of Lilian Hawkins and Tennessee Gock in preparing the paper is also gratefully acknowledged. This research was supported by the U.S. National Cancer Institute (CA-15184), the U.S. Department of Energy (DOE-DE AC03-76SF00098) and by the Armed Forces Radiobiology Research Institute, Defense Nuclear Agency, under work unit B5103. Views presented in this paper are those of the authors; no endorsement by the Defense Nuclear Agency has been given or should be inferred.

REFERENCES

1. A.A. Sandberg, Ed., The Chromosomes in Human Cancer and Leukemia, Elsevier/North-Holland, Amsterdam, 1980.

2. J.J. Yunis, C.D. Bloomfield, K. Ensrud, N. Engl. J. Med. 305, 135 (1981).

3. J.J. Yunis, M.M. Oken, M.E. Kaplan, K.M. Ensrud, R.R. Howe, and A. Theologides, N. Engl. J. Med. 307, 1231 (1982).

4. J.J. Yunis, Science 221, 227 (1983).

5. G. Kraft, Nuclear Sci. Appl. 3, 1 (1987).

6. C.R. Geard, Radiat. Res. 104, S-112 (1985).

7. C. Borek and W. Troll, Proc. Natl. Acad. Sci. USA 80, 1304 (1983).

8. C. Borek, R. Miller, C. Pa[illegible] Natl. Acad. Sci. USA 76, 1800 (1979).

9. J. Van der Veen, L. Bots, and A. Mes, Arch Gesamte Virusforsch 8, 230 (1958).

10. E.A. Blakely, P.Y. Chang, and L. Lommel, Radiat. Res. 104, S-145 (1985).

11. J.M. McCord and I. Fridovich, J. Biol. Chem. 244, 6049 (1969).

12. M.M. Bradford, Anal. Biochem. 72, 248 (1976).

13. W.W. Cleland, Adv. Enzymol. 29, 1 (1967).

14. E.A. Blakely, C.A. Tobias, T.C.H. Yang, K.C. Smith, and J.T. Lyman, Radiat. Res. 80, 122 (1979).

15. F.Q.H. Ngo, E.A. Blakely, and C.A. Tobias, Radiat. Res. 87, 59 (1981).

16. N. Albright, Radiat. Res. 112, 331 (1987).

17. W.F. Blakely, private communication (1988).

18. K. Masuda, J. Radiat. Res. 11, 107 (1970).

19. R. Railton, R.C. Lawson, and D. Porter, Int. J. Radiat. Biol. 27, 75 (1975).

20. F.Q.H. Ngo, A. Han, and M.M. Elkind, Int. J. Radiat. Biol. 32, 507 (1977).

21. S. Hornsey, U. Andreozzi, and P.R. Warren, Br. J. Radiol. 50, 513 (1977).

22. R.P. Bird, M. Zaider, H.H. Rossi, and E.J. Hall, Radiat. Res. 93, 444 (1983).

23. N.J. McNally, J. DeRonde, and M. Hinchliffe, Int. J. Radiat. Biol. 45, 301 (1984).

24. T.C.H. Yang, L. Craise, J. Howard, and C.A. Tobias (1983), Lawrence Berkeley Laboratory Annual Report 1982-83, pg 109, LBL 16840.

25. P.D. Higgins, P.M. DeLuca, Sr., D.W. Pearson, and M.N. Gould, Radiat. Res. 95, 45 (1983).

26. P.D. Higgins, P.M. DeLuca, Sr., and M.N. Gould, Radiat. Res. 99, 591 (1984).

27. F.Q.H. Ngo, E.A. Blakely, C.A. Tobias, P.Y. Chang, and L. Lommel, Radiat. Res. 115, 54 (1988).

28. E.H. Goodwin, E. Blakely, G. Ivery, and C. Tobias, Adv. in Space Res. (In press).

29. T. Terasima and L.J. Tolmach, Nature 190, 1210 (1961).

30. T. Terasima and L.J. Tolmach, Biophys. J. 3, 11 (1963).

31. W.K. Sinclair and R.A. Morton, Nature 199, 1158 (1963).

32. W.K. Sinclair and R.A. Morton, Radiat. Res. 29, 450 (1966).

33. E.A. Blakely, F.Q.H. Ngo, S.B. Curtis, and C.A. Tobias, Adv. Radiat. Biol. 11, 295 (1984).

34. W.K. Sinclair, in Proceedings of the Carmel Conference on Time and Dose Relationships in Radiation Biology as Applied to Radiotherapy, BNL Report 50203 (C-57), 1969, p. 97.

35. E.A. Blakely, P.Y. Chang, L. Lommel, F.Q.H. Ngo, K.C. Smith, M.J. Yezzi, and C.A. Tobias, Radiat. Res. 91, 300 (1982) (Abstract).

36. A.S. Baldichev, O.V. Malinovsky, L.N. Postnikov, and T.A. Sheikima, Radiobiologia 13, 57-62 (1973).

37. K. Sakai, Radiat. Res. 99, 311-323 (1984).

38. H. Ohara and T. Terasima, Exp. Cel Res. 58, 182 (1969).

39. W.K. Sinclair, in Control of Proliferation in Animal Cells, Vol. 1, eds. B. Clarkson and R. Basenga, Cold Spring Harbor Laboratory, 1974, p. 985.

40. W.K. Sinclair, Current Topics Rad. Res. Quart. 7, 264 (1972).

41. E.A. Blakely, R.J. Roots, P.Y. Chang, L. Lommel, L.M. Craise, E.H. Goodwin, E. Yee, D.P. Dodgen, and W.F. Blakely, NCI Monographs 6, 217 (1988).

42. B.P. van der Schans, O. Vos, W.S.D. Roos-Verheij, and P.H.M. Lohman, Int. J. Radiat. Biol. 50, 453-465 (1986).

43. A.F. Fuciarelli, F.Y. Shum, and J.A. Raleigh, Biochem. Biophys. Res. Commun. 134, 883-887 (1986).

44. M.L. Dirksen, W.F. Blakely, E. Holwitt, and M. Dizdaroglu, Int. J. Radiat. Biol. 54, 195 (1988).

45. W.C. Dewey, J.S. Noel, and C.M. Dettor, Radiat. Res. 52, 373 (1972).

46. S.K. Hanks, S.M. Gollin, P.N. Rao, W. Wray, and W.H. Hittelman, Chromosoma (Berl) 88, 333 (1983).

47. M. Yamoda and F. Hanaoka, Nature New Biol. 243, 227 (1973).

48. A. Giaccia, R. Weinstein, J. Hu, and T.D. Stamato, Somatic Cell and Molecular Genetics II, 485 (1985).

49. P.A. Jeggo and L.M. Kemp, Mutation Res. 112, 313 (1983).

50. L.M. Kemp, S.G. Sedgwick, and P.A. Jeggo, Mutation Res. 132, 189 (1984).

51. K.F. Weidezahn, H. Lohrer, and P. Herrlich, Mutation Res. 145, 177 (19[illegible].

52. C. Lücke-Huhle, E.A. Blakely, P.Y. Chang, and C.A. Tobias, Radiat. Res. 79, 97 (1979).

53. A. Cogoli, A. Tschopp, and P. Fuchs-Bislin, Science 225, 228 (1984).

54. A. Cogoli and A. Tschopp, Adv. Biochem. Eng. 22, 1 (1982).

55. B.B. Shank, in Space Radiation Biology and Related Topics (C.A. Tobias and P. Todd, eds.), Academic Press, New York, 1974, pg. 313.

56. I.I. Oster, Bioscience 18, 602 (1968).

57. I.I. Oster, Life Sciences and Space Research VIII, 4 (1970).

58. S.A. Kondo, Jap. J. Genet. 43, 472 (1968).

59. J.V. Slater, B. Buckhold, and C.A. Tobias, Bioscience 18, 595 (1968).

60. J.V. Slater, B. Buckhold, and C.A. Tobias, Radiat. Res. 39, 68 (1969).

61. H. Bücker, G. Horneck, G. Reitz, E.H. Graul, H. Berger, H. Höffken, W. Ruther, W. Heinrich, and R. Beaujeau, Adv. Space Res. 6, 115 (1986).

62. E.C. Keller, Jr., USAF/OSR Progr. Rep. #4, Contract F 44620-67-C-0059 (1968).

63. J.F. Weiss and K.S. Kumar, in Cellular Antioxidant Defense Mechanisms Vol. II, ed. C.K. Chow, CRC Press, Inc., Boca Raton, Florida, 1988.

64. A. Petkau, Br. J. Cancer 55 (Suppl. 8) 87 (1987).

65. T. Xu Peng, A. Moya, and F.J. Ayala, Proc. Natl. Acad. Sci., USA 83, 584 (1986).

ARMED FORCES RADIOBIOLOGY RESEARCH INSTITUTE
SCIENTIFIC REPORT
SR89-28

Pharmacology Biochemistry & Behavior, Vol. 33, pp. 549–554. Pergamon Press plc, 1989. Printed in the U.S.A. 0091-3057/89 $3.00 + .00

Characteristics of Radiation-Induced Performance Changes in Bar-Press Avoidance With and Without a Preshock Warning Cue

WALTER F. BURGHARDT, JR. AND WALTER A. HUNT[1]

Behavioral Sciences Department, Armed Forces Radiobiology Research Institute, Bethesda, MD 20814-5145

Received 15 February 1988

BURGHARDT, W. F., JR. AND W. A. HUNT. *Characteristics of radiation-induced performance changes in bar-press avoidance with and without a preshock warning cue.* PHARMACOL BIOCHEM BEHAV **33**(3) 549–554, 1989.—Rats were trained to perform one of three tasks in which responses on a lever delayed the onset of footshock for 20 sec. One task provided a warning tone beginning 15 sec after the last response on the lever and lasting for 5 sec just prior to the presentation of a shock (fixed-interval signalled avoidance), while a second task provided no external cues (unsignalled avoidance). The third task was similar to the fixed-interval signalled avoidance task, except that the warning tone preceding shock began at varying intervals after the last response on the lever (variable-inteval signalled avoidance). Animals trained on the signalled avoidance paradigms received fewer shocks than those on the unsignalled avoidance paradigm. After 10 krads of gamma radiation, animals performing on either task with cues were less able to avoid shock, although they recovered somewhat over a 90-min period. The animals not provided cues also experienced more shocks during the first 10 min after irradiation but were relatively less affected in performing the task. Response rates on the bar and the patterns of responding on these tasks were not significantly different after irradiation, except that animals responded after the onset of shock more often after irradiation than before. These results suggest that rats will continue to effectively use task related cues after irradiation, but that the relative degree of behavioral decrement may depend on the initial level of performance or possibly the complexity of the task.

Performance Ionizing radiation Avoidance Cues

BEHAVIORAL deficits are commonly observed in laboratory animals after high doses of ionizing radiation and have been found as degraded performance on a number of tasks (6). Behavioral abnormalities have been observed in victims of a number of nuclear accidents, including the one at Chernobyl (4, 7, 8). Although some of these responses could have resulted from generalized trauma, they might reflect an effect of ionizing radiation on behavior. This laboratory has been studying the ability of rats to actively avoid shock and how exposure to ionizing radiation can disrupt this behavior. Initial studies involved using a task in which animals learned to jump up onto a ledge to avoid an electrical foot-shock (5). Auditory cues were provided to alert subjects to an impending shock. The results demonstrated that doses of 2.5 to 20 krads of high-energy electrons or gamma photons degraded the performance on this active avoidance task in a dose-dependent manner. Escape behavior was unaltered. Furthermore, electrons were more effective than photons in disrupting this task.

In an attempt to characterize this effect, additional experiments were undertaken to determine whether the animals were capable of performing the required movements and whether they would ask for and use visual and auditory cues to enhance performance (2). A paradigm was used that involved responses on two levers each with different consequences (1). When one lever was pressed, an electrical shock occurring at 5-sec intervals was postponed for 20 sec. Pressing the other lever activated a visual cue (overhead light) for a 60-sec period, during which an auditory cue (tone) occurred 5 sec before the presentation of each shock. The animals rapidly learned to respond for the tone and to use it to effectively avoid shock.

A 10-krad dose of gamma photons severely disrupted the ability of animals to perform this task (2). Almost immediately after irradiation, the animals received significantly more shocks than controls. However, the animals could readily execute the required movements of pressing a bar. In fact, responding on the lever to avoid shock increased, but mostly just subsequent to the onset of shock. In addition, irradiated subjects did not continue to respond to produce the visual and auditory cues. In other words,

[1]Requests for reprints should be addressed to Walter A. Hunt.

instead of responding for the cues, the animals responded to the shocks. When subjects did use the tones after irradiation, they did so in a way which suggested that they detected the cues and were able to respond to them appropriately. In other experiments, animals were shown to receive increased shocks after doses of radiation as low as 2 krads (unpublished observations).

In the present experiments, we attempted to determine whether the presence of temporal and sensory cues influenced an animal's performance after irradiation. In one experiment, rather than require the animals to specifically respond for preshock warning cues as in the previous study (2), these auditory cues were always available (fixed-interval signalled avoidance). In another experiment, no cues other than temporal ones were available (unsignalled avoidance). A third experiment provided no predictability of the onset of shock based on temporal cues. Instead, the subject received the same average number of preshock warning cues as in the experiments using the fixed-interval signalled avoidance paradigm, except that the time of onset of the warning signal after a response was unpredictable temporally (variable-interval signalled avoidance).

METHOD

Thirty-six male Long Evans (Blue Spruce) rats (300 g) were the experimental subjects. Rats were quarantined on arrival and screened for evidence of disease by serology and histopathology before being released from quarantine. The rats were housed individually in polycarbonate isolator cages (Lab Products, Maywood, NJ) on autoclaved hardwood contact bedding ('Beta Chip' Northeastern Products Corp., Warrensburg, NY) and were provided commerical rodent chow ('Wayne Rodent Blok' Continental Grain Co., Chicago, IL) and acidified water (pH 2.5 using HCl) ad lib. Animal holding rooms were kept at 21 ± 1 C with 50 ± 10% relative humidity on a reversed, 12-hr, light:dark lighting cycle with no twilight.

The apparatus and experimental designs were similar to those previously described (2), except as indicated below. Prior to the first training session, animals were placed in the operant chambers for at least 2 hr to familiarize them with the apparatus. Thereafter, each experimental session lasted 4 hr. The animals then were trained to avoid a 0.5-sec, scrambled, electrical footshock (1.0 mA) by responding on the left lever. Responses on the right lever had no scheduled consequence in this study. A single response postponed the onset of shock by 20 sec. In the absence of responding, shock occurred at 5-sec intervals. Twelve of the rats received a 5-sec warning tone just prior to the scheduled presentation of a shock (fixed-interval signalled avoidance) (9). In this group, the onset of the warning tone always followed the last response on the lever by 15 sec. Another 12 rats received the same preshock warning tones, except that the interval between a response on the lever and the onset of the warning cue before the next scheduled shock varied with equal probability between 0.5 and 120 sec. The mean interval was 15 sec (the same as the interval in the fixed-inteval signalled-avoidance group) making the time of the onset of the warning tone in this group effectively unpredictable (variable-interval signalled avoidance). The last 12 rats were trained similarly, except no warning tones were provided (unsignalled avoidance) (10). Training was complete when the animals could successfully avoid more than 90% of the shocks that could be presented (12 min).

During the warning tone, a response on the lever terminated the warning tone and reset the response to tone interval. Responses made during shock presentation terminated both shock and warning tones and also reset the response to tone interval (response to shock interval in unsignalled avoidance). In the absence of a response in either signalled condition, shock onset followed the onset of the preshock warning tone by 5 sec. If no response was made during the shock, the tone and shock terminated simultaneously 0.5 sec after shock onset.

After training, subjects were habituated to the effects of interrupting the schedule and transporting them for irradiation. After 2 hr of performing the task on which the animals were trained, the session was suspended with the tone and response lever disabled. The animal was placed in a Plexiglas restraining tube, transported to the ^{60}Co facility, and returned without being irradiated. The session then resumed. This procedure was repeated daily until there was less than a 10% difference in the number of shocks received and in the number of responses made during the next hour, compared with those during the hour before removing the animals from the conditioning chambers.

After habituation, each group of animals who learned the fixed-interval signalled avoidance, unsignalled avoidance, or variable-interval signalled avoidance tasks was randomly divided into two subgroups, composed of six animals each. From each group of trained animals, one subgroup was irradiated with a single bilateral dose of 10 krads of gamma radiation from a ^{60}Co source at a rate of 6.6 krads/min. Control subgroups were handled identically, except they were not irradiated. The transport time from the radiation facility to the conditioning chambers was less than 5 min. At the end of the study, all animals were euthanized with a barbiturate overdose (80 mg/kg, IP) within 48 hr after irradiation. All animals were submitted for necropsy and found to be free of concurrent disease.

For radiation dosimetry, paired 50-ml ion chambers were used. Delivered dose was expressed as a ratio of the dose measured in a tissue-equivalent plastic phantom enclosed in a restraining tube to that measured free in air.

For the analysis of data, only the measurements made during the 60 min prior to and the 90 min after irradiation were used, periods when the performance of the animals was most consistent. The data collected were divided into six, 10-min blocks before removal from the apparatus for irradiation, and nine, 10-min blocks postirradiation. For response measures, each postirradiation block was totaled and expressed as the percentage of the mean number of responses for the six, 10-min periods immediately preceding irradiation. Responses from the sham-irradiated animals similarly were recorded. All other measures were presented as totals for each 10-min period. The data were analyzed statistically using multiple factor analyses of variance with repeated measures on one factor (11). Radiation dose (0 or 10 krads) was one factor, and the time after treatment was the repeated factor. The level of significance was 0.05.

RESULTS

Unirradiated animals performed well on both signalled and unsignalled avoidance paradigms. However, performance was better when auditory cues were available. Those animals provided warning tones typically received less than five shocks during a 10-min period (Figs. 1 and 2). However, animals provided no warning tones were less proficient in avoiding shock. They typically received about 8 shocks per 10-min period. $F(3,15) = 4.23$, $p < 0.05$ (Fig. 3).

Irradiated animals experienced an increased number of shocks, although they did not exhibit any gross abnormalities in spontaneous behavior and were able to move about freely. Animals performing either signalled avoidance task received approximately 10 times as many shocks during the first 10 min after irradiation [$F(1,10) = 15.69$, $p < 0.05$, for the fixed-interval signalled avoidance group; $F(1,10) = 8.01$, $p < 0.05$, for the variable-interval

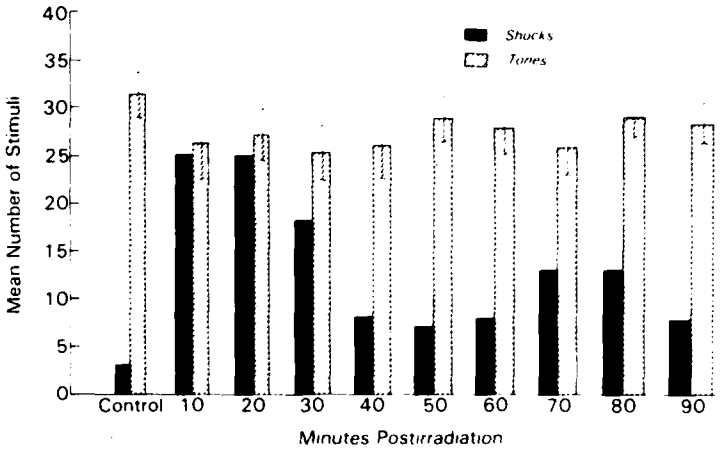

FIG. 1. Mean number of shocks and warning tones, ± SEM, received by animals trained on the fixed-interval signalled avoidance paradigm. Control values are the result of pooling the values for all subjects in the control group for the 90 min after sham irradiation. The data presented were based on observations from 6 animals.

signalled avoidance group], compared to a 2.5-fold increase in shocks received by the animals performing the unsignalled avoidance paradigm. $F(1,10) = 0.025$, $p > 0.05$. During the remaining 80 min of the session, performance improved, but the number of shocks received by animals performing the two signalled avoidance paradigms continued at a significantly higher level relative to controls. The number of warning tones provided to the animals performing on the signalled avoidance paradigms was unchanged after irradiation [$F(1,10) = 2.08$, $p > 0.05$, for the fixed-interval signalled avoidance group; $F(1,10) = 0.755$, $p > 0.05$, for the variable-interval signalled avoidance group] (Figs. 1 and 2).

Although the animal performing on any of the three paradigms experienced more shocks after irradiation, they were still able to respond on the avoidance lever. The response rates varied depending on the paradigm used. With the fixed-interval signalled avoidance paradigm the rate was lowest (63.8 ± 4.7 responses/10-min interval), while that for the unsignalled avoidance paradigm was the highest (103.1 ± 7.2 responses/10-min interval). The response rate for the variable-interval signalled avoidance group was intermediate (99.4 ± 1.4 responses/10-min interval). However, after irradiation, the average number of responses during each 10-min interval was not significantly different from controls (data not shown).

Since the rate of responding remained unchanged but the number of shocks received increased, the pattern of responding may be altered by irradiation. To test this possibility, interresponse time (IRT) histograms were constructed for the fixed-interval signalled and unsignalled avoidance groups in order to determine the distribution of responses during a session. (The data for the variable-interval signalled avoidance group were not suitable for

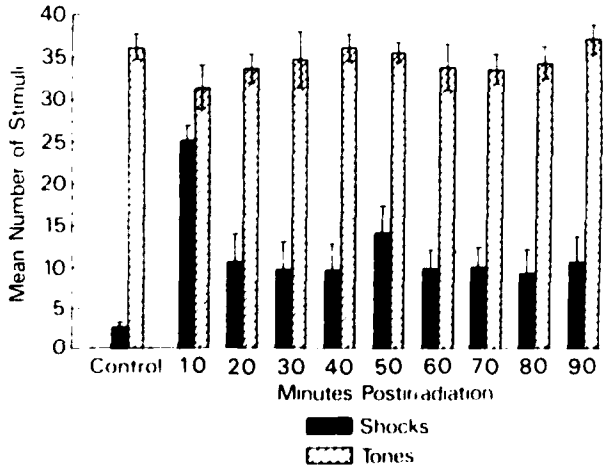

FIG. 2. Mean number of shocks and warning tones, ± SEM, received by animals trained on the variable-interval signalled avoidance paradigm. Control values are the result of pooling the values for all subjects in the control group for the 90 min after sham irradiation. The data presented were based on observations from 6 animals.

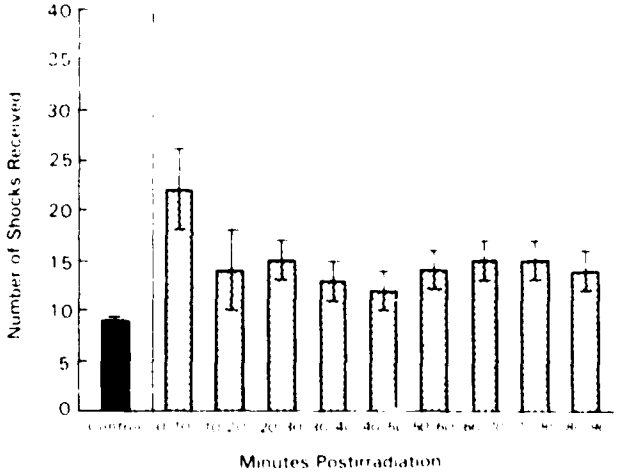

FIG. 3. Mean number of shocks, ± SEM, received by animals trained on the unsignalled avoidance paradigm. Control values are the result of pooling the values of all subjects in the control group for the 90 min after sham irradiation. The data presented were based on observations from 6 animals.

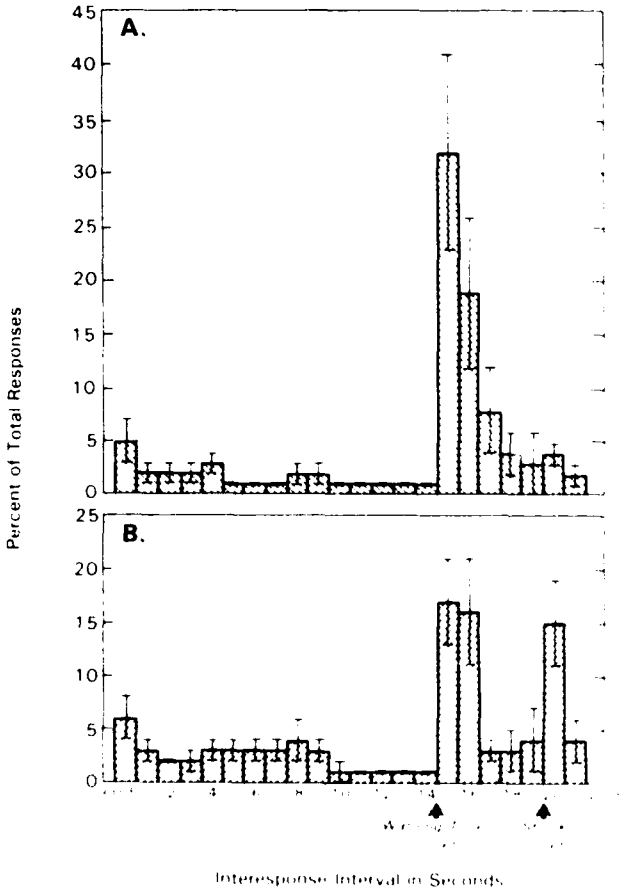

FIG. 4. (A) Interresponse distribution, ± SEM, for the control group trained on the fixed-interval signalled avoidance paradigm after sham irradiation. Arrows indicate the times of onset of warning tones and shocks. (B) Interresponse distribution, ± SEM, for the irradiated group. Scales for both graphs are identical. The mean number of responses per session was 588 ± 46. The data presented were based on observations from 6 animals.

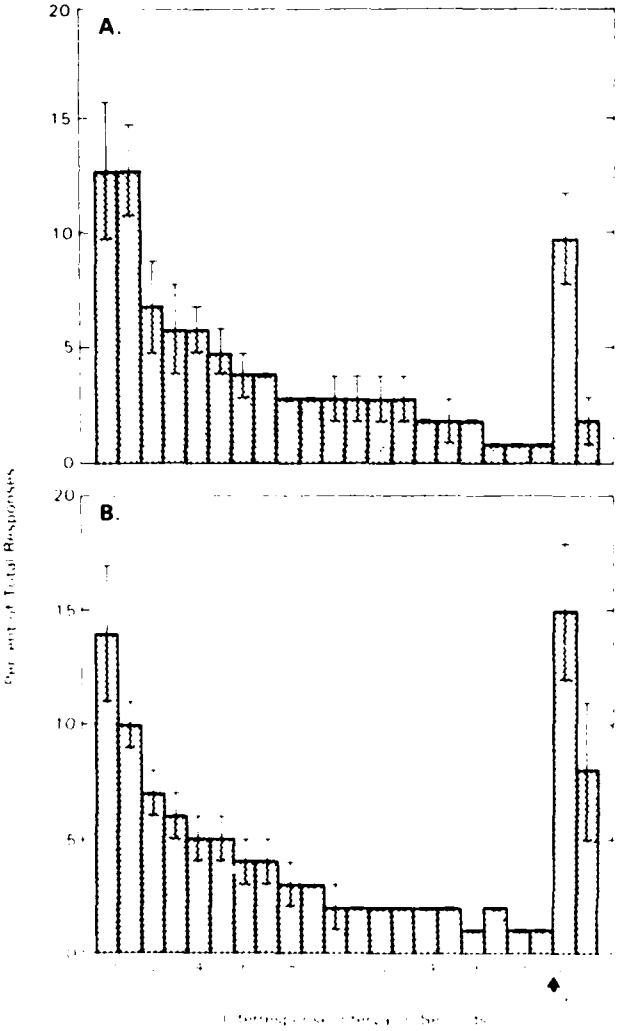

FIG. 5. (A) Interresponse distribution, ± SEM, for the control group trained on the unsignalled avoidance paradigm after sham irradiation. Arrow indicates the time of onset of shocks. (B) Interresponse distribution, ± SEM, for the irradiated group. Scales for both graphs are identical. The mean number of responses per session was 989 ± 84. The data presented were based on observations from 6 animals.

this type of analysis because the animal's response to the warning tone was not reliably related to the subject's last response and consequently showed a flat distribution. Based on the requirements of the fixed-interval signalled avoidance paradigm, the subjects, as expected, responded mostly just after the onset of the warning tone (Fig. 4A). On the other hand, the animals performing on the unsignalled avoidance paradigm often responded to the shock and continued responding for a time with short IRTs (Fig. 5A). As the IRTs lengthened, a shock eventually occurred, precipitating another period of responses with short IRTs.

The pattern of IRTs after irradiation was not greatly affected. Those animals trained on the fixed-interval signalled avoidance paradigm still responded after the warning tone (Fig. 4B). However, when subjects did not avoid shock, they usually responded just after the onset of shock. Few responses occurred at long intervals after shock. The IRTs of the irradiated animals trained on the unsignalled avoidance paradigm were essentially the same as their corresponding controls, except there were more shock elicited responses (Fig. 5B).

In order to determine whether the irradiated animals in the fixed-interval signalled avoidance group were really using the warning tones, the latencies between the presentation of the tone and responding on the avoidance lever were determined and are shown in Fig. 6. It was assumed that consistently short latencies to respond would follow the presentation of a tone. Short latencies were found in both irradiated and unirradiated animals, indicating that the animals could detect and use the tones even after irradiation.

Subjects in the variable-interval signalled avoidance group performed similarly to those in the fixed-interval signalled avoidance group (Fig. 7). The former group also responded with consistently short latencies to the onset of the warning tones in both irradiated and unirradiated conditions, indicating that even when the onset of the warning tone was made unpredictable, the animals continued to wait for it and use it as an aid in responding.

DISCUSSION

The results from this study demonstrate again that exposure to

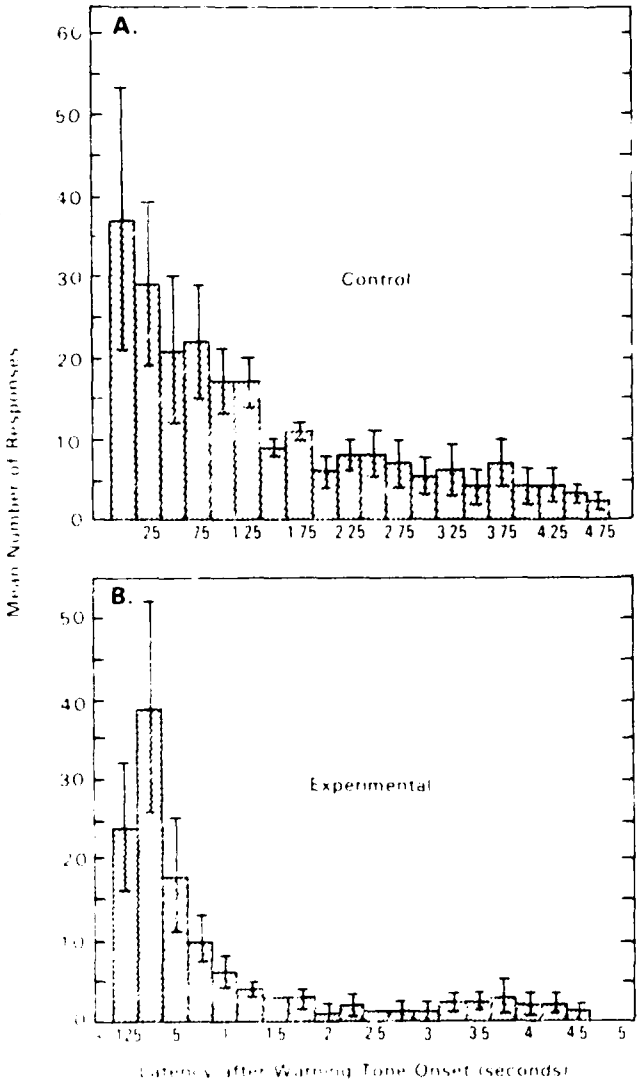

FIG. 6. (A) Latency distribution of responses, ± SEM, to the onset of the warning tone for the animals trained on the fixed-interval signalled avoidance paradigm of the control group during the 90 min after sham irradiation. (B) Latency distribution of responses, ± SEM, to the onset of the warning tone during the 90 min after irradiation. The data presented were based on observations from 6 animals.

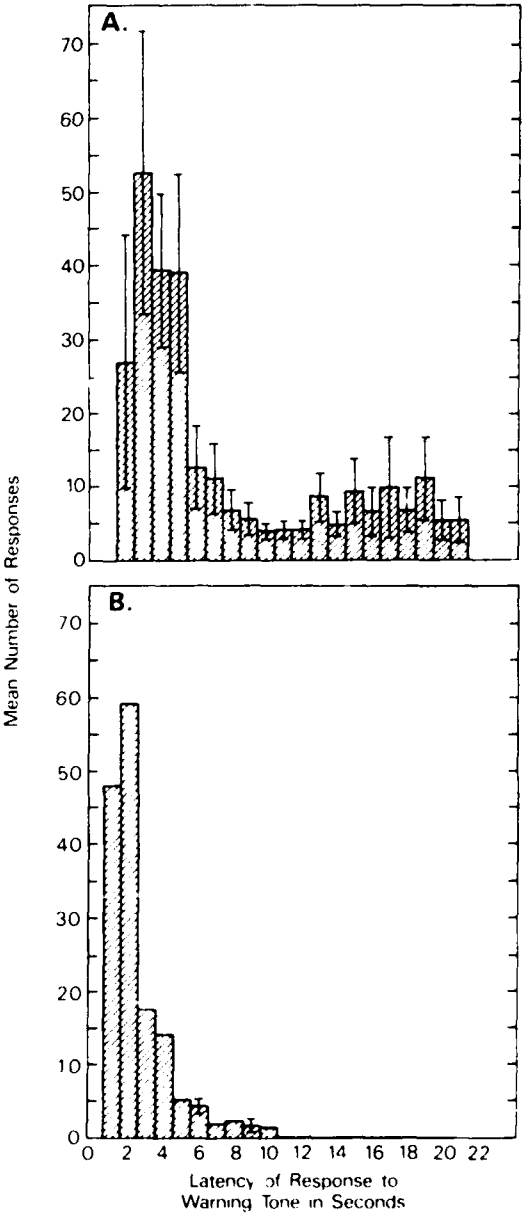

FIG. 7. (A) Latency distribution of responses, ± SEM, to the onset of the warning tone for the animals trained on the variable-interval signalled avoidance paradigm of the control group during the 90 min after sham irradiation. (B) Latency distribution of responses, ± SEM, to the onset of the warning tone during the 90 min after irradiation. Note: In some cases the SEM was too low to be graphed. The data presented were based on observations from 6 animals.

ionizing radiation can degrade performance on active avoidance paradigms and is consistent with previously published reports [2,5]. Typically, irradiated animals received more shocks than the unirradiated controls. Although performance was degraded, the animals were capable of executing the movements necessary to avoid shock. The rates and patterns of responding on the avoidance lever were generally unaltered after irradiation, except that animals performing on the two signalled avoidance paradigms responded more frequently to the shock rather than to the warning tone. Even so, it appears that subjects could detect the tones and were able to respond to them appropriately, even when the tones were temporally unpredictable.

The relative degree of behavioral decrement after irradiation appears to depend on the availability of visual and auditory cues that could be used to successfully avoid shocks. Although it can be seen from Figs. 1–3 that the number of shocks received by irradiated animals performing on the three paradigms was roughly the same, the preirradiated levels of performance were different. Prior to irradiation, animals trained on either signalled avoidance paradigm performed significantly better than those animals trained on the unsignalled avoidance paradigm, as evidenced by the fewer number of shocks received by the former animals. These findings suggest that the number and nature of cues and the consequent level of performance (presumably better with cues) have some

bearing on the likelihood of the occurrence of a radiation-induced performance decrement.

Although not the intention of the experimental design, another way to look at the relationship between cues and performance is to consider the three paradigms as requiring of the animals different levels of performance. In order for the animals trained on the two signalled avoidance paradigms to perform as well as they did, compared to those trained on the unsignalled avoidance paradigm, they needed cues to assist them. When the animals were irradiated, for some reason they did not use as many of the cues provided. Consequently, their performance was more like that of irradiated animals trained on the unsignalled avoidance paradigm in which no external cues were provided.

Why the irradiated animals were not using the cues is not clear. They apparently could detect them because responses with short latencies were still observed after presentations of the warning tones before the onset of shock even when the onset of these warning tones was unpredictable. The response pattern is not suggestive of deafness nor stupor, and the subjects were apparently not relying more on internally based time-cues rather than the tones. Another possibility is that they could maintain only temporary selective attention, rather than a more general vigilance. In addition, irradiated rats from other experiments showed no differences in their abilities to detect and respond to warm water cues (3). Rather than these performance decrements being related to abnormalities in perception, task learning, and motor function, they may result from some cognitive deficit, possibly a lack of motivation. That is, the cues and responding to these cues might become of lower value to the subject relative to other cues and behaviors.

ACKNOWLEDGEMENTS

The research was supported by the Armed Forces Radiobiology Research Institute, Defense Nuclear Agency, under work unit 00072. Views presented in this paper are those of the authors; no endorsement by the Defense Nuclear Agency has been given or should be inferred. Research was conducted according to the principles enunciated in the *Guide for the Care and Use of Laboratory Animal Resources, National Research Council*.

REFERENCES

1. Badia, P.; Culbertson, S.; Abbott, B. The relative aversiveness of signalled vs. unsignalled avoidance. J. Exp. Anal. Behav. 16: 113–131; 1971.
2. Burghardt, W. F., Jr.; Hunt, W. A. Characterization of radiation-induced performance decrement using a two-lever shock-avoidance task. Radiat. Res. 103:149–157; 1985.
3. Burghardt, W. F., Jr.; Hunt, W. A. The interactive effects of morphine and ionizing radiation on the latency of tail withdrawal from warm water in the rat. In: Proceedings of the ninth symposium on psychology in the department of defense. Colorado Springs, CO: United States Air Force Academy; 1984: 73–76.
4. Gale, R. Witness to disaster: An American doctor at Chernobyl. Life August 20: 28; 1986.
5. Hunt, W. A. Comparative effects of exposure to high-energy electrons and gamma radiation on active avoidance behavior. Int. J. Radiat. Biol. 44:257–260; 1983.
6. Hunt, W. A. Effects of ionizing radiation on behavior and the brain. In: Conklin, J. J.; Walker, R. I., eds. Military radiobiology. New York: Academic Press; 1987:321–330.
7. Karas, J. S.; Stanbury, J. B. Fatal radiation syndrome from an accidental nuclear excursion. N. Engl. J. Med. 272:755–761; 1965.
8. Shipman, S.; Lushbaugh, C. C.; Petersen, D. E.; Langham, W. H.; Harris, P. S.; Lawrence, J. N. P. Acute radiation death resulting from an accidental nuclear critical excursion. J. Occup. Med. 3:146–192; 1961.
9. Sidman, M. Some properties of the warning stimulus in avoidance behavior. J. Comp. Physiol. Psychol. 46:444–450; 1955.
10. Sidman, M. Two temporal parameters in the maintenance of avoidance behavior by the white rat. J. Comp. Physiol. Psychol. 46: 253–261; 1953.
11. Winer, B. J. Statistical principles in experimental design. New York: McGraw-Hill; 1971.

Circulatory Shock 28:257–265 (1989)

ARMED FORCES RADIOBIOLOGY RESEARCH INSTITUTE
SCIENTIFIC REPORT
SR89-29

Norepinephrine-Induced Phosphorylation of a 25 kd Phosphoprotein in Rat Aorta is Altered in Intraperitoneal Sepsis

J.A. Carcillo, R.Z. Litten, and B.L. Roth

Surgical Research Division, Naval Medical Research Institute (J.A.C., B.L.R.); and Department of Physiology, the Armed Forces Radiobiological Research Institute (R.Z.L.), Bethesda, Maryland; Department of Anesthesiology, Critical Care Medicine, Children's Hospital National Medical Center, George Washington University School of Medicine and Health Sciences, Washington, DC (J.A.C.)

An attenuation of the contractile response to norepinephrine (NE) has been previously demonstrated in rat aorta during intraperitoneal sepsis and endotoxemia. In this study, we determined whether NE-induced protein phosphorylation is altered in septic rat aorta as compared to control rat aorta. We found that the NE-induced phosphorylation of a 25 kd phosphoprotein was decreased. NE increaed phosphorylation of the 25 kd band by 54% ($P < .01$) in the control aorta but only 12% (not significant) in the septic aorta. Pyrophosphate gel purification of phosphorylated myosin showed that this 25 kd band was not related to the myosin-phosphorylated (P) light chain. Two-dimensional polyacrylamide gel electrophoresis analysis revealed that this 25 kd band represents two proteins with distinct isoelectric points of 6.5 and 6.2. These results further document that intrinsic alterations occur in the NE-mediated signal transduction system in rat aorta during sepsis and that such alterations could contribute to depressed aortic contractility.

Key words: protein phosphorylation, protein kinase, phosphoinositide metabolism, receptor, α_1-adrenoceptor

INTRODUCTION

Decreased sensitivity of the vasculature to α_1-adrenergic receptor stimulation is well described in endotoxemia and sepsis [1–3]. The rat aorta has provided a reliable

Submitted for publication December 20, 1988; revised February 22, 1989

Dr. B.L. Roth's present address is Room S-253, Stanford University Medical Center, Stanford, CA 94305

These findings were presented at the First International Shock Congress, 1987, and published in preliminary form [23].

Address reprint requests to Dr. R.Z. Litten, Department of Physiology, Armed Forces Radiobiology Research Institute, Bethesda, MD 20814

©1989 Alan R. Liss, Inc.

model in which to study this phenomenon in cecal ligation- and puncture-induced intraperitoneal sepsis [4]. Recent investigations suggest that this insensitivity correlates with intrinsic alterations in the α_1-adrenoceptor and its phospholipase C–coupled signal transduction system. In particular, we have demonstrated a marked reduction in α_1-adrenoceptor numbers as well as in basal and norepinephrine (NE)-induced phosphoinositide turnover, and calcium metabolism in aorta from this cecal ligation and puncture model of intraperitoneal sepsis [5,6].

In this study, we further examined the NE-induced signal transduction cascade in rat aorta by investigating whether alterations in protein phosphorylation occur in sepsis. A decrease in NE-mediated phosphorylation of a 25 kd phosphoprotein was observed in aorta from septic rats, further demonstrating a derangement in the NE-mediated signal transduction system during sepsis.

MATERIALS AND METHODS

Chronic Rat Sepsis Model

Male Sprague-Dawley rats (250–300 g) were obtained from Taconic Farms, Germantown, NY. Control and experimental animals were randomly subjected to sham surgery or to cecal ligation and two-hole puncture, respectively, as previously described [7]. This procedure resulted in a mortality rate of 20–30%; 24 hours after surgery, the experimental rats displayed signs of sepsis including piloerection, a bloody mucosal and nasal discharge, bloody diarrhea, and lethargy. All animals were sacrificed by decapitation and the thoracic aorta was rapidly removed and divided into 4 mm rings.

[^{32}P] Labeling of Rat Aorta

Each aortic ring was placed in a 10 × 75 mm borosilicate glass tube and incubated for 90 minutes in 0.3 ml oxygenated phosphate-free buffer (5 mM HEPES, 140 mM NaCl, 4.5 mM KCl, 1 mM $MgCl_2$, 1.5 mM $CaCl_2$, 10 mM glucose, pH 7.4, 37°C) in the presence of 10 μCi carrier-free [^{32}P] orthophosphate (8 mCi ml; Amersham). This resulted in equilibrium labeling of rat aorta. The rings were then treated for 10 min with 10 μM NE, a concentration which produced maximal aortic isometric contraction [8], or with an equivalent volume of sterile buffer solution.

The phosphorylation reaction was stopped immediately by freezing the rings in liquid nitrogen. The rings were then pulverized in liquid nitrogen and glass-to-glass homogenized in stopping solution as described by Draznin et al. [9] (100 mM NaF, 80 mM sucrose, 10 mM EDTA, pH 7.40). Protein was then determined by using the method of Bradford [10]. Ten micrograms of protein was then solubilized in 50 μl of a sodium dodecyl sulfate (SDS) solution (62.5 mM Tris, 10% glycerol, 100 mM DTT, 3% SDS pH 6.8).

Isolation of Phosphorylated Rat Aorta Myosin

The isolation of phosphorylated rat aorta myosin was carried out as previously detailed [11]. Briefly, six rat aortae were removed, divided into 4 mm rings, and placed in oxygenated phosphate-free buffer containing ^{32}P as described above. After exposure to 10 μM NE, the rings were frozen in liquid nitrogen and extracted in 16 volumes of a buffer consisting of 100 mM sodium pyrophosphate, pH 8.8, 5 mM EGTA, 50 mM sodium fluoride, 10% glycerol, 15 mM 2-mercaptoethanol, and 0.2

mM dichlorvos (serine protease inhibitor). Pyrophosphate gel electrophoresis was carried out at 0°C for 16 hours at a constant 84 V. Following electrophoresis, gels were stained briefly for 15 min in 0.1% Coomassie blue R-250, 50% methanol, and 10% acetic acid and destained in cold water. The purified myosin band was removed with a razor blade and placed on one-dimensional sodium dodecylsulfate–polyacrylamide gel electrophoresis (SDS-PAGE gel) as described below.

Gel Electrophoresis

One-dimensional SDS-PAGE was performed with 10 μg protein/50 μl SDS solution per lane. Electrophoresis on 10% SDS polyacrylamide gels with 3% stacking gels occurred as described by Laemmli [12]. Sigma molecular weight standards (Sigma Chemical Co., St. Louis, MO) were used to identify proteins. The use of protease inhibitors (30 μM PMSF, 50 μg/ml soybean trypsin inhibitor, and 50 μg/ml leupeptin) did not alter the protein or phosphorylation patterns (not shown). Therefore, they were not routinely used in this study.

Two-dimensional gel electrophoresis was performed according to modification of the procedure of Laemmli [12]: 10 μg of protein was electrofocused in 2.5 × 110 mm area tube gels containing 3% polyacrylamide, 55% urea, 2% NP-40, and 2% ampholine (1.7% of pH 3.5–10 and 0.3% of pH 5–7). The gels were equilibrated in SDS sample buffer and the second dimension was then run on 11 × 14 cm slab gels containing 10% SDS polyacrylamide gel.

Autoradiography and Quantitation

Gels were dried and phosphorylation was qualitatively determined by autoradiography with Kodak X-OMAT film. The gels were scanned and quantitated with an LKB laser densitometer. The area under the curve of all protein bands represents the total protein phosphorylation. The amount of phosphorylation of the 25 kd protein was determined by dividing the area of the 25 kd by the total area of all the proteins. This allowed determination of phosphorylation to be analyzed with equalization of samples for ^{32}P labeling.

RESULTS

Recently, attenuation of NE-induced phosphoinositide metabolism, calcium influx (calcium channel entry), and calcium efflux (intracellular calcium release) has been demonstrated in rat aorta from this model of sepsis [5,6]. Since protein phosphorylation can be influenced by increase in cytosolic calcium as well as by phosphoinositide-hydrolysis-derived diacylglycerol, we investigated whether changes in protein phosphorylation also occurred.

Aortae from cecal-ligation-and-punctured rats and from sham-operated rats were labelled with [^{32}P] orthophosphate and then exposed to 10 μM NE, a dose known to elicit maximal contraction of rat aorta [8,13]. One-dimensional gel electrophoresis of smooth muscle protein revealed a decreased NE-induced phosphorylation of the 25 kd band during sepsis (Figs. 1, 2). NE increased phosphorylation by 54% ($P < .01$) in control aorta but only by 12% (not significant) in septic aorta (Table I). There were also differences noted in equilibrium [^{32}P] labeling in control and sham tissue. The septic tissue showed greater [^{32}P] uptake into the 25 kd phosphoprotein during the basal condition (Table I). However, despite this

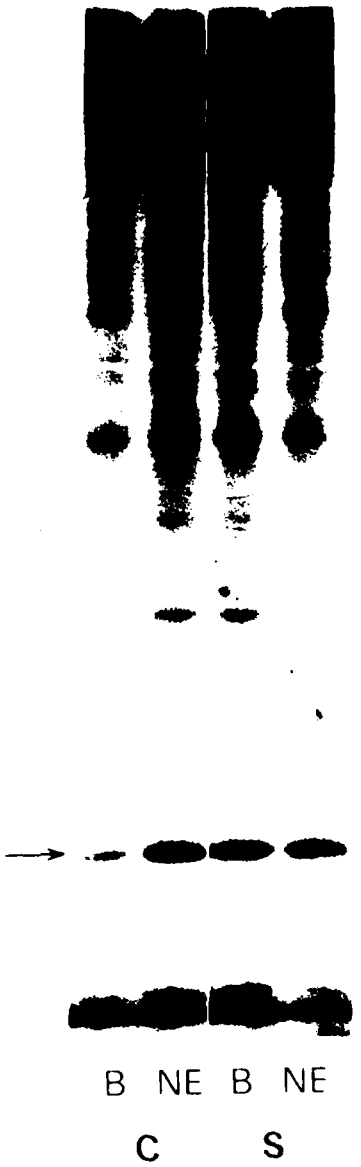

Fig. 1. One-dimensional SDS-PAGE of 10 μg aortic protein phosphorylated in the presence (NE) and absence (basal, B) of 10 μM NE in control (C) and septic (S) aortae. Arrow shows 25 kd band.

phenomena. NE-induced phosphorylation of the 25 kd phosphoprotein was significantly greater in control rats. Finally, we observed no significant differences in the total protein phosphorylation among the control and septic groups with and without NE (not shown).

To define the identity of this 25 kd band, we determined whether this represented a component of the myosin P light chain. Myosin purification from a

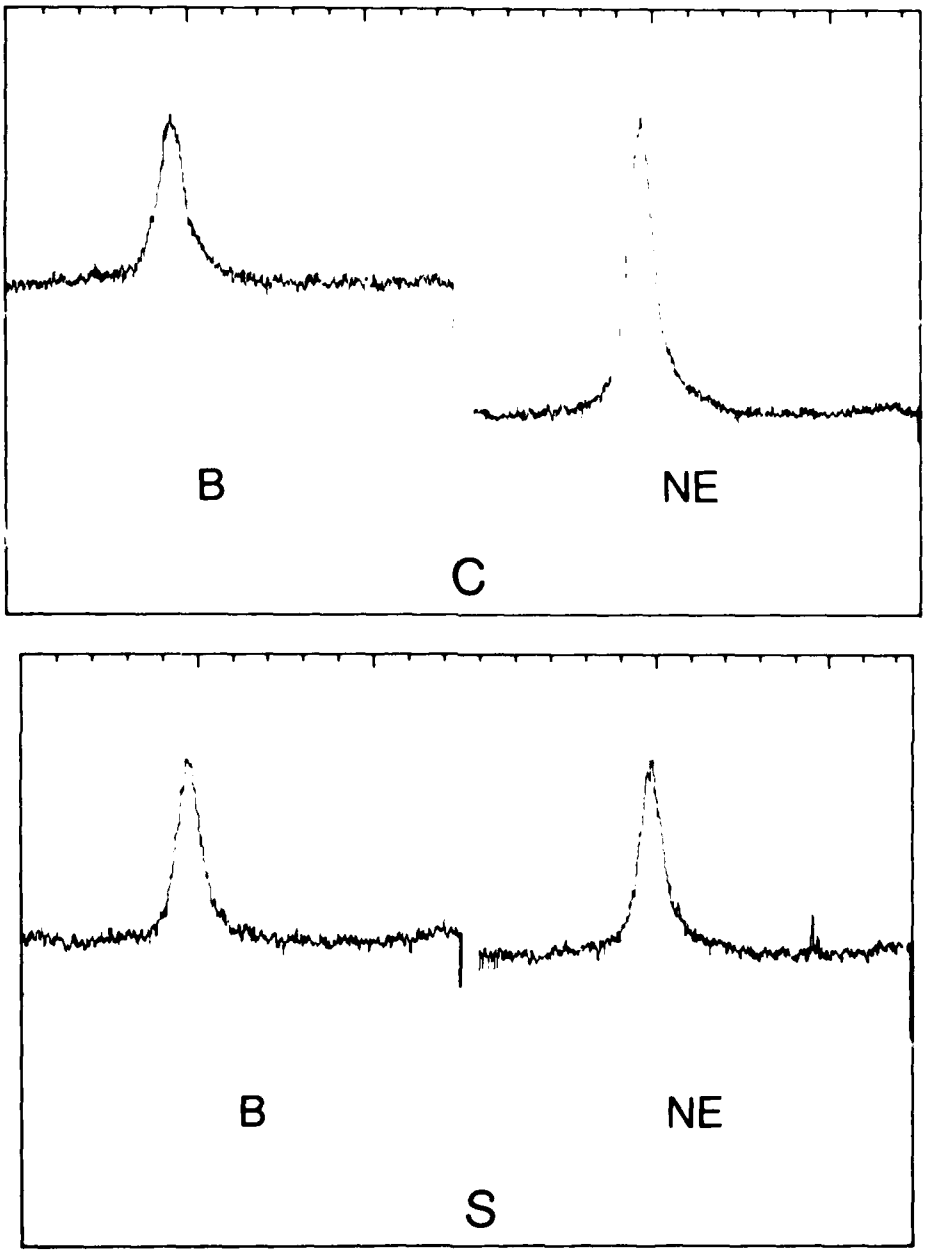

Fig. 2. Scanning densitometric analysis of 25 kd protein band after phosphorylation in the presence (NE) and absence (basal, B) of 10 μM NE in control (C) and septic (S) aortae (10 min response).

TABLE I. [^{32}P] Phosphorous Labeling of 25 kd Band†

	$\frac{\text{25kd phosphorylation}}{\text{Total phosphorylation}} \times 100$
Control	2.55 ± 0.23
Control + NE	3.93 ± 0.37*
Septic	2.93 ± 0.03
Septic + NE	3.37 ± 0.21

†Values are mean ± SE for 8 different preparations. Quantitation is described in Materials and Methods.
*$P < .01$ vs. control using Student's unpaired t-test.

control phosphorylated aorta preparation revealed phosphorylation of a 20 kd but not the observed 25 kd band. This suggested that the phosphorylated protein was not the myosin P light chain. To further identify the protein band, we submitted the phosphorylated sample to two-dimensional electrophoresis. This analysis revealed that the 25 kd band represents two distinct proteins (Fig. 3). These two proteins have isoelectric points of 6.5 and 6.2. Analysis of two-dimensional gel electrophoresis of septic aortic proteins did not show a selective attenuation of basal or NE-induced labeling in either of the two spots. Therefore, the observed alteration in phosphorylation appears to occur equally in both.

DISCUSSION

This paper demonstrates that NE-mediated phosphorylation of a 25 kd phosphoprotein is decreased in aorta from rats after cecal-ligation-and-two-hole-puncture-induced intraperitoneal sepsis. It appears that the sepsis-induced alteration in NE-mediated phospholipase C–coupled signal transduction continues to the level of protein phosphorylation. NE binding to the α_1-adrenergic receptor results in phospholipase C–mediated hydrolysis of phosphoinositides to the by-products, inositol triphosphate and diacylglycerol [14–16]. These second messengers, in turn, are thought to play a role in increased intracellular Ca^{++} release and activation of phosphorylating enzymes such as protein kinase C [17]. Thus, it would be predicted that alterations in this system would result in specific changes in protein phosphorylation, as was observed in this study.

Even though the function of the 25 kd phosphoprotein is not known, phosphorylation of this protein could be involved in the regulation of vascular smooth muscle contraction. Similar to our finding, Draznin et al. [9] found an increase in the phosphorylation of a 25 kd protein following NE activation in rat aorta. This 25 kd protein is not a myosin P light chain. Recently, Foster and Chatterjee [18] reported that a 25 kd protein is phosphorylated in skinned carotid artery following stimulation of protein kinase C with phorbol dibutyrate. This phosphorylation occurred without changes in the level of phosphorylation of the myosin P light chain, suggesting a possible role for 25 kd protein in vascular smooth muscle contraction. Since increased phosphorylation from NE continues at 10 min, one could speculate that this 25 kd

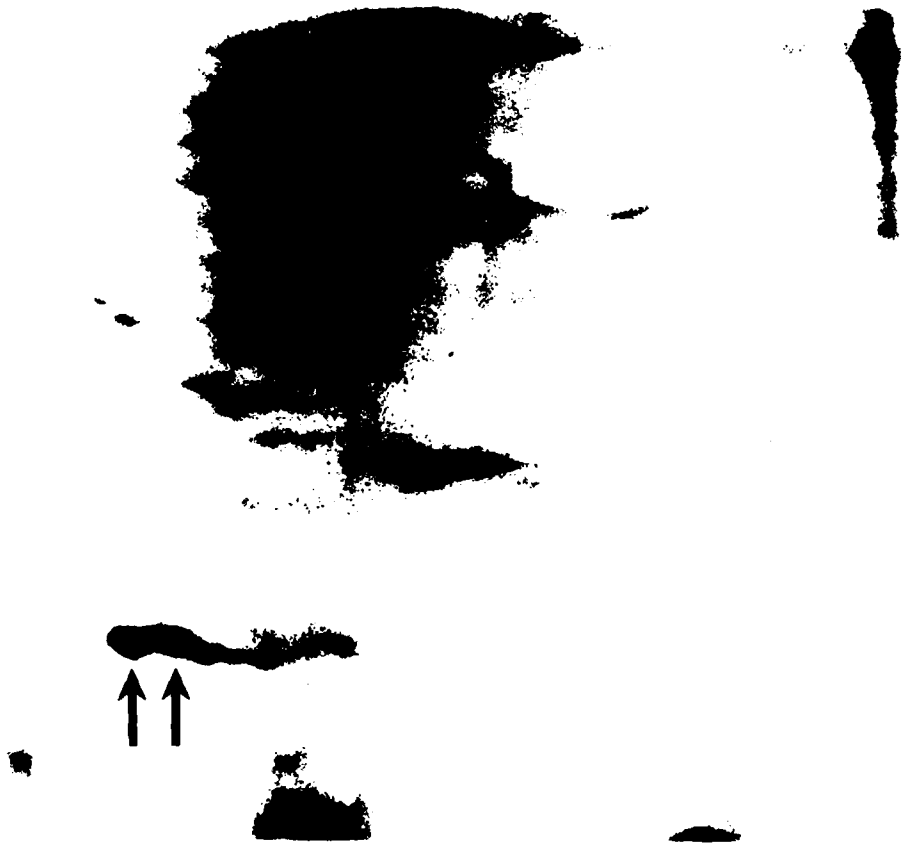

Fig. 3. Two-dimensional gel electrophoresis of band shows two distinct spots (see arrows) at isoelectric points of 6.2 and 6.5 after phosphorylation of rat aorta control. Similar findings were also observed by using aortae from septic rats.

protein has a functional role in long-term tonic contraction and hence belongs to the family of filament or latch proteins [19].

The investigation of the biochemical basis for diminished sensitivity of the vasculature as well as of the liver [20,21] to α_1-adrenergic agonist stimulation has shown fundamental and intrinsic alterations in the signal transduction system. In rat aorta, sepsis induces a marked reduction in α_1-adrenergic receptor numbers, basal phosphatidylinositol-4,5-bisphophate (PIP_2) synthesis (PIP_2 is a major substrate for the phospholipase C enzyme), basal phosphoinositide metabolism, and basal calcium efflux [5,6]. Upon α_1-adrenergic stimulation, there is also a diminution of NE-induced phosphoinositide metabolism, calcium influx and efflux, and protein phosphorylation in the aorta during intraperitoneal sepsis [5,6]. These intriguing observations suggest that intrinsic alterations in the signal transduction pathway may contribute at a molecular level to the observed alteration in α_1-adrenoceptor function in rat intraperitoneal sepsis.

These findings suggest that even though endotoxin and circulating mediators such as tumor necrosis factor, interleukin, and platelet-activating factor may play a

role in vasodilation and in diminished responsiveness to vasoconstricting agents in sepsis [22], intrinsic biochemical alterations in vascular tissue also exist. It is possible that a cause-and-effect relationship exists between these extrinsic mediators and the intrinsic biochemical alterations during sepsis. It is conceivable, for example, that tumor necrosis factor may induce α_1-adrenoceptor tachyphylaxis by an as-yet-undefined mechanism (see ref. 22 for discussion). Future experiments will be needed to test this idea.

In summary, intrinsic alterations occur in the NE-mediated signal transduction system in rat aorta in sepsis. As previously demonstrated [5,6], these changes occur at each level of the receptor-mediated signal transduction cascade.

ACKNOWLEDGMENTS

We wish to thank Ms. Carol A. Holifield for her excellent assistance in the preparation of this manuscript. This work was supported in part by Armed Forces Radiobiology Research Institute, Defense Nuclear Agency and Naval Medical Research Institute, Department of Defense, under Work Unit 70169 and Research task number MR001.01-1032. The opinions and assertions contained herein are the private ones of the authors and should not be construed as reflecting the views of the U.S. Navy, the naval service at large, the Department of Defense, or the Defense Nuclear Agency.

REFERENCES

1. Pomerantz K, Casey L, Fletcher JR, Ramwell PW: Vascular reactivity in endotoxin shock: Effect of idocaine or indomethacin treatment. Adv Shock Res 7:191–198, 1982.
2. Chernow B, Roth BL: Pharmacologic manipulation of peripheral vasculature in shock: Clinical and experimental approaches. Circ Shock 18:141–155, 1986.
3. Chernow B, Rainey TG, Late CR: Endogenous and exogenous catecholamines in critical care medicine. Crit Care Med 10:409–416, 1982.
4. Wakabayashi I, Hatake K, Kakishita E, Nagai K: Diminution of contractile response of the aorta from endotoxin-injected rats. Eur J Pharmacol 141:117–122, 1987.
5. Carcillo JA, Litten RZ, Suba EA, Roth BL: Alteration in rat aortic alpha$_1$-adrenergic receptors and alpha$_1$-adrenergic stimulated phosphoinositide hydrolysis in intraperitoneal sepsis. Circ Shock 26:331–339, 1988.
6. Litten RZ, Carcillo JA, Roth BL: Alteration in bidirectional transmembrane calcium flux occur without changes in protein kinase C levels in rat aorta during sepsis. Circ Shock 25:123–130, 1988.
7. Wichterman K, Bave AI, Chaudry IH: Sepsis and septic shock. A review of laboratory models and a proposal. J Surg Res 29:189–201, 1980.
8. Suba EA, Roth BL: Prostaglandins activate phosphoinositide metabolism in rat aorta. Eur J Pharmacol 136:325–332, 1987.
9. Draznin MB, Rapoport RM, Murad F: Myosin light chain phosphorylation in contraction and relaxation of intact rat thoracic aorta. Int J Biochem 18(10):917–928, 1986.
10. Bradford MM: A rapid and sensitive method for the quantitation of microgram quantities of protein utilizing the principle of protein dye binding. Anal Biochem 72:748–754, 1976.
11. Silver PJ, Stull JT: Quantitation of myosin light chain phosphorylation in small tissue samples. J Biol Chem 257:6137–6144, 1982.
12. Laemmli UW: Cleavage of structural proteins during the assembly of the head of bacteriophage T4. Nature 227:680–685, 1970.
13. Legan E, Chernow B, Parrillo J, Roth BL: Activation of phosphatidylinositol turnover in rat aorta by alpha$_1$-adrenergic receptor stimulation. Eur J Pharmacol 110:389–390, 1985.
14. Majerus PW, Neufield EJ, Wilson DB: Production of phosphoinositide derived messengers. Cell 37:701–703, 1984.

15. Michael RH: Inositol phospholipids and cell surface function. Biochim Biophys Acta 415:81–147, 1985.
16. Berridge MJ: Inositol trisphosphatic and diacylglycerol as second messengers. Biochem J 220:345–360, 1984.
17. Nishizuka Y: The role of protein kinase C in cell surface signal transduction and tumor promotion. Nature 308:693–698, 1984.
18. Foster CJ, Chatterjee M: A 25,000 dalton protein is phosphorylated in response to phorbol ester stimulation in skinned carotid artery. Biophys J 49:73a, 1986.
19. Rasmussen H, Takuwa Y, Park S: Protein kinase C in the regulation of smooth muscle contraction. FASEB J 1:177–185, 1987.
20. Roth BL, Spitzer JA: Altered hepatic vasopressin and α_1-adrenergic receptors after chronic endotoxin infusion. Am J Physiol 252:E699–E702, 1987.
21. Spitzer JA, Turco ER, Deaciuc IV, Roth BL: Perturbation of transmembrane signaling mechanisms in acute and chronic endotoxemia. In Schlag G, Redl H (eds): "First Vienna Shock Forum, Part A: Pathophysiological Role of Mediators and Mediator Inhibitors in Shock." Progress in Clinical and Biological Research, Vol. 236A. New York: Alan R. Liss, Inc., 1987, pp 401–418.
22. Roth BL, Suba EA, Carcillo JC, Litten RZ: Alteration in hepatic and aortic phospholipase C coupled receptor and signal transduction in rat intraperitoneal sepsis. In Roth BL, Nielsen T, McKee A (eds): "Molecular and Cellular Mechanisms of Septic Shock." New York: Alan R. Liss, Inc., 1989, pp 41–59.
23. Litten RZ, Carcillo JA, Roth BL: Vascular calcium metabolism and protein phosphorylation in rat intraperitoneal sepsis. Circ Shock 21:332, 1987.

The experiments reported herein were conducted according to the principles set forth in the *Guide for the Care and Use of Laboratory Animals*, Institute of Laboratory Animal Resources, National Research Council, DHEW, publication No. (NIH) 85-23.

RADIATION RESEARCH 119, 219–231 (1989)

ARMED FORCES RADIOBIOLOGY RESEARCH INSTITUTE
SCIENTIFIC REPORT
SR89-30

Quantitative Measurement of Radiation-Induced Base Products in DNA Using Gas Chromatography–Mass Spectrometry

ALFRED F. FUCIARELLI,*†[1] BRENT J. WEGHER,† EWA GAJEWSKI,* MIRAL DIZDAROGLU,* AND WILLIAM F. BLAKELY†

*Center for Chemical Technology, National Institute of Standards and Technology, Gaithersburg, Maryland 20899, and †Radiation Biochemistry Department, Armed Forces Radiobiology Research Institute, Bethesda, Maryland 20814-5145

FUCIARELLI, A. F., WEGHER, B. J., GAJEWSKI, E., DIZDAROGLU, M., AND BLAKELY, W. F. Quantitative Measurement of Radiation-Induced Base Products in DNA Using Gas Chromatography–Mass Spectrometry. *Radiat. Res.* **119**, 219–231 (1989).

Gas chromatography–mass spectrometry with selected-ion monitoring was used to study radiation-induced damage to DNA. Quantitative analysis of modified purine and pyrimidine bases resulting from exposure to ionizing radiation using this technique is dependent upon the selection of appropriate internal standards and calibration of the mass spectrometer for its response to known quantities of the internal standards and the products of interest. The compounds 6-azathymine and 8-azaadenine were found to be suitable internal standards for quantitative measurement of base damage in DNA. For the purpose of calibration of the mass spectrometer, relative molar response factors for intense characteristic ions were determined for the trimethylsilyl derivatives of 5-hydroxyuracil, thymine glycol, and 5,6-dihydrothymine using 6-azathymine, and for the trimethylsilyl derivatives of 4,6-diamino-5-formamidopyrimidine, 8-hydroxyadenine, 2,6-diamino-4-hydroxy-5-formamidopyrimidine, and 8-hydroxyguanine using 8-azaadenine. Accurate measurement of the yield of radiation-induced modifications to the DNA bases is also dependent upon two chemical steps in which the purines and pyrimidines are released from the sugar–phosphate backbone and then derivatized to make them volatile for gas chromatography. The completeness of these reactions, in addition to assessing the stability of the modified DNA bases in acid and their trimethylsilylated derivatives over the time necessary to complete the experimental analysis, was also examined. Application of this methodology to the measurement of radiation-induced base modification in heat-denatured, nitrous oxide-saturated aqueous solutions of DNA is presented. © 1989 Academic Press, Inc

INTRODUCTION

The interaction of ionizing radiation with cellular water results in the formation of a number of highly reactive radical species which are then capable of interacting with cellular constituents. The hydroxyl radical is the most reactive radical species that is produced, interacting via abstraction of hydrogen atoms and addition reactions on cellular constituents (for a review see Ref. (*1*)). Radiation-induced cell lethality has generally been attributed to the induction of damage in the nuclear DNA (*2*). Radia-

[1] To whom correspondence should be addressed at present address: Department of Radiation Medicine, Massachusetts General Hospital, 55 Fruit Street, Boston, MA 02114.

0033-7587/89 $3.00
Copyright © 1989 by Academic Press, Inc
All rights of reproduction in any form reserved

tion-induced damage to nucleic acid constituents manifests itself in the formation of altered purine and pyrimidine bases, altered deoxyribose moieties, abasic sites, strand breaks, and DNA–protein crosslinks (for a review see Ref. (*1*)). Repair of these structural modifications is essential to maintain the integrity of the genomic message, thereby preventing the processes of mutagenesis, cell death, and carcinogenesis (*2*).

In an effort to examine the consequences of radiation-induced modifications to DNA at the cellular level, it is necessary to develop assays to identify and measure such damage. Several types of assays have been developed to measure the yield of radiation-induced purine and pyrimidine products in DNA which include chromatographic (*3–11*), immunochemical (*12–16*), and biochemical (*17, 18*) techniques. However, all of these techniques are capable of assaying only a very limited number of modified DNA products and, because of the limitations of selectivity and sensitivity, the radiation doses used exceed those used in studies measuring biological end points.

In an effort to overcome these limitations, the technique of gas chromatography–mass spectrometry with selected-ion monitoring (GC–MS/SIM) has been pursued. This technique has been used to identify a plethora of radiation-induced purine and pyrimidine products (*19–23*) and DNA base–amino acid crosslinks (*19, 21, 24*). Further, using the GC–MS/SIM technique, detection of these products has been possible at doses lower than those reported using other methods of analysis. The GC–MS/SIM technique has been well documented for quantitative measurement of organic compounds at low concentrations in complex mixtures (*25*). However, the determination of optimum conditions for quantitative measurement of radiation-induced DNA base products by this technique has not been established. In this respect, quantitative analysis using this technique is dependent upon a number of factors including completeness of hydrolysis and derivatization reactions, stability of the products to the conditions of hydrolysis, and stability of the derivatized products over the time necessary to complete the analysis of the derivatized products. Further, selection of appropriate internal standards and calibration of the mass spectrometer with respect to the response of the internal standards and the response of authentic samples of the radiation-modified constituents under analysis are necessary for accurate measurements. This paper addresses these issues and describes the use of GC–MS/SIM for quantitative analyses of radiation-induced base modifications in DNA.

MATERIALS AND METHODS[2]

Chemicals The compounds 5-hydroxyuracil (isobarbituric acid), 8-bromoadenine, 5,6-dihydrothymine, 4,6-diamino-5-formamidopyrimidine (FAPy-adenine), 2,5,6,-triamino-4-hydroxypyrimidine, 8-azaadenine, 8-azaguanine, 6-azathymine, and calf thymus DNA were purchased from the Sigma Chemical Co. 2-Amino-6,8-dihydroxypurine (8-hydroxyguanine) was purchased from the Chemical Dynamics Corp. Nitrous oxide (ultrahigh purity) was purchased from Matheson Gas Products, Inc. Silylation grade acetonitrile and bis(trimethylsilyl)trifluoroacetamide (BSTFA) (containing 1% trimethylchlorosilane) were obtained from the Pierce Chemical Co. The *cis* isomer of 5,6-dihydroxy-5,6-dihydrothymine (thymine

[2] Mention of commercial products does not imply recommendation or endorsement by the National Institute of Standards and Technology, nor does it imply that the products identified are necessarily the best available for the purpose.

glycol) was kindly provided by Dr. E. Holwitt of the Armed Forces Radiobiology Research Institute, Bethesda, Maryland. 6-Amino-8-hydroxypurine (8-hydroxyadenine) was synthesized by treatment of 8-bromoadenine with concentrated formic acid (95%) at 150°C for 45 min and purified by crystallization from water. 2,6-Diamino-4-hydroxy-5-formamidopyrimidine (FAPy-guanine) was synthesized by treatment of 2,5,6-triamino-4-hydroxypyrimidine with concentrated formic acid and recrystallized from water (*26*).

Purity and concentration of authentic compounds. Stock solutions (0.1 mmol dm^{-3}) of each compound were freshly prepared. The purity of each compound was assessed by high-performance liquid chromatography (HPLC) using Waters 510 pump modules with a Waters automated gradient controller and a Supelco LC-18-S column (150 × 4.6 mm). Absorption spectra were obtained using a Hewlett–Packard Model 1040M linear diode array detector interfaced to a Hewlett–Packard 9000 Series 300 computer work station. An isocratic separation with a mobile phase consisting of 100% water at a flow rate of 1 ml/min was used for all compounds except for 8-hydroxyguanine. In this case, the mobile phase consisted of water with an acetonitrile gradient increasing at a rate of 1% per minute.

The concentrations of the stock solution of 5,6-dihydrothymine and *cis*-thymine glycol were determined gravimetrically. The concentrations of all other solutions were determined spectrophotometrically using their molar extinction coefficients (*26–28*). The purity of each compound was also assessed by GC–MS as described below. Appropriate corrections to the concentration of each compound were made in accordance with the HPLC and GC analyses.

Preparation of irradiated DNA samples. Calf thymus DNA (0.5 mg/ml) was dissolved in 30 mmol dm^{-3} phosphate buffer (pH 7.0) and denatured by heating the solution to 95°C for 5 min followed by rapid cooling in ice water. Aliquots of this solution were exposed to incremented doses of ionizing radiation at a dose rate of 166 Gy/min as measured by Fricke dosimetry (*29*) in a ^{60}Co γ-ray source (Gammacell-220, Atomic Energy of Canada Ltd.). Heat-denatured DNA was used for radiolysis in an attempt to maximize product yield (*30*). The solutions were bubbled with nitrous oxide for 20 min prior to, and then throughout, the irradiation interval. Nitrous oxide was used to saturate the DNA solutions in an effort to produce a spectrum of different types of radiation-induced products. Irradiated and untreated solutions of DNA were then dialyzed extensively against deionized water in SpectraPor6 dialysis membranes (molecular weight cutoff 1000, Fisher Scientific Co.). The quantity of DNA recovered following dialysis was measured spectrophotometrically (assuming that 1.0 OD_{260} = 50 μg/ml), by a modified Burton's assay (*31*), and gravimetrically following lyophilization. Calibration of the Burton's assay was accomplished by developing a calibration curve using ultrahigh purity DNA (Sigma). The measurement of the amount of DNA by spectrophotometric assay or the modified Burton's assay was in good agreement. Gravimetric measurements tended to be higher and were not used in the analysis of the data. Following lyophilization, 6-azathymine and 8-azaadenine were added to each 2.5-mg DNA sample. The optimal amount of internal standard added to these samples was determined from preliminary measurements.

Chemical hydrolysis of irradiated DNA. Conditions for optimal hydrolysis of irradiated DNA samples containing modified purines and pyrimidines were determined by measuring product release as a function of time of chemical hydrolysis. In this series of experiments, 1.0 ml of 88% formic acid was added to samples of DNA which had been irradiated to 100 Gy as described above and lyophilized. One set of these samples was subjected to high-performance liquid chromatography to monitor the loss of the DNA polymer peak and the increase in the peaks corresponding to the liberated bases. A Nucleogen DEAE 60-7 column (10 × 125 mm) (Altech) was used for separation and the mobile phase consisted of 15 mmol dm^{-3} phosphate buffer (pH 7.2) and 5 mmol dm^{-3} urea with an exponential gradient of 0–1 mol dm^{-3} KCl flowing at a rate of 2.2 ml/min. Absorption spectra and the absorbance at selected wavelengths were collected using instrumentation described above. A second set of DNA samples was hydrolyzed, derivatized, and analyzed by gas chromatography–mass spectrometry as described below. In this series of samples, release of the modified purine and pyrimidine bases was monitored as a function of hydrolysis time. From the data collected in these analyses, the optimal time for release of the DNA bases at 150°C was 30–40 min (see Results and Discussion).

Sample preparation for gas chromatography. In preliminary experiments, samples containing 75 nmol of 8-azaadenine and 6-azathymine were prepared in polytetrafluoroethylene-capped hypovials (Pierce). Following lyophilization, a 0.2-ml mixture of BSTFA and acetonitrile (1:1) was added and the mixture was heated for increasing time intervals at 130°C prior to analysis by gas chromatography with flame ionization detection (GC–FID) as described below. Once the time required for complete derivatization of

the internal standards was determined, 75 nmol of each trimethylsilylated internal standard was added to a lyophilized mixture containing 75 nmol of each of the authentic purine and pyrimidine compounds. These samples were derivatized and measured by GC–FID as described below and used to determine the time course of the derivatization reaction. To assess the stability of the trimethylsilylated base products over the course of days, 75 nmol each of the authentic purines and pyrimidines, including the internal standards, were added to hypovials. Following lyophilization, a 0.2-ml mixture of BSTFA and acetonitrile (1:1) was added to the samples, the mixture was then heated for 30 min at 130°C, and aliquots of this mixture were analyzed over a 5- to 6-day interval by GC–FID as described below.

For the measurement of the relative molar response factors for use in GC–MS/SIM sample analysis, mixtures of the internal standards and the authentic reference materials were prepared which contained 1–6 nmol of each compound. Following lyophilization, these samples were trimethylsilylated in a 0.2-ml mixture of BSTFA and acetonitrile (1:1) by heating for 30 min at 130°C prior to analysis by GC–MS/SIM as described below.

For the measurement of DNA samples, lyophilized samples of hydrolyzed DNA were derivatized by trimethylsilylation in a 0.2-ml mixture of BSTFA and acetonitrile (1:1) in the hypovials by heating for 30 min at 130°C prior to analysis by GC–MS/SIM as described below.

Analysis by gas chromatography with flame ionization detection A Varian Model 8000 gas chromatograph with a flame ionization detector, a Varian 3700 automatic sample injector, and a Hewlett–Packard Model 9000 Series 300 computer work station was used to measure completeness of the derivatization reaction and stability of the trimethylsilylated purines and pyrimidines using the identical chromatographic conditions described below.

Analysis by gas chromatography–mass spectrometry with selected-ion monitoring A Hewlett–Packard Model 5970B Mass Selective Detector controlled by a Hewlett–Packard Model 59970C computer work station and interfaced to a Hewlett–Packard 5890A gas chromatograph was used for analysis. The injection port and the GC–MS interface were kept at 250 and 270°C, respectively. The ion source was maintained at 250°C. Separations were carried out on a fused silica capillary column (12.5 m × 0.32 mm) coated with crosslinked 5% phenyl-methyl silicone gum phase (film thickness, 0.17 μm) (Hewlett–Packard). The column temperature was increased from 120 to 250°C at a rate of 8°C/min after 2 min at 120°C. Helium was used as the carrier gas at an inlet pressure of 10 kPa. Samples were injected using the split mode. Mass spectra were obtained at 70 eV.

Determination of product yield Calculation of product yields from each DNA sample incorporated relative molar response factors determined from slopes of calibration curves, measured peak areas of the ions representing the internal standards and the products of interest, and the measured amount of DNA in each sample. The slope of the best fit line obtained by linear regression analysis of these data was then used to assess product yield.

RESULTS AND DISCUSSION

Quantitative analysis of modified purine and pyrimidine bases by GC–MS/SIM is dependent upon completeness of two chemical reactions: (i) hydrolysis of the modified bases from the sugar–phosphate backbone of the DNA and (ii) derivatization of these products to make them volatile for gas chromatography. The analysis is also dependent upon stability of the modified purine and pyrimidine bases to the conditions of acid hydrolysis and stability of their trimethylsilylated derivatives to the conditions of derivatization. Further, stability of the trimethylsilylated products is required over the time necessary to complete the analysis of the experiment. Finally, to achieve quantitative measurement using selected ion monitoring, the mass spectrometer must be calibrated with respect to the signal generated by the internal standards and the compounds of interest. For this purpose, ideally a stable isotope-labeled analog of the analyte is used as an internal standard. A calibration plot is obtained for the response of the mass spectrometer to known quantities of both the analyte and the internal standard by monitoring an intense and characteristic ion of each

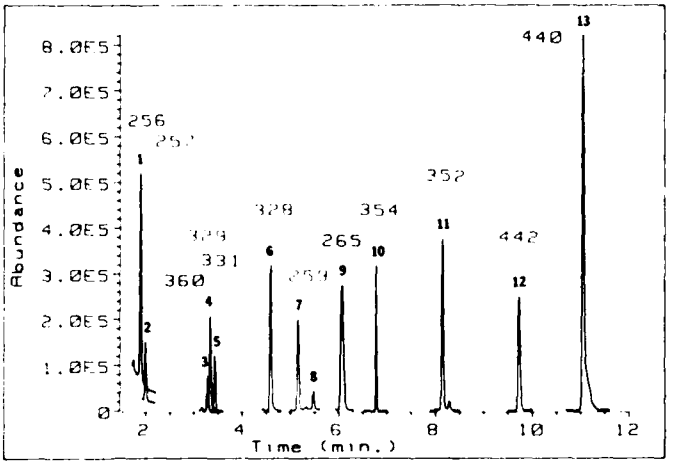

FIG. 1. Selected-ion chromatogram obtained from a trimethylsilylated hydrolysate of DNA exposed to 100 Gy of ionizing radiation in nitrous oxide-saturated solution. The ion monitored (*m/z*) for each peak is shown and peak identification is given in Table I. The mixture was separated using a temperature program from 120 to 250°C increasing at a rate of 8°C/min after 2 min at 120°C. Additional details are given in the text.

compound during the analysis (*25*). In the case of radiation-induced DNA base products, no isotope-labeled analogs are available. Therefore, a number of structurally similar compounds were evaluated for potential use as internal standards with the result that 6-azathymine and 8-azaadenine were found to be suitable for quantitation of DNA base products.

As an example of the analysis typical of that generated by GC–MS/SIM for the experiments presented herein, Fig. 1 illustrates a selected-ion chromatogram generated from a DNA sample γ-irradiated to 100 Gy in nitrous oxide-saturated aqueous solution. The chromatogram illustrates the time windows used to monitor the characteristic ions of the trimethylsilyl (Me_3Si) derivatives of the products, and their identification may be referenced in Table I. The products discussed are identified by their retention time and by selection of more than one characteristic ion to monitor simultaneously in each time window (*21*). For this analysis, approximately 3 μg of the hydrolyzed DNA sample was applied to the column. Characteristic ions for the unmodified bases were not monitored since their response would be very large relative to the modified bases. The chromatogram illustrates that the DNA base products and the internal standards can be well separated from one another (Fig. 1). Further, the chromatogram clearly demonstrates that the responses of neither the modified bases nor the internal standards, 6-azathymine and 8-azaadenine, are adversely affected by the presence of excessive quantities of unmodified bases.

The elution positions of the Me_3Si derivatives of 6-azathymine [6-azathymine $(Me_3Si)_2$] and 8-azaadenine [8-azaadenine$(Me_3Si)_2$] (peaks 1 and 9, respectively) indicate that these compounds are ideally suited for quantitative measurement by GC–MS/SIM of the modified purines and pyrimidines investigated. The trimethylsilyl derivative of 8-azaguanine was also tested as a potential internal standard. However,

TABLE I

Peak Identification in Fig. 1

Peak	*Compound*[a]	*Peak*	*Compound*[a]
1	6-Azathymine	8	(*trans*) Thymine glycol
2	5,6-Dihydrothymine	9	8-Azaadenine
3	5-Hydroxy-5,6-dihydrothymine	10	FAPy-adenine
4	5-Hydroxyuracil[b]	11	8-Hydroxyadenine
5	5-Hydroxy-5,6-dihydrouracil[c]	12	FAPy-guanine
6	5-Hydroxycytosine[d]	13	8-Hydroxyguanine
7	(*cis*) Thymine glycol		

[a] As their trimethylsilyl derivatives.
[b] 5-Hydroxyuracil is a product of the acid-induced deamination and dehydration of cytosine glycol (*35*).
[c] 5-Hydroxy-5,6-dihydrouracil is the deamination product of 5-hydroxy-5,6-dihydrocytosine (*20*).
[d] 5-Hydroxycytosine is a product of the acid-induced dehydration of cytosine glycol (*35*).

despite having an ideal elution position (approximately 9.4 min), this compound was not suitable for use as an internal standard because of its poor solubility in water. Several other reasons make these compounds a good choice for use as internal standards. These compounds are stable in acid, are available commercially, and are not formed in treated DNA. The trimethylsilylated products are stable over a period of days (data not shown) and the mass spectra of 6-azathymine$(Me_3Si)_2$ and 8-azaadenine$(Me_3Si)_2$ exhibit intense $M^{+\cdot}$ and $(M-Me)^+$ ions (m/z 271 and 256, respectively, and m/z 280 and 265, respectively).

The extent of derivatization and the stability of the trimethylsilylated derivatives of the modified purines and pyrimidines were also addressed. Derivatization of purines and pyrimidines has been known to occur over a very rapid time scale (*32–34*). However, the time dependence of the derivatization reaction for the radiation-induced purine and pyrimidine products has not been reported. Figure 2 reveals the time course of the derivatization reactions for the modified purines and pyrimidines reported herein and indicates that the reactions proceed to completion within 20 min. However, due to the number of the samples generated in these experiments and the finite time required to perform an analysis, stability of the trimethylsilyl products over the time course of days was determined. Figure 3 confirms the stability of those products over the number of days required to complete the analysis for a typical experiment. These data indicate that the derivatization proceeds very rapidly and that the trimethylsilylated products thus formed are indeed stable for sufficient time to complete the experimental analyses.

Having demonstrated that the derivatization reaction was optimized, calibration of the mass spectrometer using authentic purine and pyrimidine compounds was necessary. The mass spectrometer was calibrated by analyzing samples containing known molar amounts of the modified bases and internal standards. The ion current ratio of an ion of a compound and an ion of the internal standards was measured and plotted as a function of the ratio of the molar amounts of the compound and the internal standard. This yielded a calibration plot, in which the slope of the linear

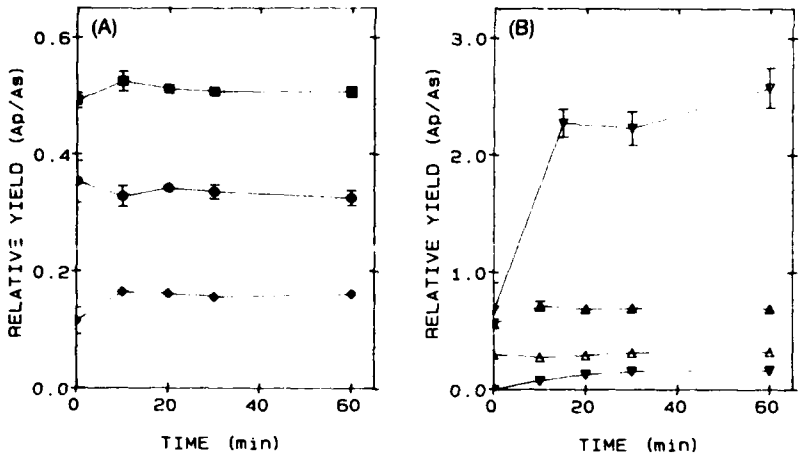

FIG. 2. Time dependence of derivatization of modified purine and pyrimidine bases. The ratio of the area of the product over that of the internal standard (A_p/A_s) as measured by GC-FID was plotted as a function of time of derivatization at 130°C. (A) Modified pyrimidines using 6-azathymine as the internal standard: (●) 5,6-dihydrothymine($Me_3Si)_2$ (*m/z* 257); (◆) thymine glycol($Me_3Si)_4$ (*m/z* 259); (■) 5-hydroxyuracil($Me_3Si)_3$ (*m/z* 329). (B) Modified purines using 8-azaadenine as the internal standard: (▲) FAPy-adenine($Me_3Si)_3$ (*m/z* 354); (△) 8-hydroxyadenine($Me_3Si)_3$ (*m/z* 352); (▼) FAPy-guanine($Me_3Si)_4$ (*m/z* 442); (▽) 8-hydroxyguanine($Me_3Si)_4$ (*m/z* 440). Each data point represents the mean (±SE) from three replicate experiments.

regression line represents the relative molar response factor (*25*). High sensitivity for product detection can be achieved by monitoring the most intense characteristic ion of the compound under analysis. In general, the most intense characteristic ions for

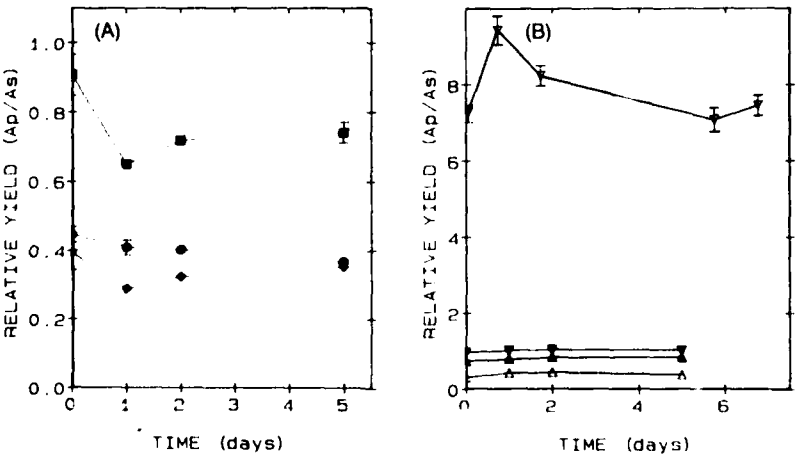

FIG. 3. Stability of modified purine and pyrimidine bases after derivatization. Data were obtained using GC-FID and plotted similar to that illustrated in Fig. 2. Modified pyrimidines (A) and purines (B) are also identified in Fig. 2. Each data point represents the mean (±SE) from three replicate experiments.

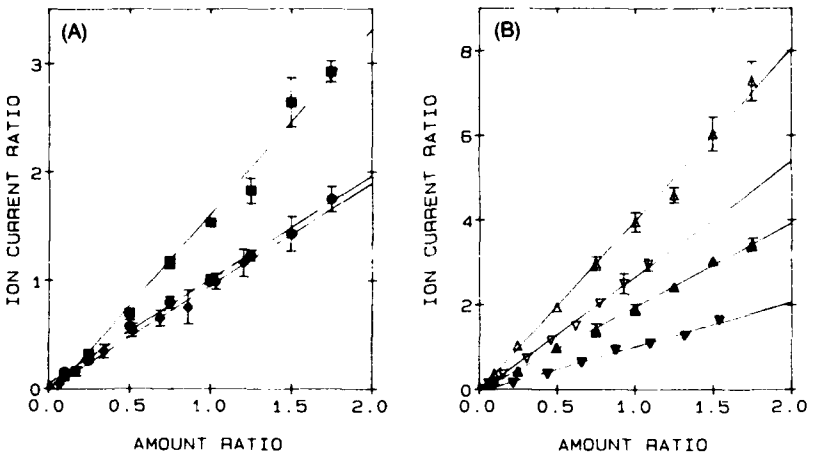

FIG. 4. (A) Calibration plots for the Me_3Si derivatives of the modified pyrimidine bases relative to 6-azathymine$(Me_3Si)_2$. The slope of the lines represents the relative molar response factors for (●) 5,6-dihydrothymine$(Me_3Si)_2$ (*m/z* 257); (◆) thymine glycol$(Me_3Si)_4$ (*m/z* 259); and (■) 5-hydroxyuracil$(Me_3Si)_3$ (*m/z* 329). (B) Calibration plots for the Me_3Si derivatives of the modified purine bases relative to 8-azaadenine$(Me_3Si)_2$. The slope of the lines represents the relative molar response factors for (▲) FAPy-adenine$(Me_3Si)_3$ (*m/z* 354); (△) 8-hydroxyadenine$(Me_3Si)_3$ (*m/z* 352); (▼) FAPy-guanine$(Me_3Si)_4$ (*m/z* 442); and (▽) 8-hydroxyguanine$(Me_3Si)_4$ (*m/z* 440). Each data point represents the mean (±SE) from three replicate experiments and the data were fitted by least-squares linear regression analysis.

the Me_3Si derivatives of the modified bases used here are the molecular ion ($M^{+\cdot}$) and the characteristic $(M-Me)^+$ ion (for the mass spectra see Refs. (*19*) and (*20*)). In the case of thymine glycol$(Me_3Si)_4$, the intense *m/z* 259 ion was used. An example of the determination of the relative molar response factors for the *m/z* 257, 329, and 259 ions of 5,6-dihydrothymine$(Me_3Si)_2$, 5-hydroxyuracil$(Me_3Si)_3$, and thymine glycol$(Me_3Si)_4$, respectively, is illustrated in Fig. 4A using the *m/z* 256 ion of 6-azathymine$(Me_3Si)_2$. Figure 4B illustrates an example of the determination of the relative molar response factors of the *m/z* 354, 352, 442, and 440 ions of FAPy-adenine$(Me_3Si)_3$, 8-hydroxyadenine$(Me_3Si)_3$, FAPy-guanine$(Me_3Si)_4$, and 8-hydroxyguanine$(Me_3Si)_4$, respectively, using the *m/z* 265 ions of 8-azaadenine $(Me_3Si)_2$. These figures indicate that the response of the mass spectrometer for these compounds in the range of the ratio of concentrations used was linear. The yield of 5,6-dihydroxy-5,6-dihydrocytosine (cytosine glycol), which is the actual radiation-induced product of the cytosine moiety in DNA (*20*), is represented by the summation of the yields of 5-hydroxycytosine and 5-hydroxyuracil. These compounds result from the acid-induced modification of cytosine glycol (*35*). In the case of 5-hydroxycytosine$(Me_3Si)_3$, the relative molar response factors were assumed to be equal to those of 5-hydroxyuracil$(Me_3Si)_3$ due to the lack of authentic compound. This assumption was based upon the similarity of the mass spectra of these compounds with respect to the ions and their relative intensities (for comparison of the mass spectra see Refs. (*20*) and (*22*)). Due to lack of authentic reference standards, relative molar response factors for the compounds 5-hydroxy-5,6-dihydrouracil [the acid-induced degradation product of 5-hydroxy-5,6-dihydrocytocine (*20*)] and 5-hy-

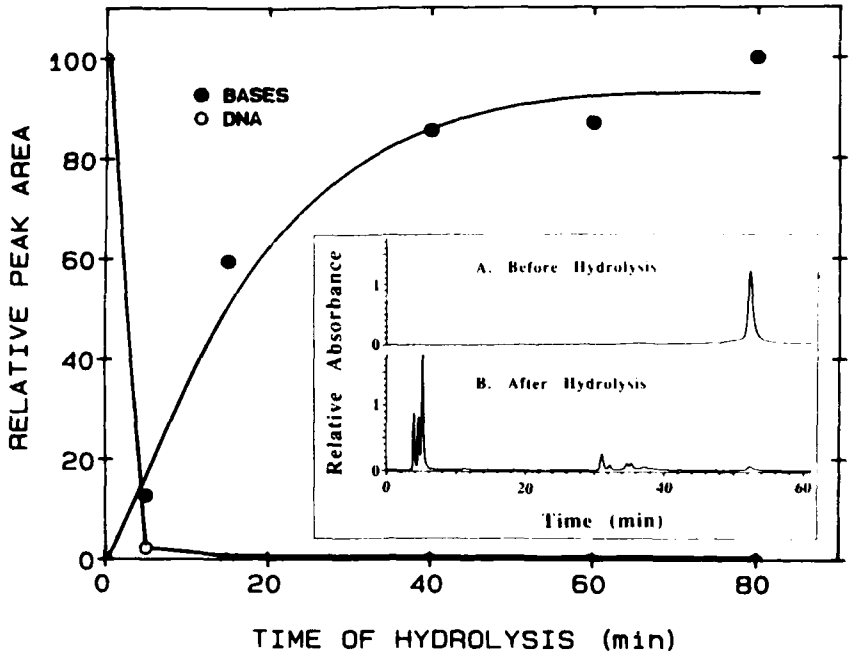

FIG. 5. Release of bases from DNA irradiated to 100 Gy in nitrous oxide-saturated aqueous solution as measured by HPLC as a function of time of formic acid hydrolysis at 150°C. The inset illustrates the HPLC chromatogram of irradiated DNA before (A) and after (B) 40 min of acid hydrolysis.

droxy-5,6-dihydrothymine were estimated from the mass spectra of these compounds and therefore may have an error associated with them. The measured relative molar response factors are not universal since they are dependent upon experimental and instrumental parameters and might also change according to the tuning conditions associated with the day to day operation of the mass spectrometer. Hence the relative molar response factors must be determined in each laboratory and measured routinely to ensure accurate measurements.

With respect to analyses of irradiated DNA samples, the modified purine and pyrimidine bases must first be released from the sugar–phosphate backbone of the DNA molecule. Removal of purine and pyrimidine bases from DNA in the presence of formic acid (*36*) is one method which has been used to assess the yield of acid-stable radiation products (*3, 11*). In the present work, release of DNA bases from a sample of DNA irradiated to 100 Gy as a function of time of hydrolysis in formic acid was followed by HPLC using an ion-exchange column capable of separating highly polymerized DNA from purines and pyrimidines. The chromatograms illustrated in the inset of Fig. 5, where the absorbance at 260 nm is monitored over the time of chromatography, reveal that high-molecular-weight DNA (retention time 52 min on chromatogram A) is hydrolyzed to the constituent bases (retention time 3–6 min on chromatogram B). The time course of this hydrolysis, as illustrated in Fig. 5, indicates that base release has gone to completion within 40 min. The peaks eluting between

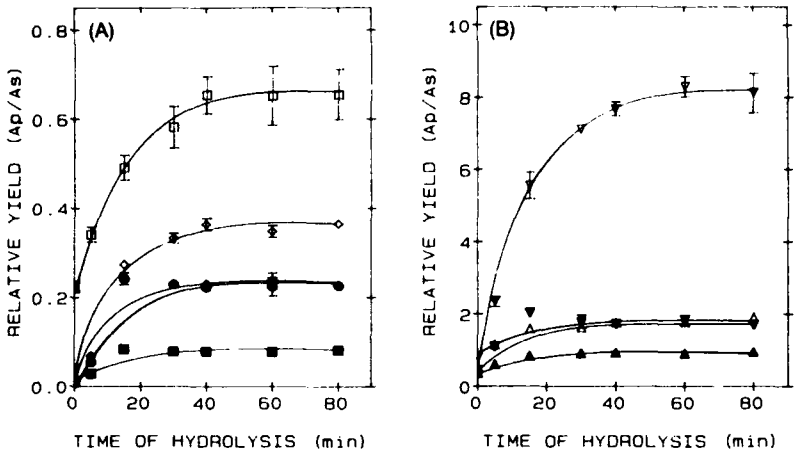

FIG. 6. Release of base products from samples of DNA irradiated to 100 Gy in nitrous oxide-saturated aqueous solution as measured by GC-MS/SIM as a function of the time of formic acid hydrolysis at 150°C. (A) Modified pyrimidines: (●) 5,6-dihydrothymine; (■) 5-hydroxy-5,6-dihydrocytosine; (◆) 5-hydroxy-5,6-dihydrothymine; (□) cytosine glycol; ( ) thymine glycol. (B) Modified purines: (▲) FAPy-adenine; (△) 8-hydroxyadenine; (▼) FAPy-guanine; (▽) 8-hydroxyguanine. Each data point represents the mean (±SE) from three replicate experiments.

30 and 40 min in the hydrolyzed sample of irradiated DNA (chromatogram B) are devoid of absorbance spectra characteristic of purine or pyrimidine constituents and are as yet unidentified. Analysis of these samples by GC–MS/SIM reveals that a plateau for release of the radiation-induced DNA base products occurs within 40 min. If the modified bases were labile under the acidic conditions used, then a decrease in their yield would occur over prolonged exposure. However, a distinct plateau was maintained for at least 80 min of heating at 150°C (Fig. 6). The data in Figs. 5 and 6 indicate that the release of modified purines and pyrimidines from the sugar–phosphate backbone of DNA is complete within 30–40 min of hydrolysis in acid at 150°C and that the products are stable under these conditions.

As a demonstration of this methodology for quantitative analysis of radiation-induced DNA base modification, product formation was assessed as a function of radiation dose. Figure 1 illustrates a selected-ion chromatogram generated from a DNA sample which was γ-irradiated to 100 Gy in nitrous oxide-saturated aqueous solution. Following analysis, the areas of the peaks representing those products listed in Table I were integrated and product yield from each sample was calculated. Figure 7 illustrates the product yield in each DNA sample in terms of micromoles per gram of DNA plotted as a function of radiation dose. Generally, products were detected in low yields in unirradiated samples (Fig. 7; Ref. (*22*)). However, product yield was found to increase linearly as a function of radiation dose in the range studied. From these data, radiation chemical yield was calculated from the slope of the best-fit lines obtained by least-squares linear regression analysis and listed in Table II. Although several studies address the yield of the radiation-induced DNA base products in air- and/or nitrogen-saturated aqueous solution (*3–6, 8–15*), no studies which permit di-

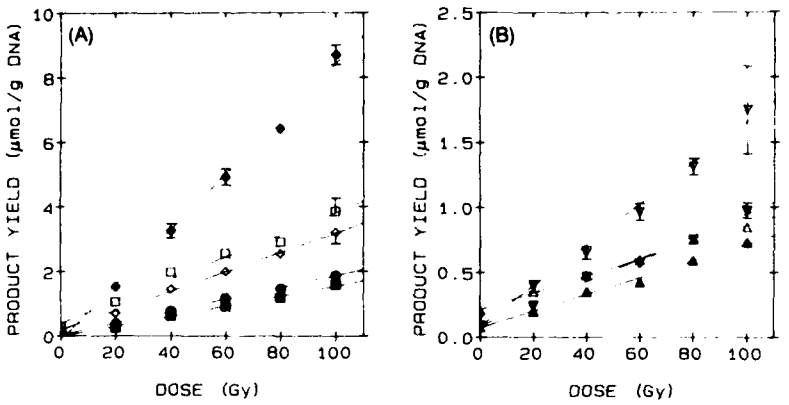

FIG. 7. Product formation resulting from exposure of nitrous oxide-saturated solutions of heat-denatured DNA to ionizing radiation. (A) Modified pyrimidines: (●) 5,6-dihydrothymine; (■) 5-hydroxy-5,6-dihydrocytosine; (◆) 5-hydroxy-5,6-dihydrothymine; (□) cytosine glycol; ( ) thymine glycol. (B) Modified purines: (▲) FAPy-adenine; (△) 8-hydroxyadenine; (▼) FAPy-guanine; (▽) 8-hydroxyguanine. Each data point represents the mean (±SE) from three replicate experiments and the data were fitted by least-squares linear regression analysis.

rect comparison of the yield of these products obtained from DNA samples irradiated in nitrous oxide-saturated aqueous solution are available.

In summary, 6-azathymine and 8-azaadenine have been suggested for use as appropriate internal standards for quantitative measurement of radiation-induced DNA base damage using the GC–MS/SIM technique and the procedure used to calibrate the mass spectrometer by experimental determination of relative molar response factors has been presented. Studies which demonstrate completeness of acid hydrolysis

TABLE II

Product Yield from DNA Samples Irradiated in Nitrous Oxide-Saturated Solutions in the Heat-Denatured Conformation[a]

Product	*Product yield* (μmol J^{-1}) × 10^{3}
5,6-Dihydrothymine	0.88
5-Hydroxy-5,6-dihydrothymine	4.05[b]
Cytosine glycol	1.63[b]
5-Hydroxy-5,6-dihydrocytosine	0.74[b]
Thymine glycol	1.43
FAPy-adenine	0.31
8-Hydroxyadenine	0.31
FAPy-guanine	0.41
8-Hydroxyguanine	0.75

[a] DNA, 0.5 mg/ml, in 30 mmol dm^{-3} phosphate buffer, pH 7.0.

[b] Relative molar response factors have been estimated.

of the DNA samples and optimization of the derivatization reactions were presented. In addition, the stability of the modified DNA bases in acid and the stability of the trimethylsilylated DNA bases over the time course required to complete analysis of a typical experiment were also described. Using this methodology, the yield of radiation-induced DNA base damage was assessed in samples of heat-denatured DNA exposed to γ radiation in nitrous oxide-saturated aqueous solution and radiation chemical yields under these conditions are reported. Quantitative measurement of a plethora of radiation-induced DNA base modifications under a variety of radiolysis conditions is now feasible.

ACKNOWLEDGMENTS

This research was supported, in part, by the Armed Forces Radiobiology Research Institute of the Defense Nuclear Agency, under Research Work Unit 00105. The authors thank Dr. E. Holwitt of the Armed Forces Radiobiology Research Institute for the kind gift of thymine glycol. The views expressed in this article are those of the authors and do not reflect the official views or position of the Department of Defense or the U.S. Government.

RECEIVED: December 12, 1988; ACCEPTED: March 21, 1989

REFERENCES

1. C. VON SONNTAG, *The Chemical Basis of Radiation Biology*. Taylor & Francis, London, 1987.
2. R. B. PAINTER, The role of DNA damage and repair in cell killing induced by ionizing radiation. In *Radiation Biology in Cancer Research* (R. E. Meyn and H. R. Withers, Eds.), pp. 59–68. Raven Press, New York, 1980.
3. R. TÉOULE, C. BERT, and A. BONICEL, Thymine fragment damage retained in the DNA polynucleotide chain after gamma irradiation in aerated solutions. II. *Radiat. Res.* **72**, 190–200 (1977).
4. A. BONICEL, N. MARIAGGI, E. HUGHES, and R. TÉOULE, *In vitro* γ irradiation of DNA: Identification of radioinduced chemical modifications of the adenine moiety. *Radiat. Res.* **83**, 19–26 (1980).
5. K. FRENKEL, M. GOLDSTEIN, and G. W. TEEBOR, Identification of the *cis* thymine glycol moiety in chemically oxidized and γ-irradiated deoxyribonucleic acid by high-pressure liquid chromatography analysis. *Biochemistry* **20**, 7566–7571 (1981).
6. L. H. BREIMER and T. LINDAHL, Thymine lesions produced by ionizing radiation in double-stranded DNA. *Biochemistry* **24**, 4018–4022 (1985).
7. K. FRENKEL, A. CUMMINGS, J. SOLOMON, J. CADET, J. J. STEINBERG, and G. W. TEEBOR, Quantitative determination of the 5-(hydroxymethyl)uracil moiety in the DNA of γ-irradiated cells. *Biochemistry* **24**, 4527–4533 (1985).
8. E. A. FURLONG, T. J. JORGENSEN, and W. D. HENNER, Production of dihydrothymidine stereoisomers in DNA by γ-irradiation. *Biochemistry* **25**, 4344–4349 (1986).
9. H. KASAI, P. F. CRAIN, Y. KUCHINO, S. NISHIMURA, A. OOTSUYAMA, and H. TANOOKA, Formation of 8-hydroxyguanine moiety in cellular DNA by agents producing oxygen radicals and evidence for its repair. *Carcinogenesis* **7**, 1849–1851 (1986).
10. G. TEEBOR, A. M. CUMMINGS, K. FRENKEL, A. SHAW, L. VOITURIEZ, and J. CADET, Quantitative measurement of the diastereoisomers of *cis* thymidine glycol in gamma-irradiated DNA. *Free Radical Res. Commun.* **2**, 303–309 (1987).
11. R. TÉOULE and A. GUY, Quantitative measurements of modified thymine residues in DNA chains by formic acid hydrolysis. *Nucleosides Nucleotides* **6**, 301–305 (1987).
12. G. J. WEST, I. W.-L. WEST, and J. F. WARD, Radioimmunoassay of a thymine glycol. *Radiat. Res.* **90**, 595–608 (1982).
13. G. J. WEST, I. W.-L. WEST, and J. F. WARD, Radioimmunoassay of 7,8-dihydro-8-oxoadenine (8-hydroxyadenine). *Int. J. Radiat. Biol.* **42**, 481–490 (1982).

14. S. A. LEADON and P. C. HANAWALT, Monoclonal antibody to DNA containing thymine glycol. *Mutat. Res.* **112,** 191–200 (1983).
15. R. RAJAGOPALAN, R. J. MELAMEDE, M. F. LASPIA, B. F. ERLANGER, and S. S. WALLACE, Properties of antibodies to thymine glycol, a product of the radiolysis of DNA. *Radiat. Res.* **97,** 499–510 (1984).
16. A. F. FUCIARELLI, G. G. MILLER, and J. A. RALEIGH, An immunochemical probe for 8,5′-cycloadenosine-5′-monophosphate and its deoxy analog in irradiated nucleic acids. *Radiat. Res.* **104,** 272–283 (1985).
17. P. V. HARIHARAN, Determination of thymine ring saturation products of the 5,6-dihydroxydihydrothymine type by the alkali degradation assay. *Radiat. Res.* **81,** 496–498 (1980).
18. H. L. KATCHER and S. S. WALLACE, Characterization of the *Escherichia coli* X-ray endonuclease, endonuclease III. *Biochemistry* **22,** 4071–4081 (1983).
19. M. DIZDAROGLU, The use of capillary gas chromatography-mass spectrometry for identification of radiation-induced DNA base damage and DNA base-amino acid crosslinks. *J. Chromatogr.* **295,** 103–121 (1984).
20. M. DIZDAROGLU, Application of capillary gas chromatography–mass spectrometry to chemical characterization of radiation-induced base damage of DNA: Implications for assessing DNA repair processes. *Anal. Biochem.* **144,** 593–603 (1985).
21. M. DIZDAROGLU, Chemical characterization of ionizing radiation-induced damage to DNA. *BioTechniques* **4,** 536–546 (1986).
22. M. DIZDAROGLU and D. S. BERGTOLD, Characterization of free radical-induced base damage in DNA at biologically relevant levels. *Anal. Biochem.* **156,** 182–188 (1986).
23. M.-L. DIRKSEN, W. F. BLAKELY, E. HOLWITT, and M. DIZDAROGLU, Effect of DNA conformation on the hydroxyl radical-induced formation of 8,5′-cyclopurine 2′-deoxyribonucleoside residues in DNA. *Int. J. Radiat. Biol.* **54,** 195–204 (1988).
24. E. GAJEWSKI, A. F. FUCIARELLI, and M. DIZDAROGLU, Structure of hydroxyl radical-induced DNA-protein crosslinks in calf thymus nucleohistones *in vitro*. *Int. J. Radiat. Biol.* **54,** 445–459 (1988).
25. J. T. WATSON, *Introduction to Mass Spectrometry*. Raven Press, New York, 1985.
26. L. F. CAVALIERI and A. BENDICH, The ultraviolet absorption spectra of pyrimidines and purines. *J. Am. Chem. Soc.* **72,** 2587–2594 (1950).
27. D. B. DUNN and R. H. HALL, In *Handbook of Biochemistry and Molecular Biology Nucleic Acids* (G. D. Fasman, Ed.), 3rd ed., Vol. 1, p. 65. CRC Press, Boca Raton, FL, 1983.
28. A. ALBERT, Chemistry of 8-Azapurines (1,2,3-Triazolo[4,5-d] pyrimidines). In *Advances in Heterocyclic Chemistry* (A. R. Katritzky, Ed.), Vol. 39, pp. 117–180. Academic Press, New York, 1986.
29. H. FRICKE and E. J. HART, Chemical dosimetry. In *Radiation Dosimetry* (F. H. Attix and W. C. Roesch, Eds.), 2nd ed., Vol. 2, pp. 167–239. Academic Press, New York, 1966.
30. J. F. WARD and I. KUO, Radiation damage to DNA in aqueous solution: A comparison of the response of the single-stranded form with that of the double-stranded form. *Radiat. Res.* **75,** 278–285 (1978).
31. K. BURTON, Determination of DNA concentration with diphenylamine. In *Methods in Enzymology* (L. Grossman and K. Moldzie, Eds.), Vol. 12, Part B, pp. 163–166. Academic Press, New York, 1968.
32. C. W. GEHRKE and D. B. LAKINGS, Gas–liquid chromatography of the purine and pyrimidine bases. *J. Chromatogr.* **61,** 45–63 (1971).
33. D. B. LAKINGS and C. W. GEHRKE, Analysis of base composition of RNA and DNA hydrolysates by gas–liquid chromatography. *J. Chromatogr.* **65,** 347–367 (1971).
34. V. MILLER, V. PACAKOVA, and E. SMOLKOVA, Gas-liquid chromatographic analysis of trimethylsilyl derivatives of pyrimidines and purines bases and nucleosides. *J. Chromatogr.* **119,** 355–367 (1976).
35. M. DIZDAROGLU, E. HOLWITT, M. P. HAGAN, and W. F. BLAKELY, Formation of cytosine glycol and 5,6-dihydroxycytosine in deoxyribonucleic acid on treatment with osmium tetroxide. *Biochem. J.* **235,** 531–536 (1986).
36. G. R. WYATT and S. S. COHEN, The bases of the nucleic acids of some bacterial and animal viruses: the occurrence of 5-hydroxymethylcytosine. *Biochem. J.* **55,** 774–782 (1953).

Reprinted from the AMERICAN JOURNAL OF VETERINARY RESEARCH, Vol. 50, No. 7, Pages 1102-1105.
© American Veterinary Medical Association, 1989. All rights reserved.

Tropism of canine neutrophils to xanthine oxidase

Dale F. Gruber, PhD, and Ann M. Farese, MA

ARMED FORCES RADIOBIOLOGY RESEARCH INSTITUTE
SCIENTIFIC REPORT
SR89-31

SUMMARY

Quantitative evaluation of neutrophil chemotaxis was performed on cells obtained by hypotonic-lysis techniques from heparinized blood samples from clinically normal dogs. The techniques resulted in neutrophil recovery rates between 60 and 80%. Chemotaxis comparisons were based on cellular migration in microchambers equipped with polycarbonate membranes with 5-μm pores. Chemoattractant comparisons were based on neutrophil migration to medium, normal canine plasma, zymosan-activated plasma, and xanthine oxidase. Cellular migration to zymosan-activated plasma in buffer (1:100 dilution) was significantly ($P < 0.001$) enhanced over random baseline medium migration. Neutrophil migrations to normal canine plasma and xanthine oxidase were quantitatively less than to zymosan-activated plasma, but were equivalent to each other and significantly greater than for random migration. Migration to xanthine oxidase was maximal at concentrations near 1 U/ml within 30 minutes.

Exposure of neutrophils to inflammatory substances initiates physiologic and metabolic changes in the cell, including ion fluxes,[1] cellular orientation or polarization,[2] locomotion,[3] lysosomal secretion,[4] and production of reactive oxygen intermediates.[5] One important intermediate of oxygen metabolism is superoxide anion. Neutrophils reportedly release superoxide anion during phagocytosis[6] or after activation by complement, aggregated immunoglobulins,[5] or endotoxins.[7] The participation, or relationship, of superoxide anion to the inflammation process has been inferred from the anti-inflammatory effects of its antagonist, superoxide dismutase.[8,9] Superoxide anion also may be produced acellularly by enzymatic action. Xanthine oxidase was the first identified biological source of superoxide anion.[10] Widely distributed, xanthine oxidase is particularly rich in lung, liver, and intestinal tissues,[11] where it exists primarily as xanthine dehydrogenase.[12] Xanthine oxidase, an oxireductase, generates superoxide anion from xanthine, hypoxanthine, and acetaldehyde substrates. Neutrophil chemotaxis toward inflammation may be related to the presence of superoxide anion.[13] Despite the fact that defective inflammatory cell migration has been associated with the pathogenesis of many diseases, little information exists on operant regulatory mechanisms. Even less is known of chemotaxis regulation in dogs, despite the fact that dogs are being used for investigation of septic shock,[14-16] pulmonary injury,[17] and myocardial infarction.[18] The study reported here was conducted to determine whether xanthine oxidase, an superoxide anion substrate, alters the directed migration of isolated canine neutrophils.

Materials and Methods

Animals—Hra Beagles (*Canis familiaris*) 1 to 2 years old and weighing 10 to 12 kg were quarantined and screened for evidence of disease before being released to experiments. Unless prescribed by protocol, subjects were not administered medication for 30 days prior to or during experimental participation. Dogs were provided commercial dog food and allowed access to tap water ad libitum. Animal-holding rooms were maintained at 21 C ± 1 C with 50% ± 10% relative humidity, using at least 10 air changes/hour of 100% conditioned fresh air. All holding rooms were maintained on a 12-hour light-dark full-spectrum photoperiod with no twilight.

Neutrophil isolation—Blood (5 ml, once/month) was drawn from each dog's lateral saphenous vein into heparinized[a] (10 U/ml of blood) syringes. Blood was washed in Hanks balanced salt solution[a] (400 × g, 10 minutes, 21 C). Contaminating RBC were lysed with 0.83% NH_4Cl[b] (10 minutes, 4 C) and washed in Hanks balanced salt solution. The leukocyte pellet was suspended in phosphate-buffered saline solution[c] supplemented with 0.2% heat-inactivated fetal bovine serum.[d] Wright-stained blood smears were prepared for differential and morphologic examinations. Complete blood cell counts were obtained by automated analysis.[e] Viability of cells isolated in this manner was > 95% when assessed by trypan blue or propidium iodide exclusion.

Chemoattractants—Zymosan-activated plasma was prepared by incubating 5 mg of zymosan[b]/ml of freshly drawn plasma for 30 minutes at 37 C. Zymosan was removed by centrifugation (400 × g, 10 minutes, 21 C). Plasma or zymosan-activated plasma chemoattractants were prepared by adding plasma to buffer at a concentration of 1:100 (v/v). Xanthine oxidase was added to phosphate-buffered saline solution at 2.5, 5, 10, and 20/1,000 (v/v). Control wells received phosphate-buffered saline solution alone.

Received for publication Mar 22, 1988.
From the Armed Forces Radiobiology Research Institute, Wisconsin Ave, Bethesda, MD 20814-5145.
Supported by the Armed Forces Radiobiology Research Institute, Defense Nuclear Agency, under work unit 00130.
The authors acknowledge the technical assistance of Kevin P. O'Halloran.

[a] Hanks balanced salt solution and preservative-free sodium heparin, Grand Island Biological Co, Grand Island, NY.
[b] Xanthine oxidase (xanthine oxireductase, grade III), superoxide oxidoreductase (superoxide dismutase), zymosan-A, and NH_4Cl, Sigma Chemical Co, St Louis, Mo.
[c] Phosphate-buffered saline solution, Biofluids Inc, Rockville, Md.
[d] Fetal bovine serum, Hyclone Laboratories, Logan, Utah.
[e] Model S, plus II, Coulter Electronics, Hialeah, Fla.

Chemotaxis assay—A 48-well microchemotaxis chamber assembly[f] was used to quantitate cellular migration by counting neutrophils that migrated through a 10-μm-thick polycarbonate polyvinyl pyrrolidone-free membrane with 5-μm pores.[g] Lower wells received chemoattractant or medium. Upper wells received a cellular mixture adjusted to contain 10^5 neutrophils. Chambers were incubated at 37 C for 1 hour. Filters were removed and the nonmigrating side was scraped clean of cells. Filters were fixed in 100% methanol for 1 minute and stained in differential stain.[h] Four high-power (100 ×) microscopic fields across the diameter of the well were examined, and the mean cellular migration per field per hour was determined.

Statistical Analysis—All data were recorded as mean ± SEM. Differences were analyzed for statistical significance, using the Student *t* test.

Results

The migratory responses of neutrophils to concentrations of xanthine oxidase between 0.125 and 1 U/ml, final volume, are depicted (Fig 1). Migration to 1 U/ml was generally better than the migration to lower concentrations, but was significantly ($P < 0.05$) increased only at 90 minutes. The highest concentration level was selected for further examination.

The migration of neutrophils to chemotaxis medium alone was enhanced by the inclusion of 1 U of xanthine oxidase/ml of medium (Fig 2). At 30 minutes' incubation, cellular migration toward 1 U of xanthine oxidase was significantly ($P < 0.01$) enhanced over that toward medium alone. This level of significance was maintained through the 90-minute incubation period.

[f] Neuro Probe Inc, Bethesda, Md
[g] Nucleopore Corp, Pleasanton, Calif
[h] Dif-Quick stain, Fischer Scientific, Silver Spring, Md

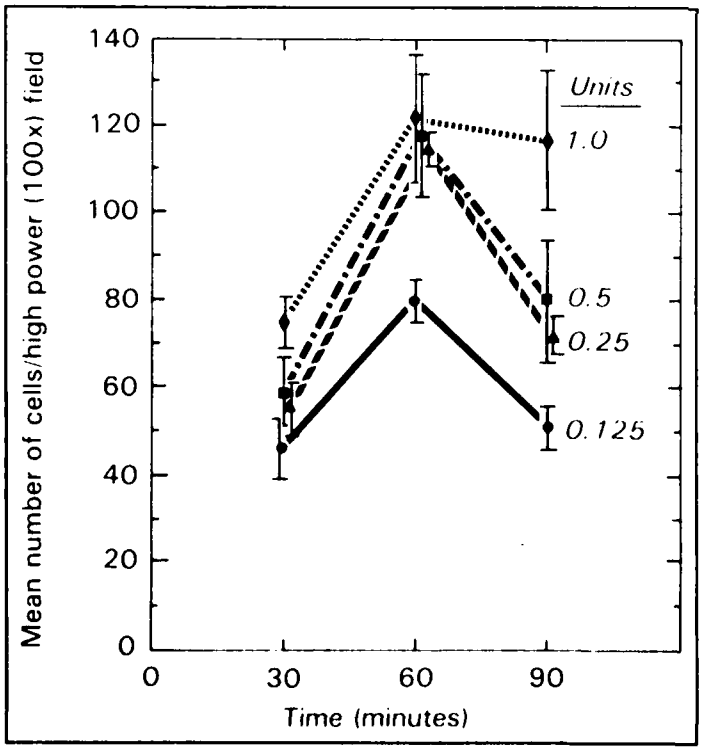

Fig 1—Migration of neutrophils to various concentrations of xanthine oxidase. Data points are the mean number (± SEM) of migrating cells per high-power field. Mean cellular migration was determined from a minimum of 4 high-power fields from triplicate samples. Minimum of 5 dogs were examined per data point.

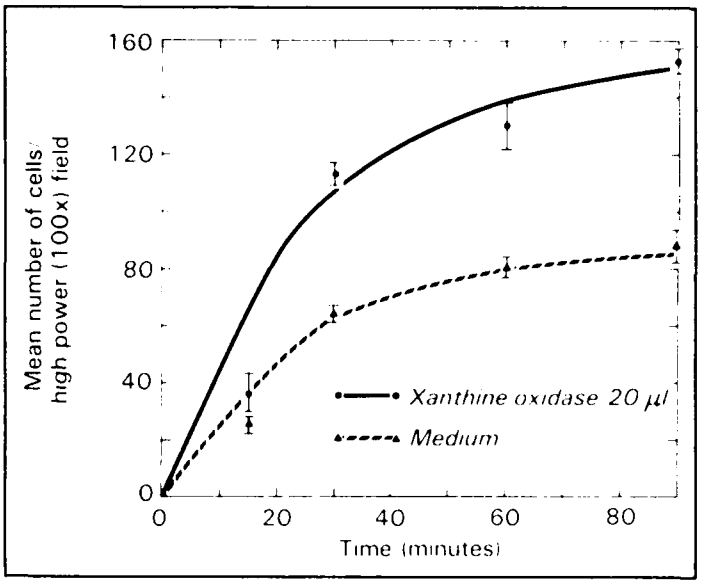

Fig 2—Migration of neutrophils to 1 U of xanthine oxidase ml of medium or to medium alone over a 90-minute period

TABLE 1 Neutrophil chemotaxis

	No.*	Mean No. of cells/HPF ± SEM	*P* vs medium
Medium	26	79 ± 3	
Plasma§	26	113 ± 6	0.001
Zymosan-activated plasma§	26	147 ± 9	0.001
Xanthine oxidase (1 U/ml of medium)	26	118 ± 6	0.001

* No. of experimental observations/10 field. HPF (high-power (100×) field. § 1:100 dilution of plasma to medium.

Migration of neutrophils to medium, normal plasma, zymosan-activated plasma and xanthine oxidase. Data are expressed as mean number of migrating cells/HPF field (± SEM) for 18 to 24 subjects.

To determine whether the chemotaxis technique was affected by cellular concentration, a titration curve was developed. Neutrophils responded to medium alone or to 1 U of xanthine oxidase ml of medium, in almost straight-line fashion (Fig 3). The cellular concentration selected for further examination was 2×10^6 cells/ml.

On the basis of the total and differential leukocyte counts obtained from the CBC counts and final cell isolates, 76% of the total available neutrophils were harvested by these techniques. Final cell isolates were almost 89% neutrophils. Viability was normally > 95% when examined by trypan blue or propidium iodide exclusion.

The mean background random migration was 79 ± 3 cells/high-power field (Table 1). The presence of 1:100 normal dog plasma in buffer increased the mean migration/high-power field to 113 ± 6 cells ($P < 0.001$). Similar concentrations of the same plasma aliquot activated by zymosan resulted in mean migration of 147 ± 9 cells/high-power field ($P < 0.001$ vs medium, $P = 0.008$ vs plasma). Xanthine oxidase added to buffer resulted in mean cellular migration of 118 ± 6 cells/high-power field ($P < 0.001$ vs medium). The migratory effect attributable to the addition of xanthine oxidase to buffer was not significantly different from the migratory effect of plasma (P

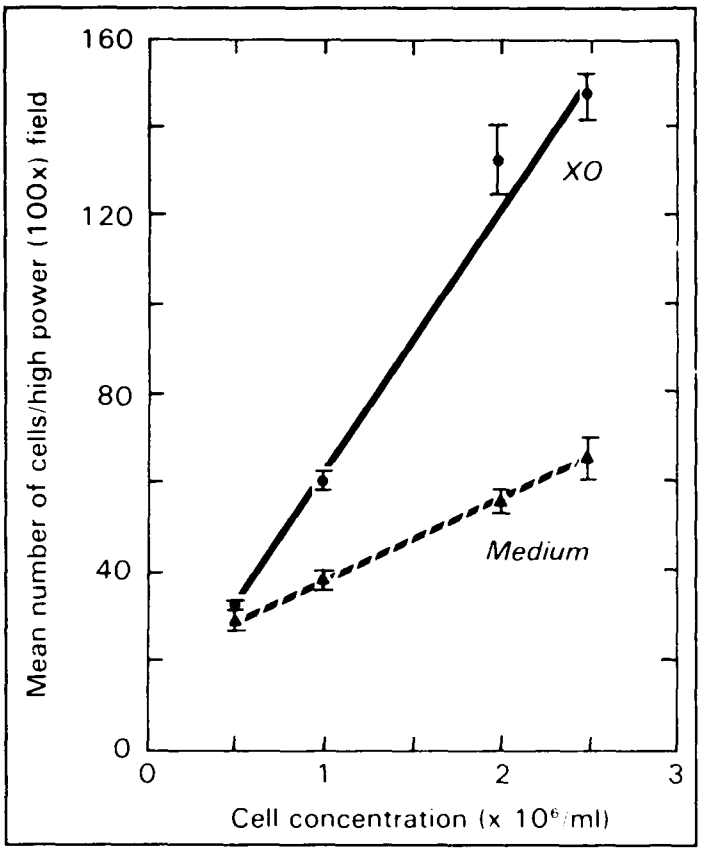

Fig 3 Migratory effects of 1 U of xanthine oxidase ml on neutrophil concentrations ranging between 0 5 and 2 5 · 1C' cells ml

· 0.5528), but was less than that for zymosan-activated plasma (P 0.02).

Discussion

The physiologic response(s) of a host to trauma includes inflammatory processes characterized by the infiltration and accumulation of neutrophils. The amplification or perpetuation of inflammatory responses depends on the emigration of normal leukocytes into the area of injury. Trauma may alter the capacity of neutrophils to migrate, thereby exacerbating existing bacterial infections into serious, often fatal, septecemia. Neutrophils migrate to injury sites by moving along concentration gradients established by intrinsic factors, eg, complement-split products or extrinsic factors, such as those elaborated by bacteria. Inflammatory cells also have been suggested as an intrinsic chemotactic source based on suppression of leukocyte infiltration after superoxide dismutase administration in rodents[17] and human beings.[20] Petrone et al[19] suggested that superoxide anion elaborated from neutrophils reacted with plasma products to generate chemotaxigenic factor(s). Superoxide dismutase administered 1 hour prior to administration of carrageenan inhibited edema and influx of neutrophils, as measured by Arthus response. Our findings suggest that xanthine oxidase, a tissue factor, has chemotaxigenic properties.

Trauma results in adenosine triphosphate catabolism and formation of the purine nucleotide precursors hypoxanthine and xanthine.[21] At the same time, xanthine dehydrogenase in tissues in proteolytically converted to xanthine oxidase.[22] The aerobic enzymatic interaction of the purine nucleotides and xanthine oxidase reduces molecular oxygen to superoxide anion and H_2O_2. Tubaro et al[23,24] reported a marked increase in the : anthine oxidase activity of neutrophils and macrophages from mice infected with *Staphylococcus aureus*. The addition of xanthine substrate to neutrophils elicited from the peritoneal cavities of clinically normal mice increased their phagocytic bactericidal activity.

It has been proposed that the protective effects of allopurinol, a competitive inhibitor of xanthine oxidase, may be related to its ability to inhibit the production of superoxide anion via it's effects on xanthine oxidase.[24] Allopurinol may reduce free radical tissue damage by inhibiting access to the xanthine oxidase substrate, thereby reducing inflammation. The participation of xanthine oxidase in the process of inflammation may be clinically relevant in instances of mechanical, thermal, reperfusion, radiation, or inflammatory injury.

References

1 Naccache PH, Showell HJ, Becker EL. Transport of sodium, potassium, and calcium across rabbit polymorphonuclear leukocyte membranes: effect of chemotactic factor. *J Cell Biol* 1977;73:428-444

2 Yuli I, Snyderman R. Rapid changes in light scattering from polymorphonuclear leukocytes exposed to chemoattracants. *J Clin Invest* 1984;73:1408-1417.

3 Zigmond SH, Hirsch JG. Leukocyte locomotion and chemotaxis. *J Exp Med* 1973;137:387-410

4 Gallin JI, Wright DG, Schiffmann E. Role of secretory events in modulating human neutrophil chemotaxis. *J Clin Invest* 1978;62:1364-1374.

5 Goldstein IM, Roos D, Kaplan HB, et al. Complement and immunoglobulins stimulate production by human leukocytes independently of phagocytosis. *J Clin Invest* 1975;56:1155-1163.

6 Babior B, Kipnes R, Curnette J. Biological defense mechanisms: the production by leukocytes of superoxide, a potential bactericidal agent. *J Clin Invest* 1973;52:741-744.

7 Guthrie LA, McPhail LC, Henson PM, et al. Priming of neutrophils for enhanced release of oxygen metabolites by bacterial lipopolysaccharide: evidence for increased activity of the superoxide-producing enzyme. *J Exp Med* 1984;160:1656-1671.

8 McCord JM. Free radicals and inflammation: protection of synovial fluid by superoxide dismutase. *Science* 1974;185:529-531

9 Frank L. Oxygen toxicity in eukaryotes. In: Oberly LW, ed. *Superoxide dismutase*. Boca Raton, Fla: CRC Press Inc, 1985;1-43

10 McCord JM, Fridovich I. The reduction of cytochrome c by milk xanthine oxidase. *J Biol Chem* 1968;243:5753-5760

11 McCord JM. The role of superoxide in postischemic tissue injury. In: Oberly LW, ed. *Superoxide dismutase*. Boca Raton, Fla: CRC Press Inc, 1985;143-150

12 Roy RS, McCord JM. Superoxide and ischemia: conversion of xanthine dehydrogenase to xanthine oxidase. In: Greenwald R, Chen G, eds. *Oxyradicals and their scavenger systems*, Vol 2. New York: Elsevier Scientific, 1983;145-153

13 Martin W, Loschen G, Gunzler WA, et al. Superoxide dismutase inhibits LTB4 induced leukotaxis. *Agents Actions* 1985;16:48-49

14 Hinshaw LB, Beller BK, Archer LT, et al. Recovery from lethal *E coli* shock in dogs. *Surg Gynecol Obstet* 1979;149:545-553

15 Wichterman KA, Baue AE, Chaudry IH. Sepsis and septic shock: a review of laboratory models and a proposal. *J Surg Res* 1980;29:189-201

16. Evans SF, Hinds CJ, Varley JG. A new canine model of endotoxin shock. *Br J Pharmacol* 1984;83:433–442.

17. Joyce LD, Smith JM, Mauer HG, et al. Zymosan-induced resistance to endotoxin and hemorrhagic shock. *Adv Shock Res* 1979;1:125–147.

18. Shatney CH, MacCarter DJ, Lillehei RC. Temporal factors in the reduction of myocardial infarct volume by methylprednisolone. *Surgery* 1976;80:61–69.

19. Petrone WF, English DK, Wong K, et al. Free radicals and inflammation: superoxide-dependent activation of neutrophil chemotactic factor in plasma. *Proc Natl Acad Sci* 1980;77:1159–1163.

20. Gyllenhammar H. Lucigenin chemiluminescence in the assessment of neutrophil superoxide production. *J Immunol Methods* 1987;97:209–213.

21. Berne RM, Rubio R. Adenine nucleotide metabolism in the heart. *Circ Res* 1974;35:109–118.

22. Tubaro E, Lotti B, Santiangeli C. Xanthine oxidase: an enzyme playing a role in the killing mechanism of polymorphonuclear leucocytes. *Biochem Pharmacol* 1980;29:3018–3020.

23. Tubaro E, Lotti B, Santiangeli C. Xanthine oxidase increases in polymorphonuclear leucocytes and macrophages in mice in three pathological situations. *Biochem Pharmacol* 1980;29:1945–1948.

24. Chambers DE, Parks DA, Ranjan R, et al. Xanthine oxidase as a source of free radical damage in ischemia. *J Mol Cell Cardiol* 1985;17:145–152.

Reprint & Copyright © by
Aerospace Medical Association, Washington, DC

ARMED FORCES RADIOBIOLOGY
RESEARCH INSTITUTE
SCIENTIFIC REPORT
SR89-32

Effects of Acute Sublethal Gamma Radiation Exposure on Aggressive Behavior in Male Mice: A Dose-Response Study

DONNA M. MAIER, M.A., Ph.D., and
MICHAEL R. LANDAUER, M.S., Ph.D.

MAIER DM, LANDAUER MR. *Effects of acute sublethal gamma radiation exposure on aggressive behavior in male mice: a dose-response study.* Aviat. Space Environ. Med. 1989; 60:774–8.

The resident-intruder paradigm was used to assess the effects of gamma radiation (0, 3, 5, 7 Gray [Gy] cobalt-60) on aggressive offensive behavior in resident male mice over a 3-month period. The defensive behavior of nonirradiated intruder mice was also monitored. A dose of 3 Gy had no effect on either the residents' offensive behavior or the defensive behavior of the intruders paired with them. Doses of 5 and 7 Gy produced decreases in offensive behavior of irradiated residents during the second week postirradiation. The nonirradiated intruders paired with these animals displayed decreases in defensive behavior during this time period, indicating a sensitivity to changes in the residents' behavior. After the third week postirradiation, offensive and defensive behavior did not differ significantly between irradiated mice and sham-irradiated controls. This study suggests that sublethal doses of radiation can temporarily suppress aggressive behavior but have no apparent permanent effect on that behavior.

KNOWLEDGE OF THE behavioral effects of low doses of acute ionizing radiation has become increasingly important in light of recent accidents involving nuclear material at Chernobyl, U.S.S.R., and Goiania, Brazil (1,20,25). Additionally, extended space missions, planned for the future, will increase astronauts' risk of exposure to radiation from solar flares and Earth's radiation belt (4). Because of the paucity of behavioral data available from victims of nuclear accidents, it is important to conduct controlled studies using animal models.

Previous radiation research has focused on a variety of behaviors, including locomotor activity, operant responding, conditioned taste aversion, conditioned avoidance responding, food and water intake, maze performance, and emesis (see 4,12,15, and 23 for reviews). In most studies, radiation produced a behavioral decrement. However, the degree and time course of the behavioral decrement varied with the behavior studied as well as with the radiation dose, quality of radiation, and animal species used (12,15,22). The complexity and physical demands of the task and, possibly, the motivation underlying its performance are involved in the different radiation-induced sequelae for various behaviors (4,8,15,19). Thus, it is necessary to assess different types of behaviors separately in order to ascertain the full range of possible radiation-induced behavioral decrement.

Our laboratory is currently exploring the consequences of radiation exposure on social behavior, an area which has not been adequately addressed in the past (19). Since mice exhibit territorial behavior under laboratory and natural conditions (2,3), a mouse model of social behavior was chosen to examine the effects of radiation on territorial aggressive behavior. The present study monitored the effects of acute, sublethal doses of gamma radiation on aggressive interactions over a 3-month period.

MATERIALS AND METHODS

Subjects: A total of 62 male Crl:CFW (SW)BR VAF/Plus Swiss-Webster mice (*Mus musculus*) from Charles River Breeding Laboratory (Raleigh, NC) (31–43 g) were used. The mice were 5.5 months old at the time of irradiation. All animals were quarantined on arrival, and representative animals were screened for evidence of disease before being released from quarantine. They were individually housed in plastic Micro-isolator cages on hardwood-chip contact bedding in an AAALAC-accredited facility. Commercial rodent chow (Wayne Lab Blox, Wayne, OH) and acidified (pH 2.5 using HCl) water were freely available (21). Animal holding rooms were maintained at 70° ± 2° F, with 50% ± 10% relative

From the Behavioral Sciences Department, Armed Forces Radiobiology Research Institute, Bethesda, MD.

This manuscript was received for review in November 1988. The revised manuscript was accepted for publication in January 1989.

Reprint requests should be addressed to Dr. Michael R. Landauer, Behavioral Sciences Department, Armed Forces Radiobiology Research Institute, Bethesda, MD 20814-5145.

humidity. The mice were on a reversed 12-h light/dark full-spectrum lighting cycle with no twilight (lights off at 0700 hours).

Radiation exposure: The mice were placed in ventilated, polycarbonate restraint devices for approximately 20 min during irradiation. Irradiation was accomplished with bilateral, whole-body exposure to gamma-ray photons from a cobalt-60 source. The mice received either 3, 5, or 7 Gy of gamma radiation administered at a dose rate of 1 Gy/min. These doses were chosen based on an LD50/30 (95% confidence limits) of 7.66 (7.50–7.82) Gy for male Swiss-Webster mice housed under our laboratory conditions. The sham-irradiated control mice were treated exactly like the irradiated mice, except that they were placed behind a lead shield and were not exposed to radiation.

Procedure: A resident-intruder paradigm, in which a resident mouse attacks an intruder that has entered its territory, was used to measure social behavior in this study (26). This paradigm has been widely used to measure offensive aggressive behavior (observed in the resident as it attacks the intruder) and defensive behavior (observed in the intruder as it defends itself from the resident) and has ethological validity as dominant mice defend their territories in the wild (2,3). The mice were individually housed 1 month before irradiation, since this has been reported to be an effective noninvasive method for inducing offensive aggressive behavior in mice (5,7,24). After 2 weeks of individual housing, each animal was brought to the test room, paired with another weight-matched mouse, and left to fight for 5 to 10 min. The animal that dominated in this encounter was subsequently designated as the resident and the subordinate animal became the intruder. Animals remained in the same resident-intruder pairs throughout the experiment, and all further testing was conducted in the resident's home cage. Resident animals were randomly assigned to four treatment groups: sham-radiation (N = 8), 3 Gy (N = 8), 5 Gy (N = 7), or 7 Gy (N = 8).

The mice were habituated to the testing room for 1 h before the test. Intruders were placed in the resident's home cage (25.7 × 15.2 × 12.1 cm) for 5 min during the dark portion of the light/dark cycle, and the mice were videotaped under infrared light. After the study was completed, the videotapes were analyzed by a scorer unaware of the treatment condition. The following behaviors displayed by the resident mouse were scored: latency to attack, number and duration of roll and tumble fights, and number of bites, lunges, and chases (2,3,26). Bites did not draw blood or leave any discernible mark on the intruder. Scored behaviors displayed by the intruder mouse were duration of defensive upright postures, number of squeaks, and number of escapes from the resident (2,3,6). The mice were tested 1 week before irradiation to ensure maintenance of the dominance relationship established between them at 2 weeks preirradiation. The baseline test was performed 2 d before irradiation. Postirradiation tests were conducted 1 to 3 h postirradiation (day 0), and days 2, 5, 7, 9, 12, 15, 19, 21, 26, 29, 48, 62, and 97 postirradiation.

Statistical analysis: The nonparametric Kruskal-Wallis and Mann-Whitney U tests were used to analyze the data (11). If the Kruskal-Wallis test revealed a significant difference among groups (which occurred on test days 0–19 postirradiation), paired comparisons of daily scores of each irradiated group with the control group were made using the Mann-Whitney U test. This was the procedure followed for each of the eight behaviors analyzed. A one-tailed alpha level ($p < 0.05$) was set for all statistical comparisons, since radiation has previously been shown to result in decrements in aggressive interactions (19).

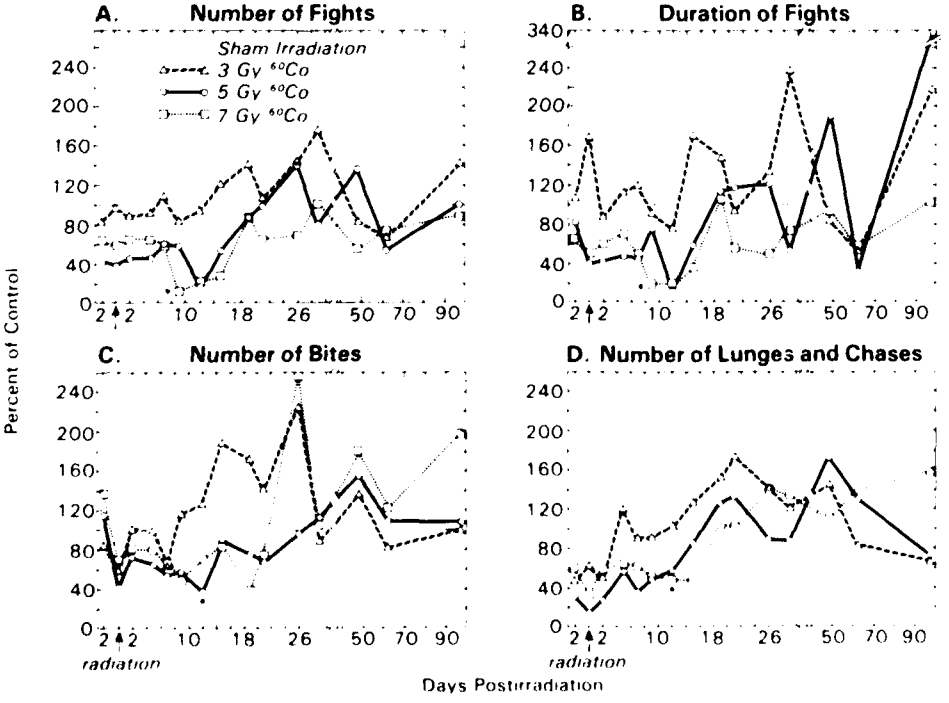

Fig. 1. Offensive aggressive behaviors displayed by resident mice in a 5-min resident-intruder test. Resident mice were sham-irradiated or exposed to 3, 5, or 7 Gy of gamma radiation on day 0. Data are presented as a percentage of control (sham-irradiated) group. (A) Number of fights, (B) Duration of fights, (C) Number of bites, and (D) Number of lunges and chases. N = 7 in the 5 Gy group; N = 8 in the other groups; *p < 0.05 when compared with controls.

RESULTS

In general, resident mice irradiated with 3 Gy did not exhibit any significant differences in offensive aggressive behavior directed toward the intruders when compared with the sham-irradiated controls (Fig. 1). Similarly, there were no differences in the defensive behaviors of the nonirradiated intruders paired with the residents treated with 3 Gy when compared with the controls (Fig. 2).

For purposes of clarification, data are illustrated as a percentage of the sham-irradiated control group in Figs. 1 and 2. The means and standard errors of all the parameters of the control group are presented in Table 1. The control group is always considered to be 100% of the response and is depicted by a solid line.

For the 5 and 7 Gy groups, significant changes in offensive behavior in the irradiated residents occurred primarily during the second week postirradiation. In the 5 Gy group, attack latency (data not shown) increased significantly on days 7 and 9 postirradiation [$U(8,7) = 54$, $p < 0.01$; $U(8,7) = 50$, $p < 0.01$] and the number of bites decreased significantly on day 12 postirradiation [$U(8,7) = 46$, $p < 0.05$] (Fig. 1). Defensive behavior emitted by the nonirradiated intruders paired with residents treated with 5 Gy also showed significant decreases, primarily in the second week postirradiation. The number of escapes and squeaks decreased significantly on day 7 postirradiation in intruders paired with residents irradiated with 5 Gy [$U(8,7) = 49.5$, $p < 0.01$; $U(8,7) = 44.5$, $p < 0.05$] (Fig. 2). Decreases in defensive behavior also occurred on day 2 postirradiation in these intruders. Both time spent in the defensive upright posture and number of escapes decreased at this time in the intruders paired with 5 Gy residents [$U(8,7) = 44$, $p < 0.05$; $U(8,7) = 44.5$, $p < 0.05$] (Fig. 2). Number of escapes also decreased significantly in these intruders on day 0 [$U(8,7) = 46$, $p < 0.05$] (Fig. 2).

In the residents treated with 7 Gy, number of fights and fight duration decreased significantly on day 9 postirradiation [$U(8,8) = 55.5$, $p < 0.01$; $U(8,8) = 53.5$, $p < 0.05$] (Fig. 1). On day 12 postirradiation, the number of lunges and chases decreased significantly [$U(8,8) = 50.5$, $p < 0.05$] (Fig. 1). Defensive behavior displayed by the nonirradiated intruders paired with residents treated with 7 Gy also showed significant decreases during the second week postirradiation. The number of escapes and squeaks decreased significantly on day 9 postirradiation [$U(8,8) = 54$, $p < 0.05$; $U(8,8) = 51$, $p < 0.05$] in intruders paired with the 7 Gy residents (Fig. 2). On day 12, both the number of squeaks and time spent in the defensive upright posture decreased significantly in these intruders [$U(8,8) = 57.5$, $p < 0.01$; $U(8,8) = 49.5$, $p < 0.05$] (Fig. 2). Time spent in the defensive upright posture also decreased significantly on day 19 postirradiation [$U(8,8) = 53$, $p < 0.05$] (Fig. 2). No significant effects were found in the 7 Gy group during the first week postirradiation.

After day 19 postirradiation, no significant differences were found between any of the irradiated groups and the sham-irradiated control group on any measure for either the residents or the intruders. Testing was stopped after day 97 postirradiation. There were no significant differences between the 5 and 7 Gy groups when the two were compared with each other.

DISCUSSION

The results of the present study indicate that gamma radiation can temporarily suppress offensive aggressive behavior during the second week postirradiation. The extent to which this finding is influenced by a generalized malaise or by reductions in spontaneous locomotor

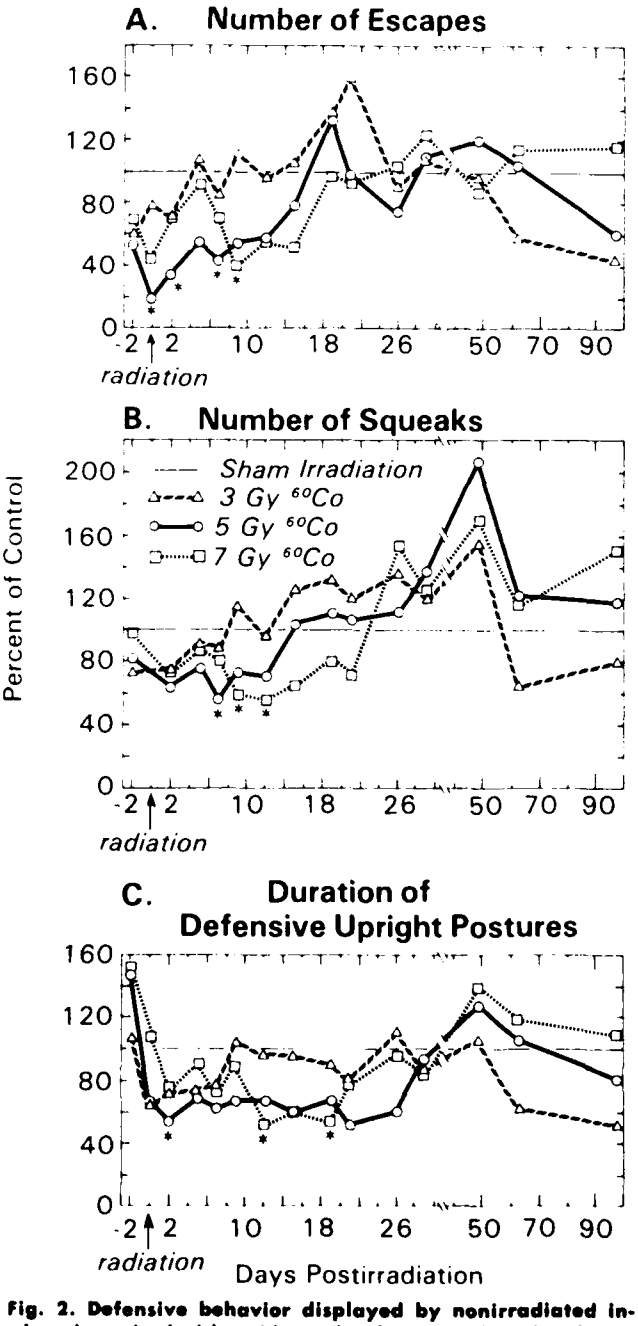

Fig. 2. Defensive behavior displayed by nonirradiated intruder mice paired with resident mice that were sham-irradiated or exposed to 3, 5, or 7 Gy of gamma radiation on day 0. Data are presented as a percentage of control (sham-irradiated) group. (A) Number of escapes, (B) Number of squeaks, and (C) Duration of defensive upright postures. N = 7 in the 5 Gy group; N = 8 in the other groups; *p < 0.05 when compared with controls.

TABLE I. MEANS (±S.E.M.) OF THE SHAM-IRRADIATED GROUP FOR BEHAVIOR OF RESIDENT MICE AND BEHAVIOR OF INTRUDER MICE OVER 3 MONTHS OF TESTING. (These values were used to compute the control lines that appear in Fig. 1 and 2.)

Offensive Aggressive Behaviors of Sham-Irradiated Residents				
Day*	No. of Fights	Fight Time**	No. of Bites	No. of Lunges/Chases
−2	4.1 (1.2)	2.7 (0.8)	12.8 (3.4)	11.6 (4.0)
0	3.9 (1.4)	3.2 (1.3)	19.6 (5.0)	12.6 (5.5)
2	2.5 (1.1)	1.8 (0.7)	9.5 (1.9)	16.4 (3.7)
5	3.1 (1.5)	2.3 (1.0)	13.0 (2.7)	8.1 (1.8)
7	2.6 (1.1)	1.8 (0.7)	13.5 (3.3)	14.5 (2.5)
9	2.3 (0.9)	1.3 (0.6)	12.3 (3.4)	11.6 (2.7)
12	1.9 (0.7)	1.4 (0.5)	12.5 (2.5)	12.5 (2.4)
15	1.9 (1.0)	1.5 (0.7)	7.6 (1.8)	9.4 (2.9)
19	1.5 (0.8)	0.9 (0.5)	9.4 (2.8)	9.9 (1.3)
21	1.8 (0.9)	1.0 (0.5)	9.9 (2.7)	8.8 (2.7)
26	1.1 (0.4)	0.8 (0.3)	6.5 (2.5)	10.4 (2.2)
29	1.6 (0.7)	1.3 (0.7)	11.5 (3.2)	8.5 (2.1)
48	1.4 (0.6)	0.9 (0.4)	5.4 (1.2)	7.0 (2.1)
62	1.9 (0.8)	1.8 (0.7)	7.1 (1.8)	7.9 (1.7)
97	1.0 (0.4)	0.7 (0.2)	6.9 (1.9)	12.4 (2.4)

Defensive Behaviors of Intruders Paired with Shammed Residents			
Day*	No. of Escapes	No. of Squeaks	Defensive Posture Time**
−2	17.1 (5.9)	63.0 (16.7)	73.8 (14.6)
0	17.0 (6.4)	***	105.8 (16.1)
2	16.0 (5.2)	51.5 (5.6)	127.1 (22.8)
5	12.1 (2.7)	58.9 (7.1)	112.6 (19.5)
7	15.1 (3.5)	56.1 (7.5)	136.0 (19.1)
9	12.8 (2.8)	45.8 (7.3)	108.5 (12.6)
12	14.1 (3.4)	47.6 (3.3)	102.0 (21.4)
15	12.3 (3.4)	32.0 (6.3)	101.4 (27.9)
19	10.9 (1.8)	39.3 (3.5)	109.4 (15.3)
21	11.1 (3.1)	38.9 (6.9)	128.1 (16.7)
26	12.8 (2.2)	36.6 (5.7)	109.8 (16.6)
29	10.3 (2.4)	34.1 (6.4)	104.0 (22.1)
48	10.3 (3.0)	24.4 (4.4)	67.6 (16.2)
62	10.4 (2.2)	34.0 (6.4)	88.9 (17.6)
97	12.6 (3.0)	31.6 (5.0)	91.5 (21.6)

* Test day with baseline test on day (−2) before sham irradiation, sham irradiation on day 0, and all other tests on days postirradiation (N = 8).
** Total duration of behavior in seconds.
*** Data lost because of technical difficulties.

activity is not clear. In a study using doses of 0.5 to 7 Gy gamma radiation, spontaneous locomotor activity and body weight in Swiss-Webster mice were temporarily decreased by 7 Gy cobalt-60 during the second and third weeks postirradiation but later recovered (16). In C57BL/6J mice, doses of 6 and 7 Gy cobalt-60 depressed locomotor activity during the second and third weeks postirradiation (17). In rats, temporary decrements in locomotor activity occurred 2 to 3 weeks following irradiation with 4 to 6.8 Gy X-rays (10,14); injection of a bone marrow suspension into rats irradiated with 6.5 Gy X-rays prevented these locomotor decrements (13). Behavioral decrements occurring in the second week postirradiation and beyond may be linked to radiation-induced suppression of hematopoietic tissue. Irradiation in the 5 to 10 Gy dose range has been found to cause a decrease in all blood cell elements including platelets, erythrocytes, lymphocytes, and granulocytes (9). The resulting anemia, inability to fight infection, and impairments in blood clotting that cause internal hemorrhaging (9), may lead to behavioral suppression until the blood cells have recovered.

Significant decreases in defensive behavior occurred on days 0 and 2 postirradiation in the nonirradiated intruders paired with residents irradiated with 5 Gy. Fight duration and number of bites in the 5 Gy residents also decreased on days 0 and 2 postirradiation, but these decreases, while marked, were not significant. The reason for these early decreases is unclear. A high degree of variability was noted on the baseline test day among the four treatment groups. This has previously been observed (19) and is due to the large amount of individual variation in aggressive behavior from day to day. Since aggressive behavior is a result of the interaction of two mice rather than a single animal performing a task alone, variability is further increased. In future studies, we plan to use a larger sample size in an attempt to reduce this variability.

In previous studies using 10 Gy cobalt-60 in Swiss-Webster mice, decreases were found in offensive be-

havior beginning on day 7 postirradiation and in spontaneous locomotor activity beginning on day 5 postirradiation (18,19). These animals did not recover normal levels of behavior and died in the second week postirradiation (18,19). In the present study, which used lower doses of radiation, no animals had died by 3 months postirradiation and a behavioral dose-response relationship was observed. A dose of 3 Gy had no effect on aggressive behavior, while doses of 5 and 7 Gy produced similar behavioral decrements. It is possible that the physiological effects produced by each dose were similar enough to produce equivalent behavioral alterations.

The results of the present study indicate a temporary deficit in offensive aggressive behavior with 5 and 7 Gy of gamma radiation along with concomitant alterations in the behavior of nonirradiated conspecifics; the latter may reflect the decline in offensive behaviors observed in the irradiated animals paired with them. Irradiation with either high-energy electrons or gamma photons has been found to decrease neurotoxin-stimulated uptake of sodium into synaptosomes in doses as low as 0.1 Gy (27). Thus, lower survivable doses may have an impact on central nervous system functioning that could underlie subtle changes in complex behaviors (23).

In conclusion, the results of the present study support our earlier finding that radiation has a suppressive effect on aggressive behavior, possibly as a result of the acute radiation syndrome (18). Previous work has demonstrated that the time course of radiation-induced behavioral suppression varies as a function of the behavior investigated (12,15,22). For example, research from this laboratory has indicated that radiation-induced decrements in locomotor activity precede deficits in aggressive behavior (18). The ability to coordinate rescue efforts following a nuclear accident or radiation exposure to space crews is of concern to both the civilian and military sectors. Radiation-induced alterations in behavior are likely to interfere with the effective functioning of teams and crews and, thus, deserve further study. The use of radioprotectants to mitigate radiation-induced behavioral deficits is, therefore, currently under investigation.

ACKNOWLEDGMENTS

The authors would like to thank H.D. Davis, M.E. Greenville, and G.J. Ruggiero for their invaluable assistance.

This research was supported by the Armed Forces Radiobiology Research Institute, Defense Nuclear Agency, under work unit 00159. Views presented in this paper are those of the authors; no endorsement by the Defense Nuclear Agency has been given or should be inferred. Research was conducted according to the principles enunciated in the "Guide for the Care and Use of Laboratory Animals," prepared by the Institute of Laboratory Animal Resources, National Research Council.

REFERENCES

1. Anspaugh LR, Catlin RJ, Goldman M. The global impact of the Chernobyl reactor accident. Science. 1988; 242:1513–9.
2. Benton D, Brain P, Jones S, Colebrook E, Grimm V. Behavioral examinations of the anti-aggressive drug Fluprazine. Behav. Brain Res. 1983; 10:325–38.
3. Blanchard RJ, O'Donnell V, Blanchard DC. Attack and defensive behaviors in the albino mouse. Aggressive Behav. 1979; 5:341–52.
4. Bogo V. Radiation: behavioral implications in space. Toxicology. 1988; 49:299–307.
5. Brain P. What does individual housing mean to a mouse? Life Sci. 1975; 16:187–200.
6. Brain PF, Benton D, Cole C, Prowse B. A device for recording submissive vocalizations of laboratory mice. Physiol. Behav. 1980; 24:1003–6.
7. Brain PF, Nowell NW. Isolation versus grouping effects on adrenal and gonadal function in albino mice. 1. The male. Gen. Comp. Endocrinol. 1971; 16:149–54.
8. Bruner A, Bogo V, Jones RK. Delayed match-to-sample early performance decrement in monkeys after cobalt-60 irradiation. Radiat. Res. 1975; 63:83–96.
9. Casarett AP. Radiation biology. Englewood Cliffs, NJ: Prentice-Hall, 1968.
10. Castanera TJ, Jones DC, Kimeldorf DJ. The effect of X-irradiation on the diffuse activity performance of rats, guinea pigs, and hamsters. Br. J. Radiol. 1959; 32:386–9.
11. Clayton KN. An introduction to statistics for psychology and education. Columbus, OH: Charles E. Merrill Publishing Company, 1984.
12. Hunt WA. Effects of ionizing radiation on behavior and the brain. In: Conklin JJ, Walker RI, eds. Military radiobiology. New York: Academic Press, 1987:321–30.
13. Jones DC, Kimeldorf DJ, Castanera TJ, Rubadeau DO, Osborn GK. Effect of bone marrow therapy on the volitional activity of whole-body X-irradiated rats. Am. J. Physiol. 1957; 189:21–3.
14. Jones DC, Kimeldorf DJ, Rubadeau DO, Osborn GK, Castanera TJ. Effect of X-irradiation on performance of volitional activity by the adult male rat. Am. J. Physiol. 1954; 177:243–50.
15. Kimeldorf DJ, Hunt EL. Ionizing radiation: neural function and behavior. New York: Academic Press, 1965.
16. Landauer MR, Davis HD, Dominitz JA, Pierce SJ. Effects of acute radiation exposure on locomotor activity in Swiss-Webster mice. Toxicologist 1987; 7:253.
17. Landauer MR, Davis HD, Dominitz JA, Pierce SJ. Dose-dependent radiation-induced alterations in ambulation and rearing over a 30-day period in C57BL/6J mice. FASEB J. 1988; 2:A1569.
18. Maier DM, Landauer MR. Radiation-induced alterations in fighting behavior and locomotor activity in mice. In: Brain PF, Olivier B, Mos J, Benton D, Bronstein PM, eds. Multidisciplinary studies on aggression. Swansea, Wales: International Society for Research on Aggression, 1988:74.
19. Maier DM, Landauer MR. Alterations in aggressive behavior of mice following exposure to gamma radiation. [Unpublished results.]
20. Marshall E. Reactor explodes amid Soviet silence. Science. 1986; 232:814–5.
21. McPherson CW. Reduction in *Pseudomonas aeruginosa* and coliform bacteria in mouse drinking water following treatment with hydrochloric acid or chlorine. Lab. Anim. Care. 1963; 13:737–44.
22. Mele PC, Franz CG, Harrison JR. Effects of sublethal doses of ionizing radiation on schedule-controlled performance in rats. Pharmacol. Biochem. Behav. 1968; 30:1007–14.
23. Mickley GA, Bogo V, West BR. Behavioral and neurophysiological changes associated with exposure to ionizing radiation. In: Walker RI, Cerveny TJ, eds. Textbook of military medicine. Vol. 1, part 2. Washington, DC: U.S. Army [in press].
24. Poshivalov VP. Some characteristics of the aggressive behavior of mice after prolonged isolation: intraspecific and interspecific aspects. Aggressive Behav. 1981; 7:195–204.
25. Roberts L. Radiation accident grips Goiania. Science. 1987; 238:1028–31.
26. Rodgers RJ. Drugs, aggression, and behavioral methods. In: Brain P, Benton D, eds. Multidisciplinary approaches to aggression research. New York: Elsevier/North Holland Biomedical Press, 1981:325–40.
27. Wixon HN, Hunt WA. Ionizing radiation decreases veratridine-stimulated uptake of sodium in rat brain synaptosomes. Science. 1983; 220:1073–4.

ARMED FORCES RADIOBIOLOGY
RESEARCH INSTITUTE
SCIENTIFIC REPORT
SR89-33

Neurotoxicology and Teratology, Vol. 11, pp. 385–393. Pergamon Press plc, 1989. Printed in the U.S.A.

0892-0362/89 $3.00 + .00

Progressive Behavioral Changes During the Maturation of Rats With Early Radiation-Induced Hypoplasia of Fascia Dentata Granule Cells

G. ANDREW MICKLEY,[1] J. LELAND FERGUSON, MAUREEN A. MULVIHILL AND THOMAS J. NEMETH

Behavioral Sciences Department, Armed Forces Radiobiology Research Institute, Bethesda, MD 20814-5145

Received 28 October 1988

MICKLEY, G. A., J. L. FERGUSON, M. A. MULVIHILL AND T. J. NEMETH. *Progressive behavioral changes during the maturation of rats with early radiation-induced hypoplasia of fascia dentata granule cells.* NEUROTOXICOL TERATOL **11**(4) 385–393, 1989. – Localized exposure of the neonatal rat brain to X-rays produces neuronal hypoplasia specific to the granule cell layer of the hippocampal dentate gyrus. This brain damage causes locomotor hyperactivity, slowed acquisition of passive avoidance tasks and long bouts of spontaneous turning (without reversals) in a bowl apparatus. Here we report how these behavioral deficits change as a function of subject aging and behavioral test replications. Portions of the neonatal rat cerebral hemispheres were X-irradiated in order to selectively damage the granule cells of the dentate gyrus. The brains of experimental animals received a fractionated dose of X rays (13 Gy total) over postnatal days 1 to 16 and control animals were sham-irradiated. Rats between the ages of 71–462 days were tested 3 separate times on each of the following 3 behavioral tests: 1) spontaneous locomotion, 2) passive avoidance acquisition, and 3) spontaneous circling in a large plastic hemisphere. Rats with radiation-induced damage to the fascia dentata exhibited long bouts of slow turns without reversals. Once they began, irradiated subjects perseverated in turning to an extent significantly greater than sham-irradiated control subjects. This irradiation effect was significant during all test series. Moreover, in time, spontaneous perseverative turning was significantly potentiated in rats with hippocampal damage but increased only slightly in controls. Early radiation exposure produced locomotor hyperactivity in young rats. While activity levels of controls remained fairly stable throughout the course of the experiment, the hyperactivity of the irradiated animals decreased significantly as they matured. The total distance traveled by irradiated rats was significantly above sham-irradiated controls at the beginning of the study but was significantly lower than controls at the conclusion. Young, irradiated rats learned a passive avoidance task more slowly than controls. They not only took more trials to meet criterion but their latency to move into an area in which they had just been shocked was significantly shorter than sham-irradiated rats. Passive avoidance learning improved in mature animals. These data suggest that radiation-induced damage to the fascia dentata produces task-dependent behavioral deficits that change as a function of subject age and/or behavioral testing.

Ionizing radiation Brain damage Hippocampus Fascia dentata Aging Maturation Behavior
Spontaneous locomotion Rotation Passive avoidance Rats Longitudinal

THE central nervous system (CNS) is most sensitive to structural damage from ionizing radiation exposure during critical periods of morphogenesis that occur prenatally and soon after birth. The consequences of radiation-induced malformations of the CNS are manifested in the function of the nervous system and in subsequent behavioral aberrations as well [for reviews see (20,35)].

Through methods that utilize precise timing of brain irradiation coupled with selective shielding techniques it has been possible to determine the behavioral changes associated with early radiation-induced damage to particular brain nuclei. Bayer and Peters have utilized these techniques to study the behavioral consequences of radiation-induced hypoplasia of the granule cells in the hippocampal dentate gyrus (fascia dentata). Since lesions of the granule cells effectively remove a major input to the hippocampus (through the perforant path from entorhinal cortex) they often produce behavioral consequences similar to total hippocampectomy (2,36). Bayer, Brunner, Hine and Altman (6) described locomotor hyperactivity, reduced spontaneous alternation in a T maze and retarded acquisition of a passive avoidance task in rats with early radiation-induced hippocampal damage. More recently, we (26) have replicated and extended this work by revealing that rats with hypoplasia of the fascia dentata granule cells exhibit perseverative spontaneous turning, with few reversals, in a bowl-shaped apparatus. These data illustrate behavioral effects of early radiation

[1]Requests for reprints should be addressed to G. Andrew Mickley, USAFSAM/RZP, Brooks AFB, TX 78235-5301

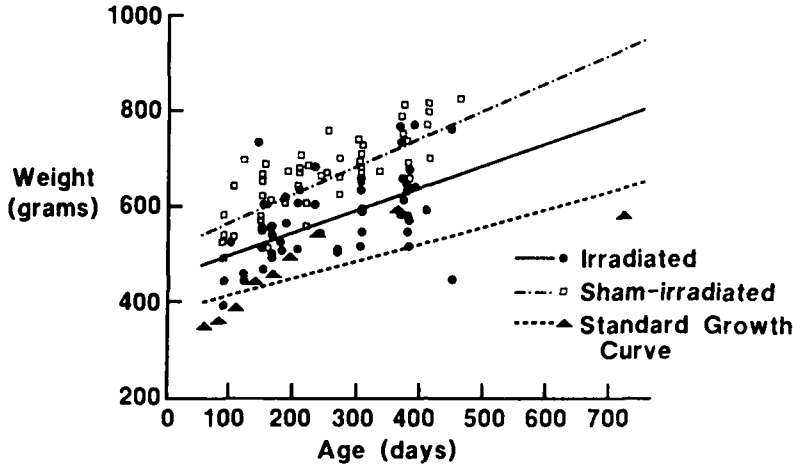

FIG. 1. Growth of irradiated and sham-irradiated rats throughout the course of this experiment. The weights presented here were recorded when subjects were being tested on the rotation measure. There are 3 data points per subject reflecting each of the 3 test series. See statistical comparisons of irradiated and sham-irradiated rat weights in the Method section of the text. Also presented for comparison are normative weights for this strain (21,32). Lines were fit using the least squares method (39).

exposure and suggest a role for hippocampal granule cells in working memory (30), response inhibition (1, 13, 19), and perhaps spatial mapping (29).

Most previous studies have described behavioral effects of radiation-induced damage to the neonatal dentate gyrus by measuring performance deficits at a single point in time. These analyses are typically done in young-adult subjects (6, 16, 36, 37). The purpose of the present experiments was to trace the consequences of early brain damage longitudinally. The same rat subjects were assessed on a battery of tests during 3 separate periods in their maturation. Here we report that radiation-induced behavioral deficits are not always stable throughout maturation. Instead, the progress of behavioral decrements following damage to the fascia dentata is task-dependent and performance may get progressively more, or less, severe as the brain-damaged animal matures.

METHOD

Subjects

Pregnant rats [Crl: CD(SD)BR] obtained from Charles River Laboratories, Kingston, NY, and screened for evidence of disease were housed in a facility accredited by the American Association for Accreditation of Laboratory Animal Care (AAALAC). Temperature and relative humidity in the animal rooms were held at 19–21 C and 50 ± 10%, respectively, with 10+ air changes hour. Full-spectrum lighting was cycled at 12 hour intervals (lights on at 0600) with no twilight. The rats used in these experiments came from a total of 19 different litters. On the day of birth (day 1) litters were culled and only 4–8 males/litter were reared together. Based on a random selection process, from 1–5 of these rats in each litter were actually used in the experiments reported here. All rats were weaned at the same time (between 23–28 days after birth) and then individually housed in microisolator, polycarbonate cages on hardwood chip contact-bedding. Rats were given ad lib Wayne Rodent Blox and acidified water (HCl, pH 2.5 to prevent the spread of *Pseudomonas*). Palatability studies indicate that animals do not prefer tap water to acidified water and that there are no deleterious effects of this water treatment over the lifetime of the subject [for review, see (38)].

Irradiated rats weighed less than sham-irradiated controls throughout most of the experiment (see Fig. 1). This weight difference was noted before weaning on postnatal day 21 [irradiated = 51.1 ± 0.8 g (SEM); sham-irradiated = 63.7 ± 1.1 g (SEM); $t(52) = 9.08$, $p<0.001$] and persisted in 71-day-old adolescents [irradiated = 356.2 ± 5.7 g (SEM); sham-irradiated = 434.2 ± 8.4 g (SEM); $t(46) = 5.79$, $p<0.001$] as well as mature (200-day-old) subjects [irradiated = 527.9 ± 10.4 g (SEM); sham-irradiated = 640.8 ± 11.2 g (SEM); $t(58) = 7.36$, $p<0.001$]. However, absolute weights for both irradiated and control rats were initially higher than published norms for this species (21,32). This may be due to the fact that litters were quite small after they were culled to contain only males. Rats raised in small litters tend to be significantly larger than are those reared in standard-sized litters (27).

The rats in the current study were sacrificed at the end of the experiment to allow histological analysis of the brain (see below). However, in another set of animals, treated identically, we found partial head irradiation did not significantly alter the life span of the animals (median = 589 days; range = 127–769; N = 40) as compared to sham-irradiated controls (median = 640 days; range = 180–782; N = 32).

See Table 1 for the number of subjects and their ages at the beginning of behavioral testing. Although their treatment was otherwise identical, some of the rats in this experiment served as "sham-surgical" controls for another study. In this context 15 of the sham-irradiated rats and 11 of the irradiated animals underwent a surgical procedure after the first behavioral test series [mean age at time of surgery = 182 ± 4 (SEM) days]. The animals were injected with atropine sulfate (0.4 mg/kg, IP) and then anesthetized with sodium pentobarbital (50 mg/kg, IP). Using aseptic techniques, the scalp was opened, a hole was drilled on both sides of the cranium adjacent to the midline, and the dura mater was broken with a probe. Following this procedure the scalp was sutured and subjects were placed back into their home cages. Full recovery was allowed since the next behavioral test series did not commence until almost 100 days after this surgery. Within each statistical analysis we compared the data derived from these animals to the data from rats not having the surgery (see Statistical Analysis section) and found them not to differ significantly.

TABLE 1

NUMBER AND AGE (DAYS) OF RATS AT THE TIME OF BEHAVIORAL TESTING*

Behavioral Measure	Test 1 N	Test 1 Age	Test 2 N	Test 2 Age	Test 3 N	Test 3 Age
Locomotor Activity						
Irradiated	21	146 ± 7†	21	279 ± 13	20	363 ± 9
Sham-Irradiated	22	133 ± 5	21	266 ± 8	22	343 ± 11
Rotation						
Irradiated	20	154 ± 10	18	268 ± 17	20	372 ± 12
Sham-Irradiated	22	145 ± 8	22	253 ± 12	22	349 ± 13
Passive Avoidance						
Irradiated	19	156 ± 12	19	276 ± 6	19	355 ± 6
Sham-Irradiated	22	146 ± 10	22	270 ± 6	22	344 ± 7

*All rats were tested on these 3 behavioral measures. Variations in N between different tests are due to slight procedural problems or equipment malfunctions that disqualified a particular subject's data from inclusion.
†Mean ± SEM.

Irradiation

Subjects from each litter were randomly assigned to either the X-irradiated or the sham-irradiated (control) group. Irradiated rats received collimated X-rays (Phillips Industrial 300 kvp X-ray machine, Phillips, Inc., Mahwah, NJ; configured with 1.5 mm of copper filtration, with a half-value layer of 2.5 mm copper) delivered dorsally, in the coronal plane, through a narrow slot in a loose-fitting whole-body lead shield. X-rays were confined to that area of the head previously determined to contain the hippocampus. Determinations of the location of the hippocampal formation relative to external landmarks (e.g., snout, eyes, ears) were made during preliminary dissections of other neonatal rats. These external landmarks were subsequently used to set the position of the slot in the lead shield during our irradiation procedure. The measurements and anatomical landmarks we used for shield placement corresponded closely to those previously reported by Bayer and Peters (7). The slot in the shield was the opening between 2 movable lead strips (22.8 × 6.8 × 2 cm) suspended just above the heads of the rats in the radiation exposure array. The opening extended laterally beyond the full width of each rat head and varied between 5–10 mm in the anterior/posterior plane in order to accommodate the growth of the head brain over the course of the radiation treatment [see (7) for a complete explanation of this procedure]. The irradiated rats were exposed to 2.0 Gray (Gy) on postnatal days 1 and 2 (day of birth = postnatal day 1), and to 1.5 Gy on postnatal days 5, 7, 9, 12, 14, and 16 for a total partial-head-only dose of 13 Gy (1 Gy = 100 rads). Doses were determined by using Exradin 0.05 cc tissue-equivalent ion chambers with calibration traceable to the National Institute of Standards and Technology. X-rays were delivered at a rate of 0.49 Gy/minute (total irradiation time = 3.5–4.0 min) at a depth of 2 mm in tissue. The sham-irradiated control rats were restrained for the same time period as the irradiated rats but were not exposed to X-rays.

The entire anterior/posterior extent of the hippocampal formation was irradiated as were brain areas dorsal and ventral to this structure [see (31) for a listing of these other brain areas]. Brain structures anterior and posterior to the slot in the lead were shielded. At the time of our postnatal radiation exposures the rat brain contained three remaining populations of dividing (and therefore radiosensitive) cells: neuronal precursors of granule cells in the hippocampus, cerebellum and olfactory bulbs (5,6). Two of these major neuronal precursor populations (in the cerebellum and olfactory bulbs) were covered by the radio-opaque shielding. Unshielded were the mitotic (radiosensitive) granule cells of the dentate gyrus and the mature neurons in other brain structures residing in the same coronal plane as the hippocampus. This procedure produces selective hypoplasia of granule cells in the dentate gyrus (7,17) while sparing the radioresistant (11,18) mature neurons of other brain structures. The technique has been validated through a variety of neuroanatomical methods (5, 17, 40).

Apparatus and Procedures

Following irradiation, rats were allowed to mature for approximately 4 months (see Table 1) before behavioral testing began. At this time, and during 2 subsequent time periods (approximately 9 and 12 months after birth) we recorded performance on 3 behavioral measures (see below). There was no systematic order in the conduct of these behavioral tests within each test series.

Spontaneous rotation. Rotation was measured in one of two opaque, sound-insulated, 60-cm diameter plastic hemispheres (bowls). Rotation within the hemisphere was inevitable since this was the primary gross movement permitted by the shape of the apparatus. Circling was measured through a projector-drive cable clipped to a wide rubber band around the rat's thorax. Following the design of Greenstein and Glick (15), the cable turned a slotted illuminated disk uncovering one of four phototransistors. The time and direction of each quarter turn in each of six, 30-minute sessions was recorded on a microcomputer.

Rats were tested at approximately the same time during the light portion of the day for six days. After each rat was put into the hemisphere and the cable clipped to its band harness, the hemisphere's sound-attenuating lid was lowered, leaving a 0.5-mm gap. Spontaneous turning was recorded for 0.5 hr. Bowls were thoroughly washed between runs. In order to control for an apparatus bias, daily runs were alternated between two test hemispheres.

Locomotor activity. Locomotor behaviors were automatically recorded using Digiscan Animal Activity Monitors, Model DCM-16 (Omnitech Electronics, Columbus, OH). Monitors consisted of a square acrylic activity arena (40 × 40 × 30 cm) and an array of infrared horizontal and vertical sensors 1 inch (2.54 cm) apart. Horizontal and vertical sensors were positioned 1.3 and 11.0 cm, respectively, above the floor of the cage. Data were processed and recorded by a Digiscan Analyzer (Omnitech, Model DCM) and an IBM-PC/XT computer.

Measurements were made in a Digiscan activity monitor for at least two 1-hour periods separated by 1 week or more. The following activity parameters were recorded during the lighted portion of the dark-light cycle: 1) Total distance traveled: a measure of horizontal locomotion that goes beyond infrared beam break counts, takes into account diagonal movements, and computes actual distance traversed; 2) Vertical activity: total number of beam interruptions that occurred in the vertical sensor (this parameter included, but was not limited to rearing; high sniffing movements were also recorded by vertical-sensor beam breaks); 3) Stereotypic movements: number of occurrences of quick (< 1 sec) repetitive breaks of the same horizontal beam.

Passive avoidance. Passive avoidance was measured within a shuttle box comprised of two compartments (each 22 × 22 × 22 cm) separated by a black plastic guillotine door. Each compartment was made of black plastic except for the top and the front walls which were clear. The goal compartment was identical to the

start box except for a small nonoperative light on the wall at the far end and a plastic food tray on this wall 2 cm off the floor. The floor was made of metal rods (0.5 cm diameter, 1.7 cm apart). Leads from a Coulbourn Instrument's (Lehigh Valley, PA) constant-current shocker (Model E13-04) were connected to the floor bars in the goal compartment but not to the bars in the start compartment.

Three to 7 days before training, rats were given daily rations of 5 g of Wayne Rodent Blox and 1–5 g of highly palatable breakfast cereal (Froot Loops™, Kellogg Company, Battle Creek, MI). For 2 to 4 days before training, each rat was allowed to fully explore the shuttle box (with cereal in the food-tray) for 15 to 45 minutes. Body weight on the first day of training averaged 87% of weight for the week prior to food reduction. During training (15 trials each day) the rat was placed in the start compartment with the divider door closed. After 5 seconds the door was raised and a timer started. The trial ended either when the rat grasped a Froot Loop™ or in 2 minutes. Between training trials, the rat was returned to its home cage for 30 seconds. Avoidance testing was started when a rat both averaged less than 10 sec per trial to grasp the food during a training session and, on the first 5 trials of the following day, had a median latency to grasp the food of 10 sec or less.

Avoidance training/testing consisted of initiating a regular training trial as usual. However, when the rat's four feet were in the goal box, the experimenter administered a 0.25 mA scrambled footshock until the rat retreated to the safe side. The rat was then returned to its home cage for 60 seconds. This procedure was repeated on subsequent trials except that the floor on the food side of the chamber was continuously electrified. The critical latency measured was the time for each rat to cross onto the shock grid. A trial was terminated if the rat either crossed onto the food/shock side of the chamber (registering a decrease in resistance across the rods) or stayed on the safe side for 120 seconds. The session (and test) was ended when the rat remained in the safe area for 120 seconds on three consecutive trials or after 20 test trials. After each session the apparatus was thoroughly cleaned and paper under the rod floor was replaced.

Histology

After behavioral testing, our rats were anesthetized and perfused with heparinized saline followed by 10% buffered formalin. Brains were embedded in paraffin, serially sectioned (6 μ) (in either the coronal or sagittal plane) and then stained with cresyl violet and luxol fast blue (23). All brains received a preliminary review to confirm radiation-induced damage to the dentate gyrus. In addition, brains sliced in the sagittal section (irradiated, N = 20; sham-irradiated, N = 20) were analyzed in more detail. A single section (approximately 1.9 mm lateral to the midline) (31) was used for this analysis to 1) estimate the degree of fascia dentata injury and 2) survey the other brain areas (olfactory bulb and cerebellum) that, although shielded from irradiation, are known to contain granule cells mitotic at the time of radiation treatment. We counted the total number of granule cells that could be visualized in the single section of the dentate gyrus used in this analysis. Cell counts were accomplished under 250× total magnification by a single observer. Nuclear cell counts were used in order to avoid the error caused by double or triple nucleoli. The size, cytoplasmic staining and nuclear structure of granule cells usually makes them distinguishable from glial cells (3,33). However, the possibility cannot be ruled out that some of the astroglial cells may have also been counted. The impact of this possible error is reduced by the fact that the number of glial cells in the fascia dentata is extremely low (22). In addition, after neonatal irradiations similar to those described here, Bayer and Altman (4) reported that the granule cell population remains significantly reduced into adulthood while the glia show an initial reduction in number followed by a complete regeneration to normal levels within 60–90 days (5). Thus our cell counts in the fascia dentata of the 1-year-old adult rat would presumably not reflect a radiation-induced alteration in glial population. Using an imaging system (Bioquant System IV, R and M Biometrics, Inc., Nashville, TN) we also derived the area of the dentate gyrus, computed the cellular density of the structure and the thickness of the granule cell layer. In order to confirm that the shielding of other brain areas was sufficient, we also counted granule cells in a 0.004 mm^2 area in the cerebellum and olfactory bulb. Further, we evaluated the sparing of other more mature, and therefore less radiosensitive, hippocampal structures by counting the thickness of the CA1 pyramidal cell layer that was dorsal to the dentate and directly in the path of the X radiation.

Using irradiation procedures similar to ours, Bayer and Peters (7) have previously determined that X irradiation destroys approximately 85% of the granule cells in the dentate gyrus of the hippocampus. This procedure spares 1) hippocampal pyramidal cells and adjacent brain nuclei (e.g., caudate) in the path of the X-rays and 2) shielded neurons anterior and posterior to the hippocampus (6,26). A foreshortening of cranial bone growth (28) and secondary brain changes in reaction to granule cell hypoplasia (40–42) may explain the slight shortening of hippocampus (2,6) and other brain structures (26) that have been previously reported.

Statistical Analyses

The effects of early radiation exposure on our behavioral parameters were evaluated through the use of analyses of covariance (ANCOVAs) with "subject age" as the covariate and "test series" (initial test and retests 2 and 3) as a within-subjects repeated measure. In one analysis of locomotor activity body weight was used as a covariate instead of "age." Initially, these analyses also included "surgery" as a factor in order to determine if the mild surgical treatment received by some of the subjects (see the Method section) significantly influenced the behavioral measures. Since no effect of surgery was revealed by these analyses, this factor was dropped in subsequent treatments of the data and the surgical groups were combined. Our analyses were conducted using the logarithms of the data in order to meet the ANCOVA assumptions of homogeneity of variance and normality of distribution (39).

In the analyses of the rotation data, the mean turning bout length for each of the 6 daily test sessions was computed by dividing the total quarter turns in the dominant direction by the number of bouts of quarter turns (without reversal of direction) in that session. Statistical comparisons were computed using each rat's average bout length score. This was the mean of the daily bout lengths for the 6 sessions in the test series.

RESULTS

In general, the data reveal that early radiation-induced granule cell hypoplasia of the fascia dentata causes 1) perseverative turning in a bowl apparatus (long turning bouts in the same direction, without reversals), 2) locomotor hyperactivity, and 3) deficits in the acquisition of a passive avoidance task. These behavioral changes were identified in young rats during the first performance tests but changed over time. Radiation-induced perseverative turning became more intense through the course of the experiment while passive avoidance acquisition improved.

TABLE 2

HISTOLOGICAL DATA DERIVED FROM ANALYSIS OF SAGITTAL SECTIONS OF RAT HIPPOCAMPUS

Anatomical Parameter	Irradiated (N = 20)	Sham-Irradiated (N = 20)	% of Control
Number of Dentate Granule Cells	177.7 (9.3)*	1771.5 (90.7)	10%
Dentate Area [sq mm]	0.5 (0.02)*	2.2 (0.15)	24%
Density of Dentate Granule Cells [sq mm]	349.1 (28.0)*	824.2 (69.9)	42%
Thickness† of Dentate Granule Cell Layer	3.4 (0.2)*	9.3 (0.4)	36%
Thickness† of CA1 Pyramidal Cell Layer	2.6 (0.1)	2.7 (0.1)	96%

*Significantly different (*t*-tests) from sham-irradiated, $p < 0.001$; Numbers are means and (in parentheses) SEMs.
†Number of cells.

Spontaneous locomotor hyperactivity was progressively reduced as subjects matured.

Histology

Exposure of a portion of the neonatal cerebral hemispheres to early, fractionated doses of ionizing radiation produced a selective reduction of granule cells of the hippocampal dentate gyrus while sparing other brain areas. Specifically, exposure of the neonatal rat hippocampus to ionizing radiation produced a significant, $t(28) = 17.5$, $p<0.001$, depletion of dentate granule cells (see Table 2). Similarly, both the areas and the granule cell densities of the irradiated dentate gyri were significantly reduced compared to those of the control rats, $t(28) = 11.4$, $p<0.001$, and, $t(28) = 6.3$, $p<0.001$, respectively. The specificity of this damage is illustrated by the sparing of the pyramidal CA1 neurons that were directly in the path of the X-rays. Irradiation produced no significant change in the thickness of the CA1 pyramidal cell layer, yet the thickness of the dentate granule cell layer was significantly reduced, $t(28) = 15.4$, $p<0.001$.

The granule cell populations (i.e., number of cells/unit area) of the olfactory bulb and the cerebellum were not significantly altered by the irradiation. Correlations were not statistically significant between granule cell densities in the dentate gyrus and those in the cerebellum or olfactory bulb. However, the granule cell densities of the cerebellum and olfactory bulb (both shielded from radiation exposure) were significantly correlated, $r(18) = .58$, $p<0.01$. These data suggest that the shielding of the olfactory bulb and cerebellum during the irradiation treatment was effective.

We also calculated correlations between anatomical data and the results of the behavioral tests of the third test series (i.e., those conducted just before the animal was sacrificed). Statistically significant negative correlations existed between, for example, the number of cells in the irradiated dentate gyrus and the length of the turning bout in the bowl apparatus, $r(18) = -0.48$, $p<0.05$. Similarly, the area of the dentate gyrus of irradiated rats was negatively correlated with horizontal activity counts, $r(18) = -0.44$, $p<0.05$, and measures of locomotor stereotypy, $r(28) = -0.39$, $p<0.05$. These data suggest that radiation-induced damage to the granule cells of the dentate gyrus predict locomotor hyperactivity and perseverative turning in a plastic hemisphere. We did not find similar correlations between our behavioral parameters and anatomical measures derived from the cerebellum or olfactory bulb.

Spontaneous Rotation

Radiation-induced hippocampal damage caused rats to make long bouts of turns in a plastic hemisphere without reversal of direction (see Fig. 2). Once they began moving in either direction, irradiated rats perseverated in that turning to an extent significantly greater than the sham-irradiated subjects, $F(1,39) = 17.09$, $p<0.001$.

The ANCOVA also revealed that there was a statistically

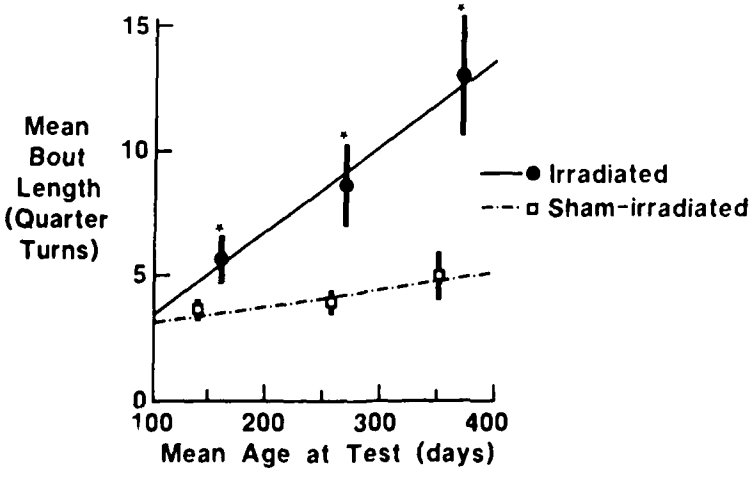

FIG. 2. Mean turning bout lengths (without reversals) in the dominant direction of movement for irradiated and sham-irradiated rats during each of 3 behavioral tests. Irradiated rats with fascia dentata damage show perseverative spontaneous turning that becomes progressively worse throughout the course of the experiment. Lines are fit using the least squares method (39). Vertical bars represent the SEMs. *Different from sham-irradiated controls $p < 0.05$.

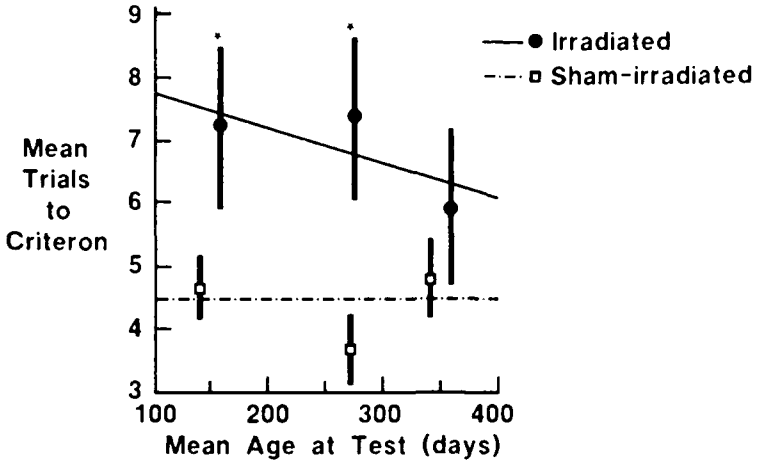

FIG. 3. Mean number of trials to achieve criterion (staying in the safe area for at least 120 seconds) on the passive avoidance task during each of the 3 behavioral test series. Irradiated rats with fascia dentata damage take longer to learn this task than do sham-irradiated controls. Lines are fit using the least squares method (39). Vertical bars represent the SEMs. *Different from sham-irradiated controls $p < 0.05$.

significant interaction between the effect of the radiation treatment and the test series, $F(2,79) = 4.17$, $p = 0.01$. These data suggest that, during the course of the experiment, perseverative turning became progressively more pronounced in irradiated animals than it did in controls. *t*-Tests comparing irradiated and sham-irradiated subjects at each test series confirmed this finding [Test series 1: $t(79) = 2.99$, $p < 0.01$; Test series 2: $t(79) = -5.72$, $p < 0.001$; Test series 3: $t(79) = -7.02$, $p < 0.001$].

The total number of quarter turns is a reflection of spontaneous activity that took place in the bowl apparatus. There was no difference between the total quarter turns exhibited by irradiated and sham-irradiated rats. However, the ANCOVA did reveal a significant decrease in this activity parameter as subjects matured [effect of the covariate of "age": $F(1,79) = 6.94$, $p = 0.01$]. It is of interest that, in mature adult animals that move less in the bowl apparatus, perseverative spontaneous turning becomes most prominent. These data suggest that increases in spontaneous perseverative turning in older subjects is not merely an outcome of enhanced frequency of turns.

Passive Avoidance

Rats with radiation-induced damage to the fascia dentata took more trials to learn the passive avoidance task, i.e., to meet a criterion of staying on the safe side for 120 seconds, $F(1,38) = 4.4$, $p = 0.04$. Irradiated rats took an average of 6.8 (±0.7, SEM) trials (over all test series) to meet this criterion while sham-irradiated rats learned the task in only 4.4 (±0.3, SEM) trials. Although the ANCOVA revealed no effect of age, there was a tendency for the data (mean trials to criterion) of the irradiated and sham-irradiated subjects to converge during the final test series (see Fig. 3). During the first 2 behavioral tests irradiated rats took more trials than did the sham-irradiated rats to meet the performance criterion [Test series 1: $t(39) = 1.80$, $p < 0.05$; Test series 2: $t(39) = 2.72$, $p < 0.01$]. During the final test series impaired reacquisition of the passive avoidance task was not observed in the rats with granule cell hypoplasia.

Irradiated rats also spent less time on the safe side of the passive avoidance chamber during the second trial (the one immediately following the first foot shock) on the test day, $F(1,38) = 5.3$, $p = 0.03$. Over all the test series, rats with radiation-induced hippocampal damage had an average latency to move onto the shock grid of only 10.8 seconds (±2.7, SEM) while sham-irradiated rats waited over twice as long (24.9 ± 4.5, SEM). According to the ANCOVA, these differences between irradiated and sham-irradiated rats did not change significantly with animal age. As Fig. 4 illustrates, however, the difference between the latencies of irradiated and sham-irradiated rats is most dramatic during the first 2 behavioral tests [Test series 1: $t(39) = 1.91$, $p < 0.05$; Test series 2: $t(39) = 2.54$, $p < 0.01$; Test series 3: not a significant difference between groups].

Learning deficits in irradiated rats with fascia dentata damage seem to be specific to passive avoidance acquisition. These animals readily learned to run to the adjacent compartment for food reward during the initial stages of training. Further, long-term retention of the learned response of running for food reward was illustrated by the fewer and fewer training trials required by the irradiated animals during the second and third behavioral test series. Thus, irradiated and sham-irradiated rats were similar in their learning and retention of this skill of shuttling from one compartment of the box to another.

Spontaneous Locomotion

Locomotor activity parameters produced by radiation-induced hippocampal damage were evident at the time of the first performance tests but changed significantly over time. After adjusting for test series in the ANCOVA, subject age seemed to affect all locomotor parameters measured: vertical activity, $F(1,77) = 6.26$, $p = 0.015$; stereotypy, $F(1,77) = 14.84$, $p = 0.0002$; and total distance traveled, $F(1,77) = 20.38$, $p < 0.0001$. Changes in spontaneous locomotion were most evident in aging subjects with radiation-induced brain damage while remaining fairly stable over time in sham-irradiated control rats (see Fig. 5). Radiation-induced changes in locomotion were dependent on the test replication within which these measures were recorded [radiation treatment × test series interactions: $F(2,77) = 3.6$–10.09, ps = 0.032–0.0001]. Subsequent *t*-tests revealed that measures of stereotypy and total distance traveled were initially higher in irradiated rats with hippocampal damage than in sham-irradiated animals [stereotypy:

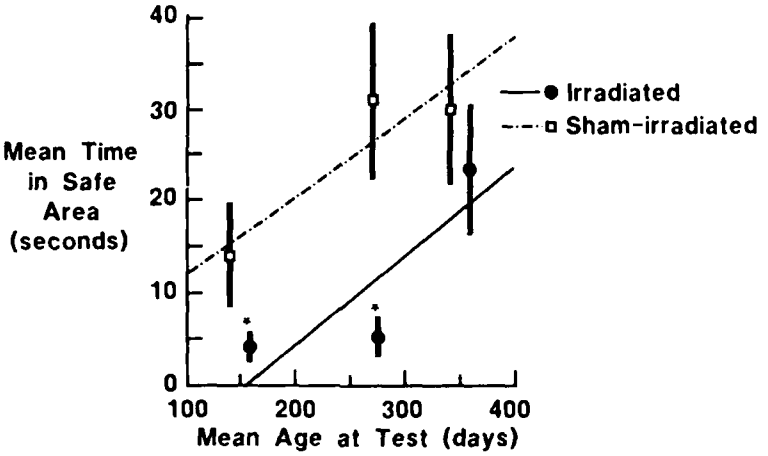

FIG. 4. Mean time (seconds) spent in the safe compartment of the passive avoidance apparatus on test trial 2 (following the initial shock in the adjacent compartment). Latencies are illustrated for each of the 3 test series. Irradiated rats with fascia dentata damage more quickly re-enter the chamber in which they have just been shocked than do sham-irradiated controls. Lines are fit using the least squares method (39). Vertical bars represent the SEMs. *Different from sham-irradiated controls $p<0.05$.

$t(77) = -3.87$, $p<0.001$; total distance: $t(77) = -3.41$, $p<0.01$]. This hyperactivity diminished and, in some cases (e.g., total distance traveled) became depressed during subsequent testing [Test series 3: $t(77) = 2.96$, $p<0.01$]. Similarly, vertical activity, which was initially as prevalent in irradiated as in control animals, was later significantly reduced in irradiated subjects [Test series 2: $t(77) = 2.91$, $p<0.01$; Test series 3: $t(77) = 4.50$, $p<0.001$].

Throughout most of this experiment, weight gains were observed both in control animals and (to a lesser extent) in irradiated subjects (see Fig. 1 and "Subject" data in the Method section). ANCOVAs used to determine the contribution of weight to the decline of stereotypy and vertical activity revealed that body weight was not a significant covariate. However, weight *was* a significant covariate within an analysis of total distance traveled, $F(1,77) = 6.83$, $p = 0.01$. Although enhanced weight may be thought to explain the reductions of spontaneous locomotion reported here, the variability of the effect of body weight on these locomotor parameters suggests that weight may actually play a more limited role in producing these behavioral declines. In this study, age seems to be a more consistent covariate of locomotor decline than is weight (see above). Further, the fact that locomotion is reduced in predominantly the irradiated rats, (subjects that

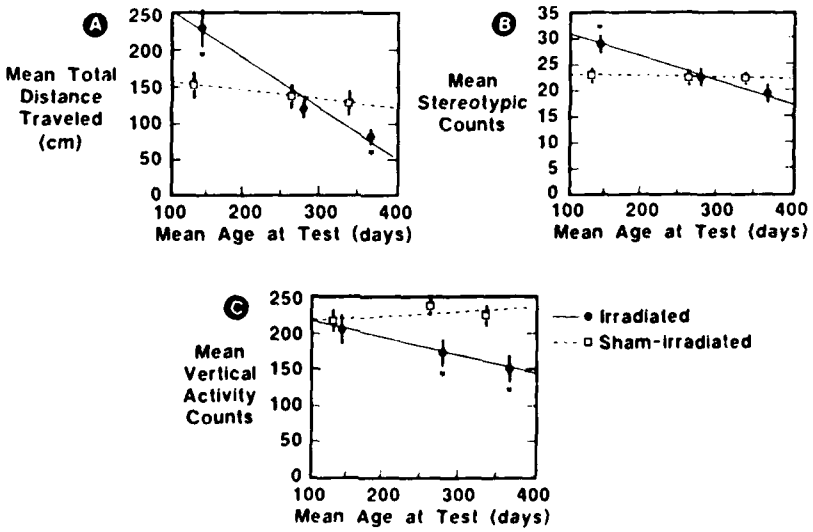

FIG. 5. Spontaneous locomotion of irradiated rats with fascia dentata damage and their sham-irradiated controls during 3 separate behavioral test series. Means for each of the following measures are illustrated. (A) Total distance traveled, (B) Stereotypy, and (C) Vertical activity (see text for definitions of these parameters). Lines are fit using the least squares method (39). Vertical bars represent the SEMs. *Different from sham-irradiated controls $p<0.05$.

weigh less than sham-irradiated animals) suggests that weight may not be a significant predictor of locomotor hypoactivity in the mature adult rats of this study.

DISCUSSION

The data reported here suggest that behavioral decrements following radiation-induced damage to the neonatal fascia dentata are task-specific and dynamic. Behavioral deficits may become more severe (e.g., spontaneous perseverative turning without reversals) or less severe (e.g., spontaneous locomotor activity) as the brain-damaged rat is retested during maturation. The progressive and task-dependant nature of these behavioral alterations highlights the need for multiple behavioral assessments throughout the development of the subject in order to fully characterize certain neurotoxic effects.

The results of the studies reported here are, in many ways, similar to those published by Brunner and collaborators (9,10). Despite the use of different experimental designs, behavioral techniques and apparatus, both of our laboratories describe a decline in spontaneous locomotion in maturing rats with radiation-induced damage to the hippocampal granule cells. This effect was marked compared to the relatively stable activity of sham-irradiated rats.

Brunner (10) also reported either 1) "persistent" deficits in the spontaneous alternation (in a T maze) of 6-month-old rats that were irradiated as neonates, or 2) a continuing "deterioration" in the spontaneous alternation of slightly older irradiated subjects (6–8 months) (9). In an important way the bowl apparatus, in which our rats spontaneously turned, is like a T maze. In the T maze there is one choice point, while the bowl gives a circular continuum of choice points. In a T maze a spontaneously alternating rat reverses direction on each discrete trial. In the bowl there is no discrete choice point. When a rat has made a full circle in the plastic hemisphere it begins to retrace the path most recently traversed. This presents an opportunity to either continue or reverse direction. The mean turning bout length is essentially a measure of alternation frequency corrected for the total number of quarter turns made. Therefore mean bout length may be considered a continuous (nondiscrete-trial) measure of spontaneous alternation. During the first behavioral test series sham-irradiated rats tended to stop and reverse direction after making almost a full circle (mean of 3.6 quarter turns) while rats with damage to hippocampal dentate granule cells continued beyond this point (to a mean of 5.9 quarter turns) before reversing direction. Our mature rats were (on average) 4 months older than Brunner and Altman's (9) oldest subject and therefore a further "deterioration" of spontaneous alternation might be expected. Indeed, our mature adult animals showed a clear lengthening of their mean circling bout and made over 10 quarter turns before alternating their direction of movement. When these data are taken in conjunction with those of Brunner (10) (who used a design that did not call for repetitive testing) we may conclude that maturation plays a dominant role in producing enhanced perseverative responding in mature rats with fascia dentata damage.

Because our rats were irradiated/sham-irradiated as neonates and then tested 3 times on 3 different behavioral measures, they received a significant amount of handling. In fact, the subjects quickly became quite tame and remained so throughout the experiment. Others have reported that neonatal handling can prevent behavioral deficits and hippocampal damage normally seen in aged animals (25). Further, Tilson and collaborators (34) suggest that handling can eliminate the rat hypermobility normally observed after colchicine-induced damage to the adult dentate gyrus. These behavioral effects of handling were observed in spite of significant decreases in both granule cell number and volume of hippocampal mossy fibers. Here we report that 1) the initial horizontal locomotor hyperactivity of our mature irradiated handled rats decreased to a level similar to, or below, that of the controls (also handled), and 2) handled animals with neonatally damaged hippocampi exhibited several behavioral deficits some of which (e.g., perseverative turning) become potentiated in the mature adult. These data may suggest some task-specific relationship between handling, early hippocampal damage and maturational effects that requires further study.

The neuronal substrate of the progressive behavioral changes that we report remains obscure. The mean percent reduction in the number of hippocampal granule cells in our rats (as compared to controls) was 90% when the subjects were sacrificed at over 1 year of age. This damage was roughly comparable to the radiation-induced hypoplasia previously reported in rats 30–125 days old (6,14). Thus the percentage of cells remaining in the damaged dentate gyrus after radiation exposure is quite stable over time and does not change in synchrony with our behavioral alterations. We know, however, that the total number of granule cells in the rat dentate gyrus is not static even in the adult. Bayer (8) has reported a 35–43% linear increase in the number of dentate granule cells between 1 month and 1 year. Others have observed significant changes in the mature hippocampus that they attribute to the development of axons and dendrites (12) or astro glia (24) rather than perikarya. Perhaps most relevant to the present study are the findings of Zimmer and his colleagues (40–42) who have shown that the brain may compensate for early radiation-induced damage to the hippocampal granule cells by stimulating dendritic growth. Their results demonstrate that a reduction of a specific neuronal population can induce: 1) a compensatory increase in the neuropil layers containing the dendrites of the remaining neurons, 2) a corresponding relative increase in their axonal projections, and 3) a shift and expansion of afferent projections to an adjacent neuronal population. Thus, although our hippocampal radiation produces damage specific to the granule cells, subsequent brain changes, in reaction to this initial damage, may produce more pervasive changes in neuroanatomy. These, or other changes in neuroanatomy/neurophysiology may contribute to the progressive behavioral changes that we observed in mature adult rats that were partially head irradiated as neonates.

Our longitudinal experiments have followed changes in the behavioral responses of rats with early radiation-induced hypoplasia of the dentate gyrus granule cells. Behaviors observed a year or more after the early brain damage are, in many ways, different from the acute behavioral response. These progressive behavioral changes may be mediated by normal developmental processes, the brain's natural compensatory reactions to early damage, experimental variables (e.g., handling) or other mechanisms that have yet to be fully elucidated.

ACKNOWLEDGEMENTS

The authors recognize the helpful technical assistance provided by Mr. Mark Postler, Ms. Diane Pickle and Dr. Cathie Alderks. The dosimetry and irradiations were performed by Mr. Douglas Eagleson and Mr. Ernest Golightly. Statistical advice was provided by Mr. William Jackson. We thank Ms. Lilly Heman-Ackah for her excellent histological assistance. This research was supported by the Armed Forces Radiobiology Research Institute, Defense Nuclear Agency, under Work Unit 00163. Views presented in this paper are those of the authors, no endorsement by the Defense Nuclear Agency has been given or should be inferred. Research was conducted according to the principles enunciated in the "Guide for the Care and Use of Laboratory Animals" prepared by the Institute of Laboratory Animal Resources, National Research Council. A portion of these data were presented at the 18th Annual Society for Neuroscience Meeting, 1988.

REFERENCES

1. Altman, J.; Brunner, R. L.; Bayer, S. A. The hippocampus and behavioral maturation. Behav. Biol. 8:557–596; 1973.
2. Altman, J. An animal model of minimal brain dysfunction. In: Lewis, M., ed. Learning disabilities and prenatal risk. Urbana and Chicago: University of Illinois Press; 1986:241–304.
3. Banks, W. J. Histology and comparative organology. A text atlas. Baltimore: Williams and Wilkins Co.; 1974.
4. Bayer, S. A., Altman, J. Hippocampal development in the rat: Cytogenesis and morphogenesis examined with autoradiography and low-level x-irradiation. J. Comp. Neurol. 158:55–80; 1974.
5. Bayer, S. A., Altman, J. Radiation-induced interference with postnatal hippocampal cytogenesis in rats and its long-term effects on the acquisition of neurons and glia. J. Comp. Neurol. 163:1–20; 1975.
6. Bayer, S. A.; Brunner, R. L., Hine, R., Altman, J. Behavioural effects of interference with the postnatal acquisition of hippocampal granule cells. Nature New Biol. 242:222–224; 1973.
7. Bayer, S. A., Peters, P. J. A method for X-irradiating selected brain regions in infant rats. Brain Res. Bull. 2:153–156; 1977.
8. Bayer, S. A. Changes in the total number of dentate granule cells in juvenile and adult rats: A correlated volumetric and ^{3}H-thymidine autoradiographic study. Exp. Brain Res. 46:315–323; 1982.
9. Brunner, R. L., Altman, J. The effects of interference with the maturation of the cerebellum and hippocampus on the development of adult behavior. In: Stein, D. G., Rosen, J. J., Butters, N., eds. Plasticity and recovery of function in the central nervous system. New York: Academic Press; 1974:129–148.
10. Brunner, R. L. A cross-sectional study of behavior at three ages after neonatal X irradiation of the hippocampus. Behav. Biol. 22:211–218; 1978.
11. Cassarett, G. W. Radiation histopathology, vol. 2. Boca Raton: CRC Press; 1980.
12. Coleman, P. D., Flood, D. G., West, M. J. Volumes of the components of the hippocampus in the aging F344 rat. J. Comp. Neurol. 266:300–306; 1987.
13. Douglas, R. J. The hippocampus and behavior. Psychol. Bull. 67:416–442; 1967.
14. Gazzara, R. A., Altman, J. Early postnatal X-irradiation of the hippocampus and discrimination learning in adult rats. J. Comp. Physiol. Psychol. 95:484–495; 1981.
15. Greenstein, S., Glick, S. D. Improved automated apparatus for recording rotation (circling behavior) in rats or mice. Pharmacol. Biochem. Behav. 3:507–510; 1975.
16. Hagghloom, S. J., Brunner, R. L., Bayer, S. A. Effects of hippocampal granule-cell agenesis on acquisition of escape from fear and one way active avoidance responses. J. Comp. Physiol. Psychol. 86:447–457; 1974.
17. Hicks, S. P. Radiation as an experimental tool in mammalian developmental neurology. Physiol. Rev. 38:337–356; 1958.
18. Hicks, S. P., D'Amato, C. J. Effects of ionizing radiation on mammalian development. In: Woollam, D. H. M., ed. Advances in teratology. London: Logos Press; 1966:195–250.
19. Kimble, D. P. Hippocampus and internal inhibition. Psychol. Bull. 70:285–295; 1968.
20. Kimeldorf, D. J., Hunt, E. L. Ionizing radiation: Neural function and behavior. New York: Academic Press; 1965.
21. Kozma, C., Cummins, L. M., Tekeli, S. The use of Long-Evans rats in long term toxicity studies. In: The laboratory animal in drug testing. Hanover: 5th ICLA Symposium; 1972.
22. Laatsch, R. H., Cowan, W. M. Electron microscope studies of the dentate gyrus of the rat: I. Normal structure with special reference to synaptic organization. J. Comp. Neurol. 128:359–395; 1966.
23. LaBossiere, E. Histological processing for the neural sciences. Springfield: Charles C. Thomas; 1976.
24. Landfield, P. W., Rose, G., Sandles, L., Wohlstadter, T. C., Lynch, G. S. Patterns of astroglial hypertrophy and neuronal degeneration in the hippocampus of aged, memory-deficient rats. J. Gerontol. 32:3–12; 1977.
25. Meaney, M. J., Aitken, D. H., van Berkel, C., Bhatnagar, S., Sapolsky, R. M. Effect of neonatal handling on age-related impairments associated with the hippocampus. Science 239:766–768; 1988.
26. Mickley, G. A., Ferguson, J. L., Nemeth, T. J., Mulvihill, M. A., Alderks, C. E. Spontaneous perseverative turning in rats with radiation-induced hippocampal damage. Behav. Neurosci. 103(4): in press; 1989.
27. Moore, B. J., Stern, J. S., Horwitz, B. A. Brown fat mediates increased energy expenditure of cold-exposed overfed neonatal rats. Am. J. Physiol. 251:R518–524; 1986.
28. Mosier, H. D., Jansons, R. A. Effect of x-irradiation of selected areas of the head of the newborn rat on growth. Radiat. Res. 43:92–104; 1970.
29. O'Keefe, J., Nadel, L. The hippocampus as a cognitive map. Oxford: Oxford University Press; 1978.
30. Olton, D. S. Memory functions and the hippocampus. In: Seifert, W., ed. Neurobiology of the hippocampus. London: Academic Press; 1983, 335–373.
31. Paxinos, G., Watson, C. The rat brain in stereotaxic coordinates. Sidney: Academic Press; 1982.
32. Polley, S. M. Growth tables for 66 strains and stocks of laboratory animals. Lab. Anim. Sci. 22:759–779; 1972.
33. Seress, L., Pokorny, J. Structure of the granular layer of the rat dentate gyrus. J. Anat. 133:188–195; 1981.
34. Tilson, H. A., Harry, G. J., Nanry, K., Rogers, B. C., Peterson, N. J., Jensen, K., Dyer, R. S. Experimental factors in the expression of hypermotility produced by intradentate colchicine: Lack of effect of GM1 ganglioside on colchicine-induced loss of granule cells and mossy fibers. J. Neurosci. Res. 17:410–416; 1987.
35. Van Cleve, C. D. Irradiation and the nervous system. New York: Rowman and Littlefield, Inc.; 1963.
36. Wallace, R. B., Kaplan, R. F., Werboff, J. Behavioral correlates of focal hippocampal X-irradiation in rats. Exp. Brain Res. 24:343–349; 1976.
37. Wallace, R. B., Graziadei, R., Werboff, J. Behavioral correlates of focal hippocampal X-irradiation in rats II. Exp. Brain Res. 43:207–212; 1981.
38. Weisbroth, S. H. Bacterial and mycotic diseases. In: Baker, H. L., Lindsey, J. R., Weisbroth, S. H., eds. The laboratory rat: vol. 1. Biology and diseases. New York: Academic Press; 1979:206–208.
39. Winer, B. J. Statistical principles in experimental design. New York: McGraw-Hill Book Company; 1971.
40. Zimmer, J., Sunde, N., Sorensen, T. Reorganization and restoration of central nervous connections after injury: A lesion and transplant study of the rat hippocampus. In: Will, B. E., Schmitt, P., Dalrymple-Alford, J. C., eds. Brain plasticity, learning and memory. London: Plenum Publishing; 1985:508–518.
41. Zimmer, J., Laurberg, S., Sunde, N. Non-cholinergic afferents determine the distribution of the cholinergic septo-hippocampal projection: A study of the AChE staining pattern of the fascia dentata and hippocampus after lesions, x-irradiation, and intracerebral grafting. Exp. Brain Res. 64:158–168; 1986.
42. Zimmer, J., Poulsen, P. H., Blackstad, J. W., West, M. J. Radiation-induced reduction of the rat dentate gyrus: Compensatory cellular and connectional changes. Soc. Neurosci. Abstr. 13:1602; 1987.

ARMED FORCES RADIOBIOLOGY RESEARCH INSTITUTE
SCIENTIFIC REPORT
SR89-34

Edited by Thomas M. Donnelly, BVSc., Dip. VP

Stomach Nodules in Pigeons

By
James B. Nold, DVM, PhD, Robert H. Weichbrod, BS, LATG, and Cathie E. Alderks, PhD

SIXTY MALE WHITE Carneau pigeons, 6 to 12 months old, were procured from a reputable supplier for subsequent use in behavioral studies. Upon receipt, the pigeons were housed individually in stainless steel cages and acclimated to the animal room environment for a period of 3 weeks. During this time the pigeons were provided grit, mixed grains, and water *ad libitum*.

Dr. Nold is Chief of the Pathology Division, Mr. Weichbrod is Chief of the Animal Husbandry Division, and Dr. Alderks is an experimental behaviorist, all at the Armed Forces Radiobiology Research Institute, Bethesda, MD 20814-5145. Reprint requests should be sent directly to Mr. Weichbrod.

Supported by the Armed Forces Radiobiology Research Institute, Defense Nuclear Agency. Views presented in this paper are those of the authors; no endorsement by the Defense Nuclear Agency has been given or should be inferred. Research was conducted according to the principles enunciated in the "Guide for the Care and Use of Laboratory Animals" prepared by the Institute of Laboratory Animal Resources, National Research Council.

The animal room was monitored at least twice daily and kept at 70°±2° F temperature and 50%±5% humidity. There were between 10 and 15 complete room air changes per hour. Following the acclimation period, the pigeons were maintained at specified weights (70%, 80%, or 100% of free-feeding weight) through individualized feeding of mixed grain. Water and grit were continued *ad libitum*. The animals were then started on behavioral training protocols.

Clinically and behaviorally the pigeon colony remained healthy. Pigeons were periodically submitted to necropsy according to protocol or at the termination of experiments. Most observed lesions were attributable to specific experimental manipulation. However, about 30 to 35% of all the pigeons (both control and treated), demonstrated a similar, distinctive gross necropsy finding: The serosal surface of the proventriculus contained multiple slightly raised black nodules of 1 to 2 mm in diameter (*see* Figure 1). The degree of involvement ranged from a half dozen nodules to total coverage of the organ. The mucosal surface was thickened and contained multiple .5 mm craterform structures with central open pores. On cut section the mucosa contained

Figure 1. Proventriculus, gizzard, and duodenum showing multiple 1 to 2 mm dark nodules in the wall of the proventriculus.

Figure 2. Proventriculus showing craterform thickening of the mucosa and cross sections of black nodules in the wall.

multiple round to oval cystic spaces filled with a black granular material, which, if squeezed, popped out, leaving a clear, mucus-filled space (*see* Figure 2). Tissue samples were taken for histology.

What's your diagnosis? How common is this problem? Why are there no clinical symptoms? Can it be treated?

DIAGNOSIS: Tetrameriasis

THE BLACK TO DARK RED nodules embedded in the mucosa of the proventriculus were gravid female nematode parasites, *Tetrameres* sp. The histologic cross sections of the proventriculus demonstrated multiple dilated gastric glands containing large, globular parasites (*see* Figure 3). One gravid female usually occupied each gland unless a much smaller male parasite was also present (*see* Figures 3 and 4). The female parasite is composed predominantly of uteri containing numerous thick-shelled embryonated and unembryonated eggs and an intestinal tract lined by uninucleated, cuboidal, epithelial cells with microvilli. *Tetrameres* sp. have a thick cuticle with bilateral alae, often prominent lateral cords, and coelomyarian-polymyarian musculature (*1*). (Body wall structure of the parasite is more easily characterized in the male than in the expanded gravid female.)

Histopathological changes in the mucosa were mild. They included compression and flattening of the secretory epithelium in affected glands and a multifocal, mild, interstitial infiltrate of lymphocytes and plasma cells. Preexisting lymphoid nodules within the mucosa often appeared enlarged with increased numbers of surrounding plasma cells. Although the affected pigeons in this report were asymptomatic, previous reports of tetrameriasis in pigeons have described clinical illness in some birds (2-4). Affected birds may show weight loss, anemia, and generalized weakness, especially after flight. Some birds may also develop diarrhea. Oral treatment with levamisole at 33 mg/kg has been the recommended method for controlling the infestation (*2*).

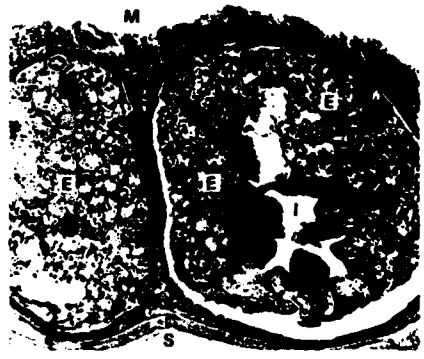

Figure 3. Cross section of two nodules, showing egg-filled globular female *Tetrameres* within dilated gastric glands. Arrow points to male parasite. Photo key—M: mucosal surface. S: serosal surface. I: intestines. E: eggs in various stages of maturation within convoluted uteri (32× original magnification).

Figure 4. Higher magnification of Figure 3, showing small male *Tetrameres* adjacent to portion of gravid female. Note distinct lateral alae and thick cuticle of male (solid arrow), and lymphocytic infiltrates in lamina propria of proventricular mucosa (open arrow). Photo key—M: mucosal glands. L: lateral cord in gravid female. E: eggs in various stages of maturation within convoluted uteri (175× original magnification)

Tetrameres sp. are spirurid nematodes in the order Spiruridae and suborder Spirurina. *Tetrameres americana* and T. columbicola are the species most described in pigeons (*2-4*). These spirurids have an indirect life cycle and require an intermediate host (*5*), such as grasshoppers, sowbugs, cockroaches, pillbugs, and earthworms. Thus, control of these vectors may help reduce the incidence of infestation. ■

References

1. Chitwood, M. and Lichtenfels, J.R. "Identification of Parasitic Metazoa in Tissue Sections." *Exp. Parasitol.* **32**:407-519, 1972.

2. Panigraphy, B. *et al.* "Diseases of Pigeons and Doves in Texas: Clinical Findings and Recommendations for Control." *J. AM. Vet. Med. Assoc.* **181**:384-386, 1982.

3. Flatt, R.E. and Nelson, L.R. "*Tetrameres americana* in Laboratory Pigeons (*Columba livia*)." *Lab. An. Care.* **19**:853-856, 1969.

4. Simpson, C.F., Carlisle, J.W., and Conti, J.A. "*Tetrameres columbicola* (Nematoda: Spiruridae) Infection of Pigeons: Ultrastructure of the Gravid Female in Glands of the Proventriculus." *Am. J. Vet. Res.* **45**:1184-1192, 1984.

5. Cram, E.B. "Developmental Stages of Some Nematodes of the Spiruroidea Parasitic in Poultry and Game Birds." *U.S.D.A. Tech. Bull.* 227, 1931.

6. Raggi, L.G. and Baker, N.F. "*Tetrameres americana* (Cram, 1927) Infection in Domestic Pigeons." *Avian Dis.* **1**:227-234, 1957.

7. Surgimoto, M. and Nishiyama, S. "On the Nematode *Tropisurus fissi spinus*." (Diesing, 1861) and Its Transmission to Chickens in Formosa." *J. Jap. Soc. Vet. Sci.* **16**:305-313, 1937.

Contributions to "What's Your Diagnosis?" by readers of LAB ANIMAL are welcomed. Selections will be made on the basis of relevancy and interest to readers. Submission of black and white illustrations or photos is encouraged. Please address contributions to Thomas M. Donnelly, LAB ANIMAL, 65 Bleecker St., New York, NY 10012.

RADIATION RESEARCH 119, 113–122 (1989)

ARMED FORCES RADIOBIOLOGY
RESEARCH INSTITUTE
SCIENTIFIC REPORT
SR89-35

An Assessment of the Behavioral Toxicity of High-Energy Iron Particles Compared to Other Qualities of Radiation

BERNARD M. RABIN,*† WALTER A. HUNT,* AND JAMES A. JOSEPH*,‡

Behavioral Sciences Department, Armed Forces Radiobiology Research Institute, Bethesda, Maryland 20814-5145, and †Department of Psychology, University of Maryland at Baltimore County, Baltimore, Maryland 21228

RABIN, B. M., HUNT, W. A., AND JOSEPH, J. A. An Assessment of the Behavioral Toxicity of High-Energy Iron Particles Compared to Other Qualities of Radiation. *Radiat. Res.* **119**, 113–122 (1989).

Conditioned taste aversion was used to evaluate the behavioral toxicity of exposure to high-energy iron particles (^{56}Fe, 600 MeV/amu) in comparison to that of gamma photons (^{60}Co), high-energy electrons, or fission neutrons. Exposure to high-energy iron particles (5–500 cGy) produced a dose-dependent taste aversion with a maximal effect achieved with a dose of 30 cGy. Gamma photons and electrons were the least effective stimuli for producing a conditioned taste aversion, with a maximal aversion obtained only after exposure to 500 cGy, while the effectiveness of fission neutrons was intermediate to that of photons and iron particles, and a maximal aversion was obtained with a dose of 100 cGy. In the second experiment, rats with lesions of the area postrema were exposed to iron particles (30 cGy), but failed to acquire a taste aversion. The results indicate that (1) high-energy iron particles are more toxic than other qualities of radiation and (2) similar mechanisms mediate the behavioral toxicity of gamma photons and high-energy iron particles. © 1989 Academic Press, Inc.

INTRODUCTION

As manned exploration of the solar system increases in the coming decades, astronauts will be leaving the protection provided by the earth's magnetic field. As a result, they will be exposed to radiation qualities and doses that will differ significantly from those experienced in earth orbit, largely from intergalactic cosmic rays. Intergalactic cosmic rays are composed of protons, alpha particles, and heavy particles with high energy and charge (HZE). The toxic effects of such exposures, particularly nausea and emesis, may interfere with the ability of astronauts to successfully complete their assigned missions. Protection against the effects of these exposures will require an understanding of the toxicity of high-energy particles and their relationship to the

‡ Present address: Gerontology Research Center, National Institute of Aging, Francis Scott Key Medical Center, Baltimore, MD 21224.

To whom address for reprint requests.

0033-7587/89 $3.00
Copyright © 1989 by Academic Press, Inc.
All rights of reproduction in any form reserved.

toxicity of other qualities of radiation and of the mechanisms by which such exposures can produce effects on behavior.

Although there has not been much research evaluating the effects of different qualities of radiation on behavioral tasks, the research that is available suggests that the toxic effects of exposure may be specific to the quality of the radiation (*1, 2*). As such, in the absence of specific data, attempts to generalize to the behavioral effects of radiation qualities that may be encountered in space based upon the effects produced by other qualities of radiation may not provide an accurate guide to the potential effects of such exposures. It may not be possible, therefore, to predict the effects of exposure to high-energy particles on behavior based upon research using other qualities of radiation. The present experiments were designed specifically to provide an initial assessment of the behavioral toxicity of high-energy iron particles in relation to other qualities of radiation and of the mechanisms by which they can affect behavior.

The behavioral task utilized for these experiments was the conditioned taste aversion. A conditioned taste aversion is acquired when a normally preferred novel tasting saccharin or sucrose solution is paired with a toxic unconditioned stimulus, such as lithium chloride or gamma or X radiation, such that the organism will avoid ingestion of that solution at a subsequent presentation. This avoidance behavior is typically acquired in a single pairing of the solution and toxin and may be observed at dose (or exposure) levels that produce no obvious signs of illness in the organism (*3*). Conditioned taste aversion is functionally related to emesis in that both responses serve to limit the intake and/or absorption of toxic substances (*4, 5*). As such the conditioned taste aversion is a standard paradigm for assessing the potential toxicity of a wide range of stimuli (*6*).

EXPERIMENT 1

The first experiment was designed to establish the dose–response relationships between exposure to high-energy ^{56}Fe particles and the acquisition of a conditioned taste aversion in comparison to exposure to other qualities of radiation.

Methods

The subjects were 248 male Crl:CD BR VAF/Plus rats (*Rattus Norvegicus*) weighing 300–400 g at the start of the experiment. Rats were quarantined on arrival and screened for evidence of disease before being released from quarantine. They were maintained in AAALAC accredited facility in plastic Microisolator cages on hardwood chip contact bedding and provided commercial rodent chow and acidified water. Animal holding rooms were maintained at 21 ± 1°C with 50 ± 10% relative humidity using at least 10 air changes per hour of 100% conditioned fresh air. The rats were maintained on a 12-h light/dark full spectrum lighting cycle with no twilight.

Procedure

The behavioral procedures have been detailed previously (*7*). Briefly, all rats were adapted to a water deprivation schedule for 5–7 days, during which they received water for 30 min each day. On the conditioning day, the rats were presented with a single calibrated drinking tube which contained a 10% sucrose solution in place of the water, and the intake was recorded. Immediately following the drinking period, the experimental animals were irradiated with one of the four qualities of radiation. The control animals were taken to the radiation source, but not exposed, to provide controls for the handling required to bring the

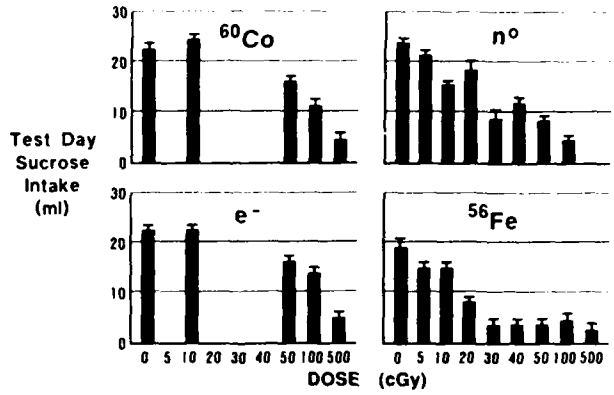

FIG. 1. Test day sucrose intake following exposure to gamma photons (^{60}Co), fission neutrons (n^0), high-energy electrons (e^-), or iron particles (^{56}Fe). Error bars indicate the standard error of the mean.

animals to the various sources. On the test day, 24 h later, the rats were again presented with the single drinking tube containing the 10% sucrose solution, and their intake was measured. Statistical analysis of the data was done using two-way analyses of variance.

Irradiation with heavy particles was done using the BEVALAC at the Lawrence Berkeley Laboratory (LBL). Groups of rats (9–12/group) were exposed to doses of 5, 10, 20, 30, 40, 50, 100, or 500 cGy of ^{56}Fe particles at an average dose rate of 10–50 cGy/min. The energy of the particles was 600 MeV/amu to take advantage of the plateau of the Bragg curve. Dosimetry was provided by the staff of the BEVALAC facility using standard procedures that have been described previously (*8, 9*).

All other irradiations were done using the sources at the Armed Forces Radiobiology Research Institute. Irradiation with fission neutrons was performed using the TRIGA reactor, which was set to deliver a neutron:gamma ratio of 20:1. The tested doses were 5, 10, 20, 30, 40, 50, or 100 cGy delivered at a dose rate of 5 cGy/min. Exposure to electrons was performed using a linear accelerator which provided 4-μs pulses (15 pulses/s) of 18.5 MeV electrons. Gamma irradiation was provided by a ^{60}Co source. For both electron and gamma irradiation, the tested doses were 10, 50, 100, or 500 cGy, at a dose rate of 130 cGy/min for electrons and 40 cGy/min for gamma rays. Radiation dosimetry was performed using paired 50-ml ion chambers. Dose was calculated using a tissue-equivalent ion chamber placed inside an acrylic rat phantom and expressed as the ratio of the dose measured in the phantom to that measured free in air (").

Results

The results are summarized in Fig. 1, which presents actual test day sucrose intake, and Fig. 2, which presents test day sucrose intake as the percentage of conditioning day intake. These figures show that the acquisition of a conditioned taste aversion following irradiation is a function of both the quality and the dose of the radiation. Both the threshold dose and the slope of the dose–response curve vary as a function of the quality of radiation.

Statistical comparisons indicated that the effects of exposure to ^{60}Co photons on the acquisition of a conditioned taste aversion were identical to those obtained following exposure to high-energy electrons. There were no differences in either the threshold at which a significant response was first observed, 50 cGy, or the dose at which the maximum taste aversion was observed.

In contrast, the behavior of both the gamma- and electron-irradiated animals differed from those exposed to fission neutrons. The threshold for observing a condi-

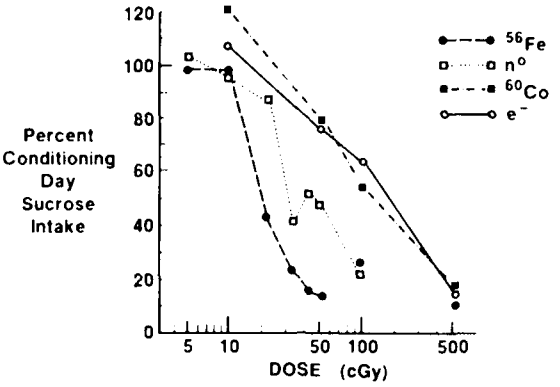

FIG. 2. Test day sucrose intake as a percentage of conditioning day intake. A taste aversion is shown as a test day intake which is less than 100% of that observed on the conditioning day.

tioned taste aversion between 10 and 20 cGy was considerably lower than that following exposure to gamma photons and electrons. In addition, as shown by the significant quality-by-dose interaction ($F(3,61) = 5.57$, $P < 0.01$), the dose–response curve following exposure to fission neutrons was steeper than that obtained with these other two qualities of radiation.

The effects of exposure to high-energy iron particles on the acquisition of a conditioned taste aversion were, in turn, significantly greater than those observed following exposure to fission neutrons ($F(1,134) = 15.59$, $P < 0.001$). Although the threshold at which a taste aversion was first observed was similar, exposure to 20 cGy produced a much greater avoidance of the sucrose following exposure to the iron particles than following exposure to neutrons. In addition, a nearly total avoidance of the conditioned stimulus was observed following exposure to only 30–40 cGy of high-energy iron particles which showed no further changes despite increasing the dose to 500 cGy. In contrast, exposure to neutrons did not produce an equivalent effect until a dose of 100 cGy had been utilized. The significant quality-by-dose interaction ($F(7,143) = 2.52$, $P < 0.05$) confirms that the pattern of responding as a function of dose was not identical between the two groups, with the animals exposed to ^{56}Fe showing a maximal aversion at a much lower dose than the animals exposed to the fission neutrons.

Discussion

These results indicate that different qualities of radiation differ in terms of their capacity to lead to the acquisition of a conditioned taste aversion. Since the taste aversion is a measure of the toxicity of a stimulus (6), the results show that these different qualities of radiation differ in terms of their toxic effect on behavior. At the lowest level of toxicity are electrons and gamma photons which show identical profiles in terms of their capacity to induce a conditioned taste aversion. The most toxic radiation stimulus is produced by exposure to high-energy iron particles, which showed the lowest threshold and steepest dose–response curve. Exposure to fission

neutrons produced intermediate levels of toxicity, both in terms of thresholds and in terms of the slope of the dose–response curve.

Previous research on a variety of physiological endpoints indicates that the relative biological effectiveness for lethality of neutron irradiation is greater than that of gamma photons (*10, 11*). Similarly, studies looking at physiological and morphological endpoints of exposure to ^{56}Fe suggest that exposure to these high-energy particles produces more damage than exposure to equivalent doses of lower linear energy transfer (LET) radiation (*12–14*). The present results are therefore consistent with these previous studies in showing increasing effects of irradiation on the acquisition of conditioned taste aversion with increasing LET.

Although there are fewer studies available examining the effects of variations in radiation quality on behavioral performance, these studies also indicate that the effect of irradiation on behavior may vary as a function of the quality of the radiation. Thus it has been reported that the frequency of vomiting is greater following exposure to a radiation field containing a higher proportion of fission neutrons to gamma photons (*15*). Similarly, studies of maze learning following irradiation of the hippocampus with ^{56}Fe particles showed deficits in performance following exposure to doses of 50 cGy (*16*). In contrast, using a different behavioral task, the accelerod which measures a motor performance decrement following high-dose irradiation, exposure to a given dose of fission neutrons or gamma photons produces the smallest decrease in performance while exposure to electrons causes the greatest decrement (*2*). The present results, showing that neutron irradiation has a greater effect on the acquisition of a conditioned taste aversion than does gamma irradiation, are consistent with the data on emesis following irradiation. This agreement between the data for taste aversion and emesis may be a reflection of the fact that taste aversion, unlike the accelerod which measured motor activity, is a behavioral measure of stimulus toxicity which is functionally related to emesis (*5*). Similarly, the present data concerning the toxicity of ^{56}Fe particles are consistent with the observations of ^{56}Fe-induced deficits in maze learning by showing that exposure to low doses of high-energy particles can produce severe effects on behavior (*16*). These data therefore suggest that the effects of radiation on behavior are a function of both the quality of the radiation and of the nature of the behavioral task.

EXPERIMENT 2

The finding that exposure to ^{56}Fe produces a conditioned taste aversion at lower doses and with a significantly steeper dose–response curve than the other qualities of radiation raises the question of whether this represents quantitative differences between the different radiation qualities, or whether it reflects the operation of fundamentally different mechanisms leading to changes in behavior.

Studies with gamma photons have shown that conditioned taste aversion following exposure to ^{60}Co requires the mediation of the area postrema (*17, 18*), the brainstem chemoreceptive trigger zone for emesis (*19*). This finding has been interpreted as indicating that the acquisition of a conditioned taste aversion following exposure to gamma radiation is a peripheral effect of the exposure: that irradiation causes the release of some humoral factor which circulates in the blood and/or cerebrospinal

fluid affecting area postrema activity which, in turn, leads to the behavioral response (5). In contrast, most research on the mechanisms by which exposure to high-energy particles affect the organism has focused on the concept of a "microlesion" (*20, 21*). This is the concept that irradiation with these particles produces a series of discrete microscopic tracks or "lesions" in the tissue, which are responsible for both the morphological and behavioral effects of exposure. Since head-only exposure to higher dose gamma photons (300 cGy) can produce a conditioned taste aversion which is partially independent of the area postrema (*22*), there is the possibility that the taste aversion seen following exposure to ^{56}Fe particles may result from direct effects on neural tissue and not from the release of a humoral mediator, as with gamma photons.

The present experiment was designed to evaluate the role of the area postrema in the acquisition of a conditioned taste aversion following exposure to high-energy iron particles to determine whether or not mechanisms similar to those observed with gamma irradiation are involved in its acquisition.

Procedure

The subjects were 57 male albino rats weighing 250–275 g at the time of surgery. Histologically verified lesions were made in the area postrema of 37 rats at AFRRI using techniques that have been detailed previously (*17*). Briefly, the rats were anesthetized with pentobarbital sodium (35 mg/kg, ip), the brainstem was exposed, and the area postrema was cauterized under direct visual control. The wound was closed and the animals were given a prophylactic injection of Bicillin (100,000 units). The 20 sham-operated controls were treated identically, except that the area postrema was not cauterized. The animals were then allowed a recovery period of 3–4 weeks before being shipped to the LBL for the remainder of the experiment.

The behavioral procedures were begun 2 weeks after the animals were shipped to LBL and were identical to those detailed above, except that only a single dose of iron particles was utilized. The rats with area postrema lesions and the sham-operated controls were each divided into two groups. The experimental subjects were 21 rats with area postrema lesions and 10 sham-operated controls which were exposed to 30 cGy ^{56}Fe particles at a nominal dose rate of 10 cGy/min. Sixteen rats with area postrema lesions and 10 sham-operated rats were treated identically, except that they were not exposed in order to serve as controls for the shipping and handling procedures.

At the conclusion of the experiment, all rats were sacrificed with an overdose of pentobarbital (50 mg), perfused with isotonic saline and 10% formalin saline, and the brains were removed for histological examination. Frozen sections were cut through the brainstem at the level of the area postrema at 50 μm and stained with thionin. Sample photomicrographs of the area postrema and a representative lesion are presented in Fig. 3.

Results

As shown in Fig. 4, lesions of the area postrema completely disrupted the acquisition of a conditioned taste aversion following exposure to high-energy iron particles. In contrast to the area postrema-operated animals, the sham-operated controls showed a significant reduction in test day sucrose intake ($F(1,29) = 22.87$, $P < 0.001$). There were no differences between the area postrema- and sham-operated groups ($F(1,24) = 1.14$, $P > 0.05$) which served as shipping and handling controls and which were not irradiated.

Histological examination of the brains of the rats indicated that, for the most part, the lesions were restricted to the area of the area postrema, although they did, in some cases, infringe upon the dorsal parts of the nucleus of the solitary tract or dorsal motor

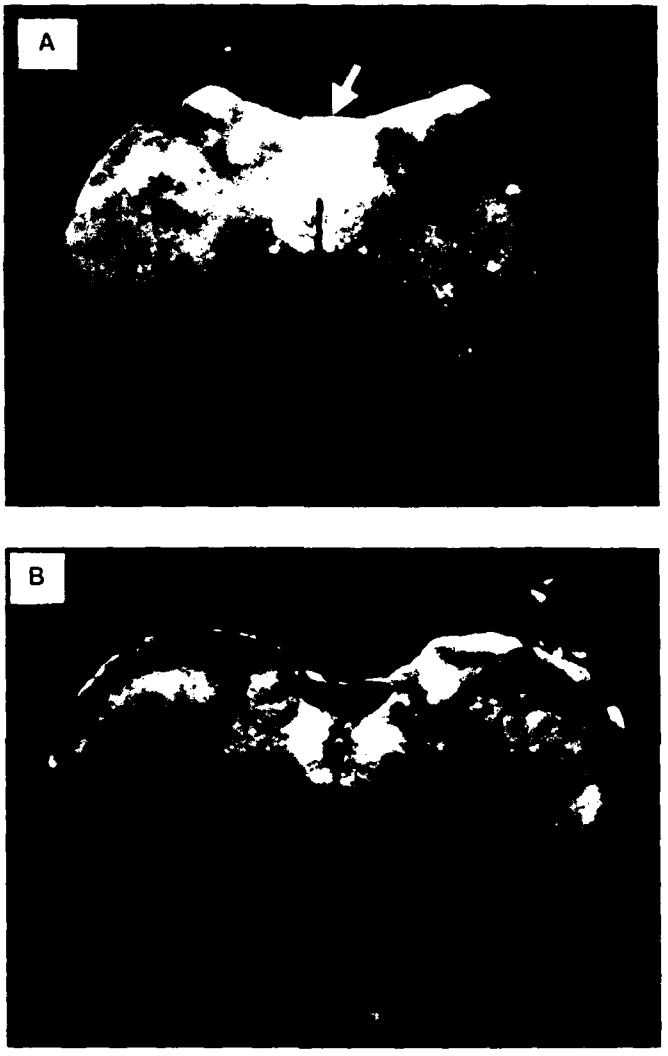

FIG. 3. Sample photomicrographs showing the area postrema in an intact sham-operated control rat (A, arrow) and a representative lesion (B).

nucleus. However, given destruction of the area postrema, there was no apparent relationship between this additional tissue destruction and the lesion effects on the acquisition of a conditioned taste aversion.

Discussion

The observation that lesions of the area postrema disrupt the acquisition of conditioned taste aversion induced by ^{56}Fe indicates that the mechanisms by which exposure to these high-energy particles exert their toxic effect on behavior are the same as

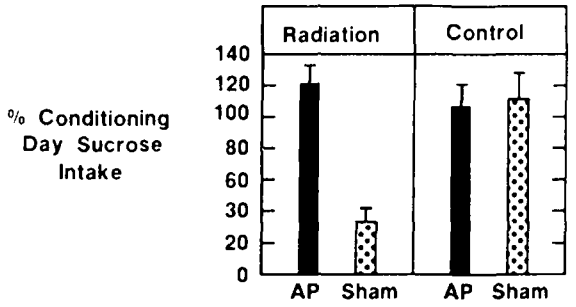

FIG. 4. Effects of area postrema lesions (AP) on the acquisition of a conditioned taste aversion following exposure to 30 cGy ^{56}Fe (Radiation) or control treatment.

those involved in the acquisition of a conditioned taste aversion following exposure to gamma photons, which also depends upon the integrity of the area postrema (*17, 18*). These data therefore suggest that the differences in toxicity obtained in the first experiment of this series are the result of quantitative and not qualitative differences between these two forms of radiation: that ^{56}Fe is a much more potent toxin than is ^{60}Co, but that both produce their effects on behavior through the operation of similar area postrema-dependent mechanisms. While these data do not directly deal with the microlesion concept, the observation that the conditioned taste aversion induced by ^{56}Fe is also dependent upon the integrity of the area postrema would be consistent with the hypothesis that this response, at this dose (30 cGy), is a peripheral effect of the exposure and does not result from the direct action of the particles on the central nervous system, as has been reported for other behavioral effects of ^{56}Fe exposure (*16*).

GENERAL DISCUSSION

The present results support the general conclusion that these different radiation qualities differ in terms of behavioral toxicity: ^{56}Fe is the most toxic, followed by fission neutrons, while ^{60}Co and electrons produce the least toxic, but identical, effects on behavior. The factors that might be responsible for this ranking are not completely clear. While it might be possible that these behavioral differences reflect differential damage to taste receptor units caused by the different qualities of radiation, resulting in a differential responsiveness to the sucrose conditioned stimulus, this does not seem likely because exposure to gamma photons and cyclotron fast neutrons produce equivalent changes in taste acuity and in detection and recognition thresholds (*23*). Another possibility is that the toxicity of radiation may be related to LET. Since the intensity of the taste aversion produced by the various qualities of radiation paralleled the LET of those radiation qualities, it may be that the behavioral toxicity of the different radiation qualities depends upon their LET. However, the basis for these differences in behavioral toxicity must await further research utilizing other high-energy heavy particles. Nonetheless, these data, in combination with previous research about the effects of different qualities of radiation, clearly suggest that the

effects of exposure on behavior are a joint function of both the specific quality of the radiation and the specific nature of the behavioral task. As a result, our ability to generalize about the potential effects of exposure to one radiation quality based upon data from another and from one endpoint to another may be very limited.

With regard to the specific effects of exposure to high-energy heavy particles on behavior, the present results are consistent with the hypothesis that these differences result from a greater effectiveness of these particles in producing the toxic reactions measured by conditioned taste aversion. These results are, in general, consistent with other research using a variety of physiological and behavioral endpoints; this indicates the significantly greater relative biological effectiveness of exposure to high-energy heavy particles (*13, 16*).

Although this research presents only an initial assessment of the behavioral toxicity of exposure to heavy particles, it does have some implications for manned flights outside the magnetic field of the earth. The relative biological effectiveness of high-energy iron particles is greater than that of gamma photons by a factor of ten, meaning that behavioral effects can be observed following exposure to doses much less than might be expected based upon the data derived from the use of gamma irradiation. As such, these results suggest that estimates of mission failure due to exposure to heavy particles may have to be revised upward.

ACKNOWLEDGMENTS

The authors acknowledge the assistance of Drs. E. John Ainsworth, Patricia Durbin, and Bernhard Ludewigt, and the staff at the Lawrence Berkeley Laboratory, without whose help these studies could not have been undertaken. We also acknowledge the support of the Computer Science Center Facilities of the University of Maryland of Baltimore County. This research was supported by the Armed Forces Radiobiology Research Institute, Defense Nuclear Agency, under work unit B4123. Views presented in this paper are those of the authors; no endorsement by the Defense Nuclear Agency has been given or should be inferred. This research was conducted according to the principles described in the "Guide for the Care and Use of Laboratory Animals" prepared by the Institute of Laboratory Animal Research, National Research Council.

RECEIVED: November 4, 1988; ACCEPTED: March 10, 1989

REFERENCES

1. W. A. HUNT, Comparative effects of exposure to high-energy electrons and gamma radiation on active avoidance behaviour. *Int. J. Radiat. Biol.* **97**, 257–260 (1983).
2. V. BOGO, Effects of Bremsstrahlung and electron radiation on rat motor performance. *Radiat. Res.* **100**, 313–320 (1984).
3. J. C. SMITH, Radiation: Its detection and its effects on taste preferences. In *Progress in Physiological Psychology* (E. Stellar and J. M. Sprague, Eds.), Vol. 4, pp. 53–117. Academic Press, New York, 1971.
4. B. M. RABIN, W. A. HUNT, A. L. CHEDESTER, and J. LEE, Role of the area postrema in radiation-induced taste aversion learning and emesis in cats. *Physiol. Behav.* **37**, 815–818 (1986).
5. B. M. RABIN and W. A. HUNT, Mechanisms of radiation-induced conditioned taste aversion learning. *Neurosci. Biobehav. Rev.* **10**, 55–65 (1986).
6. A. L. RILEY and D. L. TUCK, Conditioned taste aversions: A behavioral index of toxicity. *Ann. N.Y. Acad. Sci.* **443**, 272–292 (1985).
7. B. M. RABIN, W. A. HUNT, and J. LEE, Studies on the role of central histamine in the acquisition of a radiation-induced conditioned taste aversion. *Radiat. Res.* **90**, 609–620 (1982).

8. J. T. LYMAN and J. HOWARD, Dosimetry and instrumentation for helium and heavy ions. *Int. J. Radiat. Oncol. Biol. Phys.* **3,** 87–91 (1977).
9. J. E. AINSWORTH, Early and late mammalian responses to heavy charged particles. *Adv. Space Res.* **6,** 153–165 (1986).
10. B. C. ZOOK, E. W. BRADLEY, G. W. CASARETT, and C. C. ROGERS, Pathologic findings in canine brain irradiated with fractionated fast neutrons or photons. *Radiat. Res.* **84,** 562–578 (1980).
11. J. S. RASEY, N. J. NELSON, P. MAHLER, K. ANDERSON, K. A. KROHN, and T. MENARDI, Radioprotection of normal tissues against gamma rays and cyclotron neutrons with WR-2721: LD_{50} studies and ^{35}S-WR-2721 biodistribution. *Radiat. Res.* **97,** 598–607 (1984).
12. L. M. KRAFT and A. B. COX, Morphometric studies of heavy ion damage in the brains of rodents. *Adv. Space Res.* **6,** 251–256 (1986).
13. R. J. M. FRY, Radiation effects in space. *Adv. Space Res.* **6,** 261–268 (1986).
14. G. E. GAUGER, C. A. TOBIAS, T. YANG, and M. WHITNEY, The effect of space radiation of the nervous system. *Adv. Space Res.* **6,** 243–249 (1986).
15. G. R. MIDDLETON and R. W. YOUNG, *Neutron-Gamma Ratio and Vomiting.* Scientific Report SR75-26, Armed Forces Radiobiology Research Institute, 1975.
16. D. E. PHILPOTT and J. MIQUEL, Longterm effects of low doses of ^{56}Fe ions on the brain and retina of the mouse: Ultrastructural and behavioral studies. *Adv. Space Res.* **6,** 233–242 (1986).
17. B. M. RABIN, W. A. HUNT, and J. LEE, Attenuation of radiation- and drug-induced conditioned taste aversion following area postrema lesions in the rat. *Radiat. Res.* **93,** 388–394 (1983).
18. K.-P. OSSENKOPP, Taste aversion conditioned with gamma radiation: Attenuation by area postrema lesions in rats. *Behav. Brain Res.* **7,** 295–305 (1983).
19. H. L. BORISON, Area postrema: Chemoreceptive trigger zone for vomiting—Is that all? *Life Sci.* **14,** 1807–1817 (1974).
20. P. TODD, The evolving microlesion concept. *Adv. Space Res.* **6,** 187–189 (1986).
21. S. B. CURTIS, Lethal and potentially lethal lesions induced by radiation—A unified repair model. *Radiat. Res.* **106,** 252–270 (1986).
22. B. M. RABIN, W. A. HUNT, and J. LEE, Effects of dose and of partial body ionizing radiation on taste aversion learning in rats with lesions of the area postrema. *Physiol. Behav.* **32,** 119–122 (1984).
23. K. L. MOSSMAN, J. D. CHENCHARICK, A. C. SCHEER, W. P. WALKER, R. D. ORNITZ, C. C. ROGERS, and R. I. HENKIN, Radiation-induced changes in gustatory function: Comparison of effects of neutron and photon irradiation. *Int. J. Radiat. Biol. Oncol. Phys.* **5,** 521–528 (1979).

ARMED FORCES RADIOBIOLOGY RESEARCH INSTITUTE
SCIENTIFIC REPORT
SR89-36

0041-1337/88/4605-0655$02.00/0
TRANSPLANTATION
Copyright © 1988 by The Williams & Wilkins Co.

Vol. 46, 655–660, No. 5, November 1988
Printed in U.S.A.

L-LEUCYL-L-LEUCINE METHYL ESTER TREATMENT OF CANINE MARROW AND PERIPHERAL BLOOD CELLS

INHIBITION OF PROLIFERATIVE RESPONSES WITH MAINTENANCE OF THE CAPACITY FOR AUTOLOGOUS MARROW ENGRAFTMENT[1]

ROBERT F. RAFF,[2] EILEEN SEVERNS, RAINER STORB, PAUL MARTIN, THEODORE GRAHAM, BRENDA SANDMAIER, FRIEDRICH SCHUENING, GEORGE SALE, AND FREDERICK R. APPELBAUM

Fred Hutchinson Cancer Research Center, Seattle, Washington 98104

Incubation of canine marrow and peripheral blood mononuclear cells with L-leucyl-L-leucine methyl ester resulted in the inhibition of mitogen- and alloantigen-induced blastogenesis, the elimination of allosensitized CTL and NK activity, and prevented the development of CTL from pCTL. The effects of these incubations were similar to those described in mice and humans. Additionally, in vitro CFU-GM growth from treated canine marrow was reduced, but could be regained when the Leu-Leu-OMe–treated marrow was cocultured with either untreated autologous peripheral blood mononuclear cells or monocyte-enriched PBMC but not with untreated monocyte-depleted PBMC. Six of seven dogs conditioned with 920 cGy total-body irradiation engrafted successfully after receiving autologous marrow that was incubated with Leu-Leu-OMe prior to infusion. These cumulative results indicate that incubation with Leu-Leu-OMe is a feasible method to deplete canine marrows of alloreactive and cytotoxic T cells prior to transplantation.

The success of allogeneic marrow transplantation as treatment for malignant and nonmalignant hematopoietic diseases has been restricted by the serious complications of graft-versus-host disease (*1, 2*). Experiments in a variety of mammalian marrow transplant models have shown that removal of mature T cells from donor marrow permits engraftment without the development of GVHD (*3–6*). Based on these and similar observations, studies have been carried out to evaluate the effects of T cell depletion prior to allogeneic marrow transplantation in humans. Most studies have employed marrow treatments with anti-T cell monoclonal antibodies plus complement or with soybean agglutinin followed by E rosette formation and density gradient centrifugation (*7–9*). In general, removal of T cells has been associated with a marked decrease in both the incidence and severity of GVHD. However, the use of T cell-depleted marrow has also been associated with an increased incidence of marrow graft rejection (*10*).

This work was supported by Grants CA31787 and CA18105 from the National Cancer Institute, National Institutes of Health, DHHS, and by contract DNA 001-86-C-0192 of the Defense Nuclear Agency, Armed Forces Radiobiology Research Institute. Views presented are those of the authors; no endorsement by the Defense Nuclear Agency has been given or should be inferred. Research was conducted according to the principles enunciated in the "Guide for the Care and Use of Laboratory Animals" prepared by the Institute of Laboratory Animal Resources, National Research Council.

[2] Address reprint requests to R. F. Raff, Fred Hutchinson Cancer Research Center, 1124 Columbia Street, Seattle, WA 98104.

Recently, Thiele and Lipsky have described a dipeptide methyl ester, L-leucyl-L-leucine-methyl ester (Leu-Leu-OMe)* that can eliminate natural killer cells (NK), monocytes (Mø), and precursors of alloantigen-specific cytotoxic T cells (pCTL) from mouse spleen cell suspensions and from both mouse and human peripheral blood. This treatment leaves intact B cells, helper T cells, and murine erythroid and hematopoietic stem cells (*11–14*). In a murine histoincompatible marrow transplant model (C57BL/6J→(C57BL/6×DBA/2)F_1), treatment of donor marrow and spleen cells with Leu-Leu-OMe resulted in successful donor marrow engraftment and the development of stable long-term hematopoietic chimerism without GVHD (*14–16*). The use of Leu-Leu-OMe to treat marrow may have advantages over currently used methods. The use of Leu-Leu-OMe is very simple, requiring but a single 15-min incubation. In addition, it appears that marrow incubation with Leu-Leu-OMe results in the elimination of the cells responsible for acute GVHD while at the same time preserving hematopoietic stem cells needed for engraftment and the cells required for immune reconstitution (*15, 16*).

We and others have used dogs as a large, outbred animal model for us in experimental marrow transplantation (*17, 18*). The present studies were undertaken to determine whether the incubation of canine marrow and peripheral blood cells with Leu-Leu-OMe would yield alterations of in vitro cellular immune function comparable to those described in human and murine cells and to investigate the effects of marrow incubation with Leu-Leu-OMe on early hematopoietic progenitors and stem cells assayed for both in vitro and in vivo function.

MATERIALS AND METHODS

Dogs. Beagles, hounds, and mixed breed hounds, obtained from commercial vendors in Washington and Virginia or raised at the Fred Hutchinson Cancer Research Center (FHCRC), were dewormed and vaccinated against distemper, hepatitis, leptospirosis, and parvovirus before use in this study. All dogs were at least six months of age and were maintained at the FHCRC canine kennel facilities per guidelines stipulated by the National Academy of Sciences—National Research Council. The research protocol was approved by the Internal Animal Care and Use Committee at the Fred Hutchinson Cancer Research Center.

Medium. Waymouth's MB752/1 medium (FHCRC media preparation facility), supplemented with 0.1 mM nonessential amino acids and 100 U/ml penicillin and 100 μg/ml streptomycin (all from GIBCO).

* Abbreviations: Leu-Leu-OMe, L-leucyl-L-leucine-methyl ester; Mø, monocytes; B MLC, bulk MLC; NWNA, nylon wool nonadherent; CFU-C, colony forming unit in culture; PEDS, postendotoxin dog serum; CTAC, canine thyroid adenocarcinoma cell line.

was used for the dilution of heparinized whole blood and marrow for the cell separation procedures. Waymouth's medium supplemented as above with the addition of 10% to 20% heat-inactivated (56 C) normal pooled dog serum (M-NPS/10-20%) was used for the mixed leukocyte culture microassays, bulk MLC (B-MLC), cell-mediated lympholysis, and NK assays.

Cell preparation. Peripheral blood mononuclear cells were obtained by the centrifugation of heparinized venous whole blood (diluted 1:2 with medium) over Ficoll-Hypaque density gradients (Sp. density 1.074) as previously described (19). Bone marrow cells (BMC) for in vitro assays were obtained by syringe aspiration from the humeral head of an anesthetized dog. The marrow was diluted 1:2 with medium and overlayed onto Ficoll-Hypaque density gradients for centrifugation (1000 × g), following which the interface cells were washed once with hemolytic buffer and twice with medium. The PBMC and marrow cells were resuspended into medium for cell counts and viability assessment using the trypan-blue exclusion technique.

Monocyte-enriched cells were obtained by treating PBMC with the anticanine murine monoclonal antibody Dly 6 (20) as follows: 300×10^6 PBMC were incubated for 30 min at room temperature in 30 ml of 1:100 diluted Dly 6 (ascites containing antibody), and then an equal volume of 1:2 diluted rabbit serum complement (Pel Freeze, Rogers, AR) was added for an additional 60 min. The cells were washed once with medium, resuspended in 30 ml of 1:3 diluted rabbit serum complement, and incubated again for 60 min. After washing twice in medium, these cell suspensions contained 61±8% (SEM) viable monocytes, 16±3% lymphocytes, and 23±9% granulocytes, primarily eosinophils.

Monocyte-depleted PBMC were obtained by first passing PBMC over nylon-wool columns as previously described (21), and then transferring 30×10^6 nylon-wool nonadherent (NWNA) cells in 10 ml of medium, containing 5% fetal calf serum, into plastic petri dishes (Falcon No. 3002, Lincoln Park, NJ) for 2 hr incubation at 37 C, 7% CO_2. This depletion technique yielded approximately 95±1% lymphoid cells with greater than 90% viability and less than 3% monocytes as determined by morphologic assessment of Wright-stained cytospin preparations.

Preparation of Leu-Leu-OMe. The Leu-Leu-OMe was synthesized from L-leucyl-L-leucine (Sigma Chemical Co, St Louis, MO) as previously described (11). Qualitative assessment of Leu-Leu-OMe purity was obtained by thin-layer chromatography (TLC) (22). Briefly, 5 λ of 5×10^{-2} M solutions of L-leucine methyl ester (Leu-OMe) (dissolved in absolute methanol), L-leucine (Leu), L-leucyl-L-leucine (Leu-Leu) (both dissolved with heat and stirring in absolute methanol containing 0.5 N HCl), and the synthesized Leu-Leu-OMe were applied to precoated TLC plates (250 μM, 10×20-cm, HPTLC Kieselgel 60 (Merck), Darmstadt, West Germany), and quickly dried under a stream of warm air. The plates were developed for 2.5-hr in an enclosed, equilibrated system containing the following mixture of reagent grade solvents: chloroform, absolute methanol and acetic acid at volume ratios of 19:0.6:12.5, respectively. The migrations of the four compounds were visualized by applying an aerosol spray of 0.2% ninhydrin in ethanol and then placing the plates in a 60°C oven for 30 min. R_f values (the ratio of the distance the compound travels to the distance the solvent front travels) were calculated, in order to assess the resultant migrations, according to the following formula (22):

$$R_f = \frac{\text{distance traveled by compound}}{\text{distance traveled by solvent front}}$$

Leu-Leu-OMe was stored at −20°C in absolute methanol and, based on repeated TLC analysis, was stable for at least three months.

Incubation of PBMC or marrow cells with Leu-Leu-OMe. Equal volumes of PBMC or marrow cell suspensions and Leu-Leu-OMe at the indicated final concentrations were incubated for 15 min at room temperature. Cells for in vitro studies were washed twice and resuspended in medium. Marrow cells used for autologous infusion were incubated at cell concentrations of 20×10^6/ml in Leu-Leu-OMe solutions that contained 0.1 U/ml DNAase (Worthington Enzymes and Biochemicals, Freehold NJ). After incubation, these cells were washed, counted, and reinfused within 1–3 hr.

Mixed leukocyte culture and mitogen assays. MLCs were established, labeled with [^{3}H]thymidine, harvested, and prepared for liquid scintillation counting as previously described (23) with minor modifications. The 10^5 Leu-Leu-OMe treated or untreated responder and 10^5 irradiated (2300 rads) untreated, stimulator PBMC were cocultured in a final volume of 200 μl M-NPS/20% per well. Mitogen stimulation was assessed by adding either 375 μg/ml PHA (DIFCO, Detroit MI), 200 μg/ml Con A, (Calbiochem, San Diego CA), or 200 μg ml PWM (GIBCO, Grand Island, NY) to 10^5 treated or untreated responder cells in a final volume of 200 μl of M-NPS/20%. All cultures were established in triplicate in microtiter plates (Costar No. 3799, Cambridge MA) for 7 days at 37 C, 7% CO_2 in a humidified incubator.

Bulk MLC (B-MLC) and cell mediated lympholysis assays. Bulk MLCs were established using either untreated or Leu-Leu-OMe treated PBMC or marrow cells as responders, and untreated, irradiated PBMC as stimulators, to generate CTL for CML assays, as previously described (19), with modifications. CTL were derived from these cultures to form two CML assay groups: (1) responder PBMC or marrow cells treated with Leu-Leu-OMe or MeOH on day 0 prior to mixing with irradiated stimulator PBMC in B-MLC (day 0); and (2) Leu-Leu-OMe or MeOH treatment of 7-day B-MLC generated CTL (day 7). CTLs were mixed at a 50:1 effector:target ratio, with ^{51}Cr-labeled Na_2CrO_4 (300–500 μCi/ml, NEN, Wilmington DE) Con A stimulated PBMC targets. Cultures of PBMC to be used for targets in the CML assays were established on the same day of B-MLC, and stimulated with Con A on day 4 of culture. The 4-hr ^{51}Cr release assay was performed as previously described (19). The mean spontaneous maximum ^{51}Cr release ratio was 16±1% (± SEM), while maximum release (total ^{51}Cr incorporation was 90±2% for targets used in this series of CML assays.

Proliferation of treated or untreated responder PBMC or marrow cells in 7-day B-MLC was measured by distributing 200-μl aliquots from each B-MLC flask into triplicate microculture wells and labeling for 7 hr with [^{3}H]thymidine. Cell harvest and liquid scintillation counting were performed as described for MLC (23).

Natural killer cell (NK) assays. Leu-Leu-OMe or MeOH treated or untreated PBMC and marrow cells were assayed for NK activity against a ^{51}Cr-labeled canine thyroid adenocarcinoma cell line (CTAC) in a 18-hr assay with the percentage of ^{51}Cr release calculated as previously described (24).

In vitro marrow cultures for CFU-GM growth. Leu-Leu-OMe and MeOH treated and untreated marrow cells were tested for in vitro hematopoietic progenitor growth using an agar based colony formation assay that utilizes postendotoxin dog serum (PEDS) as the source of colony-stimulating factor (25). Growth of granulocyte-macrophage colonies (CFU-GM) was assayed in cultures containing 10^5 or 3×10^5 treated or untreated marrow cells only, and in cultures in which marrow cells were cocultured with either 10^5 autologous PBMC, Mø-enriched or Mø-depleted PBMC, or Leu-Leu-OMe treated PBMC incubated with 1000 μM Leu-Leu-OMe. Cultures were incubated in triplicate for 10 days in a 37 C, 7% CO_2 humidified incubator and CFU-GM colonies were enumerated as previously described (25).

Autologous marrow transplantation. Marrow for autologous transplantation was obtained by a vacuum pump aspiration procedure (26), processed over a Ficoll-Hypaque density gradient and incubated with Leu-Leu-OMe. All recipients were conditioned with 920 cGy total body irradiation delivered as a single exposure from two opposing ^{60}Co sources at 7.0 cGy/min (26). The recipients were infused with treated autologous marrow within 3 hr of TBI. Supportive care pre- and posttransplantation with antibiotics, iv fluids, and whole blood transfusions, was given as previously described (27). In addition, recipients were given oral antibiotics (Neomycin sulfate and polymyxin B sulfate) daily for five days before TBI and posttransplant until the granulocyte count reached 500/mm

RESULTS

Thin-layer chromatographic analysis of synthesized Leu-Leu-OMe. Three batches of Leu-Leu-OMe were synthesized for use in the in vitro studies and autologous transplant experiments described. Consistent R_f values were obtained for each batch of Leu-Leu-OMe and for the three control compounds tested. Within the Leu-Leu-OMe, there was a secondary spot that migrated with a R_f value equal to that observed for the L-Leucyl-L-leucine. The consistency of the R_f values indicated that constant yield and purity was achieved with minimal batch-to-batch variations.

Viability of PBMC and marrow cells after incubation with Leu-Leu-OMe. The viability of treated PBMC and marrow cells was assessed within 1 hr after incubation with Leu-Leu-OMe. There was no significant difference in viabilities observed in cells treated with either Leu-Leu-OMe (up to 1000 μM), 0.5% MeOH in PBS, or PBS only. No time-course studies were done to assess the viability of PBMC and marrow cells more than 1 hr after incubation with Leu-Leu-OMe.

Elimination of alloantigen responsiveness and mitogen induced lymphocyte blastogenesis by incubation of PBMC with Leu-Leu-OMe. PBMC were treated at either 2×10^6 or 20×10^6/ml with Leu-Leu-OMe and tested in micro-MLC, and blastogenesis assays (Fig. 1). In all assays there was a Leu-Leu-OMe dose-dependent reduction in the proliferative response such that virtually no blastogenesis was observed after incubation with 1000 μM Leu-Leu-OMe.

Treatment of 20×10^6 responder PBMC or marrow cells before bulk MLC resulted in similar Leu-Leu-OMe dose-dependent reductions in proliferative response (data not shown). The marrow cells gave a lower baseline level of [^{3}H]thymidine incorporation and were more sensitive than the PBMC to treatment with Leu-Leu-OMe (data not shown). Treatment of PBMC/marrow cells with 0.5% MeOH in PBS had no effect on the alloproliferative response in B MLC (data not shown).

Elimination of the generation of antigen specific cytotoxic T lymphocytes by incubation of PBMC and marrow cells with Leu-Leu-OMe. The effect of Leu-Leu-OMe on the generation of antigen-specific cytotoxic T cells was measured by incubating responder PBMC and marrow cells with Leu-Leu-OMe (day 0 treatment), and then testing these cells in a standard CML assay after 7 days of culture in B MLC. Treatment with 1000 μM Leu-Leu-OMe eliminated the generation of cytolytic activity against ^{51}Cr labeled alloantigen specific Con A stimulated PBMC (Fig. 2). These results indicated that the generation of CTL from precursors is sensitive to incubation with Leu-Leu-OMe. The effect of Leu-Leu-OMe incubation on CTL already generated in 7 day bulk MLC (day 7 treatment) was also evaluated. This treatment eliminated antigen-specific cytolytic activity (Fig. 2). Treatment with 0.5% MeOH either on day 0 or day 7 did not interfere with either the development of CTL or the specific cytolysis of targets assayed on day 7 (data not shown).

Elimination of NK activity after incubation of PBMC and marrow cells with Leu-Leu-OMe. Marked diminution of NK activity, in a dose dependent manner, was seen after incubation of PBMC or marrow cells with Leu-Leu-OMe, and NK activity was essentially eliminated after treatment with 1000 μM Leu-Leu-OMe (Fig. 3).

In vitro CFU-GM colony assay after incubation with Leu-Leu-OMe.

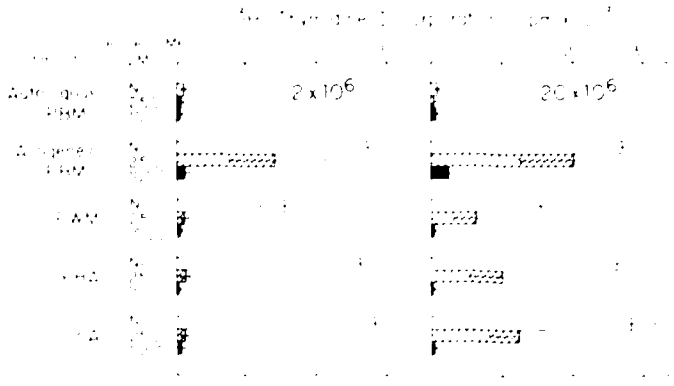

FIGURE 1. Effect of Leu-Leu-OMe on alloantigen- and mitogen-induced lymphocyte blastogenesis. Data for [^{3}H]thymidine incorporation are mean cpm ± SEM from multiple assays in which PBMC were treated at concentration of 2×10^6 or 20×10^6 cells/ml.

FIGURE 2. CML assays illustrating the effect of Leu-Leu-OMe treatment on p CTL (day 0) or on 7-day B MLC generated CTL (day 7), derived either from PBMC or BMC. The ordinate indicates mean percentage of ^{51}Cr release ± SEM using specific alloantigen sensitizing ^{51}Cr labeled Con A stimulated PBMC as targets.

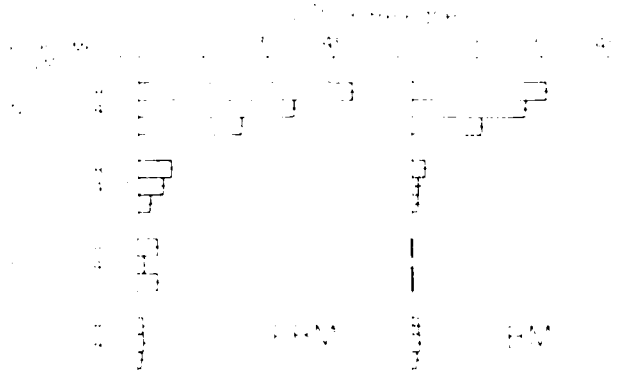

FIGURE 3. Leu-Leu-OMe treatment of PBMC and BMC eliminates NK cytolytic activity. The ordinate indicates mean percentage of ^{51}Cr release ± SEM from CLV-2 at three different effector/target (E:T) ratios. For this series of assays the mean spontaneous release of ^{51}Cr from targets was 2.1% ± SEM of 0.6% (maximum release of ^{51}Cr by detergent lysis was 64%).

treatment of marrow cells. There was a marked reduction in CFU-GM colony growth obtained from marrow cells incubated with varying concentrations of Leu-Leu-OMe (Table 1). Minimal CFU-GM growth was observed with 10^5 Leu-Leu-OMe treated marrow cells per plate were cultured. There was some recovery of CFU-GM growth when the cell number was increased to 3×10^5 treated marrow cells per plate, but only to a level that was approximately 25% of that observed with 3×10^5 untreated marrow cells. Addition of either untreated, autologous PBMC or Mø-enriched autologous PBMC increased CFU-GM growth, but not to the levels observed with untreated marrow cells in similar cocultures. The addition of Mø-depleted or Leu-Leu-OMe treated autologous PBMC to treated marrow cells did not augment growth.

The effect of incubating marrow cells with Leu-Leu-OMe on autologous marrow engraftment. Six of the seven dogs given Leu-Leu-OMe treated autologous marrow engrafted and did so with kinetics similar to those seen in recipients of untreated autologous marrow (Table 2 and Fig. 4). Platelet counts returned to normal levels between 20 to 30 days posttransplant. Dog C521 did not survive past day 20 posttransplant. After Leu-Leu-OMe incubation, the marrow cells from this dog were clumped and had only 20% viability, resulting in the infusion of a very low marrow cell dose. The marrow from C580 was incubated with the same concentration of Leu-Leu-OMe as C521, but the treated marrow cells of C580 did not clump and this dog survived with rapid engraftment. Dog BB8701 had to be euthanized on day 19 posttransplant due to an accidental, severe, foot injury that failed to respond to treatment, but did show evidence of engraftment as indicated by a rise in WBC and the marrow cellularity at autopsy.

DISCUSSION

Thiele and Lipsky have demonstrated that exposure of mouse spleen cells or human peripheral blood leukocytes to Leu-Leu-OMe depletes these populations of monocytes, NK cells, and cytotoxic lymphocytes at both the precursor and effector stages of differentiation, without apparently affecting other cell populations (*11–13*). They further showed that incubation of mixtures of murine marrow and spleen cells with Leu-Leu-OMe did not interfere with engraftment and could, in certain circumstances, prevent GVHD (*14–16*). In the studies presented here, we found that canine peripheral blood and marrow cells behave similarly following exposure to Leu-Leu-OMe with the elimination of functional monocytes, NK cells, and alloantigen-sensitized CTL, and inhibited the development of CTL from pCTL. Further, we found that incubation of marrow cells with Leu-Leu-OMe (even at very high doses) did not inhibit autologous engraftment in recipients conditioned with 920 cGy TBI. These studies also demonstrated that the treatment of canine

TABLE 1. In vitro CFU-GM colony growth from marrow cells incubated with varying concentrations of Leu-Leu-OMe

Leu-Leu-OMe (μM)	CFU-GM colonies obtained from CFU-C cultures[a]									
	10^5 BMC cocultures[b]					3×10^5 BMC cocultures[b]				
	No coculture	10^5 PBMC	10^5 Mø enriched	10^5 Mø depleted	10^5 Leu-Leu-OMe treated PBMC	No coculture	10^5 PBMC	10^5 Mø enriched	10^5 Mø depleted	10^5 Leu-Leu-OMe treated PBMC
Nil	66±13	84±9	96±15	76±23	78±13	207±15	255±18	348±9	288±7	252±17
250	0.4±0.2	64±32				55±31	178±63			
500	0	14±8				3±2	51±24			
1000	1.2±0.5	10±3	29±11	2±1	2±0.6	8±3	42±3	74±29	0.3±0.3	3±1
2000	2±1	5±2				2±0.8	13±5			
4000	0.7±0.6	11±5				0.9±0.5	16±9			

Represented are mean values ± SEM, obtained from multiple experiments in which triplicate CFU-GM cultures were established for each parameter tested.

[a] All cocultures employed autologous cells. The limited yield of Mø prevented coculture with all concentrations of Leu-Leu-OMe tested. There was no CFU-GM growth when untreated PBMC (between 10^5 to 6×10^5/ml) were cultured without marrow cells.

[b] The concentration of marrow cells treated was constant at 20×10^6/ml.

TABLE 2. Recipients conditioned with 920 cGy TBI and receiving Leu-Leu-OMe treated autologous marrow[a]

Dog ID	[Leu-Leu-OMe][b] (μM)	No. viable *treated* BMC infused ($\times10^8$/kg)	Survival (*days post* BMT)	*Cause of death*	*Marrow cellularity*
C563	1000	1.4	152	Sodium pentothal[c]	Normocellularity (3 cell lines)
BB8701	1000	0.7	19	Sodium pentothal[d]	75% of Normocellularity (3 cell lines)
C622[e]	1000	1.41	>124	Still living	Normocellularity (3 cell lines)
C521	2000	0.052	20	Pneumonia; sepsis	Focal hematopoiesis
C580	2000	1.67	173	Sodium pentothal[c]	Normocellularity (3 cell lines)
B950	4000	1.3	114	Sodium pentothal[c]	Normocellularity (3 cell lines)
C662	4000	1.5	112	Sodium pentothal[c]	Normocellularity (3 cell lines)

[a] *Autologous marrow aspiration, BMC treatment, and infusion on same day as 920 cGy TBI to recipient (BMT: bone marrow transplant).*

[b] 20×10^6 BMC/ml treated with Leu-Leu-OMe.

[c] Viability of bone marrow cells infused determined by trypan blue stain exclusion technique.

[d] Sodium pentothal injection for euthanasia at end of study.

[e] The Leu-Leu-OMe treated autologous marrow was frozen and stored at −80 C for one week prior to reinfusion. The procedure for marrow cryopreservation was as described (26).

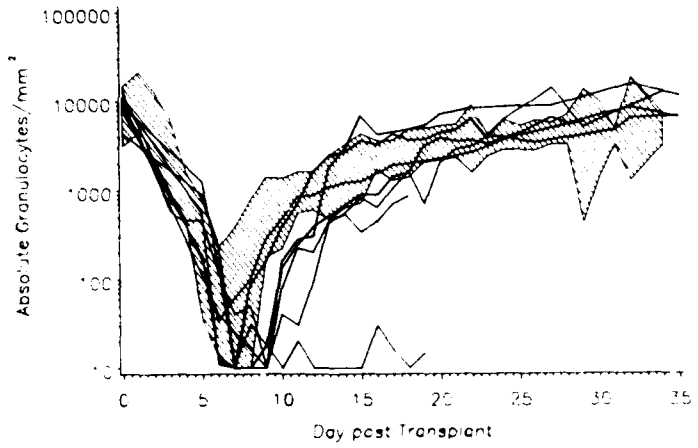

FIGURE 4. Hematologic recovery in recipients conditioned with 920 cGy TBI and infused with Leu-Leu-OMe-treated autologous marrow. The ordinate indicates the absolute granulocyte counts obtained daily posttransplant until death or recovery to the normal range. The shaded area represents the normal range (mean ± SD) of recovery observed in 16 dogs conditioned with 920 cGy TBI and given untreated autologous marrow (*98*).

marrow cells with Leu-Leu-OMe, in a concentration-dependent fashion, could reduce or eliminate in vitro CFU-GM growth. This reduction could be partially reversed with the addition of unfractionated autologous PBMC or Mø-enriched PBMC but not with Mø-depleted PBMC or autologous PBMC treated in vitro with Leu-Leu-OMe. Our assay employs postendotoxin-treated dog serum as a source of colony-stimulating factor. Reversal of the effects of Leu-Leu-OMe on CFU-GM growth by monocytes demonstrated the monocyte dependence of this CFU-GM assay system and suggests that PEDS does not act directly as a single factor on the granulocyte/macrophage progenitors.

Marrows were treated at two different cell concentrations in anticipation that this procedure might be useful for allogeneic marrow transplantation in large animals and possibly in man. Reduction or elimination of various cells involved either in response to alloantigen stimulation (MLC, pCTL, CTL) or NK function could be accomplished by treating PBMC or marrow cells at 20×10^7/ml with 1000 μM Leu-Leu-OMe. The murine models using H2-disparate P→F$_1$ marrow donor/recipient pairing showed that Leu-Leu-OMe treatment could prevent acute GVHD. The resultant chimeras developed normal cellular immune responses and showed donor and host-specific immunologic tolerance (*16*). The cell concentration treated in those studies was 2×10^7/ml, and the highest concentration of Leu-Leu-OMe used was 250 μM. Cell concentration directly influenced the concentration of Leu-Leu-OMe required to achieve a given effect. Thus, in the present study when the cell concentration was increased tenfold, the concentration of Leu-Leu-OMe had to be increased approximately fourfold to achieve the same inhibition of cellular immune functions. The potential problem of larger cell numbers and expanded marrow volumes needed for the transplantation of larger animals can be circumvented by increasing the concentration of Leu-Leu-OMe.

Data in the canine model suggest that Leu-Leu-OMe should be explored further as a possible substitute for other currently used methods of marrow T cell depletion. It needs to be determined whether treatment of marrow with Leu-Leu-OMe will leave behind a population of cells that facilitate engraftment and recovery of immunity while removing cytotoxic T cells that may comprise the major population of cells involved in the development of acute GVHD.

Acknowledgments. We thank Ray Colby, Greg Davis, Susan DeRose, Cassandra Beckham, and the Fred Hutchinson Cancer Research Center hematology and pathology technical staffs for expert technical assistance during this study. We also thank Kendall of the FHCRC Shared Word Processing facility for her excellent work in this manuscript preparation.

REFERENCES

1. Storb R, Thomas ED. Graft-versus-host disease in dogs and man: the Seattle experience. Immunol Rev 1985; 88: 215.
2. Storb R. Critical issues in bone marrow transplantation. Transplant Proc 1987; 19: 2774.
3. Korngold R, Sprent J. Lethal graft-versus-host disease after bone marrow transplantation across minor histocompatibility barriers in mice: prevention by removing mature T cells from marrow. J Exp Med 1978; 48: 1687.
4. Kolb HJ, Rieder I, Rodt H, et al. Anti-lymphocytic antibodies and marrow transplantation: VI. Graft-versus-host tolerance in DLA-incompatible dogs after in vitro treatment of bone marrow with absorbed antithymocyte globulin. Transplantation 1979; 27: 242.
5. Wagemaker G, Vriesendorp HM, van Bekkum DW. Successful bone marrow transplantation across major histocompatibility barriers in rhesus monkeys. Transplant Proc 1981; 13: 875.
6. Vallera DA, Soderling CCB, Carlson GJ, Kersey JH. Bone marrow transplantation across major histocompatibility barriers in mice: effect of elimination of T cells from donor grafts by treatment with monoclonal Thy-1.2 plus complement or antibody alone. Transplantation 1981; 31: 218.
7. Martin PJ, Hansen JA, Buckner CD, et al. Effects of in vitro depletion of T cells in HLA-identical marrow grafts. Blood 1985; 66: 664.
8. Mitsuyasu RT, Champlin RE, Gale RP, et al. Treatment of donor bone marrow with monoclonal anti-T-cell antibody and complement for the prevention of graft-versus-host disease. Ann Intern Med 1986; 105: 20.
9. Reisner Y, Kapoor N, Kirkpatrick D, et al. Transplantation for severe combined immunodeficiency with HLA-A, B, D, DR incompatible parental marrow cells fractionated by soybean agglutinin and sheep red blood cells. Blood 1983; 61: 341.
10. Storb R. The role of T cells in engraftment: experimental models, clinical trials. In: Gale RP, Champlin R, eds. Progress in bone marrow transplantation. New York: Liss, 1987: 23.
11. Thiele DL, Lipsky PE. Regulation of cellular function by products of lysosomal enzyme activity: elimination of human natural killer cells by a dipeptide methyl ester generated from L-leucine methyl ester by monocytes or polymorphonuclear leukocytes. Proc Natl Acad Sci USA 1985; 82: 2468.
12. Thiele DL, Lipsky PE. Modulation of human natural killer cell function by L-Leucine methyl ester: monocyte-dependent depletion from human peripheral blood mononuclear cells. J Immunol 1985; 134: 786.
13. Thiele DL, Lipsky PE. The immunosuppressive activity of L-leucyl-L-leucine methyl ester: selective ablation of cytotoxic lymphocytes and monocytes. J Immunol 1986; 136: 1038.
14. Charley M, Thiele DL, Bennett M, Lipsky PE. Prevention of lethal murine graft versus host disease by treatment of donor cells with L-leucyl-L-leucine methyl ester. J Clin Invest 1986; 78: 1415.
15. Thiele DL, Charley MR, Calomeni JA, Lipsky PE. Lethal graft-versus host disease across major histocompatibility barriers: requirement for leucyl-Leucine methyl ester sensitive cytotoxic T cells. J Immunol 1987; 138: 51.
16. Thiele DL, Calomeni JA, Lipsky PE. Leucyl-leucine methyl ester

treatment of donor cells permits establishment of immunocompetent parent → F_1 chimeras that are selectively tolerant to host alloantigens. J Immunol 1987; 139: 2137.
17. Vriesendorp HM, van Bekkum DW. Bone marrow transplantation in the canine. In: Shifine M, Wilson FD, eds. The canine as a biomedical research model. Oak Ridge, TN: DOE Technical Information Center, 1980: 153.
18. Storb R, Deeg HJ. Contributions of the dog model in marrow transplantation. Plasma Ther Transfus Technol 1985; 6:303.
19. Raff RF, Storb R, Ladiges WC, Deeg HJ. Recognition of target cell determinants associated with DLA-D-locus-encoded antigens by canine cytotoxic lymphocytes. Transplantation 1982; 40: 323.
20. Wulff JC, Durkopp N, Aprile J, et al. Two monoclonal antibodies (DLy-1 and DLy 6) directed against canine lymphocytes. Exp Hematol 1982; 10: 609.
21. Atkinson K, Deeg HJ, Storb R, et al. Canine lymphocyte subpopulations. Exp Hematol 1980; 8: 821.
22. Pairia DL, Lampman GM, Kriz GS Jr. In: Introduction to organic laboratory techniques. Philadelphia: Saunders, 1976: 599.
23. Raff RF, Deeg HJ, Farewell VT, DeRose S, Storb R. The canine major histocompatibility complex: population study of DLA-D alleles rising a panel of homozygous typing cells. Tissue Antigens 1983; 21: 360.
24. Loughran TP Jr, Deeg HJ, Storb R. Morphologic and phenotypic analysis of canine natural killer cells: evidence for T cell lineage. Cell Immunol 1985; 95: 207.
25. Raff RF, Deeg HJ, Loughran TP Jr, et al. Characterization of host cells involved in resistance to marrow grafts in dogs transplanted from unrelated DLA-non-identical donors. Blood 1986; 68: 861.
26. Ladiges WC, Storb R, Graham T, Thomas ED. Experimental techniques used to study the immune system of dogs and other large animals. In: Gay WI, Heavner JE, eds. Methods of animal experimentation; vol 7: research surgery and care of the research animal; part C. Orlando, FL Academic, (in press).
27. Storb R, Rudolph RH, Kolb HJ, et al. Marrow grafts between DL-A-matched canine littermates. Transplantation 1973; 15: 92.
28. Deeg HJ, Meyers JD, Storb R, Graham TC, Weiden PL. Effect of trimethoprim-sulfamethoxazole on hematological recovery after total body irradiation and autologous marrow infusion in dogs. Transplantation 1979; 28: 243.

Received 28 March 1988.
Accepted 10 May 1988.

ARMED FORCES RADIOBIOLOGY RESEARCH INSTITUTE
SCIENTIFIC REPORT
SR89-37

0022-1554/89/$3.30
The Journal of Histochemistry and Cytochemistry
Copyright © 1989 by The Histochemical Society, Inc.
Vol. 37, No. 9, pp. 1319-1328, 1989
Printed in U.S.A.

Rapid Communication

Localization of Cyclo-oxygenase and Prostaglandin E_2 in the Secretory Granule of the Mast Cell

ELSA A. SCHMAUDER-CHOCK[1] and STEPHEN P. CHOCK[2]

Department of Experimental Hematology, Armed Forces Radiobiology Research Institute, Bethesda, Maryland 20814-5145 (EAS-C), and The Department of Medicinal Chemistry, Division of Experimental Therapeutics, Walter Reed Army Institute of Research, Washington, DC 20307 (SPC)

Received for publication June 7, 1989; accepted June 14, 1989 (9C1715).

The application of anti-cyclo-oxygenase and anti-prostaglandin E_2 immunoglobulins to A23187-stimulated rat connective tissue mast cells has permitted the localization of cyclo-oxygenase activity (prostaglandin H_2 synthetase) and the site of prostaglandin E_2 (PGE_2) formation in the secretory granules. Because binding was carried out after stimulation but before dehydration and embedding, we have limited the loss of these antigens due to normal degradation and to aqueous and solvent washes. As this method permits labeling of exposed cell surfaces, only granules that have been exteriorized can be labeled. Contrary to what might have been expected, no labeling was associated with plasma membranes or with any portion of damaged cells. Antibodies to PGE_2 were bound evenly over the surface of the granule matrix, whereas antibodies to cyclo-oxygenase appeared to be bound to strands of proteo-heparin projecting from the surface of the granule matrix. Where granule matrix had become unraveled and dispersed, label appeared to adhere throughout the ribbon-like proteo-heparin strands. These results support our previous conclusion that the secretory granule is the site of the arachidonic acid cascade during exocytosis. (*J Histochem Cytochem 37:1319-1328, 1989*)

KEY WORDS: Cyclo-oxygenase; Prostaglandin E_2; Secretory granules; Mast cell; Exocytosis; Lipid mediators; Inflammation; Arachidonic acid; Eicosanoids; Immunocytochemistry

Introduction

It has long been assumed that the cell membrane is the source of phospholipid which provides the arachidonic acid required for synthesis of prostaglandins and other eicosanoids (1-5). Eicosanoid release has also been assumed to occur as a result of cell and membrane damage (3,4). However, membrane damage cannot be the source for the large pool of free arachidonic acid required for eicosanoid synthesis, as calcium ionophore-stimulated release of eicosanoids from neutrophils can occur without damage to membrane or loss of cell function (6). In addition, macrophages that produce large amounts of eicosanoids are known to contain no stored free arachidonic acid (7). These contradictions are compounded when one considers that phospholipase A_2, the enzyme necessary for arachidonic acid release from phospholipid, requires millimolar calcium concentrations for its activity (4,8). This calcium requirement cannot be met by a membrane bilayer source.

Recently, we found that the secretory granules of the mast cell contain a large non-bilayer phospholipid store (9). During granule activation, a portion of this phospholid spontaneously assembles into vesicles as a result of a water influx from the cytoplasm into the granule (9-11). Fusion of these newly assembled membrane vesicles with the perigranular membrane enables the activated granule to enlarge and its perigranular membrane to lift from the surface of the granule matrix. The contact and fusion of the expanding perigranular membrane with the plasma membrane culminate in exocytosis (10-13). Like many other secretory systems, the mast cell also produces a variety of lipid-derived mediators, such as prostaglandins and leukotrienes, during histamine release (14). Because mast cell phospholipid contains a high concentration of arachidonic acid (15), the remaining matrix-bound phospholipid would be a convenient arachidonic acid source for eicosanoid synthesis if the enzymes of the arachidonic acid cascade are also found in the granule. To this end, we have demonstrated that the mast cell granule not only contains the substrate for eicosanoid synthesis but also contains the machinery for rapid production of eicosanoids during granule activation (16). In this communication, we further establish that the granule is the site as well as the source of eicosanoid production, by localizing the presence of cyclo-oxygenase and its product, prostaglandin E_2 (PGE_2) to the granule matrix using immunocytochemical techniques.

Materials and Methods

Rat serosal mast cells were obtained by peritoneal lavage according to a pub-

[1] Correspondence to: Dr. Elsa A. Schmauder-Chock, Armed Forces Radiobiology Research Institute, Bethesda, MD 20814-5145.
[2] Recipient of The National Research Council Senior Research Associateship.

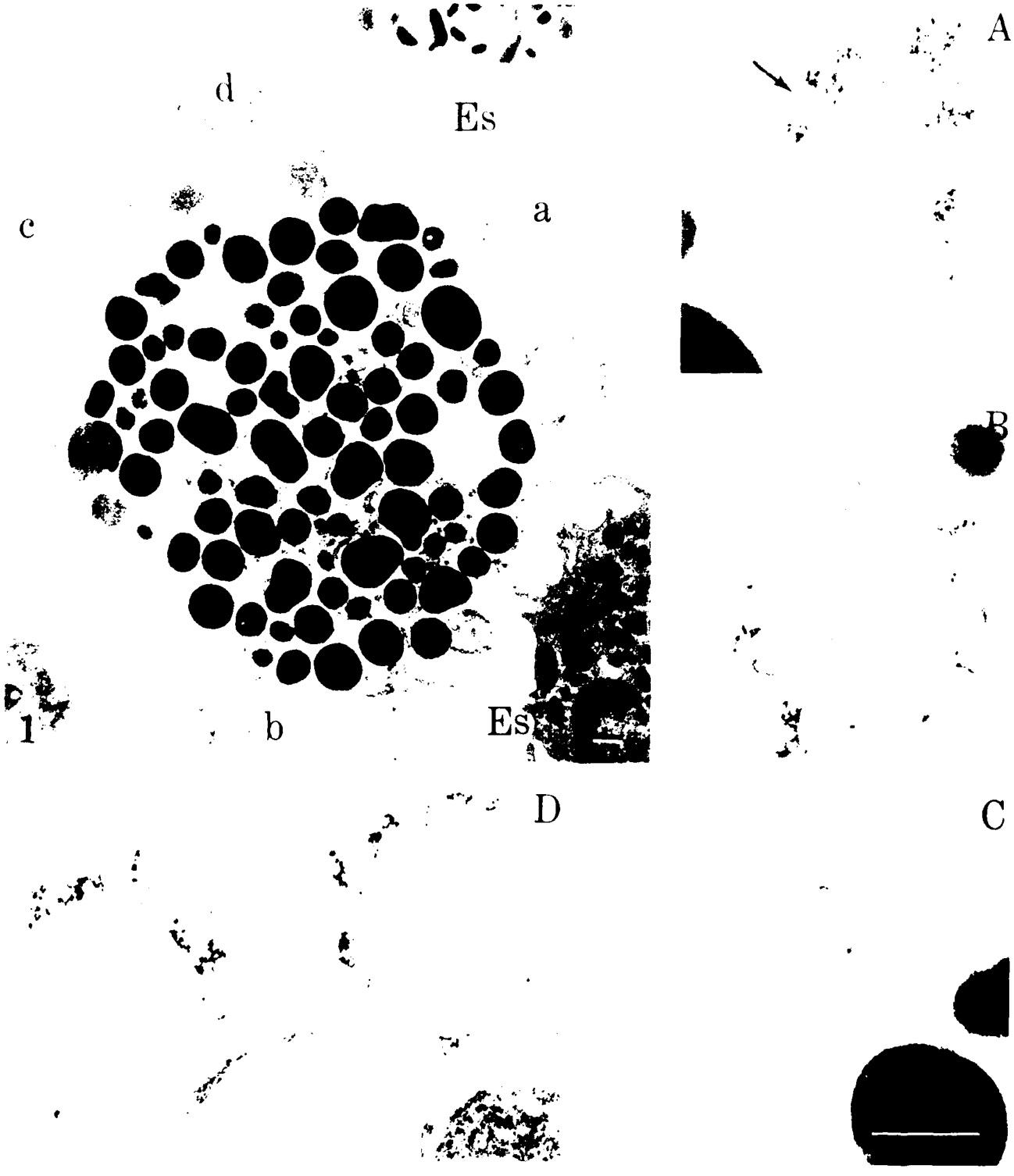

Figure 1 Cyclo-oxygenase localization in mast cells stimulated with A23187. The cyclo-oxygenase activity was localized by using monoclonal anti-cyclo-oxygenase antibodies and the resulted antigen–antibody complex was visualized ultrastructurally by binding of ferritin-conjugated antibodies. The ferritin label was confined to the strands of proteo-heparin projecting from the surface of the secreted granules. Eosinophils (Es) showed no label. Membrane vesicles were often seen in association with secreted granules (arrow). (**A–D**) High-magnification images of areas marked a through d. Original magnification × 10,120, **A–D** × 36,550. Bars = 0.5 μm.

Figure 2 Association of cyclo-oxygenase with vesicles assembled from granule matrix phospholipid. The presence of cyclo-oxygenase activity, as visualized by the ferritin label, is seen to decorate the secreted membrane vesicles (arrow). (**A–D**) High-magnification images of serial sections of the cluster of vesicles. *Note that the damaged mast cell (•) shows no ferritin label.* Original magnification × 11,362; **A–D** × 48,375. Bars = 0.5 μm

Figure 3. Control experiment for cyclo-oxygenase localization. Secreting mast cells incubated with pre-immune serum in place of the anti-cyclo-oxygenase antibodies show essentially no ferritin label. (**Inset**) High-magnification image of the granule (arrow). Original magnification × 10,350; **inset** × 40,850. Bars = 0.5 μm.

lished procedure (9), except that plain normal Hank's balanced salt solution (HBSS) was used as a lavage buffer. After one wash with HBSS and centrifugation at 30 × g for 10 min, mast cells were activated by suspension in HBSS containing 1 μg/ml A23187 for 5 min at 20°C. The reaction was stopped and cells were fixed by the addition of an equal volume of fixative containing 5% glutaraldehyde, 100 mM cacodylate, and 4 mM $MgCl_2$. After a 30-min incubation at 20°C, the cells were washed three times with HEPES-buffered saline (0.15 M NaCl and 20 mM HEPES, pH 6.8). Each wash was for 15 min with gentle agitation and was followed by a 2-min 1500-rpm centrifugation in a Beckman microfuge 12. During the third wash, the cell suspension was divided into aliquots for the various intended experiments. After centrifugation, the cell pellets were re-suspended in the respective antibodies or in pre-immune serum for the corresponding control experiments.

For localization of cyclo-oxygenase, the cells were re-suspended and incubated for 75 min with monoclonal mouse anti-cyclo-oxygenase immunoglobulin G_1 (Cayman Chemical; Ann Arbor, MI) diluted to an approximate concentration of 50 μg/ml in HEPES-buffered saline containing 20 μM digitonin (Fluka; Buchs, Switzerland) and 10 mM EDTA. A cell sample for the corresponding control experiment was incubated in pre-immune mouse serum diluted to 50 μg/ml in the same buffer.

For localization of PGE_2, the cells were incubated for 75 min with polyclonal rabbit anti-PGE_2 immunoglobulin G (Cayman Chemical) diluted to about 50 μg/ml as for the anti-cyclo-oxygenase antibody. The corresponding control was incubated with pre-immune rabbit serum at about 50 μg/ml.

After incubation, the cells were treated with three 5-min washes in HEPES-buffered saline to remove unbound antibodies. To visualize the immunogenic activity of the cyclo-oxygenase, both the control and the experimental samples were incubated with about 1 mg/ml ferritin-conjugated goat anti-mouse IgG antiserum (Cappel, West Chester, PA) for 60 min, followed by three 5-min washes with HEPES-buffered saline to remove unbound ferritinated antiserum. To visualize the PGE_2, the control and the experimental samples were incubated with diluted ferritin-conjugated goat anti-rabbit IgG antiserum (Sigma, St. Louis, MO) for 60 min, followed by washes to rid of excess unbound antibodies. Similarly, gold-conjugated antiserum (Sigma) was also used in place of the ferritin-conjugated antisera for ultrastructural localization of PGE_2.

After a last wash to rid the cells of the unbound heavy metal-conjugated antisera, the specimens were osmicated for 20 min in 1% osmium tetroxide, followed by routine dehydration and embedding in Epon 812 according to established procedures (12). Unstained thin sections were examined with a Phillips 400 transmission electron microscope.

Results

Cyclo-oxygenase Localization

The application of monoclonal anti-cyclo-oxygenase antibodies to A23187-stimulated peritoneal lavage cells permitted the ultrastruc-

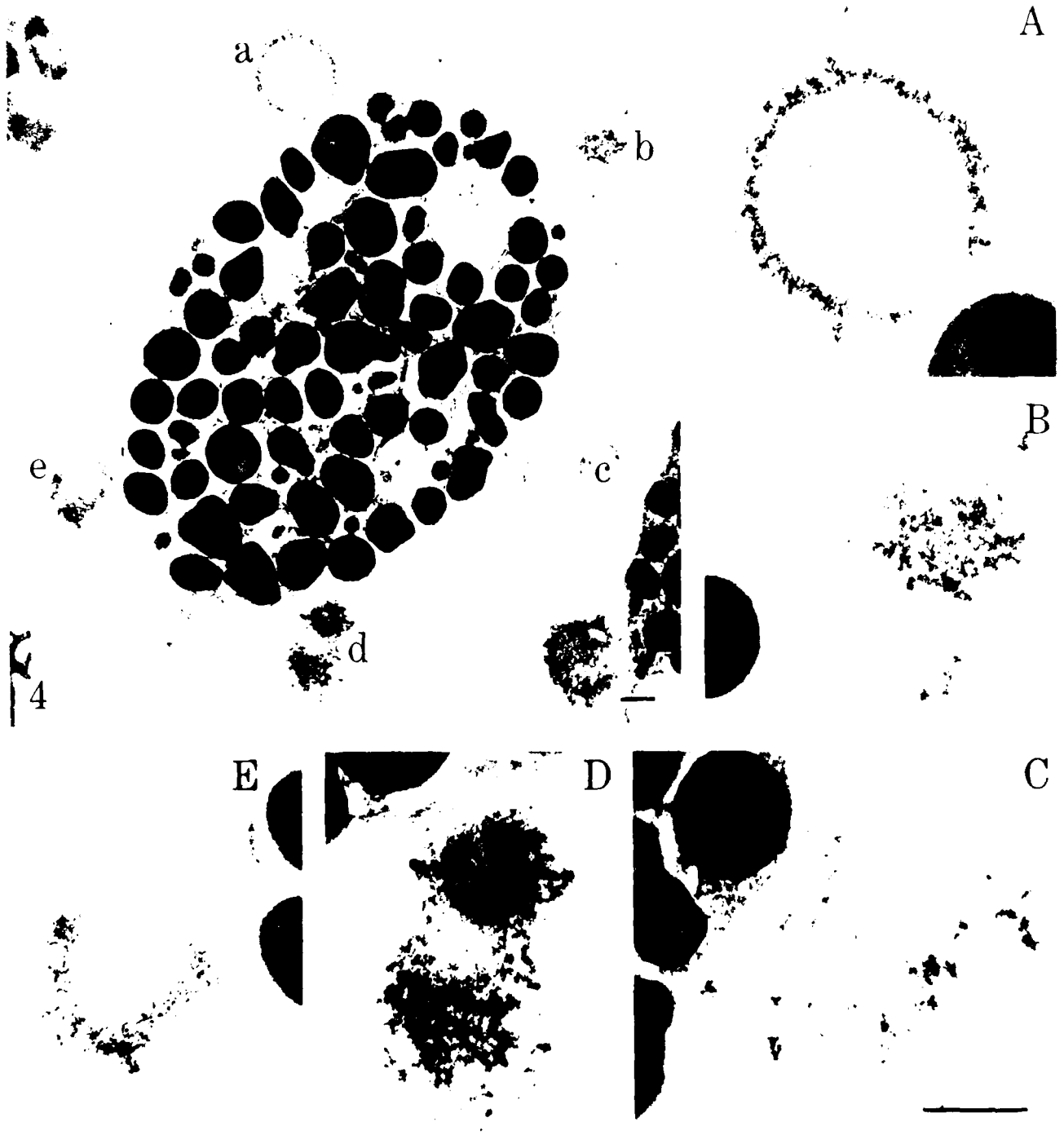

Figure 4 Localization of the secretory granule as the site of PGE_2 production. Mast cells were stimulated with A23187 and PGE_2 was localized by using a polyclonal anti-PGE_2 antibody. The resulting antigen–antibody complex was visualized ultrastructurally by binding of ferritin-conjugated IgG. PGE_2 is confined to the exposed surface of the secreted granules. (**A–E**) High-magnification images of areas labeled a through e. Original magnification × 11,730, **A–E** × 34,400. Bars = 0.5 μm.

tural localization of cyclo-oxygenase to the secretory granule of the mast cell. The association of cyclo-oxygenase with secreted mast cell granule matrix was readily visualized (Figure 1). Antibody binding was prominently localized to the proteo-heparin strands projecting from the surfaces of the secreted granules. All secreted mast cell granules were labeled. Binding was not seen in the interior of the granules. This may indicate the inaccessibility of the condensed granule matrix to the antibodies. Dispersed granules which re-

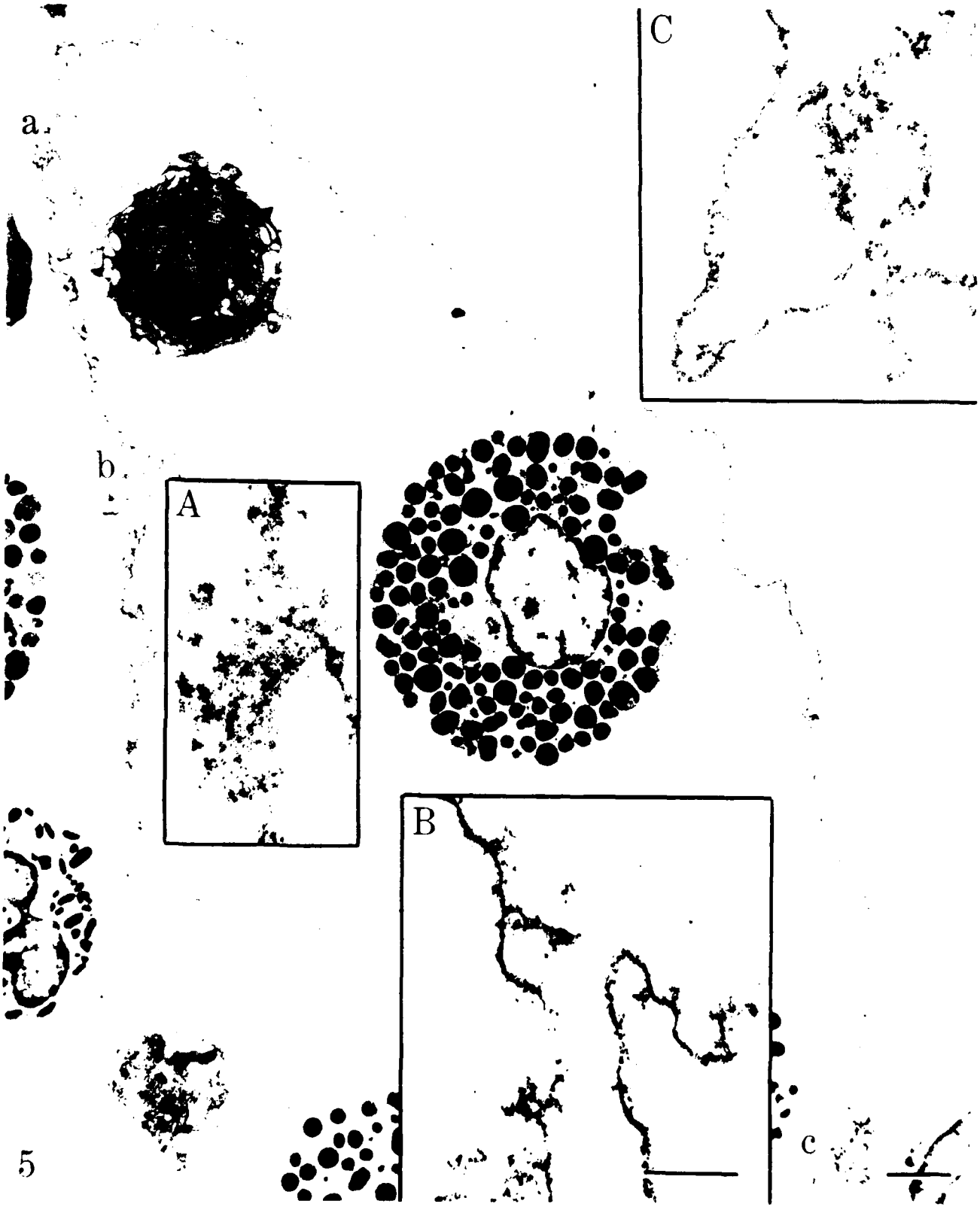

Figure 5 PGE_2 localization on unraveled secreted granule Complete unraveling of a secreted granule has permitted visualization of PGE_2 binding on the ribbon-like proteo-heparin strand Bar at the lower right-hand corner = 2 μm Insets **A**, **B**, and **C** correspond to areas a, b, and c on the strand Even distribution of ferritin label on the matrix proteo-heparin strands can be observed Original magnification × 5698, **A–C** × 33,325 Inset bar = 0 5 μm

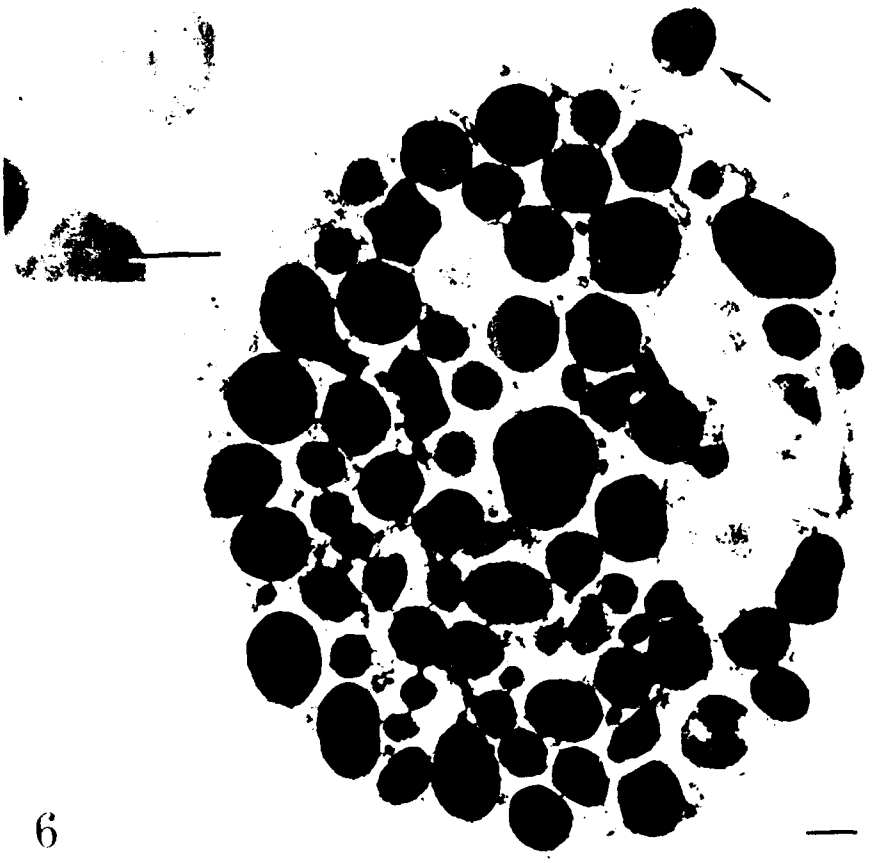

Figure 6. Control experiment for PGE_2 localization. Parallel experiment in which pre-immune serum is used in place of the polyclonal anti-PGE_2 antiserum. (**Inset**) High-magnification of the secreted granule (arrow). Original magnification × 13,570; **inset** × 24,725. Bars = 0.5 μm.

6

mained within the confines of the cell but which were in communication with the outside via a pore often had little or no label. No cyclo-oxygenase was localized to the plasma membranes of any cell type present in the lavage.

The lipid nature of the granule contents could be seen, to a limited extent, with the appearance of a single vesicle adjacent to a secreted granule (Figure 1A). It became more apparent in Figure 2, where a large cluster of vesicles was associated with a partially secreted mast cell. This mass of vesicles was prominently labeled for cyclo-oxygenase, especially in the intervesicular regions of the mass.

A control cell which received pre-immune serum rather than anti-cyclo-oxygenase antibodies is shown in Figure 3. The absence of label on the secreted granules of the control cells illustrated the specificity of the antigen antibody reaction.

Prostaglandin E_2 Localization

The application of polyclonal anti-PGE_2 antibodies to A23187-stimulated peritoneal lavage cells has established the mast cell granule as the site of PGE_2 synthesis during histamine release (Figure 4). All secreted mast cell granules were labeled. Although other granule-containing cell types were present at the lavage, including eosinophils and neutrophils, these cells did not appear to have undergone secretion and were generally not associated with PGE_2 label. Antibody binding was predominantly localized to the periphery of the secreted granules. Unlike the cyclo-oxygenase label which was apparent on the proteo-heparin projections from the granule matrix, the PGE_2 label was distributed evenly and in a more continuous fashion on the surface of the matrix. This suggests a strong hydrophobic interaction between the PGE_2 and the hydrophobic components of the matrix.

It is not uncommon to find extruded granules that have become so dispersed and unraveled that they reveal their proteo-heparin cores as being made up of long ribbon-like strands (17). A portion of an unraveled granule can be seen in Figures 5A–5C. The adherence of the label throughout the strand indicates that much of the newly synthesized prostaglandin remains bound to the granule matrix long after the extrusion of the granule. We never observed any gradient of label in association with the granule matrix. The label was always tightly associated with the matrix protein and did not appear to diffuse from this bound state.

Results of the control experiment in which cells received pre-immune serum rather than PGE_2 antibodies can be seen in Figure 6. The absence of label in the control sample lends credence to the results. The localization of both the cyclo-oxygenase and its

Figure 7 Ultrastructural visualization of PGE_2 antigen–antibody complex using a gold-conjugated antibody. Parallel experiment as in Figure 4, except that a gold-conjugated IgG antibody was used in place of the ferritin-conjugated one for visualization of PGE_2. Like the ferritin label, the gold label is also confined to exposed surfaces of secreted granules, especially in areas where the granule is more dispersed and accessible to label penetration. Original magnification × 34,425. Bar = 0.5 μm.

product, PGE_2, further supports the conclusion that the secretory granule is the site of the arachidonic acid cascade during exocytosis.

Analogous experiments which substituted the ferritin-conjugated antiserum with a gold-conjugated antiserum in the second antibody incubation were also carried out. The results were in agreement with those using ferritin-conjugated antibody for visualization of the antigens. Figure 7 shows a typical result using the immunogold method for localization of PGE_2.

Discussion

In agreement with our previous biochemical evidence, our current ultrastructural results also confirm the fact that the secretory granule of the mast cell is the site of cyclo-oxygenase activity and prostaglandins synthesis during exocytosis. Because we applied antibodies to secreting whole cells, the labeling was limited to exposed surfaces. The fact that only the matrices of the secreted granules were labeled (Figures 1, 4, 5, and 7) implies the presence of an eicosanoid-synthetic machinery in the secretory granule.

Contrary to what might have been expected, cell plasma membranes were never labeled with either cyclo-oxygenase or PGE_2 activity. Disrupted cells, broken or damaged as a result of handling, also gave no evidence of cyclo-oxygenase activity or PGE_2 localization, even though the antibodies often had access to internal cytosolic locations (Figure 2).

Prostaglandin E_2 appeared to be bound to the granule matrix even when the granule was unraveled (Figure 5). Since PGE_2 is very hydrophobic, as evidenced by its low solubility in water, much of it may have remained bound to the hydrophobic matrix after secretion. Many cells of the immune system, such as neutrophils and macrophages, are rapidly attracted to secreted mast cell granules because their secretion is associated with the production of the so-called "slow-reacting substances of anaphylaxis" (SRSA). These SRSA, which are primarily leukotrienes, are potent leukocyte chemoattractants. In Figure 8, a granulocyte appears to be phagocytosing a labeled mast cell granule. Since the eicosanoids, as represented by PGE_2, remain bound to the granule matrix via hydrophobic interaction, it seems possible that these bound lipid mediators may confer a signal to the phagocytosing cells by activating their cell surface receptors at the points of contact. The phagocytosis of the granule matrix would result in formation of a lysosome which contains lipid mediators. However, it is also conceivable that mediator-containing vesicles, such as some of those shown in Figure 2, may fuse directly with a target cell on contact. Their fusion would result in the direct release of lipid mediators into the cytoplasm of the

Figure 8 Phagocytosis of ferritin-labeled secreted mast cell granule by granulocyte. A granulocyte is seen in the process of phagocytosing a mast cell granule (arrow) which has been labeled with ferritin for PGE_2 activity. Original magnification × 10,580. Bar = 1 μm.

target cell. The internalization of non-membrane-delimited mediators opens up the possibility of some yet unknown intracellular functions for the lipid mediators. A role of arachidonic acid metabolites as intracellular modulators of K^+ channel has been recently suggested (18).

Previously, eicosanoid synthesis was considered to originate from membrane phospholipid (1–5), with damage to these membranes as the event that made phospholipid available for eicosanoid synthesis. Our results indicate that prostaglandin formation may actually be the result of receptor-mediated granule exocytosis. The coupling of granule activation to triggering of the arachidonic acid cascade explains why, for the mast cell, the initial time course of histamine release closely parallels the time course for prostaglandin production (14,19). This explanation is also consistent with the coincident production of eicosanoids with the process of secretion in other secretory systems (20,21).

In the eicosanoid biosynthetic cascade, the first requirement for the synthesis of prostaglandins is availability of phospholipid. In the mast cell granule, this is easily met by the existence of a large non-bilayer phospholipid store bound to the granule matrix (9). The second requirement is a phospholipase to liberate the arachidonic acid from the phospholipid. Since arachidonic acid is usually esterified in the sn-2 position of phospholipid (7), the presence of a phospholipase A_2 is implied. The existence of a phospholipase A_2 in the mast cell granule has now been verified in our laboratory (submitted for publication). In fact, the formation of PGE_2 from endogenous granule phospholipid detected here by using a specific antibody to PGE_2 is in itself strong evidence for the presence of a phospholipase A_2 in the granule. This phospholipase A_2, like that found in the pancreas and in the macrophage, requires high calcium concentrations for its activity (4,8). This requirement can be easily met in the granule (22), but not by a membrane bilayer source. The phospholipase A_2 of macrophage granules was assumed to be bound to the granule membrane (4). In the mast cell, our studies suggest that it is bound to the granule matrix instead. The third requirement in the pathway is the presence of a cyclo-oxygenase, the topic of this study, to catalyze the conversion of arachidonic acid to PGE_2. Current theory had also placed this enzyme, along with other key enzymes of the cascade, in or on the plasma membrane. However, it should be pointed out here that fragmented granule matrix components can be easily sedimented with the microsomal fraction at 100,000 × g. Therefore, it is possible to confuse granule matrix components with membrane components. This confusion becomes more obvious in experiments involving the use of fragmented cells or tissues as starting materials. Our observations indicate that cyclo-oxygenase is tightly bound to the matrix of the secretory granule, where a large amount of phospholipid is stored. All these points, taken together, suggest that the secretory granule contains all the necessary ingredients to function as an eicosanoid-producing entity during granule exocytosis.

There are many inconsistencies surrounding the current dogma which places the prostaglandin-synthesizing machinery on the plasma membrane. Aside from the difficulty of coping with the consequence of placing many membrane-destructive enzymes on the plasma membrane, this concept also provides no credible explanation of how hydrophobic products such as prostaglandins can be released from their hydrophobic membrane environment during exocytosis. More serious challenge to this dogma ensues after the identification of a key enzyme in the cascade, prostaglandin D-isomerase, being a cytosolic enzyme instead of an expected membrane enzyme (23). This difficulty of placing the cyclo-oxygenase complex on the plasma membrane while the D-isomerase/synthetase is in the cytosol, has been pointed out by Giles and Leff (24). Furthermore, the use of immunocytochemical technique also failed to demonstrate the presence of cyclo-oxygenase on the plasma membrane (25). Our present finding of localizing both the substrate and the necessary enzymes of the cascade to the secretory granules not only can overcome the difficulties facing the current dogma but also can provide the physical basis for linking of granule activation to the production of eicosanoids during exocytosis (16).

We now understand that stimulus in the form of trauma, infection, or radiation causes certain cells to secrete and thus produce various lipid mediators which can initiate an inflammatory response. Many of these mediators are also potent chemotactic factors. The involvement and the recruitment of the cells of the immune system into the site of inflammation usually results in tissue destruction. Under physiological conditions, the process of inflammation is self-contained in the sense that the release of a deleterious mediator eventually elicits the release of opposing factors via a feedback mechanism. This line of thinking is consistent with the concept of Chandler and Fulmer, who suggested that the inflammation-promoting eicosanoids are released to initiate an inflammatory response and that this inflammatory state is later terminated by the release of immunosuppressive eicosanoids (26). Many studies on the roles of eicosanoids in the mechanism of inflammation and how they interact with the various lymphokines, helper cells, and suppressor cells to elicit a specific immune response have been published (27–30). The localization of the site of eicosanoid production to the secretory granule and the linking of their production to the process of secretion will lead to a better understanding of the mechanism of inflammation and open the way to specific manipulation of the immune system.

Acknowledgments

We wish to thank Mr Joe L. Parker and Ms Christine S. Cho for technical assistance.

Animal usage was in compliance with the Animal Welfare Act and the NIH Guide for the Care and Use of Laboratory Animals.

Literature Cited

1 Smith WL. Prostaglandin biosynthesis and its compartmentation in vascular smooth muscle and endothelial cells. Annu Rev Physiol 1986; 48:251

2 Miyamoto T, Yamamoto S, Hayaishi O. Prostaglandin synthetase system: resolution into oxygenase and isomerase components. Proc Natl Acad Sci USA 1974;71:3695

3 Flower RJ, Blackwell GJ. The importance of phospholipase A_2 in prostaglandin synthesis. Biochem Pharmacol 1976;25:285

4 Lanni C, Franson RC. Localization and partial purification of a neutral-active phospholipase A_2 from BCG-induced rabbit alveolar macrophages. Biochim Biophys Acta 1981;658:54

5 Van der Ouderaa FJ, Buytenhek M, Nugteren DH, Van Dorp DA. Purification and characterisation of prostaglandin endoperoxide synthetase from sheep vesicular glands. Biochim Biophys Acta 1977;487:315

6 Stenson WF, Parker CW. Metabolism of arachidonic acid in ionophore-stimulated neutrophils. J Clin Invest 1979;64:1457

7 Sahu S, Lynn WS. Lipid composition of human alveolar macrophages. Inflammation 1977;2:83

8 De Haas GH, Gonsen PPM, Pieterson WA, Van Deenen LLM. Studies on phospholipase A and its zymogen from porcine pancreas. III. Action of the enzyme on short chain lecithins. Biochim Biophys Acta 1971;239:252

9 Chock SP, Schmauder Chock EA. Phospholipid storage in the secretory granule of the mast cell. J Biol Chem 1989;264:2862

10 Chock SP, Chock ES. A two-stage fusion model for secretion. Fed Proc 1985;44:1524

11 Chock SP, Schmauder Chock EA. *Evidence of de novo membrane generation in the mechanism of mast cell secretory granule activation.* Biochem Biophys Res Commun 1985;132:154

12 Schmauder Chock EA, Chock SP. Mechanism of secretory granule exocytosis: can granule enlargement precede pore formation? Histochem J 1987;19:413

13 Schmauder Chock EA, Chock SP. New membrane assembly during exocytosis. In Bailey GW, ed. Proc 45th Annu Meeting Electron Microsc Soc America. San Francisco: San Francisco Press, 1987:782

14 Metcalfe DD, Kalmer M, Donlon MA. The mast cell. CRC Crit Rev Immunol 1981;3:23

15 Strandberg K, Westerberg S. Composition of phospholipids and phospholipid fatty acids in rat mast cells. Mol Cell Biochem 1976;11:105

16 Chock SP, Schmauder Chock EA. *Synthesis of prostaglandins and eicosanoids by the mast cell secretory granule.* Biochem Biophys Res Commun 1988;156:1308

17 Chock SP, Schmauder Chock EA. The mast cell granules: a phospholipid source for prostaglandins synthesis. In Walden TL, Hughes HN, eds. Prostaglandins and lipid metabolism in radiation injury. New York: Plenum Press, 1987:127

18 Kurachi Y, Ito H, Sugimoto T, Shimizu T, Miki I, Ui M. Arachidonic acid metabolites as intracellular modulators of the G protein-gated cardiac K^+ channel. Nature 1989;337:555

19 Ishizaka T, Ishizaka K. Activation of mast cells for mediator release through IgE receptors. Prog Allergy 1984;34:188

20 Slivka SR, Insel PA. α_1-Adrenergic receptor-mediated phosphoinositide hydrolysis and prostaglandin E_2 formation in Madin-Darby canine kidney cells. J Biol Chem 1987;262:4200

21 Reichman M, Nen W, Hokin LE. Highly sensitive muscarinic receptors in the cerebellum are coupled to prostaglandin formation. Biochem Biophys Res Commun 1987;146:1256

22 Chock ES, Donlon MA, Fiori CE, Catravas GN. Elemental analysis for calcium in rat peritoneal mast cell granules. J Cell Biol 1982;95:409a

23 Shimizu T, Yamamoto S, Hayaishi O. Purification and properties of prostaglandin D synthetase from rat brain. J Biol Chem 1979;254:5222

24 Giles H, Leff P. The biology and pharmacology of PGD_2. Prostaglandins 1988;35:277

25 Rollins TE, Smith WL. Subcellular localization of prostaglandin-forming cyclo-oxygenase in Swiss mouse 3T3 fibroblasts by electron microscopic immunocytochemistry. J Biol Chem 1980;255:4872

26 Chandler DB, Fulmer JD. Prostaglandin synthesis and release by subpopulations of rat alveolar macrophages. J Immunol 1987;139:893

27 Michelassi F, Shahinian HK, Ferguson MK. Effects of leukotrienes B_4, C_4, and D_4 on rat mesenteric microcirculation. J Surg Res 1987;42:475

28 Kunkel SL, Chensue SW, Phan SH. Prostaglandins as endogenous mediators of interleukin 1 production. J Immunol 1986;136:186

29 Tilden AB, Balch CM. A comparison of PGE_2 effects on human suppressor cell function and on interleukin 2 function. J Immunol 1982;129:2469

30 Wasserman J, Hammarstrom S, Petrini B, Blomgren H, von Stedingk LV, Vedin I. Effects of some prostaglandins and leukotrienes on lymphocytes, monocytes and their activity in vitro. Int Arch Allergy Appl Immun 1987;83:39

AD-A214 900 AFRRI (ARMED FORCES RADIOBIOLOGY RESEARCH INSTITUTE) 2/2
REPORTS JULY AUGUST SEPTEMBER 1989(U) ARMED FORCES
RADIOBIOLOGY RESEARCH INST BETHESDA MD NOV 89
UNCLASSIFIED F/G 6/15 NL

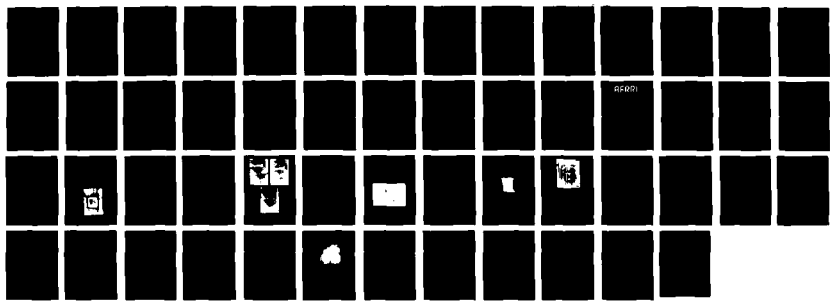

RADIATION RESEARCH 119, 101–112 (1989)

ARMED FORCES RADIOBIOLOGY
RESEARCH INSTITUTE
SCIENTIFIC REPORT
SR89-38

Radioprotection of Mice with Interleukin-1: Relationship to the Number of Spleen Colony-Forming Units

G. N. SCHWARTZ

Transplantation Laboratory, American Red Cross, Rockville, Maryland 20855

AND

M. L. PATCHEN, R. NETA, AND T. J. MACVITTIE

Experimental Hematology Department, Armed Forces Radiobiology Research Institute, Navy Medical Command, National Capital Region, Bethesda, Maryland 20814-5145

SCHWARTZ, G. N., PATCHEN, M. L., NETA, R., AND MACVITTIE, T. J. Radioprotection of Mice with Interleukin-1: Relationship to the Number of Spleen Colony-Forming Units. *Radiat. Res.* **119**, 101–112 (1989).

Compared to saline-injected mice 9 days after 6.5 Gy irradiation, there were twofold more Day 8 spleen colony-forming units (CFU-S) per femur and per spleen from B6D2F1 mice administered a radioprotective dose of human recombinant interleukin-1-α (rIL-1) 20 h prior to their irradiation. Studies in the present report compared the numbers of CFU-S in nonirradiated mice 20 h after saline or rIL-1 injection. Prior to irradiation, the number of Day 8 CFU-S was not significantly different in the bone marrow or spleens from saline-injected mice and rIL-1-injected mice. Also, in the bone marrow, the number of Day 12 CFU-S was similar for both groups of mice. Similar seeding efficiencies for CFU-S and percentage of CFU-S in S phase of the cell cycle provided further evidence that rIL-1 injection did not increase the number of CFU-S prior to irradiation. In a marrow repopulation assay, cellularity as well as the number of erythroid colony-forming units, erythroid burst-forming units, and granulocyte-macrophage colony-forming cells per femur of lethally irradiated mice were not increased in recipient mice of donor cells from rIL-1-injected mice. These results demonstrated that a twofold increase in the number of CFU-S at the time of irradiation was not necessary for the earlier recovery of CFU-S observed in mice irradiated with sublethal doses of radiation 20 h after rIL-1 injection. © 1989 Academic Press, Inc

INTRODUCTION

Previous studies demonstrated that more mice survived after exposure to otherwise lethal doses of γ radiation or cytoxan if they had been administered a single injection of recombinant interleukin-1 (rIL-1) 18–24 h before these hematopoietic suppressive treatments (*1–5*). Associated with the increased survival, there was an earlier recovery of mature cells in the blood and hematopoietic colony-forming cells in the bone marrow (*2–5*). Similarly, an earlier recovery of CFC was observed in mice administered rIL-1 prior to sublethal doses of radiation (*3, 4*). The physiological mechanisms pro-

0033-7587/89 $3.00
Copyright © 1989 by Academic Press, Inc
All rights of reproduction in any form reserved

moting the earlier recovery of CFC after irradiation of mice pretreated with rIL-1 are not well understood.

In mice, assays for spleen colony-forming units (CFU-S) have provided useful and sensitive measurements of damage and recovery of bone marrow cells after irradiation (*6, 7*). However, CFU-S represent a heterogeneous population of cells that varies in time of appearance (*8*), cell cycling characteristics (*7, 9, 10*), and potential for self-renewal (*7, 11, 12*). These subpopulations of CFU-S have been shown to differ in their tissue distribution (*7, 11–13*), radioprotective ability after transplantation (*11, 14*), and sensitivity to irradiation (*9, 10, 13, 15–17*). Neta *et al.* (*18*) demonstrated that injection of murine rIL-1 induced an increase in the number of endogenous CFU-S. However, they reported that the increase in endogenous CFU-S observed after rIL-1 injection was not necessarily predictive of radioprotection (*18*). Others demonstrated that an increase in the number of endogenous CFU-S is not always correlated with earlier bone marrow recovery or increased survival (*19–21*). Determinations of the effect of rIL-1 injection on the number and cell cycle status of other populations of CFU-S may be useful in further delineating the mechanisms responsible for the earlier hematopoietic recovery that occurs after irradiation of rIL-1-injected mice.

The studies in the present report were done to investigate the changes in CFU-S number and the proportion of CFU-S in S phase of the cell cycle in tissues of normal mice that had occurred by 20 h after a single injection of a radioprotective dose of rIL-1. Data in an earlier report demonstrated that 150 ng rIL-1 from the same stock solutions as used in the present studies increased the number of B6D2F1 mice that survived after 10.5 Gy irradiation from 7 ± 13.1 to 85 ± 7.1% (*4*). Also, compared to saline-injected mice, there was an earlier recovery of erythroid and granulocyte-macrophage hematopoietic colony-forming cells in the bone marrow of rIL-1 injected mice 8 days after 6.5 Gy irradiation (*4*). In the present report, compared to saline-injected mice, there were twofold more Day 8 CFU-S in both bone marrow and spleens from rIL-1-injected mice 9 days after 6.5 Gy irradiation. At the time of irradiation, the number and seeding efficiency of Day 8 CFU-S and Day 12 CFU-S were compared for rIL-1-injected mice and saline-injected mice. The decrease in CFU-S after hydroxyurea injection was used to measure the proportion of CFU-S in S phase of the cell cycle. Also, bone marrow cells from rIL-1-injected and saline-injected mice were assayed for their ability to repopulate the bone marrow and spleens of lethally irradiated mice.

MATERIALS AND METHODS

Mice

B6D2F1, or (C57Bl/6J × DBA/2)F1, female mice were purchased from Jackson Laboratories (Bar Harbor, ME). Upon arrival, mice were maintained in an AAALAC-accredited facility. They were housed 10 per cage in plastic microisolator cages on hardwood-chip contact bedding and were allowed food (Wayne Rodent Blox) and HCl acidified water (pH 2.4) *ad libitum*. Animal holding rooms were maintained at 70 ± 2°F and 50 ± 10% relative humidity using at least 10 air changes per hour of 100% conditioned fresh air and exposed to full-spectrum light from 6:00 AM to 6:00 PM. Upon arrival, mice were tested for *Pseudomonas* contamination and quarantined until test results were obtained. Only healthy mice were released for experimentation. Twelve- to 16-week-old mice were used for these studies. Research was conducted ac-

cording to the principles enunciated in the "Guide for the Care and Use of Laboratory Animals" prepared by the Institute of Laboratory Animals Resources, National Research Council.

Irradiation

Mice were exposed bilaterally to γ radiation at a dose rate of 0.40 Gy/min from a ^{60}Co radiation source. Mice received total-body doses of 6.5 Gy for sublethal radiations studies and 10.5 Gy for CFU-S and bone marrow and spleen repopulation studies.

Treatment with Interleukin-1 (rIL-1)

Purified human recombinant IL-1-α a generous gift from Dr. S. Gillis of Immunex (Seattle, WA), was used in these studies. The rIL-1 (three different lots) was supplied in a solution of phosphate-buffered saline at pH 7.2 with a specific activity of 7.5×10^6 U IL-1/mg protein, and aliquots were maintained at −70°C. Immediately before use, stock solutions of rIL-1 were diluted with pyrogen-free saline (McGaw). In a volume of 0.5 ml 75, 150, or 200 ng was administered to normal mice by intraperitoneal injection. The mean body weight of mice used in these studies was 27 ± 2.5 g so that the average dose of rIL-1 was approximately 5.6 μg/kg body wt. Control animals were administered 0.5 ml saline at the same time. Endotoxin (LPS) contamination in rIL-1 stock solutions was measured by the *Limulus* lysate assay. On the basis of these results less than 0.2 ng of LPS was administered per injection.

Preparation of Cell Suspensions

Mice were sacrificed by cervical dislocation, and the femurs and spleens were excised. Cells were flushed from the bone marrow with Hanks' balanced salt solution without Ca^{++} or Mg^{++} (HBSS; Grand Island Biological Co., Grand Island, NY) using a syringe and 25 gauge needle. Spleen cells were obtained by using a syringe plunger to disperse spleen cells through a wire screen (Millipore). Bone marrow and spleen cells were then dispersed through a 25 gauge needle until a single cell suspension was obtained. All cell concentrations were determined by hemacytometer counts.

Bone Marrow and Repopulation Assay

Bone marrow cells from mice 20 h after saline or rIL-1 injection were diluted, and 2×10^4, 2×10^5, or 2×10^6 cells were infused into a caudal vein of individual mice 24 h after 10.5 Gy irradiation. Four and 12 days later, bone marrow and spleen cells were assayed for cellularity and hematopoietic colony-forming cell content.

Assays for in Vitro Colony-Forming Cells

Granulocyte-macrophage colony-forming cells (GM-CFC) were assayed using the double-layer agar technique basically as described by Hagan *et al* (22). The culture medium was double strength CMRL-1066 culture medium (Connaught Medical Research Laboratory) containing 10% (vol/vol) fetal calf serum, 5% (vol/vol) horse serum, 5% trypticase soy broth, 0.02 g/ml L-asparagine, and penicillin–streptomycin. In the bottom layer of 35-mm plastic petri dishes was 1 ml of a 1:1 mixture of culture medium and 1.0% agar (Bactoagar, Difco) containing 10% (vol/vol) L-929 cell conditioned medium as a source of colony-stimulating activity. The top layer contained 1 ml of a 1:1 mixture of culture medium and 0.66% agar containing bone marrow or spleen cells. Cultures were incubated at 37°C in 5% humidified CO_2 in air. After 10 days of culture, colonies greater than 50 cells were scored as GM-CFC.

Determinations of erythroid colony-forming units (CFU-E) and erythroid burst-forming units (BFU-E) were made using a plasma clot culture system basically as described by Weinberg *et al* (23). Iscove's modified Dulbecco's medium (Grand Island Biological Co.) was substituted for α medium. Cells were plated with 0.25 U/ml (for CFU-E) or 3.0 U/ml (for BFU-E) anemic sheep plasma, step III erythropoietin (Connaught Laboratories, Inc., Lot No. 3092-2) as 0.4-ml plasma clots in four-well Nunclone culture dishes (Nunc). CFU-E and BFU-E cultures were placed into a humidified 37°C incubator with 5% CO_2 for 2.5 and 8 days, respectively. Cultures were then harvested, fixed, stained, and evaluated as described by McLeod *et al* (24).

Assay for Spleen Colony-Forming Units

Determinations of CFU-S were done basically as described by Till and McCulloch (6). Background colony counts were determined from irradiated mice injected with HBSS. An irradiation dose of 10.5 Gy was sufficient to reduce background Day 8 and Day 12 macroscopic colonies to a mean ± SD of 0.0 ± 0.0 (n = 23 mice) and 0.1 ± 0.4 (n = 38 mice), respectively. In survival studies, the mean survival time of mice not transfused with bone marrow or spleen cells after exposure to 10.5 Gy radiation was 13 ± 2.5 days (n = 78). Cell suspensions were diluted and injected into a caudal vein of each mouse. After 8 or 12 days, the spleens were removed and placed into Bouin's fixative, and the number of macroscopic colonies was counted. Five to seven mice were injected with cells for each group in individual studies. The mean ± SD was calculated from the mean CFU-S numbers from each group in individual studies.

Determination of CFU-S Seeding Efficiencies

Twenty-four-hour seeding efficiencies were determined for both Day 8 and Day 12 CFU-S in bone marrow from saline- or rIL-1-injected mice (7, 25, 26). In these studies, Day 8 and Day 12 CFU-S per femur were determined for saline- or rIL-1-injected mice. Bone marrow cells (5×10^6) from the same suspensions were also transfused into another group of 6–10 mice after their exposure to 10.5 Gy radiation (primary recipients). After 24 h, 7.5×10^6 (for Day 8 CFU-S) or 3.7×10^6 (for Day 12 CFU-S) splenic cells from the primary recipients were slowly infused into a caudal vein of mice exposed to 10.5 Gy radiation 24 h earlier (secondary recipients). The number of colonies on spleens from secondary recipients was counted on Day 8 or Day 12. This number was used to calculate the number of CFU-S per spleen from primary recipients. The percentage of bone marrow derived CFU-S that had seeded into the spleens of primary recipients by 24 h was calculated by dividing CFU-S recovered/spleen of primary recipient mice by the number of CFU-S in bone marrow cells from nonirradiated saline- or rIL-1-injected mice.

Determination of CFU-S in S Phase of the Cell Cycle

The percentage of CFU-S in S phase of the cell cycle was determined basically as described by Rickard *et al.* (27). Mice were administered 900 mg/kg body wt hydroxyurea (Sigma) in Dulbecco's phosphate-buffered saline (PBS; Grand Island Biological Co.) by intraperitoneal injection. Control groups of mice were administered PBS without hydroxyurea at the same time. Tissues were assayed for surviving CFU-S 2.5 to 3 h later. The number of CFU-S in hydroxyurea-injected mice was compared to the number in PBS-injected mice, and the percentage decrease in CFU-S after hydroxyurea was calculated as the percentage of CFU-S in S phase of the cell cycle for rIL-1-injected mice and saline-treated mice.

Statistics

The two-tailed Student's t test was used to test for significant differences in cellularity and colony-forming cells per tissue between groups of mice.

RESULTS

Effect of rIL-1 on Early Recovery of CFU-S after Sublethal Irradiation

The number of Day 8 CFU-S per femur was determined for mice exposed to a radiation dose of 6.5 Gy 20 h after saline or rIL-1 injection. Five, 9, and 12 days after irradiation, the number of CFU-S was twofold greater in bone marrow from rIL-1-injected mice than in bone marrow from saline-injected mice. The values were similar to Day 12 CFU-S values previously reported (*4*). Also, 9 days after exposure to 6.5 Gy radiation, the number of Day 8 CFU-S/spleen was twofold greater ($P < 0.01$) for rIL-1-injected mice (111 ± 23.5) than for saline-injected mice (55 ± 17.0). These results demonstrate that rIL-1 injection induced an earlier recovery of CFU-S in both

bone marrow and spleens of mice injected with 150 or 200 ng rIL-1 20 h prior to irradiation.

Number of Spleen Colony-Forming Units after rIL-1 Injection

The content of CFU-S was measured in bone marrow and spleens from nonirradiated mice 20 h after saline or rIL-1 injection (Table I). The number of Day 8 CFU-S/femur was not significantly different ($P > 0.05$) for mice 20 h after injection with saline or 75-200 ng rIL-1. Also, the number of Day 12 CFU-S/femur and Day 8 CFU-S/spleen was similar for mice 20 h after saline injection or rIL-1 injection. Seeding efficiencies for both Day 8 and Day 12 CFU-S from the bone marrow of saline-injected mice were not significantly different from seeding efficiencies determined for CFU-S in bone marrow from rIL-1-injected mice (Table IIA). Thus the number of CFU-S/femur after correction for seeding efficiencies was also similar for saline-injected mice and rIL-1-injected mice. These results demonstrate that rIL-1 injection did not induce a change in the number or seeding efficiencies of Day 8 and Day 12 CFU-S in mice prior to irradiation.

Effect of rIL-1 on Sensitivity of CFU-S to Hydroxyurea

The decrease in CFU-S after hydroxyurea injection was used to determine the percentage of CFU-S that were in S phase of the cell cycle 20 h after rIL-1 injection. The number and percentage of Day 8 CFU-S surviving after treatment with hydroxyurea was not significantly different for saline-injected mice and rIL-1-injected mice (Table IIB). In one study, the number of Day 12 CFU-S sensitive to hydroxyurea was also similar for mice 20 h after saline or rIL-1 injection. These results demonstrate that a twofold increase in the number of CFU-S/femur in S-phase of the cell cycle 20 h after rIL-1 injection was not necessary for the earlier recovery of CFU-S observed in rIL-1-injected mice after 6.5 Gy.

Recovery of Colony-Forming Cells after Bone Marrow Transplantation

In a bone marrow repopulation assay, the recovery of CFU-E, BFU-E, and GM-CFC was determined for lethally irradiated mice receiving bone marrow cells from saline-injected mice or rIL-1-injected mice (Table III). Similar numbers of cells and Day 8 CFU-S from saline-injected or rIL-1-injected donor mice were transfused into lethally irradiated mice. Four and 12 days later, bone marrow cellularity and content of colony-forming cells were not significantly different for either group of recipient mice. Fewer GM-CFC per spleen were observed in recipients of bone marrow cells from rIL-1-injected donor mice. These studies demonstrate that at 4 and 12 days, there was no evidence that bone marrow cells from rIL-1-injected mice accelerated hematopoietic recovery of lethally irradiated recipient mice.

DISCUSSION

Data in this report demonstrated that a single injection of rIL-1 administered to B6D2F1 mice 20 h prior to sublethal irradiation promoted an earlier recovery of Day 8 CFU-S in the bone marrow and spleen. Data in this report and a previous report

TABLE I

Spleen Colony-Forming Units (CFU-S) in Tissues of Mice 20 h after Saline or rIL-1 Injection[a]

	Day 8 CFU-S/femur (× 10³) injection[b]		*Day 12 CFU-S/femur (×10³) injection*[b]		*Day 8 CFU-S/spleen (×10³) injection*[b]	
Study no	*Saline (n)*[c]	*rIL-1 (n)*[c]	*Saline (n)*[c]	*rIL-1 (n)*[c]	*Saline (n)*[c]	*rIL-1 (n)*[c]
A. 75 ng rIL-1						
1[d]	2.3 ± 0.2 (7)	2.2 ± 0.6 (7)			2.0 ± 0.4 (7)	1.5 ± 0.6 (7)
B. 150 ng rIL-1						
		2.0 ± 0.3 (7)				1.7 ± 0.5 (7)
2[d]	4.5 ± 0.6 (5)	4.0 ± 1.0 (5)				
3[d]	3.8 ± 0.4 (5)	4.1 ± 0.5 (5)	3.7 ± 0.9 (3)		1.0 ± 0.2 (4)	1.2 ± 0.3 (5)
4[d]	4.3 ± 0.8 (5)	3.3 ± 0.6 (6)			0.8 ± 0.3 (6)	0.9 ± 0.4 (6)
5	3.6 ± 0.9 (6)	3.5 ± 0.9 (6)				
6	4.5 ± 0.2 (5)	4.1 ± 0.5 (5)			2.0 ± 0.5 (5)	2.4 ± 0.6 (5)
7[d]			4.5 ± 1.0 (4)	3.0 ± 1.0 (3)		
8[d]			3.9 ± 0.5 (4)	3.4 ± 0.6 (5)		
C. 200 ng rIL-1						
9[d]	4.5 ± 0.9 (5)	3.4 ± 0.5 (5)	5.8 ± 1.3 (3)	3.5 ± 0.9 (5)	1.8 ± 0.5 (5)	1.0 ± 0.3 (4)
10	3.7 ± 0.5 (5)	3.8 ± 0.1 (5)	2.6 ± 1.1 (5)	2.6 ± 0.0 (5)		
11[d]	4.0 ± 1.6 (4)	4.1 ± 0.2 (5)				

[a] Female B6D2F1 mice, 12–16 weeks old, were administered 0.5 ml saline or 75, 150, or 200 ng rIL-1 20 h prior to assays.

[b] Cells were pooled from both femurs and spleens from three mice per group in each study; values represent the means ± SD of mean colony values in individual studies.

[c] Number of mice.

[d] Groups of mice were also evaluated for survival or bone marrow recovery after 6.5 Gy irradiation.

TABLE II

Effect of rIL-1 Injection on Bone Marrow CFU-S Seeding Efficiencies and Survival after Hydroxyurea Injection of Saline or rIL-1 Injected Mice[a]

Measurement[c]	*Treatment*[b]	
	Saline injection (n)[d]	*rIL-1 injection (n)*[d]
A. Seeding efficiencies		
Day 8 CFU-S	2.4 ± 0.4 (3)	2.7 ± 0.7 (3)
Day 12 CFU-S	3.1 ± 0.1 (2)	4.4 ± 0.2 (2)
B. Survival of Day 8 CFU-S after hydroxyurea injection		
Number/Femur ($\times 10^3$)		
Noninjected mice	4.0 ± 0.35 (3)	3.6 ± 0.42 (3)
Injected mice	3.5 ± 0.65 (3)	3.0 ± 0.36 (3)
% Surviving after injection	88 ± 9.1	84 ± 17.1

[a] B6D2F1 female mice, 12–16 weeks old.

[b] Mice were administered 0.5 ml saline or 150 ng rIL-1 20 by ip injection 20 h prior to administration of hydroxyurea (900 mg/kg body wt) or saline.

[c] Cells were pooled from both femurs of three mice per group in each study, 2.5 to 3 h after hydroxyurea injection; values represent the means ± SD of mean values from individual studies.

[d] Number of studies.

(*4*) demonstrated that, compared to saline-injected mice, there were twofold more Day 8 and Day 12 CFU-S per femur of rIL-1-injected mice 5–12 days after 6.5 Gy irradiation. Results in this report further demonstrate that the earlier recovery of CFU-S observed in rIL-1-injected mice was not due to a twofold increase in numbers of CFU-S at Day 8 or Day 12 or porportion of CFU-S in S phase of the cell cycle at the time of irradiation. Also, in a marrow repopulation assay, the recovery of erythroid and granulocyte-macrophage colony-forming cells in bone marrow of lethally irradiated recipients of bone marrow cells from saline-injected mice was similar to the recovery in recipients of bone marrow cells from rIL-1-injected mice.

In some studies, the fraction of CFU-S in injected bone marrow cells that lodged in the spleen and proliferated to form colonies was decreased for populations of CFU-S in S phase of the cell cycle (*28, 29*). For example, 24 h after endotoxin injection the number of CFU-S per femur was decreased by 50%, but when corrected for a lower seeding efficiency in the spleen (i.e., f-fraction) there was no difference in the number of CFU-S from control and treated mice (*29*). In the present studies, there was no significant difference in the 24-h seeding efficiency of Day 8 and Day 12 CFU-S in bone marrow from saline-injected mice and rIL-1-injected mice. In general, the ratio of 2-h seeding efficiency:24-h seeding efficiency has been reported to be approximately 3:1 (*11*). In the present studies, the 24-h seeding efficiency for Day 8 CFU-S was lower than expected from the 13.4% 2-h seeding efficiency previously reported for similarly aged female B6D2F1 mice (*30*). This lower value was observed for both saline-injected mice and rIL-1-injected mice. Saline injection alone may have stimulated some CFU-S into cell cycle. In one study, the percentage of mice surviving >30

TABLE III

Bone Marrow Recovery in Irradiated Recipients of Bone Marrow Cells from Mice 20 h after Saline or rIL-1 Injection

Assay[b] (% of normal values)	Time after transplantation and source of donor cells[a]				
	Day 4		Day 12		
	Saline donors	rIL-1 donors	Saline donors	rIL-1 donors	No cells
Bone marrow					
Cells	3.4 ± 0.1	3.3 ± 0.2	69 ± 25	75 ± 33	13
CFU-E	3.8 ± 1.1	4.2 ± 2.4	117 ± 1	140 ± 32	12
BFU-E	0.3 ± 0.5	0.5 ± 0.7	43 ± 12	43 ± 4	0
GM-CFC	1.7 ± 0.7	0.8 ± 0.5	13	11	0.1
Spleen					
Cells	6.1 ± 0.6	5.7 ± 0.2	94 ± 7.8	90 ± 2.7	5.8
CFU-E	8.0 ± 6.9	5.6 ± 3.0	605 ± 61	714 ± 216	0
GM-CFC	56 ± 9.6	19.3 ± 6.0[c]	ND	ND	ND

[a] B6D2F1 female mice, 12–16 weeks old, were administered 0.5 ml saline or 150 ng rIL-1. Bone marrow cells (2×10^6) from mice 20 h after saline or rIL-1 injection were injected into B6D2F1 mice that had received a radiation dose of 10.5 Gy. CFU-S values in 2×10^6 cells from saline-injected mice were 620 ± 84 and 620 ± 78; CFU-S values for 2×10^6 cells from rIL-1-injected mice were 660 ± 262 and 600 ± 156.

[b] Values are the means ± SD of mean values from two studies.

[c] Significantly different from values for recipients of cells from saline-injected mice ($P < 0.05$)

days after 10.5 Gy irradiation was similar for noninjected mice (1/10), saline-injected mice (1/10), and mice injected with heat-inactivated rIL-1 (1/10). That study demonstrated that the possible stimulation of CFU-S into cell cycle after saline injection did not result in an increase in the number of mice surviving after irradiation. Similarities in CFU-S numbers and seeding efficiencies further demonstrated that a twofold increase in the number of CFU-S at the time of irradiation was not necessary for the earlier recovery of CFU-S observed in mice after 6.5 Gy irradiation.

Neta *et al.* (*31*) suggested that one possible mechanism for the radioprotective effects of rIL-1 might be that rIL-1 injection induces bone marrow cells into a radioresistant late S phase of the cell cycle. Reports on differences in the radiosensitivity of cycling and noncycling populations of CFU-S are not definitive (*9, 10, 13, 15–17*). This may be due to the heterogenity of CFU-S, as well as to the difficulty in establishing and maintaining a synchronized population of CFU-S *in vivo*. Several studies indicated that some subpopulations of CFU-S in S phase of the cell cycle were more resistant to radiation injury than noncycling CFU-S (*9, 10, 15*). Dumenil *et al.* (*32*) demonstrated that a decrease in seeding efficiency was not always observed when there was an increase in the proportion of CFU-S in S phase of the cell cycle. Therefore, in the present studies, the decrease in the number of CFU-S after hydroxyurea injection was used to determine the percentage of CFU-S in S phase of the cell cycle. The decrease in the number of Day 8 and Day 12 CFU-S in the bone marrow after hydroxyurea injection was similar for saline-injected mice and rIL-1-injected mice.

Thus, within the limits of these assays, it does not appear that the twofold increase in the number of CFU-S after 6.5 Gy irradiation of rIL-1-injected mice can be accounted for by a similar increase in number of CFU-S in S-phase of the cell cycle. However, the effect of rIL-1 injection on the number of endogenous CFU-S in S phase of the cell cycle was not investigated in studies for this report. Boggs and Boggs (*10*) suggested that the earlier hematopoietic recovery observed after irradiation of endotoxin-injected mice was a result of an increase in the proportion of endogenous CFU-S in S phase of the cell cycle. Further studies of the effects of rIL-1 injection on cell cycle kinetics of subpopulations of CFU-S will be important to further delineate the mechanisms for the earlier hematopoietic recovery after irradiation of rIL-1-injected mice.

Others demonstrated that CFU-S in the bone marrow were induced into cell cycle within 24 h after endotoxin injection (*29*). The increase in the number of CFU-S in S phase of the cell cycle after endotoxin injection might be related to the replacement of CFU-S and other hematopoietic colony-forming cells lost due to mobilization of CFU-S from the bone marrow to the blood and the spleen early after endotoxin injection (*29*). In the present studies, 20 h after rIL-1 injection, there was no increase in the number of CFU-S in the spleen or in the number of CFU-S decreased after hydroxyurea injection. Also, the numbers of endogenous CFU-S reported for mice administered similar doses of rIL-1 used in the present studies were low (*18*) compared to the numbers reported for mice after injection of glucan (*33*) or endotoxin (*19*). These results suggest that mobilization of CFU-S from the bone marrow to the spleen early after the injection of the doses of rIL-1 used in the present studies was minimal. This may be one reason for the observations in the present studies in which the number of CFU-S in S phase of the cell cycle in the bone marrow was not increased in mice 20 h after rIL-1 injection.

A previous report demonstrated that rIL-1 injection did not prevent the expression of radiation-induced long-term decreases in the number of CFU-S (*4*). Also, the number of Day 8 and Day 12 CFU-S per femur was similar for saline-injected mice and rIL-1-injected mice 2 and 24 h after their irradiation (*4*). Those studies demonstrated that rIL-1 injection did not protect CFU-S from radiation injury or decrease their radiosensitivity (*4*). However, rIL-1 injection may induce an increase in a subpopulation of CFU-S with a greater capacity for repair of radiation damage. Studies by Till and McCulloch (*34*) suggested that endogenous CFU-S have a greater capacity for repair of radiation damage than CFU-S (*10*). Neta *et al.* (*18*) demonstrated that rIL-1 injection induced an increase in the number of endogenous CFU-S. However, an increase in the number of endogenous CFU-S has not always been associated with earlier bone marrow recovery or increased survival (*19–21*). Another possible mechanism for the earlier recovery of CFU-S after irradiation of rIL-1-injected mice is that rIL-1 injection may induce an earlier recruitment of surviving CFU-S into cell cycle after irradiation, as proposed by Smith *et al.* (*35*) for the radioprotective effects of endotoxin.

Manori *et al.* (*36, 37*) demonstrated that IL-1 containing supernatants were radioprotective when added to T cells within less than 24 h after their irradiation. This effect was related to the induction of IL-2 by IL-1 (*37*). *In vitro* studies demonstrated that IL-1 induced a manyfold increase in the production of colony-stimulating activ-

ity or factors for erythroid, granulocyte, macrophage, and multipotential colony-forming cells from a variety of cell types that include cells of the hematopoietic microenvironment (*38–42*). For example, IL-1 has been shown to induce the expression of genes for granulocyte-macrophage colony-stimulating factors, granulocyte colony-stimulating factors, and IL-6 from cell lines derived from endothelial, fibroblast, and bone marrow stromal cells (*38–41*). The maximum amounts of colony-stimulating factors occurred 8–48 h after addition of rIL-1 to cell lines (*40, 42*). *In vitro* studies demonstrated that hematopoietic functions of bone marrow stromal cells, thought to make up part of the hematopoietic microenvironment, are relatively radioresistant (*43, 44*). After radiation doses of 13–500 Gy, stromal cells still supported prolonged production of GM-CFC or produced granulocyte-macrophage colony-stimulating factors. Also, after exposure to 500 Gy radiation, murine bone marrow stromal cells still were able to respond to endotoxin by increased production of colony-stimulating factors (*43*). The production and release of colony-stimulating factors from accessory cells that make up part of the hematopoietic microenvironment may be one mechanism for the earlier bone marrow recovery observed in mice irradiated after rIL-1 injection.

ACKNOWLEDGMENTS

We are grateful to Mr. Michael White, Ms. Rita Hardy, Mr. Richard Brandenburg, and Ms. Kristina Palomba for their excellent technical assistance. We also thank Drs. D. D. Dooley and C. L. Dorian for their editorial assistance. The views presented in this paper are those of the authors; no endorsement by the Defense Nuclear Agency has been given or should be inferred. This research was supported by the Armed Forces Radiobiology Research Institute, Defense Nuclear Agency under Research Work Units 00132 and 03147 and NIH Grant BSRG 2 S07 RR05737.

RECEIVED: September 28, 1988; ACCEPTED: March 13, 1989

REFERENCES

1. R. NETA, S. DOUCHES, and J. J. OPPENHEIM, Interleukin-1 is a radioprotector. *J. Immunol.* **136,** 2483–2485 (1986).
2. M. P. CASTELLI, P. L. BLACK, M. SCHNEIDER, R. PENNINGTON, F. ABI, and J. E. TALMADGE, Protective, restorative, and therapeutic properties of recombinant human IL-1 in rodent models. *J. Immunol.* **140,** 3830–3837 (1988).
3. G. N. SCHWARTZ, T. J. MACVITTIE, R. M. VIGNEULLE, M. L. PATCHEN, S. D. DOUCHES, J. J. OPPENHEIM, and R. NETA, Enhanced hematopoietic recovery in irradiated mice pretreated with interleukin-1 (IL-1). *Immunopharmacol. Immunotoxicol.* **9,** 371–389 (1987).
4. G. N. SCHWARTZ, R. NETA, R. M. VIGNEULLE, M. L. PATCHEN, and T. J. MACVITTIE, Recovery of hematopoietic colony-forming cells in irradiated mice pretreated with interleukin-1 (IL-1). *Exp. Hematol.* **16,** 752–757 (1988).
5. V. S. GALLICCHIO, Accelerated recovery of hematopoiesis following sub-lethal whole body irradiation with recombinant murine interleukin-1 (IL-1). *J. Leuk. Biol.* **43,** 211–215 (1988).
6. J. E. TILL and E. A. MCCULLOCH, A direct measurement of the radiation sensitivity of normal bone marrow cells. *Radiat. Res.* **14,** 213–222 (1961).
7. J. GIDALDI, I. FEHER, and S. ANTAL, Some properties of the circulating hemopoietic stem cells. *Blood* **43,** 573–580 (1974).
8. M. C. MAGLI, N. N. ISCOVE, and N. ODARTCHENKO, Transient nature of early haematopoietic spleen colonies. *Nature* **295,** 527–529 (1982).

9 S. S. Boggs, D. R. Boggs, and G. J. Nell, Cycling characteristics of endogenous spleen colony-forming cells as measured with cytosine arabinoside and methotrexate. *J. Lab. Clin. Med.* **82,** 727–739 (1973).

10. S. S. Boggs and D. R. Boggs, Cell cycling characteristics of exogenous spleen colony-forming units. *J. Lab. Clin. Med* **82,** 740–753 (1973).

11 S. K. Lahiri and L. M. Pluznik, Distribution and multiplication of colony-forming units from bone marrow and spleen after injection into irradiated mice. *Cell Tissue Kinet.* **2,** 21–28 (1969).

12 F. C. Monette, Antibodies against pluripotent stem cells: Their use in studying stem cell function. *Blood Cells* **5,** 175–191 (1979).

13 L. Siminovitch, J. E. Till, and E. A. McCulloch, Radiation responses of hemopoietic colony-forming cells derived from different sources. *Radiat. Res.* **24,** 482–492 (1965).

14 R. Schofield, A comparative study of the repopulating potential of grafts from various haemopoietic sources: CFU repopulation. *Cell Tissue Kinet.* **3,** 119–130 (1970).

15 J. J. Chaffey and S. Heilman, Differing responses to radiation of murine one marrow stem cells in relation to the cell cycle. *Cancer Res.* **31,** 1613–1615 (1971).

16 J. F. Dupuan and L. E. Feinendegen, Radiosensitivity of the colony-forming cells of the mouse bone marrow. *Proc. Soc. Exp. Biol. Med.* **134,** 319–321 (1970).

17 M. P. Steger, L. E. Feinendegen, S. K. Lahiri, and E. P. Cronkite, Relative number and proliferation kinetics of hemopoietic stem cells in the mouse. *Blood Cells* **5,** 211–236 (1979).

18 R. Neta, J. J. Oppenheim, S. D. Douches, P. C. Giclas, R. J. Imbro, and M. Karin, Radioprotection with IL-1. Comparison with other cytokines. *Prog. Immunol* **5,** 900–908 (1986).

19 G. E. Hanks and E. J. Ainsworth, Endotoxin protection and colony-forming units. *Radiat. Res.* **32,** 367–382 (1967).

20 M. L. Patchen, Use of glucan-p and sixteen other immunopharmaceutical agents in prevention of acute radiation injury. *Comments Toxicol.* **2,** 217–231 (1988).

21 W. W. Smith, G. Brecher, R. A. Budd, and S. Fred, Effects of bacterial endotoxin on the occurrence of spleen colonies in irradiated mice. *Radiat. Res.* **27,** 369–374 (1966).

22 M. P. Hagan, T. J. MacVittie, and D. P. Dodgen, Cell kinetics of GM-CFC in the steady state. *Exp. Hematol* **13,** 532–538 (1985).

23 S. R. Weinberg, E. G. McCarthy, T. J. MacVittie, and S. J. Baum, Effect of low-dose irradiation on pregnant mouse haemopoiesis. *Br. J. Haematol.* **48,** 127–135 (1981).

24 D. L. McLeod, M. M. Shreeve, and A. A. Axelrad, Improved plasma system for production of erythrocytic colonies in vitro: Quantitative assay for CFU-E. *Blood* **44,** 517–534 (1974).

25 L. Siminovitch, E. A. McCulloch, and J. E. Till, The distribution of colony-forming cells among spleen colonies. *J. Cell. Comp. Physiol* **62,** 327–336 (1963).

26 B. I. Lord, The relationship between spleen colony production and spleen cellularity. *Cell Tissue Kinet* **4,** 211–216 (1971).

27 K. A. Rickard, R. K. Shadduck, D. E. Howard, and F. Stohlman, Jr., A differential effect of hydroxyurea on hemopoietic stem cell colonies in vitro. *Proc. Soc. Exp. Biol. Med* **134,** 152–156 (1970).

28 F. C. Monette and J. B. DeMello, The relationship between stem cell seeding efficiency and position in cell cycle. *Cell Tissue Kinet* **12,** 161–175 (1979).

29 P. J. Quesenberry, A. Morley, M. Ryan, D. Howard, and F. Stohlman, Jr., The effect of endotoxin on murine stem cells. *J. Cell. Physiol* **82,** 239–244 (1973).

30 M. P. Hagan and T. J. MacVittie, CFUs kinetics observed in vivo by bromodeoxyuridine and near-uv light treatment. *Exp. Hematol* **9,** 123–128 (1981).

31 R. Neta, M. P. Sztein, J. J. Oppenheim, S. Gillis, and S. D. Douches, The in vivo effects of interleukin-1. I. Bone marrow cells are induced to cycle after administration of interleukin-1. *J. Immunol* **139,** 1861–1866 (1987).

32 D. Dumenil, E. Laurel, and E. Frindel, Effects of various treatments of CFU-S seeding efficiency in mice. *Exp. Hematol* **12,** 749–752 (1984).

33 M. L. Patchen and T. J. MacVittie, Comparative effects of soluble and particulate glucans on survival in irradiated mice. *J. Biol. Resp. Modifiers* **5,** 45–60 (1986).

34 J. E. Till and E. A. McCulloch, Early repair processes in marrow cells irradiated and proliferating in vivo. *Radiat. Res.* **18,** 96–105 (1963).

35 W. W. SMITH, G. BRECHER, S. FRED, and R. A. BUDD. Effect of endotoxin on the kinetics of hemopoietic colony-forming cells in irradiated mice. *Radiat. Res.* **27**, 710–717 (1966).

36 I. MANORI, A. KUSHELEVSKY, S. SEGAL, and Y. WEINSTEIN. Effect of radiation on the production of interleukins and T-lymphocyte activities. *J. Natl. Cancer Inst.* **74**, 1215–1220 (1985).

37 I. MANORI, A. KUSHELEVSKY, and Y. WEINSTEIN. Analysis of interleukin 1 mediated radioprotection. *Clin. Exp. Immunol.* **63**, 526–532 (1986).

38 Y. YANG, T. SHICKWANN, G. G. WONG, and S. C. CLARK. Interleukin-1 regulation of hematopoietic growth factor production by human stromal fibroblasts. *J. Cell. Physiol.* **134**, 292–296 (1988).

39 K. D. RENNICK, G. YANG, I. GEMMOT, and L. LEE. Control of hemopoiesis by a bone marrow stromal cell clone: Lipopolysaccharide- and interleukin-1-inducible production of colony-stimulating factors. *Blood* **69**, 682–691 (1987).

40 K. KAUSHANSKY, N. LIN, and J. W. ADAMSON. Interleukin 1 stimulates fibroblasts to synthesize granulocyte-macrophage and granulocyte colony-stimulating factors. *J. Clin. Invest.* **81**, 92–97 (1988).

41 K. M. ZSEBO, V. N. YUSCHENKOFF, S. SCHIFFER, D. CHANG, E. MCCALL, C. A. DINARELLO, M. A. BROWN, B. ALTROCK, and G. C. BAGBY, JR., Vascular endothelial cells and granulopoiesis: Interleukin-1 stimulates release of G-CSF and GM-CSF. *Blood* **71**, 99–103 (1988).

42 J. R. ZUCALI, C. A. DINARELLO, D. J. OBLON, M. A. GROSS, L. ANDERSON, and R. S. WEINER. Interleukin 1 stimulates fibroblasts to produce granulocyte-macrophage colony-stimulating activity and prostaglandin E 2. *J. Clin. Invest.* **77**, 1857–1863 (1986).

43 R. J. GUALTIERI. Consequences of extremely high doses of irradiation on bone marrow stromal cells and the release of hematopoietic growth factors. *Exp. Hematol.* **15**, 952–957 (1987).

44 J. LAVER, W. EBELL, and H. CASTRO-MALASPINA. Radiobiological properties of the human hematopoietic microenvironment: Contrasting sensitivities of proliferative capacity and hematopoietic function to in vitro irradiation. *Blood* **67**, 1090–1097 (1986).

RADIATION RESEARCH 119, 313–324 (1989)

ARMED FORCES RADIOBIOLOGY RESEARCH INSTITUTE
SCIENTIFIC REPORT
SR89-39

Survival after Total-Body Irradiation. I. Effects of Partial Small Bowel Shielding[1]

R. M. VIGNEULLE,* H. M. VRIESENDORP,† P. TAYLOR, W. BURNS,* AND T. PETKEY*

* *Armed Forces Radiobiology Research Institute, Bethesda, Maryland 20814-5145, and*
† *Johns Hopkins Oncology Center, Baltimore, Maryland 21205*

VIGNEULLE, R. M., VRIESENDORP, H. M., TAYLOR, P., BURNS, W., AND PETKEY, T. Survival After Total-Body Irradiation. I. Effects of Partial Small Bowel Shielding. *Radiat. Res.* **119**, 313–324 (1989)

The small intestine of the rat was shielded during total-body irradiation (TBI) to evaluate the effects of radiation dose and length of intestine shielded on survival. Sprague–Dawley rats were anesthetized in groups of 10. Using aseptic surgical procedures 80, 40, 20, or 10 cm, or none of the proximal or distal small intestine were temporarily exteriorized and shielded during irradiation with photons from an 18 MeV linear accelerator. Less than 17% of the dose was delivered to the shielded intestines. In unshielded animals deaths occurred from Days 4 to 6 with 13, 15, or 17 Gy and from Days 8 to 30 with 9, 11, and 12 Gy. However, in all animals exposed to 15 Gy with all or part of the small intestine shielded, survival was increased to between 5 and 9 days. Shielding of the distal small intestine was more effective in prolonging survival than shielding of the proximal small intestine. The previously identified target of radiation damage in the small intestine is the crypt stem cell. In this study, the analysis of histological specimens of shielded and irradiated small intestine suggested that humoral factors also influence intestinal histology and survival after irradiation. These humoral factors are thought to originate from the irradiated body tissues, the shielded proximal intestine, and the shielded distal intestine. Further studies are required to identify these factors and to determine their mode of action and their therapeutic potential after radiation damage to the small intestine.

INTRODUCTION

Total-body irradiation (TBI) of experimental animals has been studied to explore treatment options for victims of accidental radiation exposures or for patients in need of a bone marrow transplant (*1*). Dose-effect studies of TBI have been reported in a number of animal species since 1945 (*2, 3*). There is a threshold dose for lethality with total-body irradiation which varies between species. After a TBI dose just above the threshold dose, animals begin to die during the second week postirradiation from

Supported by the Armed Forces Radiobiology Research Institute, Defense Nuclear Agency, under Work Units B3161 and 107. Views presented in this paper are those of the authors; no endorsement by the Defense Nuclear Agency has been given or should be inferred. Research was conducted according to the principles enunciated in the "Guide of the Care and Use of Laboratory Animals" prepared by the Institute of Laboratory Animal Resources, National Research Council.

0033-7587/89 $3.00

the sequelae of bone marrow aplasia, i.e., hemorrhage and/or infection. A further increase in TBI dose decreases survival to between 4 and 6 days. At these higher doses, death is caused by intestinal damage that leads to fluid and electrolyte loss (*3*). After very high doses (>100 Gy) of TBI, death will ensue within hours due to respiratory and cardiac arrest caused by radiation damage in the central nervous system. For low-LET TBI, the relationship of dose to survival is different for each species. In a given species, these patterns occur in clearly separate dose ranges (*4*). Bone marrow transplantation can protect an irradiated individual after low-dose TBI (e.g., a single dose of ≤10 Gy) (*5, 6*). With an appropriate bone marrow transplantation protocol, survival will occur at twice the dose that is lethal in animals without transplantation. When TBI is combined with bone marrow transplantation, the intestinal tract becomes the dose-limiting tissue for acute side effects of radiation. Fluid and electrolyte replacement, as well as total microbiologic gastrointestinal decontamination, have proven to be useful in decreasing radiation-induced intestinal toxicity. However, the TBI dose is increased by only 1 to 2 Gy (i.e., ≤12.5 Gy) (*7–10*). The crypt stem cell of the small intestine has been identified as a critical target for radiation injury of the intestine (*2, 3*). The number or function of crypt stem cells that survive radiation is not readily influenced by currently available therapeutic agents. Other studies with intestinal shielding during TBI appear to indicate that factors other than crypt stem cells also influence survival (*11–13*). The identification of these factors might be useful for the treatment of intestinal radiation injury.

The present study was initiated in rats to explore new pathophysiological mechanisms in acute intestinal radiation damage.

MATERIALS AND METHODS

Animals

Purpose-bred Sprague–Dawley rats 6 to 8 weeks old and weighing 200–300 g were quarantined on arrival and screened for evidence of disease and pseudomonas before being released. They were maintained in an AAALAC-accredited facility caged in pairs and provided commercial rat food pellets and acidified tap water (pH 2.5) *ad libitum*. Animal holding rooms were maintained at 21 ± 2°C with 50 ± 10% relative humidity using at least 10 air changes per hours of 100% conditioned fresh air. They were on a 12-h light/dark full-spectrum light cycle with no twilight.

Surgery and Anesthesia

General anesthesia was maintained during surgical procedures using Ketamine Hydrochloride (50 mg/kg) in combination with Xylazine (10 mg/kg) given intramuscularly and supplemented as needed. Aseptic procedures were used. A midline abdominal incision was made, and the portion of the small intestine to be shielded was exteriorized. Hemorrhage was not normally a problem in this surgical procedure; however, if it occurred, 4-0 chromic gut suture material was used to ligate bleeding vessels. The exteriorized portion of the intestine was tagged with colored nonabsorbable suture material. The animal was irradiated as described below. After irradiation, the small bowel was repositioned in the abdominal cavity and the abdominal wall was closed using single interrupted 4-0 monofilament nylon sutures. The skin was closed with clamps. Anesthesia was maintained during this entire time (approximately 40 min). Pedal reflex was monitored to assure maintenance of adequate anesthesia depth. Animals were allowed to regain consciousness in individual cages after completion of the irradiation exposure and surgical closure. The influence of anesthesia and surgery on survival after TBI was analyzed by irradiating animals in the same restraint

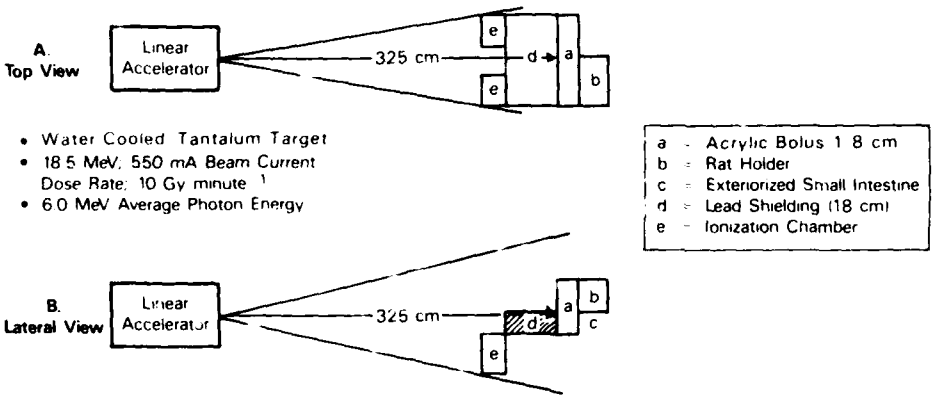

FIG. 1. Physical setup for exposure to 18 MeV linear accelerator (LINAC)

holders with or without anesthesia. All of the animals without anesthesia and some of the animals under anesthesia did not undergo surgery.

Irradiation

An 18 MeV Linac Accelerator was used at a dose rate of 10 Gy/min. A bremsstrahlung beam with an average energy of 6 MeV was produced by electrons impinging on a 4-mm water-cooled tantalum target. The dose per pulse was determined prior to irradiation of each group of animals. The restraint device allowed for shielding of the exteriorized portion of the small intestine with 18 cm of lead during irradiation. Figure 1 is a diagram of the physical setup. Ten centimeters of the small intestine or multiples thereof was shielded while the remainder of the rat's body was exposed. The following intestinal segments were shielded: the first 10, 20, or 40 cm of the proximal small intestine; the last 10, 20, or 40 cm of the distal small intestine; the middle 40 cm of the small intestine; or the entire 80 cm of the small intestine. Every radiation exposure was monitored by two ionization chambers in the field that were calibrated to the midline dose in a rat phantom for each irradiation day. The actual dose delivered was always within ± 3% of the prescribed dose.

Dose measurements were made with ionization chambers and thermoluminescent dosimeters (TLDs) placed in an acrylic rat phantom. Ionization chambers were used to determine the dose rate according to the protocol established by Task Group 21 of the American Association of Physicists in Medicine (*14*). The TLDs were used to determine dose uniformity and the effectiveness of the shielding.

Animal Care after Irradiation

Rats remained in individual cages after the irradiation. They were evaluated for appetite, hydration, health status, and diarrhea twice a day during the normal work week and once daily during the weekends. Moribund animals were euthanized by CO_2 inhalation.

Morphometric Analysis

Computerized morphometric studies (Bioquant System IV; R & M Biometrics, Inc., Nashville, TN 37850) were performed on tissues obtained from moribund animals. The small intestine samples were taken at 5, 10, 20, 40, 60, and 70 cm of an average 80 cm total length. The samples at 20 (proximal) and 60 cm (distal) were selected for complete histological and statistical analysis. The tissues were fixed in 10% buffered formalin. Transverse sections were embedded in paraffin. Five micron sections were cut, placed on glass slides, and stained with hematoxylin and eosin. At least five slides per animal were analyzed for

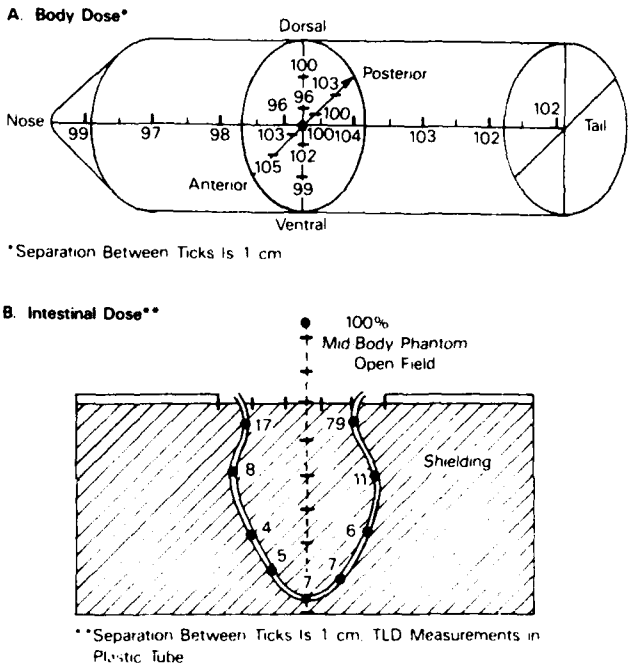

FIG. 2. Relative dose distribution in plastic rat phantom in percentage of dose in midphantom using intestinal shielding. The same orientation is used for A and B.

each sample. Tissues of three or more animals were used per parameter. Only crypts containing viable cells were counted. Crypts were scored per millimeter of circumference. Crypt depth was recorded in millimeters. Crypt depth was measured from the base of the villus to the muscularis mucosa. The base of the villus was determined by comparing several adjacent villi and drawing an arbitrary line through the assumed beginning of the villus and the top of the crypt. Villus height and villus-crypt length were measured in millimeters. Cell numbers were analyzed for the combined length from the bottom of the crypt to the top of the villus, because the division between villus and crypt was considered arbitrary.

RESULTS

Dosimetry

Dosimetry results are summarized in Fig. 2. The rat's body received a homogeneous dose (maximum/minimum ratio 1.08). The shielded intestine positioned more than 5 mm from the edge of the shield received less than 17% of the midline body dose.

Dose-Effect Curve

The $LD_{50/30}$ was 10.0 Gy while the $LD_{50/6}$ was 12.5 Gy. Anesthesia increased both of these LD_{50}'s by approximately 1.0 Gy (Fig. 3). The addition of surgery decreased the LD_{50} for the intestinal syndrome death by approximately 0.5 Gy.

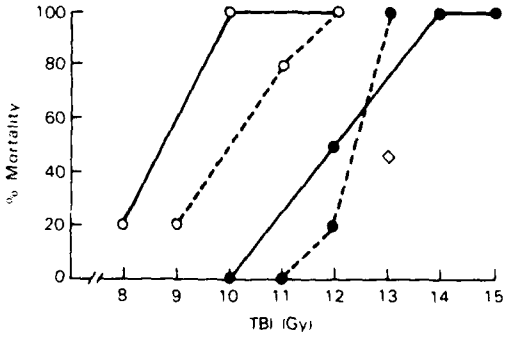

FIG. 3. Lethality after total-body irradiation in anesthetized and unanesthetized rats. Ten to 20 rats per point. Solid circles indicate death before Day 6 (intestinal syndrome). Open circles indicate death before Day 30 (hematopoietic syndrome). The diamond symbol indicates animals that died before Day 6 that received anesthesia but no surgery. The broken lines connect results in rats that received anesthesia and surgery. The drawn lines connect results in rats that did not receive anesthesia or surgery.

Shielding of the Small Intestine

Shielding of as little as 10 cm of the small intestine increased survival time significantly ($P < 0.05$). Shielded animals died between days 5 and 9 after TBI (see Fig. 4

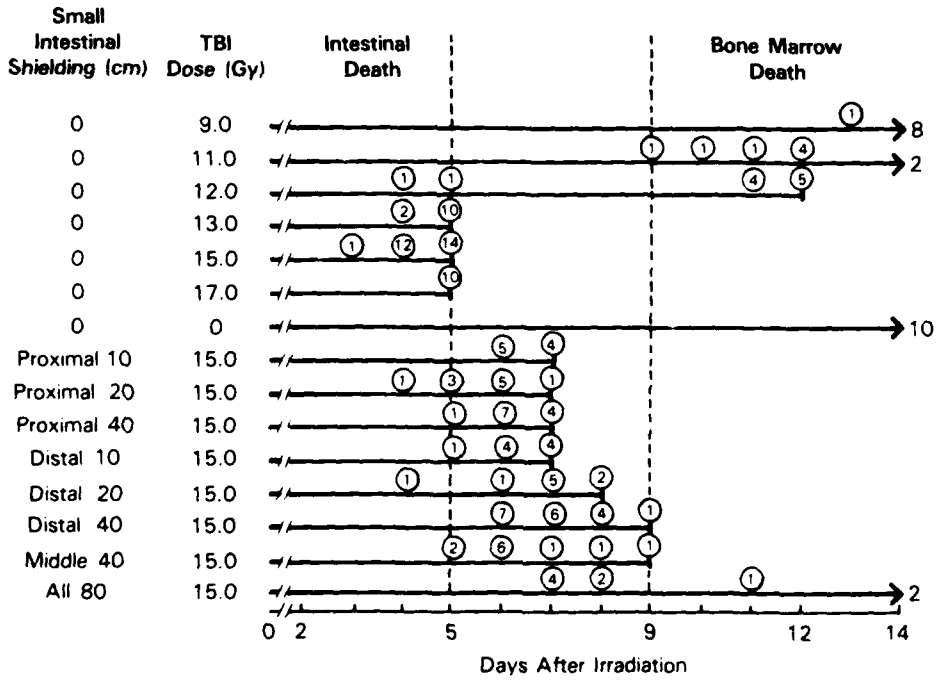

FIG. 4. Mortality of irradiated and shielded rats after total-body irradiation. Ten to 20 rats per point. Number of deaths per day is circled. Day of death of last animal is indicated by vertical mark. Continuation of survival is indicated by >mark and the number of survivors to Day 14 is indicated.

TABLE I

Survival Time of Rats after 15.0 Gy Irradiation

Small intestine subsection	*Shielding (cm)*	*Group N*	*Mean survival (days ± SEM)*
Entire	0	27	4.6 ± 0.21
Proximal	10	9	6.4 ± 0.18[a]
Proximal	20	10	5.6 ± 0.26[a,b]
Proximal	40	12	6.2 ± 0.17[a,c]
Distal	10	9	6.3 ± 0.23[a]
Distal	20	9	7.1 ± 0.20[a,b]
Distal	40	18	6.8 ± 0.18[a,c]
Middle	40	11	6.3 ± 0.36[a]
Entire	80	9	9.2 ± 0.99[a]

[a] ($P < 0.05$) significant difference from 0 cm (no shielding).
[b,c] ($P < 0.05$) significant difference between shielding groups.

and Table I). Shielding of the proximal small intestine was less effective than distal shielding. A gradual increase in survival time of shielded animals was noted with increasing length of intestine shielded. In contrast, the dose–effect TBI studies in unshielded animals showed a discontinuous distribution of survival times, i.e., ≤Day 5 for intestinal syndrome death and ≥Day 9 for hematopoietic syndrome death. The survival times of animals in different groups are shown in Table I and were compared using a *t* test.

Histopathology of Shielded and Irradiated Small Intestine

The highest number of crypts was found in the unirradiated proximal small intestine. Shielding protected the crypts in the distal small intestine completely (100%) but was less effective in the proximal small intestine (75%). Proximal shielding increased survival of crypts in the irradiated distal small intestine by 35% (Fig. 5, see ascending arrow). However, distal shielding did not increase the number of crypts per millimeter in the proximal and irradiated small intestine (Fig. 5, see descending arrow).

Proximal shielding did not change crypt depth in the irradiated distal intestine. In contrast, shielding the distal small intestine increased the crypt depth in the irradiated proximal small intestine (Fig. 6, see arrows). Crypt depth in the shielded distal small intestine was significantly increased compared to the unirradiated control on Day 6 ($P < 0.01$). However, this effect was transient since it was no longer observed on Day 7.

Villus height was greater in the unirradiated proximal small intestine than in the unirradiated distal small intestine ($P \leq 0.01$). Villus height in the proximal small intestine was decreased by irradiation and conserved by shielding (Fig. 7). Distal shielding did not alter villus height in the irradiated proximal small intestine. However, with proximal shielding, the villus height in the irradiated distal small intestine was significantly ($P \leq 0.01$) greater than the unirradiated control (Fig. 7, ascending

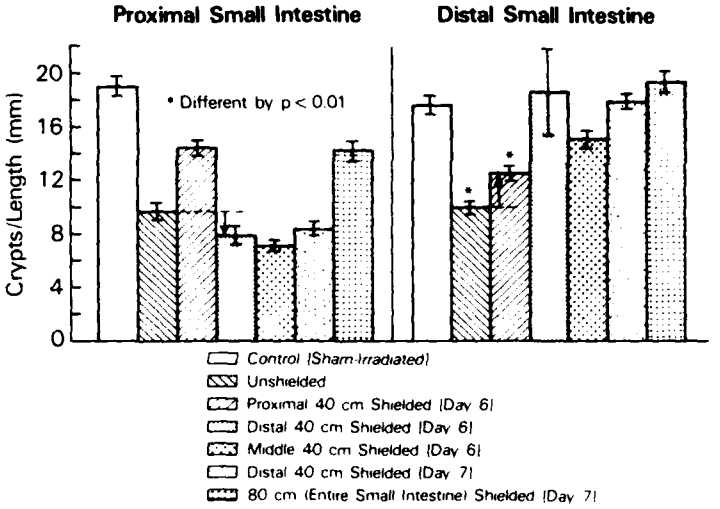

FIG. 5. Crypts per millimeter length after shielding rat small intestines from 15 Gy total-body irradiation.

arrow). With distal shielding, the villus height in the distal-shielded small intestine was increased to 200% of the unirradiated controls. This effect appeared to be sustained until at least Day 7 (Fig. 7, descending arrow).

Results were best explained by the release of humoral factors (see Discussion). Humoral factors produced in *shielded* segments of the small intestine appeared to induce

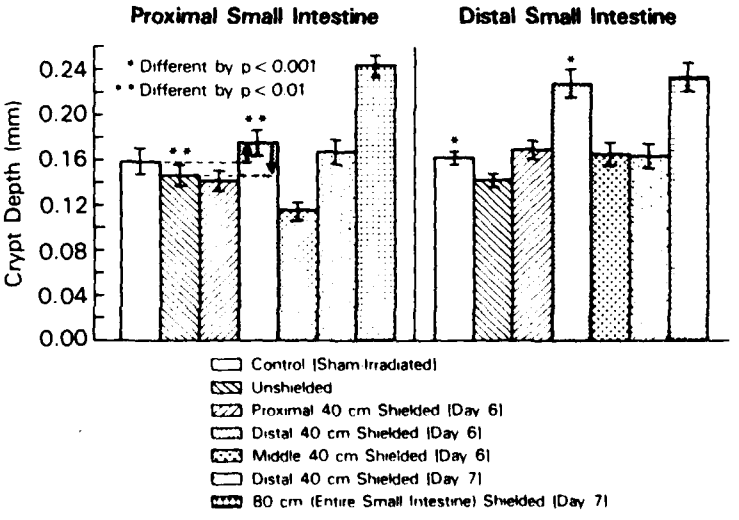

FIG. 6. Crypt depth in millimeters after shielding rat small intestines from 15 Gy total-body irradiation.

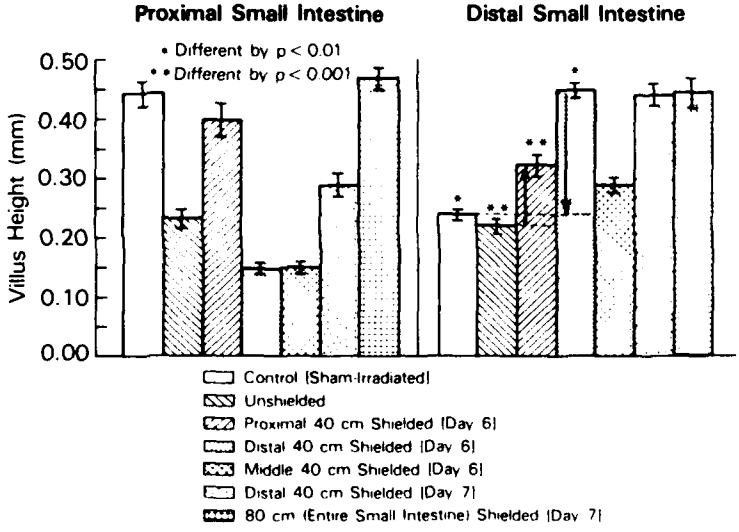

FIG. 7. Villus height in millimeters after shielding rat small intestines from 15 Gy total-body irradiation.

cell replication in the *irradiated* small intestine (Fig. 8, see arrows). Humoral factors released by the tissues that were *irradiated* influenced the *shielded* distal small intestine. The cell number in *shielded* distal small intestine was decreased compared to unirradiated controls (Fig. 8), whereas the villus–crypt length in the same tissue was

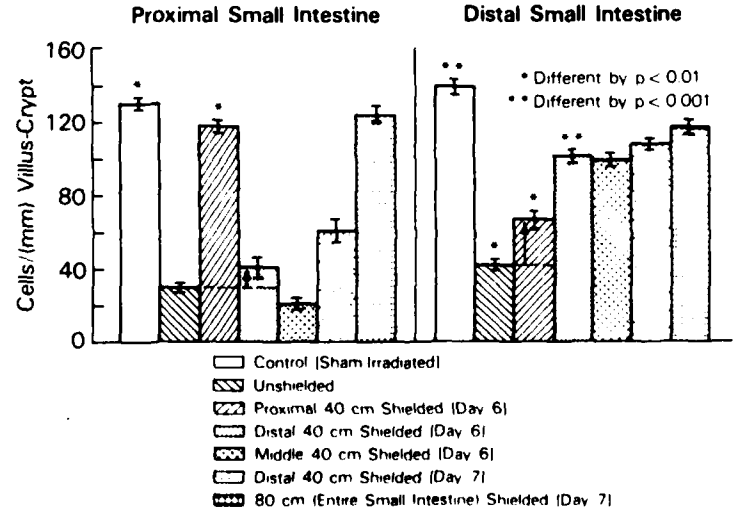

FIG. 8. Number of cells per villus to crypt length after shielding rat small intestines from 15 Gy total-body irradiation. *P* values apply to labeled bars in the same anatomical location only.

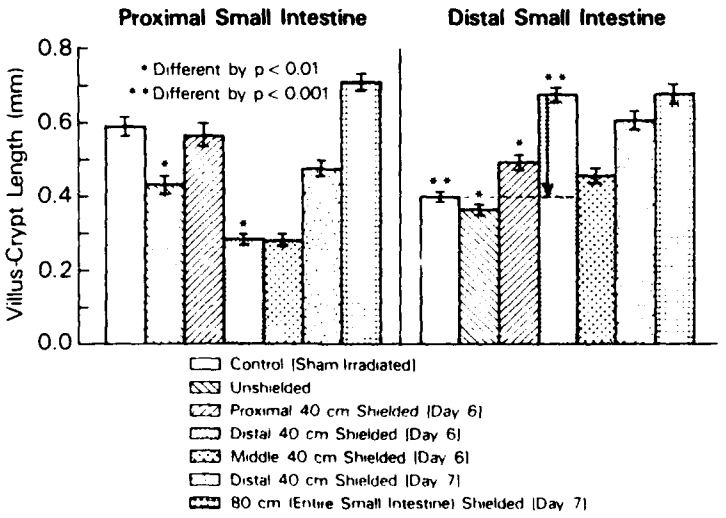

FIG. 9. Villus to crypt length after shielding rat small intestines from 15 Gy total-body irradiation. *P* values apply to labeled areas in the same anatomical location only.

increased compared to unirradiated controls (Fig. 9, see arrow), indicating that cell size had increased.

In summary, the supportive evidence that the *shielded* proximal small intestine influenced the *irradiated* distal small intestine, probably by release of a humoral factor was (a) accelerated regeneration of crypts (Fig. 5); (b) increased villus height (Fig. 7); and (c) increased cell number (Fig. 8). Similarly, that the *shielded* distal small intestine influenced the *irradiated* proximal small intestine was indicated by (a) increased crypt depth (Fig. 6) and (b) increased cell number (Fig. 8). Humoral factors released by *irradiated* tissues appeared to increase cell size in the *shielded* distal small intestine only (Figs. 8 and 9).

DISCUSSION

Shielding the small intestine from radiation improved survival and resulted in changes in the intestinal mucosa. These studies required the use of anesthesia (Ketamine and Xylazine) which introduced a dose-modifying factor of approximately 1.15. The $LD_{50/30}$ and the $LD_{50/6}$ for mice restrained during TBI without anesthesia are also higher than for unrestrained animals.[2] The radioprotective effect of anesthesia or restraint has been attributed to various mechanisms which include: (i) modulation of the central nervous system;[2] (ii) the induction of hypoxia in cells; and (iii) a direct radioprotective effect (*15, 16*). In contrast, radio*sensitization* by anesthetic

[2] H. J. Keizer, Protection of Hematopoietic Stem Cells during Cytotoxic Treatment. Ph.D. thesis, State University of Leiden, 1976.

agents has also been observed in normal and malignant tissues in mice (*17–19*). There is a need for further clarification of the interactions between anesthesia and radiation.

Shielding the small intestine from radiation increases the survival time. Data in Fig. 4 indicate that intestinal shielding changed the time of death of rats given 15 Gy TBI to a period midway between the classic intestinal syndrome (4–6 days) and the classic hematopoietic syndrome (9–30 days). If the intestinal crypt stem cells were the only determinant of survival after TBI, shielding of the small intestine should increase survival into the range associated with hematopoietic syndrome ($\geq$9 days) as soon as enough crypt stem cells are shielded. However, since this was not observed, factors other than the intestinal crypt stem cells appear to influence survival. The survival times obtained in shielded animals in our experiments are similar to those observed by previous investigators (*11–13*). However, we were able to quantify the effects of shielding the small intestine more precisely by: (a) using higher energy photons that allowed for more precise shielding; (b) using a more detailed dosimetry; (c) comparing our results to a TBI dose–effect curve for unshielded animals; and (d) making a quantitative morphometric analysis of shielded and irradiated small intestine histology after irradiation. The strip of shielded intestine that received a higher dose than the rest of the shielded intestine is so small that it is not considered to influence our results (see Fig. 2).

The protective effects of shielding from radiation can be explained in several ways. One possibility is that cells may migrate from shielded to irradiated sites. The classic example is the protective effect of spleen or leg shielding in the lower lethal TBI dose range (*20*). It has been shown that hematopoietic recovery results from migration of stem cells from the shielded body areas (*21–23*). Recovery from intestinal radiation damage is unlikely to occur by migration of stem cells from shielded small bowel to irradiated small bowel. Instead, we postulate that humoral substances contribute to recovery from intestinal radiation injury. Humoral substances are released after irradiation and may influence the intestinal mucosa at shielded or irradiated sites by stimulating cell proliferation, cell traffic, or cell function after TBI. Prior studies of intestinal growth control mechanisms have indicated that intraluminal as well as circulatory factors are involved (*24*). The observation that shielding of the distal small intestine influenced the mucosal histology of the irradiated proximal small intestine supports the idea of a systemic transport of such a humoral factor and not intraintestinal lumen transport of that particular factor.

Humoral factors released by irradiated tissues would appear to differ from those released by shielded tissues. The former produce changes in intestinal cell size, the latter in intestinal cell proliferation (see Figs. 8 and 9). Irradiated tissues might release factors from cells damaged by radiation. In contrast, shielded tissues can produce factors actively as part of a physiological response to damaged intestinal mucosa. Known factors that should be considered include (i) pleiotropic growth regulators (hormones) such as gastrin, glucagon, thyroid hormone, or others (*24*); (ii) chalones that specifically suppress intestinal growth and change in concentration after irradiation (*25*); and (iii) growth factors which are not identified yet that are specific for the intestinal mucosa renewal system and comparable to factors identified for the hematopoietic system (*26*). The nature and number of humoral factors involved in

regeneration of intestinal tissues after irradiation can be determined only by biochemical identification, separation, purification, and testing of such factors by bioassay systems. The findings in this communication provide a good start for such assays.

ACKNOWLEDGMENTS

We thank Drs. Thomas J. MacVittie, Jim Nold, Pamela Gunter-Smith, Ruth Neta, and Steve Stiefel for helpful discussions.

RECEIVED: November 8, 1988; ACCEPTED: April 11, 1989

REFERENCES

1. H. M. VRIESENDORP and T. J. MACVITTIE, Animal models for radiation accidents. In *Controversies in Bone Marrow Transplantation* (R. P. Gale and R. Champlin, Eds.), pp. 659–670. Liss, New York, (1989).
2. H. QUASTLER, Studies on roentgen death in mice I. Survival time and dosage. *Am. J. Roentgenol* **54**, 449–456 (1945).
3. V. P. BOND, T. M. FLIEDNER, and J. O. ARCHAMBEAU, *Mammalian Radiation Lethality. A Disturbance in Cellular Kinetics*. Academic Press, New York, 1965.
4. V. P. BOND, Radiation mortality in different mammalian species. In *Comparative Cellular and Species Radiosensitivity* (V. P. Bond and T. Sugahara, Eds.), pp. 5–19. Igaku Shoin, Tokyo, 1969.
5. E. LORENZ, D. E. UPHOFF, T. R. REID, and E. SHELTON, Modification of irradiation injury in mice and guinea pigs by bone marrow injections. *J. Nat. Cancer Inst.* **12**, 197–201 (1951).
6. H. JAMMET, G. MATHE, B. PENDIC, J. P. DUPLAN, B. MAUPIN, R. LATARGET, D. KALIC, I. SCHWARZENBERG, Z. DJUKIC, and J. VIGNE, Etude de six cas d'irradiation totale aigue accidentelle. *Rev. Fr. Etud. Clin. Biol.* **4**, 210–225 (1959).
7. S. T. TAKETA, Water-electrolyte and antibody therapy against acute (3- to 5-day) intestinal radiation death in the rat. *Radiat. Res.* **16**, 312–317 (1964).
8. R. J. M. FRY, A. B. REISKIN, W. KISIELESKI, A. SALTESE, and E. STAFFELDT, Radiation effects and cell renewal in rodent intestine. In *Comparative Cellular and Species Radiosensitivity* (V. P. Bond and T. Sugahara, Eds.), pp. 255–270. Igaku Shoin, Tokyo, 1969.
9. H. M. VRIESENDORP, P. HEIDT, and C. ZURCHER, Gastrointestinal decontamination of dogs treated with total body irradiation and bone marrow transplantation. *Exp. Hematol.* **9**, 904–916 (1981).
10. R. A. CONARD, E. P. CRONKITE, G. BRECHER, and C. P. A. STROME, Experimental therapy of the gastrointestinal syndrome produced by lethal doses of ionizing radiation. *J. Appl. Physiol.* **9**, 227–233 (1956).
11. M. N. SWIFT and S. T. TAKETA, Modification of acute intestinal radiation syndrome through shielding. *Am. J. Physiol.* **185**, 85–91 (1956).
12. H. QUASTLER, E. F. LANZL, M. E. KELLER, and J. W. OSBORNE, Acute intestinal death. Studies on roentgen death in mice. III. *Am. J. Physiol.* **164**, 546–556 (1951).
13. V. P. BOND, M. N. SWIFT, A. C. ALLEN, and M. C. FISHLER, Sensitivity of abdomen of rat to x-irradiation. *Am. J. Physiol.* **164**, 323–330 (1956).
14. Task Group 21, Radiation Therapy Committee, AAPM, A protocol for the determination of absorbed dose from high-energy photon and electron beams. *Med. Phys.* **10**, 741–771 (1983).
15. J. WONDERGEM, J. HAVEMAN, E. VAN DER SCHUEREN, H. VAN DEN HOLVEN, and K. BREUR, The influence of misonidazole on the radiation response of murine tumors of different size: possible artifacts caused by pentobarbital sodium anesthesia. *Int. J. Radiat. Oncol. Biol. Phys.* **7**, 755–760 (1981).
16. P. W. SHELDON and A. M. CHU, The effects of anesthetics on the radiosensitivity of a murine tumor. *Radiat. Res.* **79**, 568–578 (1979).
17. H. D. SUIT, R. S. SEDLACEK, G. SILVER, and D. DOSORETZ, Pentobarbital anesthesia and the response of tumor and normal tissue in the C3Hf/Sed mouse to radiation. *Radiat. Res.* **104**, 47–65 (1985).

18. J. DENEKAMP, N. H. A. TERRY, P. W. SHELDON, and A. M. CHU, The effect of pentobarbital anaesthesia on the radiosensitivity of four mouse tumours. *Int. J. Radiat. Biol.* **35**, 277–280 (1979).
19. H. B. KAL and J. F. GAISER, The effect of anaesthesia on the radiosensitivity of rat intestine, foot skin and R-1 tumours. *Int. J. Radiat. Biol.* **37**, 447–450 (1980).
20. L. O. JACOBSEN, E. A. MARKS, M. J. ROBSON, E. GASTON, and R. E. ZIRKLE, The effect of spleen protection on mortality following x-irradiation. *Lab. Clin. Med.* **34**, 1538–1543 (1949).
21. L. E. FORD, J. L. HAMERTON, D. W. H. BARNES, and J. F. LOUTIT, Cytological identification of radiation chimeras. *Nature* **177**, 452–454 (1956).
22. O. VOS, J. A. G. DAVIDS, W. W. H. WEYSEN, and D. W. VAN BEKKUM, Evidence for the cellular hypothesis in radiation protection by bone marrow cells. *Acta Physiol. Pharmacol. Neth.* **4**, 482–486 (1956).
23. P. C. NOWELL, L. J. COLE, J. G. HABERMEYER, and P. L. ROAN, Growth and continued function of rat marrow cells in x-irradiated mice. *Cancer Res.* **16**, 258–261 (1956).
24. R. C. N. WILLIAMSON, Intestinal adaptation. Structural, functional and cytokinetic changes. *N. Engl. J. Med.* **298**, 1393–1402 and 1444–1450 (1978).
25. R. M. KLEIN and J. C. MCKENZIE, The role of cell renewal in the ontogeny of the intestine. II. Regulation of cell proliferation in adult, fetal, and neonatal intestine. *J. Pediatr. Gastroenterol. Nutr.* **2**, 204–208 (1983).
26. S. C. CLARK and R. KAMEN, The human hematopoietic colony stimulating factors. *Science* **236**, 1229–1237 (1987).

AFRRI

TECHNICAL REPORT

Laboratory x-ray irradiator for cellular radiobiology research studies: Dosimetry report

T. H. Mohaupt
G. H. Zeman
W. F. Blakely
M. M. Elkind

AFRRI TR89-1

DEFENSE NUCLEAR AGENCY
ARMED FORCES RADIOBIOLOGY RESEARCH INSTITUTE
BETHESDA, MARYLAND 20814-5145

APPROVED FOR PUBLIC RELEASE; DISTRIBUTION UNLIMITED

REVIEWED AND APPROVED

GEORGE W. IRVING, III
Col, USAF, BSC
Director

SECURITY CLASSIFICATION OF THIS PAGE

REPORT DOCUMENTATION PAGE

1a REPORT SECURITY CLASSIFICATION	1b RESTRICTIVE MARKINGS
2a SECURITY CLASSIFICATION AUTHORITY	3 DISTRIBUTION / AVAILABILITY OF REPORT
2b DECLASSIFICATION / DOWNGRADING SCHEDULE	
4 PERFORMING ORGANIZATION REPORT NUMBER(S)	5 MONITORING ORGANIZATION REPORT NUMBER(S)
6a NAME OF PERFORMING ORGANIZATION / 6b OFFICE SYMBOL (If applicable)	7a NAME OF MONITORING ORGANIZATION
6c ADDRESS (City, State, and ZIP Code)	7b ADDRESS (City, State, and ZIP Code)
8a NAME OF FUNDING SPONSORING ORGANIZATION / 8b OFFICE SYMBOL (If applicable)	9 PROCUREMENT INSTRUMENT IDENTIFICATION NUMBER
8c ADDRESS (City, State, and ZIP Code)	10 SOURCE OF FUNDING NUMBERS

PROGRAM ELEMENT NO	PROJECT NO	TASK NO	WORK UNIT ACCESSION NO

11 TITLE (Include Security Classification)

12 PERSONAL AUTHOR(S)

13a TYPE OF REPORT	13b TIME COVERED FROM ____ TO ____	14 DATE OF REPORT (Year, Month, Day)	15 PAGE COUNT

16 SUPPLEMENTARY NOTATION

17 COSATI CODES			18 SUBJECT TERMS (Continue on reverse if necessary and identify by block number)
FIELD	GROUP	SUB-GROUP	

19 ABSTRACT (Continue on reverse if necessary and identify by block number)

Dosimetry measurements were performed on a 50 kVp laboratory x-ray irradiator for cellular radiobiology research. The measurements were done with a parallel-plate ionization chamber, which had a thin aluminized-mylar window, and an extrapolation chamber. Intercomparison of dosimetry data from the two independent methods showed excellent agreement. Results are presented for radiation dose rate, uniformity, and beam quality for operation of the tungsten target, beryllium window x-ray tube at 50 kVp, 20 mA, and with filters either 0.012 mm, 0.180 mm, or 0.633 mm thick, for arrays positioned at a range of distances from the x-ray tube. The data in this report establish a dosimetric link between the cellular radiobiology research to be performed at AFRRI with the 50 kVp laboratory x-ray irradiator and the landmark work performed by Elkind and Sutton (1960) with a similar device.

20 DISTRIBUTION / AVAILABILITY OF ABSTRACT ☐ UNCLASSIFIED/UNLIMITED ☐ SAME AS RPT ☐ DTIC USERS	21 ABSTRACT SECURITY CLASSIFICATION
22a NAME OF RESPONSIBLE INDIVIDUAL	22b TELEPHONE (Include Area Code) / 22c OFFICE SYMBOL

DD FORM 1473, 84 MAR — 83 APR edition may be used until exhausted. All other editions are obsolete. SECURITY CLASSIFICATION OF THIS PAGE

12. Current addresses are as follows:

[a]Nuclear Medicine Department
Great Lakes Naval Hospital
Great Lakes, IL 60008-5237

[b]Radiation Protection Department
AT&T Bell Laboratories
600 Mountain Avenue
Murray Hill, NJ 07974-2070

[c]Department of Radiology and
Radiation Biology
Colorado State University
Ft. Collins, CO 80523

CONTENTS

	Page
INTRODUCTION	3
MATERIALS AND METHODS	4
Irradiator	4
Beam Filtration	4
Culture Dish Arrays	5
Radiation Detectors	7
RESULTS	9
Tube Potential and Timer Accuracy	9
Focal Spot Measurements	10
Beam Quality	10
Parallel-plate Window Transmission	12
Intercomparison	12
Dosimetry Measurements	17
SUMMARY	21
REFERENCES	22
ACKNOWLEDGMENTS	22
APPENDIX A	23
APPENDIX B	24
APPENDIX C	25

INTRODUCTION

In 1985, the Armed Forces Radiobiology Research Institute (AFRRI) acquired a 60 kVp x-ray irradiator (figure 1) from Argonne National Laboratory, Argonne, IL, for cellular radiobiology experiments. This irradiator is similar to one used by Elkind and Sutton (1) for their landmark investigations. The shielding, space, and logistical requirements for the irradiator are minimal, allowing it to be conveniently located in a typical laboratory. Because of its simplicity of operation and inherent safety mechanisms, an investigator or technician can qualify easily to use the radiation source independently.

This report describes the dosimetry methods used to calibrate the beams planned for cell irradiations. Measurements of exposure rate, beam quality, and field uniformity were made with a thin-window, parallel-plate ionization chamber. Elkind and Sutton (1) used a variable-volume extrapolation chamber to provide dosimetry for their irradiator because of its excellent capability of measuring low-energy photons. We had the good fortune to use Elkind's variable-volume extrapolation chamber for comparison with the parallel-plate chamber. Comparison of the dosimetry data showed very good agreement between results obtained by the two methods.

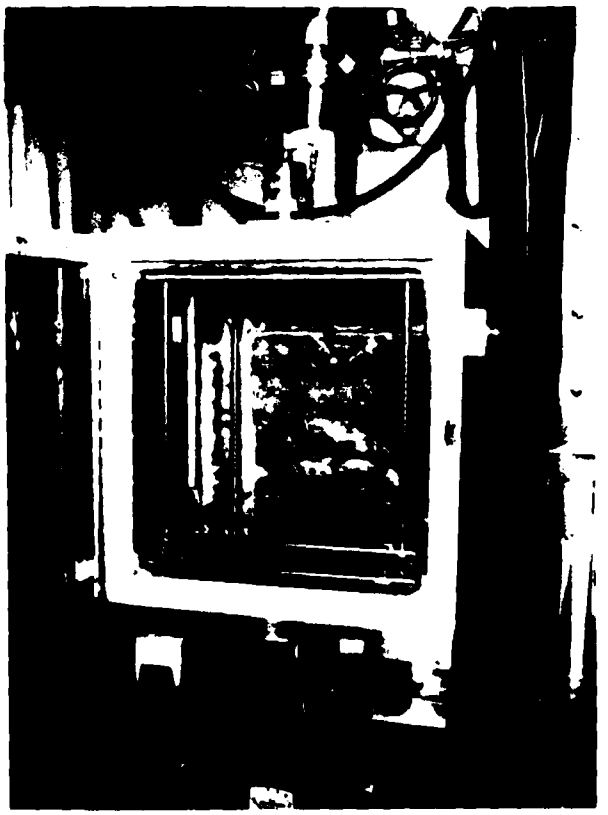

Figure 1. AFRRI laboratory irradiator for cellular radiobiology.

MATERIALS AND METHODS

Irradiator

The x-ray irradiator consists of a x-ray machine (Model No. DXE-225, General Electric Company, Milwaukee, WI), a x-ray tube (Model No. OEG-60, Machlett Laboratories Inc, Stamford, CT), and a shielded cabinet. The x-ray machine operated at peak voltages and currents of up to 60 kVp and 25 mA, respectively. The tube head is water-cooled for continuous operation. The tungsten target angle is 45 degrees to minimize anode heel effects. The tube window has an inherent filtration of 1.5 mm of beryllium (Be), which allows passage of a significant portion of the low-energy x rays. The irradiation time is controlled by a microprocessor-based solid-state timer (Model CX300, Eagle Signal Industrial Controls, Davenport, WI).

The irradiation cabinet has interior dimensions of 56 cm by 42 cm by 45 cm. The inner walls (including the door, top, and bottom) are lined with 2 mm of lead for effective personnel protection. A plastic shelf inside the chamber provides a stable, highly repeatable platform for experimental dosimetry devices and cell samples. The shelf is movable in the vertical (Z) axis by increments of 1 cm. The Z axis is at the center of crossed lines etched into the plastic shelf.

Radiation surveys at the exterior surface of the irradiator during operation at maximum power have shown no radiologic hazard due to beam leakage, thereby permitting experimental preparations to proceed in the lab during irradiation. The only detectable response was 0.5 mrem/hour on contact with the x-ray tube. At 10 cm from the tube, this response was negligible. As a precaution, two safety lights (and an audible alarm, if activated) alert occupants in the laboratory when x rays are being generated. Also, an interlock mechanism prevents the machine from working when the cabinet door is open and automatically turns the irradiator off when the door is opened during operation.

Beam Filtration

Aluminum (Al) filters were added at the exit port of the Be window to increase the effective energy of the x-ray beam by removing many of the low-energy x rays (2). Three thicknesses of Al (that is, 0.633 mm, 0.180 mm, and 0.012 mm) were used for all dosimetric measurements. The tube voltage and current used were 50 kVp and 20 mA, respectively. The 0.633-mm Al filter was used for intercomparison measurements because it simulates a field at the National Institute of Standards and Technology (NIST), Gaithersburg, Maryland, and was used to calibrate the parallel-plate ion chamber. The 0.180-mm Al filter is comparable to that used by Elkind (1). The 0.012-mm Al filter provides negligible filtration of low-energy x rays, hence, it offers a higher dose rate.

Culture Dish Arrays

Typically, cells are maintained in tissue culture petri dishes under monolayer growth conditions bathed in nutrient media to a depth of about 3 to 5 mm (approximately 5 ml per 60-mm-diameter dish or 20 ml per 100-mm-diameter dish). The petri dish is capped with a plastic cover approximately 1 mm thick, which assists both to maintain sterility and to decrease evaporative loss of media.

The x-ray energy spectrum produced at a peak voltage of 50 kV and with added Al filters readily undergoes attenuation by the plastic tissue-culture petri dish covers or the culture media. For example, using a beam hardened with 0.180 mm of Al the attenuation due to the medium can be as high as 60%, and the plastic cover will reduce the beam an additional 15%. Further, inconsistencies in the thickness of medium above the cells can result in large changes in the x-ray energy spectra reaching the cells. To avoid these problems, Elkind and Sutton (1) irradiated cells with a minimum of absorbing material between the radiation source and biological target. An ultra-thin cover of plastic wrap (Saran) secured in a plastic ring with brass screws substitutes for the petri dish cover during irradiations and decreases the possibility of contamination without severely diminishing the photon fluence Further, all excess culture media was aspirated from the petri dish, leaving the cells without a significant media-induced shielding during irradiation.

Reproducibility of the positioning of the biological target material relative to the radiation source was accomplished in the following manner. Either 60-mm or 100 mm-diameter tissue-culture petri dishes were placed on the plastic tray in custom acrylic holders to provide several arrays for irradiation (figure 2). The petri dish array was centered on the Z axis of the irradiator by a centering plate. Cell cultures can be irradiated at room temperature or at the temperature of ice water. For ice water irradiations, an adaptor raises the large petri dish by 1 cm for ice water to be placed beneath the cell plate, thereby facilitating a common vertical scale (3).

2a

2b

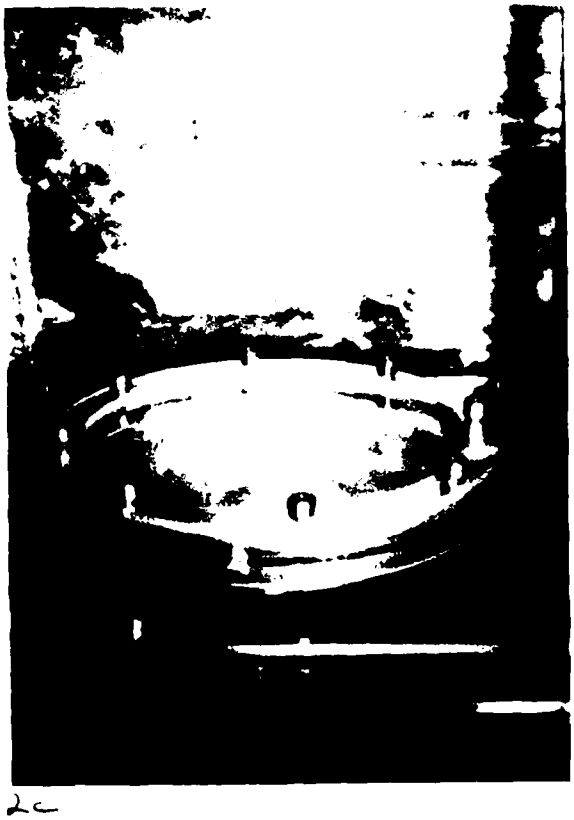

2c

Figure 2. Culture dish arrays: a. 100-mm diameter; b. 60-mm diameter; c. 60-mm diameter in three dish array.

Radiation Detectors

Parallel-Plate Ionization Chamber

A parallel-plate ionization chamber made by Capintec, Inc. (Model No. PS-033, Pittsburg, PA) was used to measure the exposure rate. Its thin window has a thickness of 0.5 mg/cm^2 of aluminized mylar, and its sensitive volume is 0.5 cm^3. The detector body is made of polystyrene. The chamber was calibrated at NIST with two x-ray fields (table 1) (4). Appendix A shows the NIST energy spectrum for the unshielded, 20 kVp calibration field and an energy spectrum with irradiation parameters similar to the NIST L50 x-ray field (5). The difference between the calibration factors for the two beams was 2.4%. This indicated that the chamber response changed minimally over a range of low energies. Charge accumulation was made with a Keithley Model 616 digital electrometer (Cleveland, OH) for the duration of exposure. Collecting charge was the appropriate method of ionization measurement because this is the mode used by NIST to calibrate the chamber. The half-value layer (HVL) is the thickness of material required to reduce an x-ray beam to half its original intensity. The homogeneity coefficient is simply the ratio of the first and second HVL's. Appendix B shows the method of calculation for exposure and dose rates.

Preliminary measurements on the x-ray irradiator indicated that the parallel-plate chamber showed negligible ion recombination characteristics and polarity differences. Readings taken over several days at the same position showed a precision of ±1.5%.

Table 1. NIST Calibration Parameters of Parallel-Plate Chamber

NIST field	kVp	Added filter (mm Al)	HVL (mm Al)	Homogeneity coefficient	Calibration factor (R/nC)
L20	20	None	.071	.76	6.349
L50	50	.639	.75	.58	6.502

Elkind Variable-Volume Extrapolation Chamber

An extrapolation chamber is an ionization chamber in which the sensitive volume may be accurately changed by varying the separation distance between the window and collecting plate. It is a fundamental method of measuring exposure rate so that instrument calibration is unnecessary (6). Appendix C shows the derivation of the equations used to compute exposure rate from extrapolation chamber measurements. The extrapolation chamber (figure 3) used for comparison with the parallel-plate chamber is a custom device provided by Dr. M. M. Elkind. The chamber has a 50-μm-thick Be window (1) and a dual anode with collecting surface diameters of 1 cm and 4 cm. The potential difference applied to the collecting plate was -1,500 volts per centimeter with respect to the Be window. The collected current was read on the same electrometer as used with the parallel-plate chamber. (The difference between the electrometer current (nA) and charge (nC/sec) modes was measured to be 1.6% with a Keithley 261 Picoampere source in conjunction with a Hewlett-Packard 85 computer and 3421A Data Acquisition/Control Unit (Corvallis, OR).)

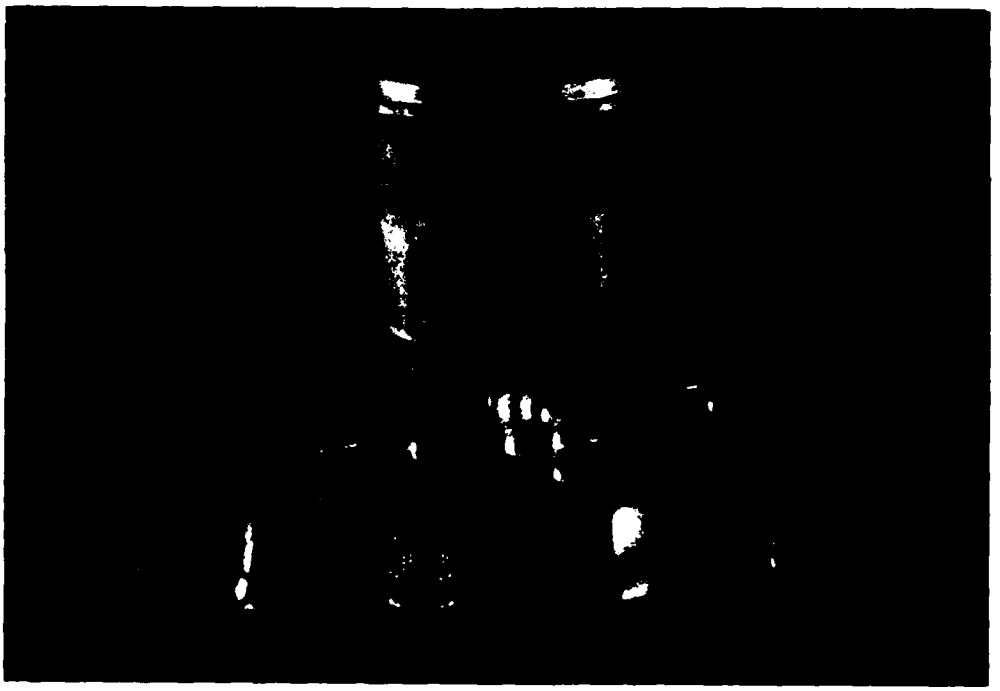

Figure 3. Elkind's extrapolation chamber with collecting plate.

RESULTS

Tube Potential and Timer Accuracy

Peak tube potential and quality assurance measurements for timer accuracy were made with a Mini-X kVp/Timer Meter (RTI Electronics Lab, AB, Sweden). The Mini-X was capable of accurately measuring x-ray tube voltage down to 44 kVp and timer accuracy for times up to 20 seconds. The measured value of kVp from the Mini-X agreed with the x-ray generator settings of 50 kVp and 55 kVp to within +/- 1% and at 45 kVp to within 3.5%. The x-ray timer setting was consistently 2% higher than the time measured by the Mini-X. This difference is due partly to the fact that the x-ray timer indicated the full exposure time while the Mini-X displayed the time that the exposure rate exceeded 75% of the maximum. To further evaluate the timer accuracy, charge was collected by the parallel-plate chamber over a range of exposure times for each beam quality (figure 4). The slopes of the fitted values have units of nC/sec. Comparison of each slope with the measured current shows an overresponse of the charge readings relative to the current readings by an average of 1.5%. This agrees with measurements taken with the picoampere source. The intersection of each line with the time axis shows negligible offset from the origin.

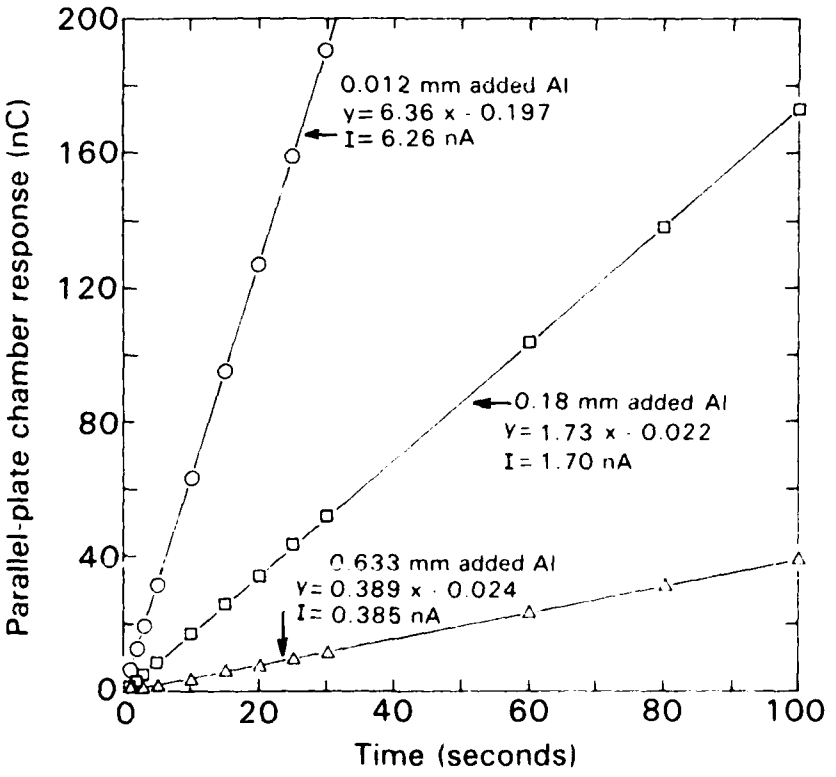

Figure 4. X-ray timer evaluation.

Focal Spot Measurements

The focal spot is the area on the target that accelerated electrons strike to produce x rays, and it correlates to the effective source size. The focal spot image of the irradiator was recorded on radiographic film through a pinhole aperture of 0.2 mm in a sheet of 1.6-mm lead placed midway between the source and the film. The size of the effective focal spot was calculated to be 6 mm by 7 mm using a similar triangles technique (7). Figure 5 shows an enlargement of the focal spot radiographic image.

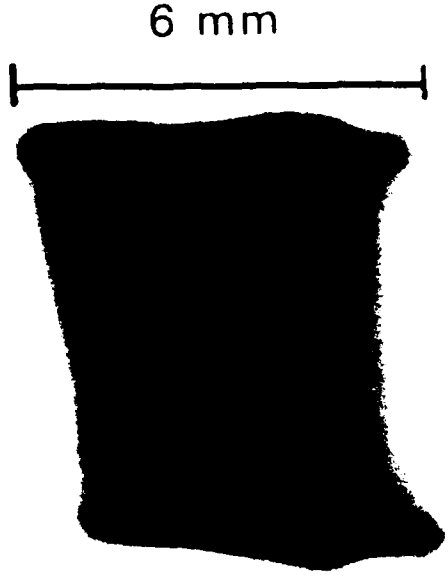

Figure 5. Enlargement of focal spot image.

Beam Quality

When an energy spectrum of an x-ray beam is not available, its penetrability or quality is described in terms of its HVL. The material of choice for measuring beam quality of this irradiator is Al. Because of the space limitation inside the irradiator chamber, ideal conditions for measuring HVL's as described by Trout (8) could not be attained. To approximate the ideal conditions, the distance between the source and the parallel-plate chamber was 36.8 cm with the filter placed halfway between. A collimator arrangement (figure 6) restricted the beam to the chamber's window. Table 2 shows beam quality data for several thicknesses of added Al at 50 kVp and no added Al at 20 kVp. The approximate equivalent photon energy for each beam's HVL was referenced from Johns and Cunningham (7).

Figure 6. Collimator arrangement used for half-value layer measurements.

Table 2. Parameters of Beam Quality

kVp	Added filter (mm Al)	HVL (mm Al)	Homogeneity coefficient	Approximate equivalent energy (keV)
20	none	0.058	0.80	8
50	.012	.077	.70	9
50	.18	.16	.67	10
50	.633	.53	.63	19

The measured HVL values for the 20 kVp and 50 kVp/0.633 mm Al measurements are significantly lower than the respective NIST L20 and L50 HVL values shown in table 1. The differences, which indicate the AFRRI x-ray unit has a softer energy spectra, are likely due to the various ways the tube potential is supplied. The NIST power supply is constant potential whereas the laboratory x-ray irradiator potential is half-wave rectified single phase.

Parallel-plate Window Transmission

The ability of the parallel-plate chamber to transmit low-energy photons through the aluminized mylar window was tested by measuring x-ray transmission through mylar. The HVL of mylar for two different x-ray beams was measured with the collimator system. The two beams were 50 kVp with 0.633 mm of added Al and 20 kVp with no added filtration. The measured HVL's were 876 and 94.4 mg/cm^2 for the 50 kVp and 20 kVp beams, respectively. The calculated attenuation due to the chamber window is 0.04% and 0.30% for each of the respective beams. This method provided an approximation because the mylar attenuators were not aluminized.

Intercomparison

Intercomparison between the parallel-plate ionization chamber and the extrapolation chamber was made with AFRRI's laboratory x-ray irradiator to verify the parallel-plate chamber's ability to measure low-energy exposures. The parameters measured were (a) exposure rate, (b) falloff with increasing vertical (Z axis) distance, (c) falloff in field size (X-Y axes), and (d) output charges with current and voltage. The amount of added filtration used was 0.633 mm of Al. Unless altered for experimental purposes, the tube voltage, current, and source-to-detector distance (SDD) were set at 50 kVp, 20 mA, and 19.2 cm, respectively.

Comparison of Exposure Rates

Ionization current measurements were made while changing the distance separating window and collecting plate of the extrapolation chamber. These measurements were repeated for both of the available plate collecting diameters on Elkind's extrapolation chamber. The results of these measurements are presented in figure 7. The slope of the fitted line for each set of measurements, when applied to equation 1 of appendix D, resulted in the exposure rate at the midpoint of the chamber. The intercepts of the extrapolated lines on the abscissa fell at about 0.09 cm.

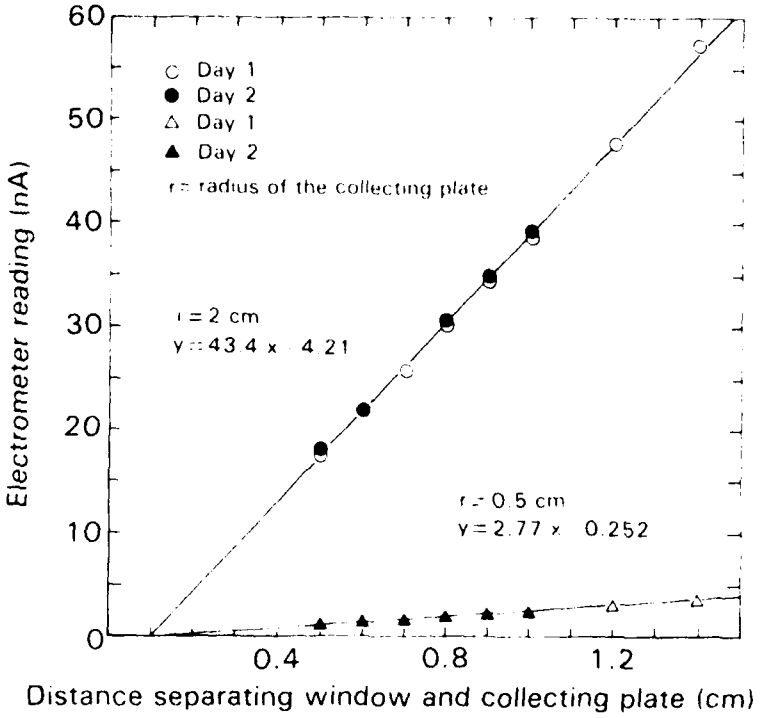

Figure 7. Effect of changing volume on extrapolation chamber.

Table 3 shows the values used to evaluate the exposure rate. The average exposure rate of the four extrapolation measurements was 10.5 R/sec, with a standard deviation representing 1.6% of the mean. The exposure rate as measured by the parallel-plate chamber was 10.6 R/sec. The method used to calculate the exposure rate to the parallel-plate chamber is equation 1 in appendix B. The excellent agreement between these two methods establishes a link between the landmark radiobiology experiments of Elkind and colleagues at the Argonne National Laboratory and those performed with the new unit at AFRRI.

Table 3. Exposure Rate Evaluation of Extrapolation Chamber and Parallel-Plate Chamber

Chamber*	Day	Diameter (cm)	Temperature (C°)	P (mm Hg)	Slope (ΔA Δh)	X intercept (cm)	X (R sec)
EC	1	4	22.6	753.8	43.8	0.107	10.6
EC	1	1	22.6	753.8	2.78	.093	10.7
EC	2	4	23.1	757.0	42.7	.081	10.3
EC	2	1	23.1	757.0	2.74	.083	10.5
PPC	NA	NA	NA	NA	NA	NA	10.6

*EC = extrapolation chamber; PPC = parallel-plate chamber.

Inverse Square Measurements

The measurement of beam falloff with increasing distance from the source was made with the parallel-plate and extrapolation (4-cm diameter only) chambers. Figure 8 shows the ratio of the observed to expected values at successive distances from the source. The point of normalization was 19.2 cm from the source. After 16 cm, the falloff of both chambers yielded an inverse square relationship to within 1%. Additional measurements were made by the parallel-plate chamber along the same axis with added filters of 0.180 mm and 0.012 mm Al. Figure 8 compares these data and shows that filtration with thinner filters caused greater deviation from the inverse square law. This was the expected result because air acted as an effective attenuator for the low-energy x rays transmitted through the thin filters. The slopes of the two lines were approximately 0.006 cm^{-1}, which was consistent with the linear attenuation coefficient for 10 keV x rays in air (7).

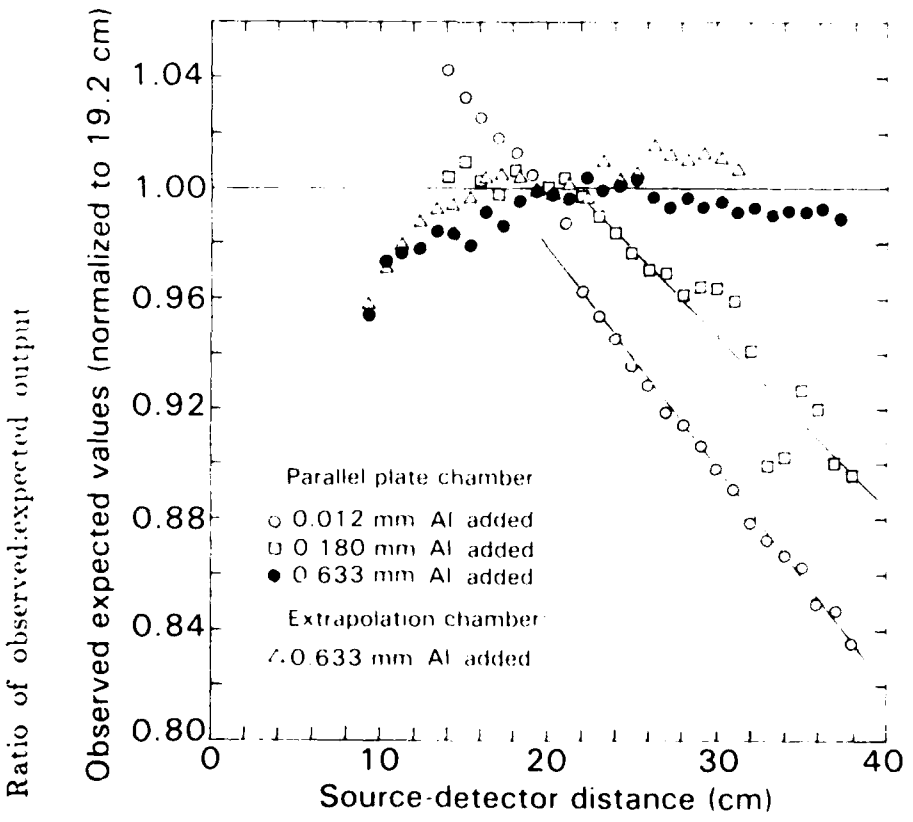

Figure 8. Radiation output measurements normalized to expected values. Expected values were calculated using the inverse square law referenced to the output at 19.2 cm distance.

Beam Falloff in the X-Y Plane

Beam intensity measurements in the horizontal plane at 19.2 cm were made with the parallel-plate and extrapolation (4-cm diameter only) chambers. The measurements were made diverging from the geometrical center toward the front, back, left, and right. The values were normalized to the geometrical center. Figure 9 shows field distribution was in excellent agreement between the parallel-plate chamber and 4-cm-diameter extrapolation chamber. The center of the field was at the geometrical center of the beam for both chambers. The diameters of the fields for 95%, 92.5%, and 90% uniformity are 4.7 cm, 6.3 cm, and 7.3 cm, respectively.

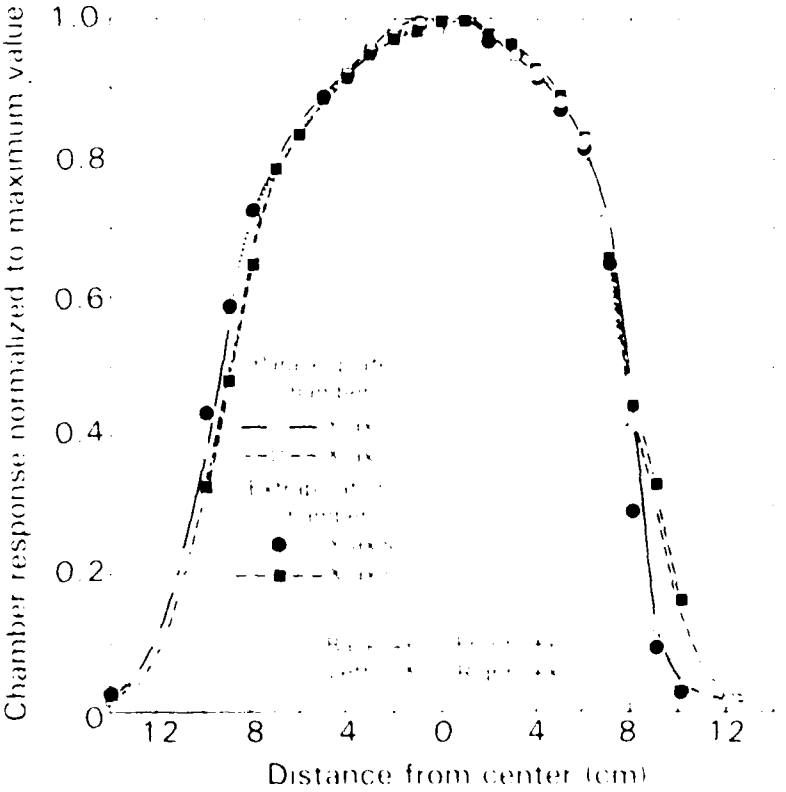

Figure 9. Intercomparison of field uniformity measurements.

Tube Current and Voltage

The linearity of the x-ray output with tube current over a range of 8 mA to 25 mA was evaluated by the parallel-plate chamber and both collection plate diameters of the extrapolation chamber. Figure 10 shows the tube current dependence of each ionization chamber's response as normalized to its sensitive volume. The results show excellent agreement and linearity over the entire range of x-ray tube current.

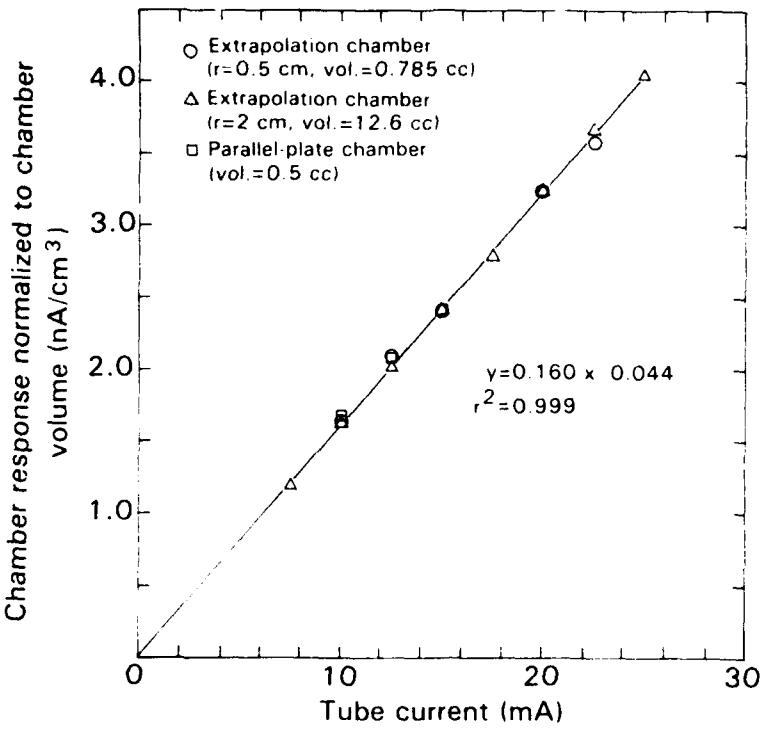

Figure 10. Linearity of x-ray output with tube current.

Figure 11 shows the effect of varying tube voltage on each chamber's volume-normalized response. Agreement between the two anode diameters of the extrapolation chamber was quite good. Agreement of the parallel-plate chamber was also good at lower voltages, but shows an overresponse at higher voltages, which peak at 5% at 50 kVp. The data in figure 11 were fitted with both linear and power function curves, as shown. Both the linear and power function correlation coefficients were greater than 0.995.

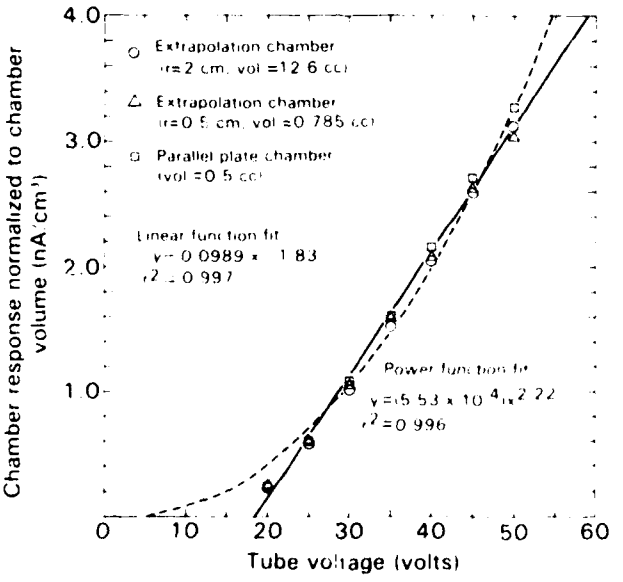

Figure 11. X-ray output as a function of tube voltage.

Dosimetry Measurements

The cellular dose was calculated from parallel-plate measurements taken along the Z axis for three beam parameters. The beam parameters were 50 kVp with added filtration of 0.633 mm, 0.180 mm, and 0.012 mm Al. Equation 2 of appendix B shows the method of dose calculation. Tables 4-6 show the dose rate at incremental distances from the source at the geometrical center for the single-plate arrays. The hole number is the position where the plate was placed to attain the respective source-to-cell distance. One shelf height was for the room temperature setup and the other was for the ice water setup. The uniformity measurements at each distance were derived from falloff measurements in the X-Y plane at several Z-axis positions for each beam. From those measurements, cones of uniformity were constructed to ensure 90%, 92.5%, and 95% uniformity across the plate. Thus, an investigator can use the dose rate and uniformity that best suits the experimental needs.

While taking beam profile measurements with the thinner filters, we observed that the point of maximum beam intensity was offset from the vertical axis towards the back of the cabinet (-Y direction). This effect was enhanced at greater source-to-detector distance (SDD). The displacement for the 0.180-mm Al beam was 0.3 cm at 15 cm SDD and increased to 1 cm at 40 cm SDD. The displacement of the 0.012-mm Al beam was 0.5 cm at 15 cm SDD and increased to about 2 cm at 40 cm SDD. While this effect was not fully characterized, it probably resulted from a variation in the x-ray energy spectrum across the x-ray beam in the direction of the anode-cathode axis. Because the offset varied with both the SDD and added filtration, the irradiation arrays were left in place at the X-Y plane origin. As a result, the cone of uniformity was slightly narrower than if it had been centered at the point of peak intensity. In the worst case, the deviation of the maximal intensity from the intensity at the geometric axis was 0.5%.

Incomplete aspiration of culture medium from the petri dishes before irradiation can markedly influence the uniformity of cellular x-ray dosage. This was demonstrated by the results of a pilot experiment on x-ray dose response and cell survival that used the 0.012 mm Al filter. An anomalous cluster of cell colonies around the periphery of the culture plate was observed in the high radiation dose samples. Investigation into this abnormality suggested that this effect was produced by the shielding of x rays by a meniscus of excess culture fluid that was created by not aspirating all of the excess cell culture medium from the petri dish. This was confirmed by repeating the experiment with complete medium aspiration (that is, all of the excess medium was removed), which resulted in the elimination of the ring of colonies. Upon the addition of incremental amounts of medium, the medium-induced shielding around the outer edge reappeared. Figure 12 shows cell survival populations after staining when the culture medium had been aspirated completely, followed by the addition of

Table 4. Dose Rate Chart of 0.633-mm Al Beam

Hole # Room temp	Hole # Ice water	Shelf height SDD (cm)	Dose rate (cGy/s)	Uniformity of cell irradiation (percentage) 60-mm dish	100-mm dish	Array of 3 60-mm dishes
9	10	15.3	14.6	92.5	NA	NA
10	11	16.3	12.8	92.5	NA	NA
11	12	17.3	11.4	95	NA	NA
12	13	18.3	10.2	95	NA	NA
13	14	19.3	9.17	95	90	NA
14	15	20.3	8.29	95	90	NA
15	16	21.3	7.53	95	92.5	NA
16	17	22.3	6.87	95	92.5	NA
17	18	23.3	6.29	95	92.5	NA
18	19	24.3	5.87	95	92.5	NA
19	20	25.3	5.33	95	92.5	NA
20	21	26.3	4.94	95	92.5	NA
21	22	27.3	4.58	95	92.5	90
22	23	28.3	4.26	95	95	90
23	24	29.3	3.98	95	95	90
24	25	30.3	3.72	95	95	90
25	26	31.3	3.48	95	95	92.5
26	27	32.3	3.27	95	95	92.5
27	28	33.3	3.08	95	95	92.5
28	29	34.3	2.90	95	95	92.5
29	30	35.3	2.74	95	95	92.5
30	31	36.3	2.59	95	95	92.5
31	32	37.3	2.45	95	95	92.5
32	33	38.3	2.33	95	95	92.5
33	34	39.3	2.21	95	95	92.5
34	35	40.3	2.10	95	95	92.5
35	36	41.3	2.00	95	95	92.5
36	37	42.3	1.91	95	95	92.5
37	NA	43.3	1.82	95	95	95

Table 5. Dose Rate Chart of 0.180-mm Al Beam

Hole # Room temp	Hole # Ice water	Shelf height SDD (cm)	Dose rate (cGy/s)	Uniformity of cell irradiation (percentage) 60-mm dish	100-mm dish	Array of 3 60-mm dishes
9	10	15.3	71.6	92.5	NA	NA
10	11	16.3	62.7	92.5	NA	NA
11	12	17.3	55.4	92.5	NA	NA
12	13	18.3	49.4	92.5	NA	NA
13	14	19.3	44.2	95	NA	NA
14	15	20.3	39.7	95	NA	NA
15	16	21.3	36.0	95	90	NA
16	17	22.3	32.7	95	90	NA
17	18	23.3	29.9	95	90	NA
18	19	24.3	27.4	95	90	NA
19	20	25.3	25.1	95	90	NA
20	21	26.3	23.2	95	92.5	NA
21	22	27.3	21.5	95	92.5	NA
22	23	28.3	20.0	95	92.5	NA
23	24	29.3	18.5	95	92.5	NA
24	25	30.3	17.3	95	92.5	NA
25	26	31.3	16.2	95	92.5	NA
26	27	32.3	15.2	95	92.5	90
27	28	33.3	14.2	95	92.5	90
28	29	34.3	13.4	95	92.5	90
29	30	35.3	12.6	95	95	90
30	31	36.3	11.9	95	95	90
31	32	37.3	11.2	95	95	90
32	33	38.3	10.6	95	95	90
33	34	39.3	10.1	95	95	90
34	35	40.3	9.5	95	95	92.5
35	36	41.3	9.1	95	95	92.5
36	37	42.3	8.6	95	95	92.5
37	NA	43.3	8.21	95	95	95

Table 6. Dose Rate Chart of 0.012-mm Al Beam

Hole # Room temp	Hole # Ice water	Shelf height SDD (cm)	Dose rate (cGy/s)	Uniformity of cell irradiation (percentage) 60-mm dish	100-mm dish	Array of 3 60-mm dishes
9	10	15.3	293	90	NA	NA
10	11	16.3	255	92.5	NA	NA
11	12	17.3	224	92.5	NA	NA
12	13	18.3	198	92.5	NA	NA
13	14	19.3	176	95	NA	NA
14	15	20.3	158	95	NA	NA
15	16	21.3	142	95	90	NA
16	17	22.3	128	95	90	NA
17	18	23.3	117	95	90	NA
18	19	24.3	106	95	90	NA
19	20	25.3	97.4	95	92.5	NA
20	21	26.3	89.5	95	92.5	NA
21	22	27.3	82.5	95	92.5	NA
22	23	28.3	76.2	95	92.5	NA
23	24	29.3	70.6	95	92.5	NA
24	25	30.3	65.6	95	92.5	NA
25	26	31.3	61.1	95	92.5	90
26	27	32.3	57.0	95	92.5	90
27	28	33.3	53.4	95	95	90
28	29	34.3	50.0	95	95	90
29	30	35.3	47.0	95	95	90
30	31	36.3	44.1	95	95	90
31	32	37.3	41.6	95	95	90
32	33	38.3	39.3	95	95	92.5
33	34	39.3	37.1	95	95	92.5
34	35	40.3	35.1	95	95	92.5
35	36	41.3	33.3	95	95	92.5
36	37	42.3	31.6	95	95	92.5
37	NA	43.3	NA	95	95	92.5

up to 0.5 ml of medium before irradiation. Notice that a shielding effect was present with as little as 0.1 ml of medium added to the dish. A similar effect was present for the triple-dish array.

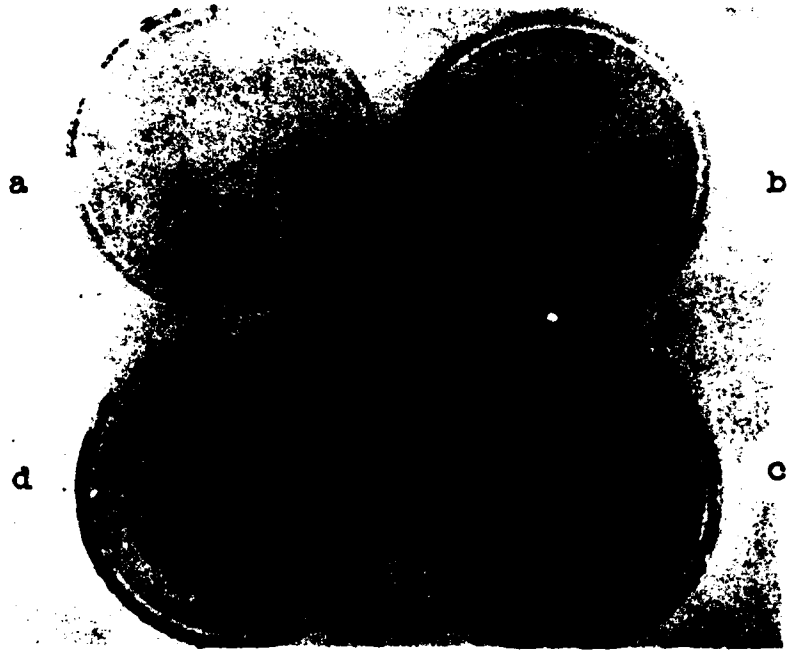

Figure 12. Meniscus effect for essentially unfiltered (0.012 mm Al) beam. The cell cultures were aspirated to completeness with increasing amounts of culture fluid added: (a) O ml, (b) 0.1 ml, (c) 0.3 ml, and (d) 0.5 ml.

SUMMARY

Dosimetry measurements have been performed on the AFRRI laboratory x-ray irradiator for three different cell culture dish arrays positioned at a range of distances from the x-ray tube. The device used for these measurements was a parallel-plate ionization chamber with a thin aluminized-mylar window. Intercomparison with an extrapolation chamber showed excellent agreement between these independent measurement methods. Results are presented for radiation dose rate, uniformity, and beam quality for operation of the tungsten target, Be window x-ray tube at 50 kVp, 20 mA, and with filters either 0.012 mm, 0.180 mm, or 0.633 mm thick. The data in this report establish a dosimetric link between the cellular radiobiology research to be performed at AFRRI with the laboratory x-ray irradiator and the landmark work performed by Elkind and Sutton (1) with a similar device.

REFERENCES

1. Elkind, M. M., and Sutton, H. Radiation response of mammalian cells grown in culture. Radiation Research 13: 556-593, 1960.

2. Christensen, E. E., Curray III, T. S., Dowdey, J. E. An Introduction to the Physics of Diagnostic Radiology. Lea and Febiger Pub., Philadelphia. 1978.

3. Personal communications with M. M. Elkind, June 1986.

4. Report of Calibration. DG 8454/85, TFNG45095. National Bureau of Standards, Gaithersburg, MD, 30 October 1985.

5. Seelentag, W. W., Panzer, W., Drexler, G., Platz, L., and Santner, F. A catalogue of spectra for the calibration of dosimeters. GSF-KBericht S 560. Gesellschaft fur Strahlen-und Umweltforschung mbH, Munich, Federal Republic of Germany, 1979.

6. Radiation Dosimetry, 2nd Ed. Vol. II: Instrumentation. Attix, F., and Roesch, C., eds. Academic Press, New York, 1966.

7. Johns, H. E., and Cunningham, J. R. The Physics of Radiology, 4th ed. C. Thomas Pub., Springfield, IL, 1983.

8. Trout, E. D., Kelly, J. P., and Lucas, A. C. Determination of half value layer, American Journal of Roentgenology 84: 729-740, 1960.

ACKNOWLEDGMENTS

The authors would like to thank Dr. Colin K. Hill for his helpful discussions and advice in planning this project. We would like to especially thank Mr. Franklin M. Sharpnack for the construction of the petri dish holders and acrylic positioning devices for the x-ray irradiator. We would also like to thank Mr. Scott Hawkins for the copious dosimetry measurements he made, which are included in this report. Finally, we acknowledge and thank Dr. Michael P. Hagan for his invaluable assistance and guidance in numerous aspects of this project.

APPENDIX A. X-RAY ENERGY SPECTRA

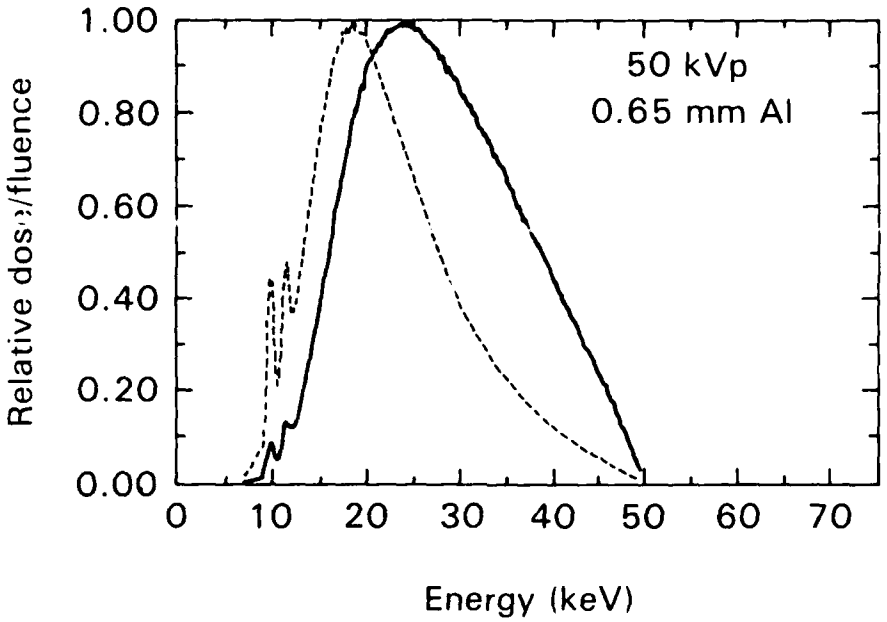

Figure A-1. X-ray energy spectrum for 50 kVp and 0.65 mm Al filtration. The solid line shows the spectral distribution of x-ray energy, and the dash line shows that of x-ray fluence. Redrawn from reference (5).

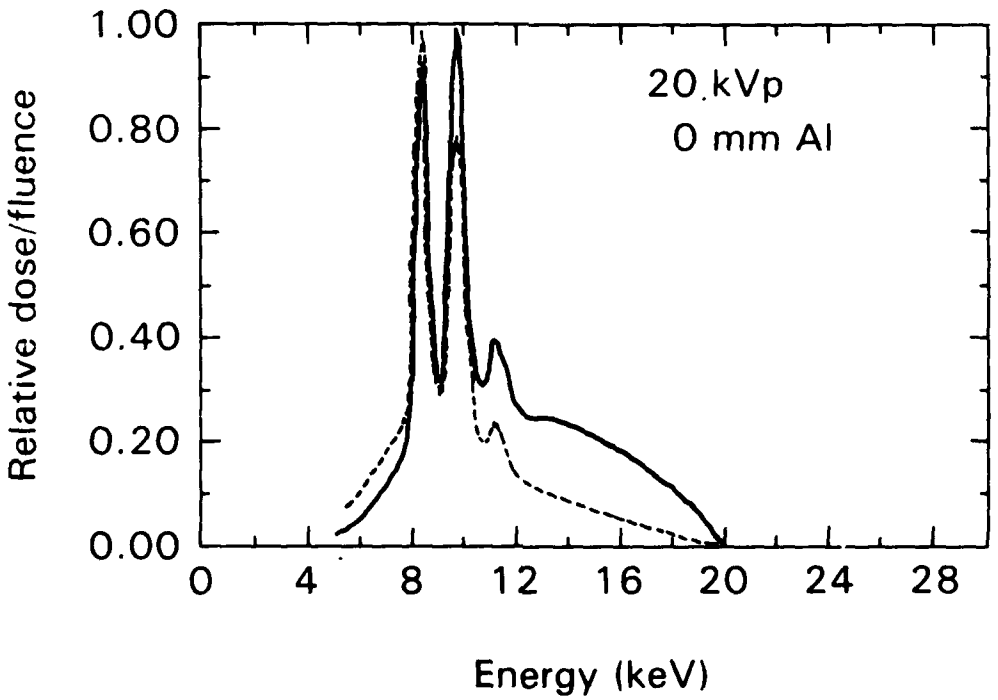

Figure A-2. X-ray energy spectrum for 20 kVp and no added filtration. The solid line shows the spectral distribution of x-ray energy, and the dash line shows that of x-ray fluence. Redrawn from reference (5).

APPENDIX B. EXPOSURE AND DOSE CALCULATIONS FOR THE PARALLEL-PLATE IONIZATION CHAMBER

$$\dot{X} = (\Delta Q/\Delta t)\ N_x\ k_{tp} \qquad \text{(B-1)}$$

where $\dot{X}$ = exposure rate in R/s

ΔQ = charge collected over time interval Δt (nC/s)

N_x = chamber calibration factor (see table 1). The calibration factor whose HVL and homogeneity factor most closely resembles the values measured for each field was chosen for that field. The uncertainty in applying this method is approximately 1%.

= 6.502 R/nC for 0.633 mm added Al beam

= 6.349 R/nC for 0.180 mm added Al beam

= 6.348 R/nC for 0.012 mm added Al beam

k_{tp} = correction to standard room temperature and pressure

$$\dot{D} = \dot{X}\ f_{water}\ k_{bs}\ k_{sw} \qquad \text{(B-2)}$$

where $\dot{D}$ = absorbed dose rate to cell medium (cGy/s)

f_{water} = factor that converts exposure in air to dose in water, which approximates the cell media. This is an energy dependent value, although it varies less than 2.5% over the equivalent energy ranges involved (7).

= 0.886 for 0.633 mm added Al beam

= 0.902 for 0.180 mm added Al beam

= 0.905 for 0.012 mm added Al beam

k_{bs} = correction for backscatter. This correction was assumed to be 1.00 because the amount of plastic behind the ionization chamber was approximately the same as behind the cells.

k_{sw} = correction for attenuation due to plastic wrap. This correction was only applied to the 0.633 mm Al beam. Plastic wrap was included in the measurements of the other fields.

= 1.02 for 0.633 mm added Al beam

APPENDIX C. DERIVATION OF EXPOSURE RATE CALCULATION FOR EXRAPOLATION CHAMBER (3)

a. Definition of Exposure:

1 R in dry air for x or γ rays = 1 esu charge / cm^3 at STP

$\therefore$ 1 R = 3.336×10^{-10} C/cm^3

b. Conversion of C/cm^3 to amp-s/cm^3 at STP

Given: 1 amp = 1 C/s

1 C = 1 amp-s

$\therefore$ 1 R = 3.336×10^{-10} amp-s/cm^3

and 1 R/s = 3.336×10^{-10} amp/cm^3

c. Define:

$$K = \frac{1 \text{ R/s}}{3.336 \times 10^{-10}} = 2.998 \times 10^{9} \left[(\text{R/s})/(\text{amp/cm}^3)\right]$$

d. $$\dot{X} = \frac{K \, dQ/dt}{V_{STP}} = K \left[\frac{\text{R/s}}{\text{amp/cm}^3}\right] \frac{I \text{ (amp)}}{V_{STP} \text{ (cm}^3\text{)}}$$

$$= 2.998 \times 10^{9} \, (I/V_{STP})$$

where I = current of charge generated in air volume V at STP conditions

e. Volume of a right circular cylinder (V) = $\pi r^2 h$
where r is the radius and h is the height
Correct the air volume to room temperature and standard pressure.

$$V_{STP} = \left[\frac{295.15}{T + 273.15}\right] \left[\frac{P}{760}\right] (\pi r^2 h)$$

where T is the air temperature in ^{o}C and P is the atmospheric pressure in mm of mercury.

$$f. \quad \dot{X} = 2.457 \times 10^{9} \left[\frac{T + 273.15}{P}\right] \left[\frac{I_c}{r^2 h}\right] \qquad (C\text{-}1)$$

where r = the extrapolation effective radius (cm)
I_c/h = slope of line from chamber response (amp) vs. separation of window-anode (cm)
h = separation distance of the extrapolation chamber window from the anode

END

FILMED

1-90

DTIC